

# **Development of Robust Control Strategies for Autonomous Underwater Vehicles**

*Dissertation submitted in partial fulfillment  
of the requirements of the degree of*

***Doctor of Philosophy***

*in*

**Electrical Engineering**

*by*

***Debabrata Atta***  
**(Roll No.508EE102)**

*based on research carried out  
under the supervision of*

***Prof. Bidyadhar Subudhi***



**Department of Electrical Engineering  
National Institute of Technology Rourkela**

**June 2017**



## **CERTIFICATE OF EXAMINATION**

01/06/2017

Roll Number : 508EE102

Name: *Debabrata Atta*

Title of Dissertation: *Development of Robust Control Strategies for Autonomous Underwater Vehicles*

We the below signed, after checking the dissertation mentioned above and the official record book(s) of the student, hereby state our approval of the dissertation submitted in partial fulfillment of the requirements of the degree of Doctor of Philosophy in Electrical Engineering at National Institute of Technology Rourkela. We are satisfied with the volume, quality, correctness, and originality of the work.

---

Prof. D. R. K. Parhi  
(Member, DSC)

---

Prof. S. K. Behera  
(Member, DSC)

---

Prof. K. B. Mohanty  
(Member, DSC)

---

Prof. A. K. Panda  
(Chairman, DSC)

---

Prof. B. Subudhi  
(Supervisor)

---

Prof. A. K. Deb  
(External Examiner)



Department of Electrical Engineering  
**National Institute of Technology Rourkela**

**CERTIFICATE**

This is to certify that the work presented in the dissertation entitled “**Development of Robust Control Strategies for Autonomous Underwater Vehicles**” submitted by Debabrata Atta, Roll Number 508EE102, is a record of original research carried out by him under my supervision and guidance in partial fulfillment of the requirements of the degree of Doctor of Philosophy in Electrical Engineering. Neither this dissertation nor any part of it has been submitted earlier for any degree or diploma to any institute or university in India or abroad.

Place:

Date:

---

Prof. Bidyadhar Subudhi  
(Supervisor)

## **Declaration of Originality**

I, Debabrata Atta, Roll Number 508EE102 hereby declare that this dissertation entitled **“Development of Robust Control Strategies for Autonomous Underwater Vehicles”** presents my original work carried out as a doctoral student of NIT Rourkela and, to the best of my knowledge, contains no material previously published or written by another person, nor any material presented by me for the award of any degree or diploma of NIT Rourkela or any other institution. Any contribution made to this research by others, with whom I have worked at NIT Rourkela or elsewhere, is explicitly acknowledged in the dissertation. Works of other authors cited in this dissertation have been duly acknowledged under the sections Reference or Bibliography. I have also submitted my original research records to the scrutiny committee for evaluation of my dissertation.

I am fully aware that in case of any non-compliance detected in future, the Senate of NIT Rourkela may withdraw the degree awarded to me on the basis of the present dissertation.

DEBABRATA ATTA



## **ACKNOWLEDGEMENTS**

I would like to gratefully acknowledge the enthusiastic supervision and guidance of Prof. Bidyadhar Subudhi during this work. He is my source of inspiration. As my supervisor, his insight observations and suggestions helped me to establish the overall direction of the research and contributed immensely to the success of the work.

I express my sincere gratitude to Doctoral Scrutiny Committee Chairman Prof. A.K.Panda and its members Prof. D.R.K Parhi, Prof. S.K.Behera, Prof. K.B.Mohanty for their suggestion to improve my work. I am also very much obliged to Head of the Department Prof. J.K.Satapathy for providing possible facilities. I also express my earnest thanks to Prof. S.Ghosh, and Prof. S. Maity for their detailed comments and suggestions during the final phases of the preparation of this thesis.

I acknowledge all staffs, research scholars, friends and juniors, especially Raja Rout, Basant Sahoo, Satyam Bonala, Rudra Prasad Das, Rajeswari Pradhan, Soumya Mahapatro, Murlidhar Killi, Subhashish Mahapatra, Subhrajit Mahapatra, Debashish Jena, Santanu Pradhan of Center for Industrial Electronics and Robotics, Department of Electrical Engineering, NIT, Rourkela for helping me during my research work.

Finally, I would like to thank my beloved parents, father-in-law, mother-in-law and especially my wife for their endless encouragement for pursuing my research.

DEBABRATA ATTA



# Abstract

---

The resources of the energy and chemical balance in the ocean sustain mankind in many ways. Therefore, ocean exploration is an essential task that is accomplished by deploying Underwater Vehicles. An Underwater Vehicle with autonomy feature for its navigation and control is called Autonomous Underwater Vehicle (AUV). Among the task handled by an AUV, accurately positioning itself at a desired position with respect to the reference objects is called set-point control. Similarly, tracking of the reference trajectory is also another important task. Battery recharging of AUV, positioning with respect to underwater structure, cable, seabed, tracking of reference trajectory with desired accuracy and speed to avoid collision with the guiding vehicle in the last phase of docking are some significant applications where an AUV needs to perform the above tasks. Parametric uncertainties in AUV dynamics and actuator torque limitation necessitate to design robust control algorithms to achieve motion control objectives in the face of uncertainties. Sliding Mode Controller (SMC),  $H_\infty / \mu$  synthesis, model based PID group controllers are some of the robust controllers which have been applied to AUV. But SMC suffers from less efficient tuning of its switching gains due to model parameters and noisy estimated acceleration states appearing in its control law. In addition, demand of high control effort due to high frequency chattering is another drawback of SMC. Furthermore, real-time implementation of  $H_\infty / \mu$  synthesis controller based on its stability study is restricted due to use of linearly approximated dynamic model of an AUV, which hinders achieving robustness. Moreover, model based PID group controllers suffer from implementation complexities and exhibit poor transient and steady-state performances under parametric uncertainties. On the other hand model free Linear PID (LPID) has inherent problem of narrow convergence region, i.e. it can not ensure convergence of large initial error to zero. Additionally, it suffers from integrator-wind-up and subsequent saturation of actuator during the occurrence of large initial error. But LPID controller has inherent capability to cope up with the uncertainties. In view of addressing the above said problem, this work proposes wind-up free Nonlinear PID with Bounded Integral (BI) and Bounded Derivative (BD) for set-point control and combination of continuous SMC with Nonlinear PID with BI and BD namely SM-N-PID with BI and BD for trajectory tracking. Nonlinear functions are used for all P,I and D controllers (for both of set-point and tracking control) in addition to use of nonlinear tan hyperbolic function in SMC(for tracking only) such

that torque demand from the controller can be kept within a limit. A direct Lyapunov analysis is pursued to prove stable motion of AUV. The efficacies of the proposed controllers are compared with other two controllers namely PD and N-PID without BI and BD for set-point control and PD plus Feedforward Compensation (FC) and SM-NPID without BI and BD for tracking control.

Multiple AUVs cooperatively performing a mission offers several advantages over a single AUV in a non-cooperative manner; such as reliability and increased work efficiency, etc. Bandwidth limitation in acoustic medium possess challenges in designing cooperative motion control algorithm for multiple AUVs owing to the necessity of communication of sensors and actuator signals among AUVs. In literature, undirected graph based approach is used for control design under communication constraints and thus it is not suitable for large number of AUVs participating in a cooperative motion plan. Formation control is a popular cooperative motion control paradigm. This thesis models the formation as a minimally persistent directed graph and proposes control schemes for maintaining the distance constraints during the course of motion of entire formation. For formation control each AUV uses Sliding Mode Nonlinear PID controller with Bounded Integrator and Bounded Derivative. Direct Lyapunov stability analysis in the framework of input-to-state stability ensures the stable motion of formation while maintaining the desired distance constraints among the AUVs.

**Keywords:** AUV, Parametric uncertainties, Actuator saturation, Nonlinear PID, Integrator wind-up, Sliding Mode Control, , Cycle Free Minimally Persistent Formation, Cascaded system.

# Contents

	Abstract	vii
	Contents	ix
	List of symbols	xv
	List of Abbreviations	xvii
	List of Figures	xix
	List of Tables	xx
<b>Chapter-1</b>	<b>Introduction</b>	<b>1</b>
1.1	Evolution of Underwater Vehicles	1
1.1.1	Manned Submersible Vehicles	2
1.1.2	Remotely Operated Vehicles (ROV)	2
1.1.3	Hybrid ROV	3
1.1.4	Autonomous Underwater Vehicle	4
1.2	Motivation behind the Research in AUV	9
1.2.1	Mission	9
1.2.2	Applications of AUVs	10
1.3	Advantages of Multi-AUV Dynamic System	11
1.4	Challenges in AUV Research	13
1.4.1	The Control Issues and Autonomy	13
1.4.2	Communication	14
1.5	Motivation of the Thesis	16
1.6	Objectives of this Research Work	17
1.7	Organization of the Thesis	18
<b>Chapter-2</b>	<b>Literature Review on Control Strategies of AUV</b>	
2.1	Introduction	21
2.2	Motion Control Objectives	22
2.2.1	Navigation	22
2.2.2	Path Tracking/ Trajectory Tracking	23
2.2.3	Path Following	25
2.2.4	Point Stabilization and Regulatory Problems	27
2.2.5	Line-of-sight (way-point) Guidance Based Path Following	27
2.2.6	Cross-Track Control	28
2.2.7	Region-Based Tracking	28
2.2.8	Homing and Docking	29
2.3	Control Architectures	30
2.3.1	Deliberative Architectures	30

2.3.2	Behavioral Architectures	31
2.3.3	Hybrid Architectures	31
2.4	Control Algorithms	32
2.4.1	Traditional Controllers	32
2.4.1.1	PID Type Control	32
2.4.1.2	Robust Control	35
2.4.1.3	Robust/Optimal Control	37
2.4.1.4	Optimal Control	41
2.4.1.5	Adaptive Control	42
2.4.1.6	Intelligent Control	45
2.4.1.7	Behavior Based Scheme	46
2.4.1.8	Geometric Control	47
2.4.1.9	Some Lyapunov based Controller	49
2.4.1.10	Passivity Based Control	51
2.4.1.11	Energy Based Control	51
2.4.1.12	Switched Seesaw Control	52
2.4.2	Hybrid Controllers	53
2.4.2.1	$H_{\infty}$ Optimal PID	53
2.4.2.2	Adaptive Sliding Mode Control	53
2.4.2.3	Adaptive Optimal Control	54
2.4.2.4	Adaptive Supervisory Control	54
2.4.2.5	Fuzzy Sliding Mode Control	55
2.4.2.6	Adaptive Fuzzy Logic Control	55
2.4.2.7	Adaptive Fuzzy Sliding Mode Control	56
2.4.2.8	Neural Sliding Mode Control	56
2.4.2.9	Neural Network Based Time Optimal Sliding Mode control	56
2.4.2.10	Neuro-Fuzzy Control	56
2.4.2.11	Adaptive Neuro-Fuzzy Control	57
2.4.2.12	Adaptive Backstepping	57
2.4.2.13	Adaptive- Behavior-based Control Strategy	57
2.4.2.14	Adaptive PD Set Point Control	58

2.4.2.15	Synthesis Method	59
2.5	Control of Multiple AUVs under Cooperative Motion	59
2.5.1	Architecture of Cooperative Motion Control System of AUVs	59
2.5.1.1	Decision Making Strategies	61
2.5.1.1.1	Centralized	62
2.5.1.1.2	Decentralized	63
2.5.1.1.3	Combination of Centralized and Decentralized	66
2.5.1.1.4	Distributed	66
2.5.1.2	Coordination Strategies	67
2.5.1.2.1	Leader Follower	68
2.5.1.2.2	Consensus	70
2.5.1.2.3	Potential Field Approach	73
2.5.1.2.4	Virtual Structure/Body/Leader	76
2.5.1.2.5	Behavioral	77
2.5.1.2.6	Graph Based Coordination	77
2.5.2	Objectives of Cooperative Motion of Multiple AUVs	79
2.5.2.1	Formation Acquisition	79
2.5.2.2	Cooperative Path Following and Navigation	79
2.5.2.3	Cooperative Path Planning	79
2.5.2.4	Cooperative Target Following/ Target Tracking	79
2.5.2.5	Cooperative LOS/ Target Tracking	80
2.5.2.6	Region-based Tracking	80
2.5.2.7	Rendezvous	80
2.6	Remarks on Literature review Conducted	82
2.7	Scope of Use of N-PID like Controllers for AUV	85
2.8	Advantages of Directed Graph Based Coordination Strategy	88
2.9	Chapter Summary	94
<b>Chapter-3</b>	<b>Robust Set-Point Control of AUV using Nonlinear PID controller with Bounded Integral and Bounded Derivative</b>	
3.1	Introduction	97
3.2	Kinematics and Dynamics of an AUV	99

3.2.1	Kinematics of AUV	99
3.2.2	Dynamics of AUV	101
3.3	Problem Formulation	103
3.4	Properties of Dynamic Parameters of AUV	104
3.5	Mathematical Preliminaries	105
3.6	N-PID with BI and BD Control Law	107
3.7	Closed-Loop Set-Point Error Dynamics of AUV	109
3.8	Stability Analysis	110
3.9	Results and Discussion	117
3.9.1	Simulation Results with Analysis	119
3.9.1.1	PD (roughly tuned gains) on AUV dynamics with and without Uncertainties	119
3.9.1.2	PD (roughly tuned gains) on AUV dynamics with and without Uncertainties	122
3.9.1.3	PD (sufficiently tuned minimum gains) on AUV dynamics with uncertainties	125
3.9.1.4	N-PID with BI and BD and N-PID without BI and BD on AUV dynamics with uncertainties	127
3.10	Chapter Summary	133
<b>Chapter-4</b>	<b>Robust Tracking of AUV using Sliding Mode Nonlinear PID controller with Bounded Integral and Bounded Derivative</b>	
4.1	Introduction	137
4.2	Mathematical Preliminaries	139
4.3	Definition of Reference AUV	140
4.4	Problem Formulation	141
4.5	SM-N-PID Control Law with Bounded Integral and Bounded Derivative	142
4.6	Dynamics of AUV in Terms of Trajectory Tracking Error	145
4.7	Stability Analysis	146
4.8	Simulation Results and Discussion	161
4.8.1	Simulation Results with Analysis	166
4.8.1.1	PD plusFeedforward Compensation (roughly tuned gains) on AUV Dynamics without and with Uncertainties	166
4.8.1.2	PD plusFeedforward Compensation (sufficiently tuned gains) on AUV Dynamics Uncertainties	169
4.8.1.3	Tracking of sinusoidal path by application of SM- N-PID with BI and BD & SM-N-PID without BI and BD	173
4.9	Chapter Summary	177



<b>Chapter-5</b>	<b>Directed Graph Based Formation Control of Multiple Autonomous Point Agents and Extension to AUVs</b>	
5.1	Introduction	179
5.2	Background	180
5.3	Application of Graph Theory in Formation Control	182
5.3.1	Definitions associated with Rigid Graph	182
5.3.2	Definitions associated with Persistent Graph	183
5.3.3	Construction of cycle free minimally persistent (CFMP) graph	185
5.3.3.1	Henneberg construction (directed case) containing vertex addition	185
5.4	Problem Formulation	187
5.4.1	Agent Kinematics	189
5.4.2	Problem Statement	190
5.5	Development of Formation Control Strategy for the System of Point Agents	190
5.5.1	Development of Control Law for the Leader	192
5.5.2	Development of Control Law for the First Follower	193
5.5.3	Control Law for Ordinary Follower-1	196
5.5.4	Control Law for Ordinary Follower-2	198
5.6	Simulation Results and Discussions	202
5.6.1	Observations	204
5.7	CFMP Formationwith AUV Dynamics	210
5.8	Problem Formulation	211
5.8.1	Problem Statement	213
5.9	Development of Control Strategyof CFMP formation with AUV Dynamics	214
5.9.1	Trajectory Tracking and Development of Control Law of Global Leader	214
5.9.2	Trajectory Generation and Development of Control Lawfor Followers	216
5.9.2.1	Trajectory Generation and Development of Control Lawfor First Follower	216
5.9.2.2	Trajectory Generation and Development of Control Lawfor Ordinary Follower	219
5.10	Simulation Results and Observations	222
5.11	Chapter Summary	224

<b>Chapter-6</b>	<b>Directed Distance-Based Decentralized Robust Tracking Control of Formation of Multiple AUVs</b>	
6.1	Introduction	227
6.2	Preliminaries	228
6.2.1	Problem Description	228
6.2.2	Trajectory Generation and its boundedness and formulation of desired state	232
6.2.2.1	Trajectory generation and design of DSO	232
6.2.2.2	Boundedness of trajectories of followers corresponding to bounded trajectory of GB	241
6.2.2.3	Desired Steady State of system of AUVs	241
6.2.3	Problem statement	243
6.3	Notations and Definitions on Input to State Stability (ISS) and Cascaded System Stability	244
6.4	Controller Design	246
6.5	Closed Loop Dynamics of $k^{\text{th}}$ AUV in terms of Trajectory Tracking Error	248
6.6	Stability Analysis	249
6.7	Results and Discussion	268
6.8	Chapter Summary	271
<b>Chapter-7</b>	<b>Conclusions and Suggestions for Future Work</b>	
7.1	Overall Conclusions of the Thesis	273
7.2	Contributions of the Thesis	274
7.3	Suggestions for the Future Work	276
	Appendix	277
	References	283

# List of Symbols

$\Re$	The set of real numbers
$\Re^n$	The set of real $n$ vectors
$\Re^{m \times n}$	The set of real $m \times n$ matrices
$\ X\ $	Euclidean norm of a vector or a matrix $X$
$\in$	Belongs to
$<(\leq)$	Less than (Less than equal to)
$>(\geq)$	Greater than (Greater than equal to)
$\neq$	Not equal to
$\forall$	For all
$\rightarrow$	Tends to
$y \in [a, b]$	$a \leq y \leq b; y, a, b \in \Re$
$[0]$	A null matrix with appropriate dimension
$I$	An identity matrix with appropriate dimension
$X^T$	Transpose of matrix $X$
$X^{-1}$	Inverse of $X$
$\lambda(X)$	Eigenvalue of $X$
$\lambda_{max}(X)$	Maximum eigenvalue of $X$
$\lambda_{min}(X)$	Minimum eigenvalue of $X$
$\det(X)$	Determinant of matrix $X$ ,
$\text{diag}(x_1, x_2, \dots, x_n)$	A diagonal matrix with diagonal elements $x_1, x_2, \dots, x_n$



## List of Abbreviations

<b>Abbreviations</b>	<b>Description</b>
<b>AUV</b>	Autonomous Underwater Vehicle
<b>Deep Submergence Vehicle</b>	DSV
<b>ROV</b>	Remotely Operated Vehicle
<b>HROV</b>	Hybrid Remotely Operated Vehicle
<b>ODIN</b>	Omni-Directional Intelligent Navigator
<b>BAUV</b>	Biorobotic Autonomous Underwater Vehicle
<b>SMC</b>	Sliding Mode Control
<b>PD</b>	Proportional plus Derivative
<b>LPID</b>	Linear Proportional plus Integral plus Derivative Controller
<b>PI<sup>2</sup>D</b>	Proportional plus derivative with Double Integration ( $I^2$ ) action
<b>SP-D-NI</b>	Saturated Proportional plus Derivative plus Nonlinear Integral
<b>N-PID</b>	Nonlinear Proportional plus Integral plus Derivative Controller
<b>N-PID with BI and BD</b>	N-PID with Bounded Integral and Bounded Derivative
<b>PD plus FC</b>	PD plus Feedforward Compensation
<b>SM -N-PID with BI and BD</b>	Sliding Mode Nonlinear PID with BI and BD
<b>CFMP</b>	Cycle free Minimally Persistent Formation
<b>IRF</b>	Inertial Reference Frame
<b>BRF</b>	Body-Fixed Reference Frame
<b>CoM</b>	Centre of Mass
<b>CPDI</b>	Continuously Piecewise Differentiable Increasing
<b>RA</b>	Reference AUV
<b>SQP</b>	Sequential Quadratic Programming
<b>GB</b>	Global Leader
<b>FF</b>	First Follower
<b>OF</b>	Ordinary Follower
<b>DGT</b>	Dynamically Generated Trajectory
<b>DSO</b>	Desired State Observer
<b>ISS</b>	Input to State Stability



## List of Figures

Sl No.	Figure Name	Page No.
1.1	Manned Submersible Vehicle: JAGO, ALVIN , Pisces V	2
1.2(a)	Remotely Operated Vehicles: DSL-120A (USA), Hercules (USA)	3
1.2(b)	KAIKO ROV	4
1.3	Nereus: An HROV Woods Holes Oceanographic Institution (WHOI), USA 2009	5
1.4	ODIN AUV	6
1.5	REMUS AUV	6
1.6(a) and 1.6(b)	Prototype and mechanical configuration of autonomous robotic fish	8
1.7	BioroboticAUV (BAUV) developed by Naval Undersea Warfare Center (NUWC), Newport, RI	8
2.1	Evolution of Motion Control of AUV	21
2.2	Typical Navigation System of AUV	24
2.3(a)	Path following	24
2.3(b)	Path Tracking	24
2.4	Path tracking control of an AUV	25
2.5	Path following control of an AUV	26
2.6	Set point control	27
2.7	Way-point guidance based tracking of a part of a sinusoidal path	28
2.8	Dynamic moving region in region based tracking control	29
2.9	Difference between deliberative and reactive control architectures for AUVs	30
2.10	Behaviour-Based Controller	48
2.11	A general framework of cooperative motion control of multiple AUVs	61
2.12	A typical centralized cooperative motion control scheme for multi-AUV system	63
2.13(a)	Decentralized Control with one to one unidirectional communication	64

2.13(b)	Decentralized Control with two to one unidirectional communication	64
2.14	A typical combination of centralized and decentralized cooperative scheme of Multi-AUV system	65
2.15(a)	Distributed Control with one to one bidirectional communication	67
2.15(b)	Distributed Control with manyto one bidirectional communication	67
2.16	Control scheme based on a decentralized leader-follower approach	69
2.17	Basic building blocks of control scheme based on consensus coordination for a group of AUVs.	71
2.18(a)	Potential function between $j$ th and $k$ th AUV	74
2.18(b)	Potential function between $k$ th AUV and $m$ th virtual Body	74
2.19	Potential field based coordination between two AUVs	74
2.20	Controller structure system of an AUV in potential field based coordination	76
2.21	Cooperative path following of three AUVs	80
2.22	Cooperative target following of three AUVs	81
2.23	Cooperative Line of Sight (LOS) target tracking of two AUVs	81
2.24	Rendezvous of four AUVs	82
3.1	Kinematic Description of AUV	100
3.2	Element $f_i(x_i)$ of function vectors $f(x)$	106
3.3	Controller structure for set-point control of AUV using N-PID with BI and BD	109
3.4	Position errors vs. time (PD with and without uncertainties)	120
3.5	Error in orientation vs. time (PD with and without uncertainties)	120
3.6	Errors in linear velocities vs. time (PD with and without uncertainties)	121
3.7	Error in angular velocity vs. time (PD with and without uncertainties)	121
3.8	Control forces vs. time (PD with and without uncertainties)	121
3.9	Control torque vs. time (PD with and without uncertainties)	122
3.10	Position errors vs. time (PD with large P & D)	123



3.11	Error in orientation vs. time (PD with large P & D)	123
3.12	Errors in linear velocities vs. time (PD with large P & D)	123
3.13	Error in angular velocity vs. time (PD with large P & D)	124
3.14	Control forces vs. time (PD with and without uncertainties)	124
3.15	Control torque vs. time (PD with large P & D)	124
3.16	Position errors (suff. tuned gains) vs. time	125
3.17	Error in orientation (suff. tuned gains) vs. time	125
3.18	Errors in linear velocities (suff. tuned gains) vs. time	126
3.19	Error in angular velocity (suff. tuned gains) vs. time	126
3.20	Control forces (suff. tuned gains) vs. time	126
3.21	Control torque (suff. tuned gains) vs. time	127
3.22	Position errors vs. time (N-PID with BI and BD & N-PID without BI and BD)	129
3.23	Orientation error vs. time (N-PID with BI and BD & N-PID without BI and BD)	130
3.24	Error in angular velocity error vs. time (N-PID with BI and BD & N-PID without BI and BD)	130
3.25	Errors in linear velocities vs. time (N-PID with BI and BD & N-PID without BI and BD)	130
3.26	Control forces vs. time (N-PID with BI and BD & N-PID without BI and BD)	131
3.27	Control torque vs. time (N-PID with BI and BD & N-PID without BI and BD)	131
3.28	Saturation of actuator w.r.t. control force	135
3.29	Saturation of actuator w.r.t. control torque	135
3.30	Set-Point Control of Autonomous Underwater Vehicle using N-PID with BI Control Strategy	136
4.1	Motion of an AUV on a planar path	139
4.2	Tracking controller structure of AUV using SM-N-PID with BI and	144

## BD

4.3	Position errors vs. time (PD plus FC with and without uncertainties)	167
4.4	Orientation error vs. time (PD plus FC with and without uncertainties)	167
4.5	Errors in linear velocities vs. time (PD plus FC with and without uncertainties)	167
4.6	Error in angular velocity vs. time (PD plus FC with and without uncertainties)	168
4.7	Control forces vs. time (PD plus FC with and without uncertainties)	168
4.8	Control torque vs. time (PD plus FC with and without uncertainties)	168
4.9	Position errors vs. time (PD plus FC sufficiently tuned)	170
4.10	Orientation error vs. time (PD plus FC sufficiently tuned)	170
4.11	Errors in linear velocities vs. time (PD plus FC sufficiently tuned)	170
4.12	Error in angular velocity vs. time (PD plus FC sufficiently tuned)	171
4.13	Control forces vs. time (PD plus FC sufficiently tuned)	171
4.14	Control torque vs. time (PD plus FC sufficiently tuned)	172
4.15	Position errors vs. time (SM-N-PID with BI and BD & SM-N-PID without BI and BD)	173
4.16	Orientation error vs. time (SM-N-PID with BI and BD & SM-N-PID without BI and BD)	173
4.17	Errors in linear velocities vs. error time (SM-N-PID with BI and BD & SM-N-PID without BI and BD)	174
4.18	Linear in angular velocity vs. time (SM-N-PID with BI and BD & SM-N-PID without BI and BD)	174
4.19	Control forces (N) vs. time (SM-N-PID with BI and BD & SM-N-PID without BI and BD)	174
4.20	Control torque (N-m) vs. time (SM-N-PID with BI and BD & SM-N-PID without BI and BD)	175
4.21	Tracking of sinusoidal trajectory by an AUV on the application of SM-N-PID controller with BI and BD	177
5.1	Henneberg construction for making leader-follower type formation	186

	from four agents	
5.2	Quadrilateral formation of four point agents with leader-follower structure	188
5.3	Motion of leader and first follower for a very small duration of time	196
5.4	Motion of leader, first follower and ordinary follower-1 for a very small duration of time	199
5.5	Straight line motion of formation of four agents with leader-follower structure	205
5.6	Motion of formation of four agents with leader-follower structure with circular path tracked by leader	206
5.7	Motion of quadrilateral formation of leader-follower structure corresponding to sinusoidal path tracking of leader	207
5.8	Plot of $d_1, d_2, d_3, d_4$ and $d_5$ vs. time corresponding to straight line trajectory tracking of leader	209
5.9	Plot of $d_1, d_2, d_3, d_4$ and $d_5$ vs. time corresponding to circular trajectory tracking of leader	209
5.10	Plot of $d_1, d_2, d_3, d_4$ and $d_5$ vs. time corresponding to sinusoidal trajectory tracking of leader	210
5.11	Triangular formation of three AUVs with leader-follower structure	212
5.12	Motion of Leader and First Follower for a very small duration of time ( $dt$ )	215
5.13	Controller Structure for Global Leader	216
5.14	Controller Structure of $k$ th. AUV	218
5.15	Locus of leader, first follower and ordinary follower for straight line trajectory tracking of leader	223
5.16	Motion of different AUVs for first six instants of time	223
5.17	Plots of distances among three AUVs during formation tracking	224
6.1	Cycle free minimally persistent formation of a group of AUVs	229
6.2(a)	Motion of FF and GB	238

6.2(b)	Motion of FF and GB	238
6.3	Motion of three followers in a triangular subgroup of CFMP formation	239
6.4	Cascaded system of GB and FF	250
6.5	Cascaded system of GB and FF and OF	250
6.6	Distance errors among AUVs vs. time	269
6.7	Error in orientations among AUVs vs. time	270
6.8	Orientation error of leader vs. time	270
6.9	Error in angular velocity vs. time	270
6.10	Error in linear velocities of leader vs. time Tracking of	271
6.11	Tracking of sinusoidal path by global leader and corresponding generated trajectory tracking of first follower , ordinary follower-1 in a CFMP formation	271

# List of Tables

Sl No	Description	Page No
3.1	Force and torque limits [24] of actuator	118
3.2	Information about initial and final state	119
3.3	Values of gains of different controllers	127
3.4	Values of parameters of nonlinear functions for different controllers	129
3.5	Observations from the simulation of application of different set point controllers on AUV dynamics	132
3.6	List of parameters of AUV [24] and $\pm 10\%$ variation in their nominal values	134
4.1	Force and torque limits [24] of actuator	162
4.2	Information about initial state and error	163
4.3	Velocity and acceleration limits [24] of actuator	163
4.4	Values of parameters of nonlinear functions of SM-N-PID with BI and BD & SM-N-PID without BI and BD	164
4.5	Values of gains of different controllers	165
4.6	Observations from the simulation of application of different tracking controllers on AUV dynamics.	176
5.1	Instantaneous and desired distance constraints among different agents	188
5.2	Formation specifications, size of simulations steps, simulation environment	202
5.3	Initial position of agents and information about leader trajectories	203
5.4	Observations of distances from simulation for motion control of quadrilateral formation during the period of $t=0$ s to $t=0.08$ s	208
5.5	Formation specifications, size of simulation steps, initial position state, trajectory information of leader	222
6.1	Information about initial state and initial error in state of global leader	268
6.2	Information about desired distances and initial errors in distances	268

6.3	Table 6.3 Values of parameters of controllers for different controllers	269
A.6.1	The value of second derivative of $F_1$ correspond to $\sin \theta$ and $\cos \theta$	280







# **Chapter 1**

## **Introduction**

Ocean is the main resource of the energy and chemical balance that sustain mankind whose future is very much dependent on the living and nonliving resources in the oceans. Oceans' activities are also critically relevant to climate changes. Therefore, various studies are conducted for ocean exploration and intervention. Autonomous Underwater Vehicles (AUVs) have been a popular and effective means for ocean exploration and intervention as they make it possible to go far beneath the ocean surface, collect first-hand information about how the oceans work, and furthermore perform intervention tasks.

### **1.1 Evolution of Underwater Vehicles**

AUV is an underwater robotic device which can drive through the underwater propulsion system without any human intervention. Thus, it is self-piloted and uses the feedback received from the surrounding in order to determine its actions and movement during operation. Studies on Unmanned Underwater Vehicles (UUVs) have increased especially in the last two-three decades. Many examples of Remotely Operated Vehicles (ROVs) and AUVs were developed and used successfully for various applications. Four types of underwater vehicles reported in literature [2],[4],[7],[9] such as manned submersible vehicles, remotely operated vehicles (ROV), hybrid ROV and AUV.

### ***1.1.1 Manned Submersible Vehicles***

Underwater vehicles can carry out complicated tasks because of human intelligence. However, they have short endurance due to human physical and psychological limitations, and are expensive to operate because of the effort needed to ensure human safety. There are two categories under the manned underwater vehicles namely large sized submarines and small sized submarines. First one is operated by a crew which can reside on it for long periods. This category belongs to military submarines. The second one is intended for deeper exploration. JAGO (2006) of Germany at Leibniz Institute of Marine Sciences (IFM-GEOMAR) (2006), ALVIN (1998) of USA Navy at the Woods Hole Oceanographic Institute and Pisces V, deep-submergence vehicle(DSV) at the NOAA Hawaii's Undersea Research Laboratory(1973) are examples of manned submersible vehicles. These vehicles can make direct observations of the deep seas. Manned submersibles cannot stay underwater for long duration; however, crew safety is always an important consideration.

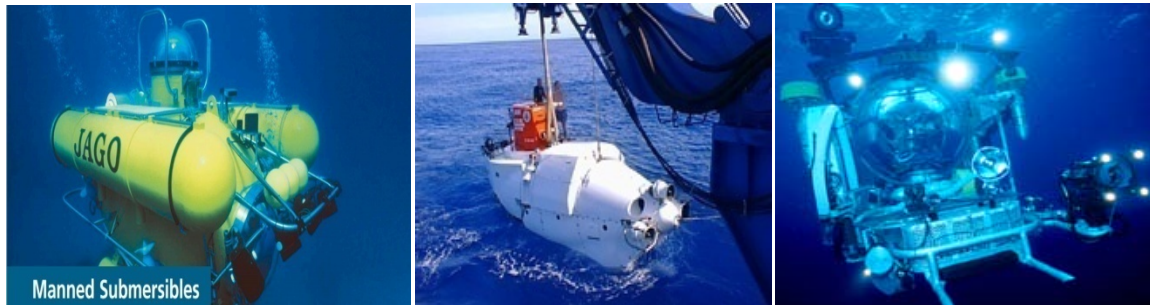


Fig. 1.1(a) Manned Submersible Vehicle: JAGO [1], ALVIN [2], Pisces V [3]

### ***1.1.2 Remotely Operated Vehicles (ROV)***

These [4],[5],[6],[13] are unmanned, tethered vehicles with adjacent cables to transfer power, sensor data and control commands between the operators on the surface and the ROV. These are usually launched from surface ships. They can also carry out complicated tasks via tele-operation

by human pilots on the surface ships. Even though their operations are often limited by operator fatigue, they are free from the safety concern of on-board human operators and have almost unlimited endurance in the ocean, compared to manned submersibles and transmit data constantly. ROVs often bristle with manipulator arms, cameras, lights and sensors to "see" and "feel" for their operators. Fig. 1.2(a) and 1.2(b) show different ROVs. However, the dragging force on the tether, time delay, and operator fatigue make ROV difficult to operate and the daily operating cost is still very expensive. KAIKO from the Japanese Marine–Earth Science and Technology Center (JAMSTEC) was the most advanced ROV ever operated at an 11000-m depth. Unfortunately, KAIKO was lost during the operation in 2003 as the tether was snapped due to bad weather.

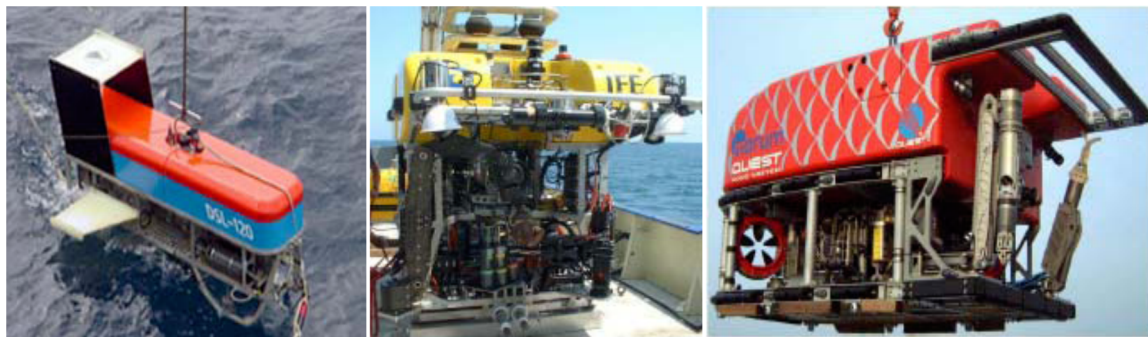


Fig. 1.2(a) Remotely Operated Vehicles: DSL-120A (USA) [4], Hercules (USA) [5], and MARUM (Germany) [6]

Canada (Vancouver) based advanced ROV is Seamor ROV[13]. These vehicles are light weight and can be easily deployed, retrieved and transported.

### ***1.1.3 Hybrid ROV (HROV)***

Hybrid ROV can operate untethered, when near the surface, in order to explore large areas. To descend to great depths, however, it is tethered with a thin optical fiber cable, operated by pilots aboard the ship. This enables it to make deep dives while being highly maneuverable. An HROV has been reported in [4].

#### ***1.1.4 Autonomous Underwater Vehicles (AUVs):***

With advances in automation technology, and ability to create smarter robots, more explorations are being conducted by autonomous vehicles. In underwater application this fact allows for accessing to higher risk areas, longer time underwater, and more efficient exploration as compared to human occupied/tethered underwater vehicles.

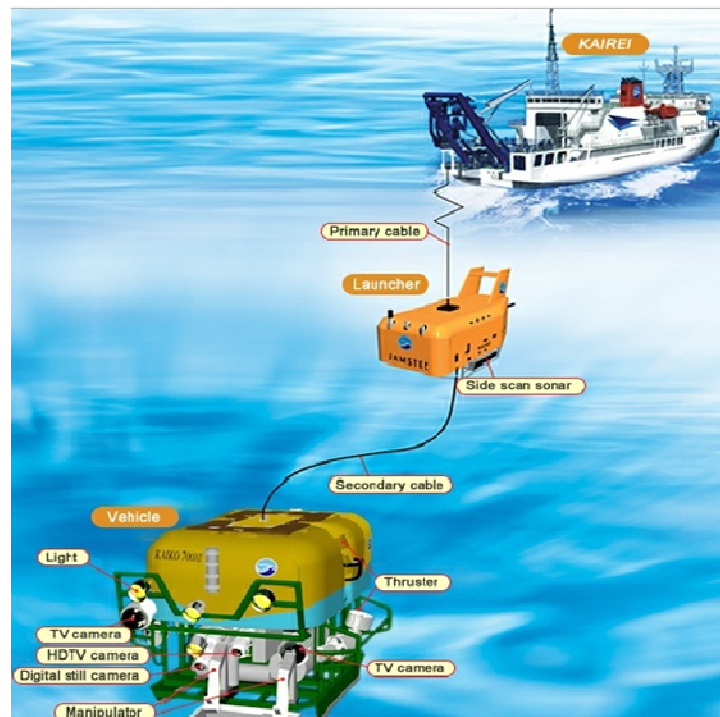


Fig. 1.2(b) KAIKO ROV [7]

These vehicles are designed to be agile, versatile and robust. Autonomy of a vehicle adds to its versatility. Therefore, for the last 25 years much research has been directed into designing AUVs that perform a multitude of tasks far surpassing the abilities of human divers and small human-driven submarines. Tasks range from long term gathering of ocean samples to 3-D mapping of underwater caverns and never before seen areas. Also, these vehicles can dive deeper and remain at depth longer without risking human lives.

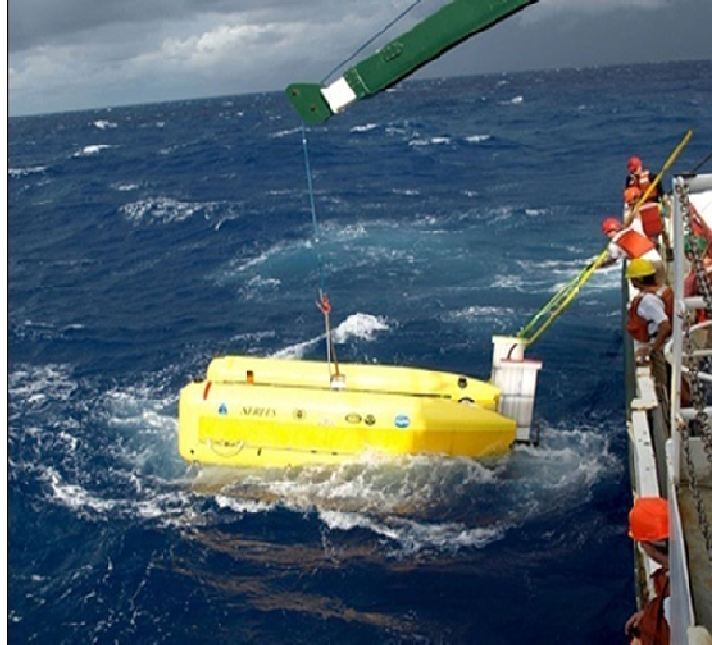


Fig 1.3 Nereus: An HROV Woods Holes Oceanographic Institution (WHOI), USA 2009[4]

AUVs are therefore unmanned, tether-free, powered by onboard energy sources e.g. batteries fuel cells, equipped with various navigation sensors such as inertial measurement unit (IMU), sonar sensor, laser ranger, and pressure sensor, and controlled by onboard computers for given missions. AUVs are free-swimming marine robots that require little or no human intervention. These are more mobile and could have much wider reachable scope than ROV. On-board power and intelligence could help AUV self-react properly to changes in the system and its environment, avoiding any disastrous situation like the KAIKO case. With the continuous advance in control, navigation, artificial intelligence, material science, computer, sensor, and communication, AUVs have become a very attractive platform in exploring the oceans.

According to operating mechanism there are three types of AUVs namely traditional propeller-driven AUV, biorobtic AUV and AUV gliders are reported in literature[9],[11],[18] so far.

## ***Propeller Driven AUV***

These AUVs rely on propulsion technique for their motion. A propeller, type of fan, is driven by brushed/brushless motor. Mechanical power generated from motor provides rotational motion to propeller by suitable power transmitter arrangement. Due to this rotational motion a pressure difference is produced between the forward and rear surfaces of the airfoil-shaped blade of fan and water is accelerated behind the blade. Consequently, a thrust is acted on AUV and it goes under motion. Propeller dynamics may be explained by both Bernoulli's Principle and Newton's Third Law. Conventional propeller used for marine AUV is termed as a screw propeller or screw. Propeller-driven AUVs come in a variety of shapes and sizes, and are built for a wide range of purposes. Numerous AUV prototypes have been proposed in different Universities/Institutes/research organizations in USA. ODIN [88] in Fig.1.4, REMUS [9] in Fig.1.5, ODYSSEY [10] are most popular among them. Scientists at California Polytechnic State University use a REMUS (Remote Environmental Monitoring Units) AUV, developed by WHOI and Hydroid, Inc., shown in Fig.1.5, to monitor and map toxic blooms of *Karenia Brevis* on the west Florida coast.

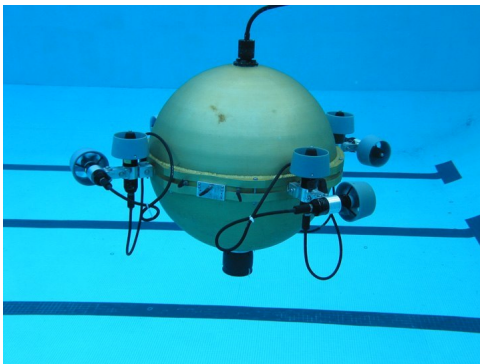


Fig. 1.4 ODIN AUV [88]



Fig. 1.5 REMUS AUV [9]

## ***Biorobotic Autonomous Undersea Vehicles***

These underwater robot work on bionic propulsion mechanism [15], concept borrowed from biological mechanism of nature. Small size, good maneuverability, direct operation on fin are several advantages of these vehicles. Although several advantages are there, biorobotic AUV are still active research.

The research in bio-robotic undersea vehicles [11],[17] has been greatly benefitted and inspired from the significant advances in three disciplines, namely the biology-inspired high-lift unsteady hydrodynamics,artificial muscle technology and neuroscience-based control. Several bio-robotic AUVs are reported in literature as follows.

*Dolphin Biosonar and Biorobotic AUV:* Mine detection is an important function of AUVs. U.S. Navy Marine Mammal Systems sets a false alarm in detection system in which levels achieved by dolphin biosonar [14] plays a significant role to reduce the dependence on human diver.

*Robotic Fish AUV:* Compared with propeller-driven engineering underwater vehicles, fish in nature have been evolving their aquatic locomotion abilities for millions of thousands of years, achieving superb swimming performances and surpassing man-made underwater vehicles in many respects, such as high propulsive efficiency, great agility, low noise, station-keeping ability, and acceleration. Taking advantage of recent progress in robotics, control technology, artificial intelligence, and hydrodynamics of fishlike swimming, new materials, sensors, and actuators, emerging research has focused on developing novel fish like vehicles, aiming to incorporate biological principles into engineering practice. First fish-like robot, RoboTuna, was developed by Triantafyllou [4] in 1994. The robotic fish [16] is composed of several elements: a



rigid main body, a tail fin, and two pectoral fins. Prototype and mechanical configuration of an autonomous robotic fish is shown in Fig.1.6.

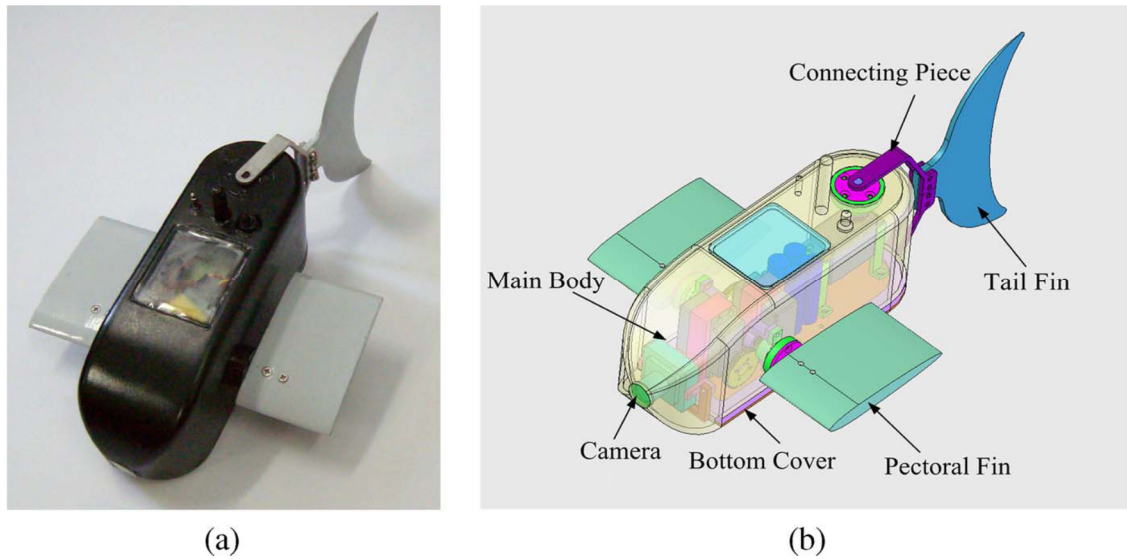


Fig 1.6(a) and (b) Prototype and mechanical configuration of autonomous robotic fish [16]

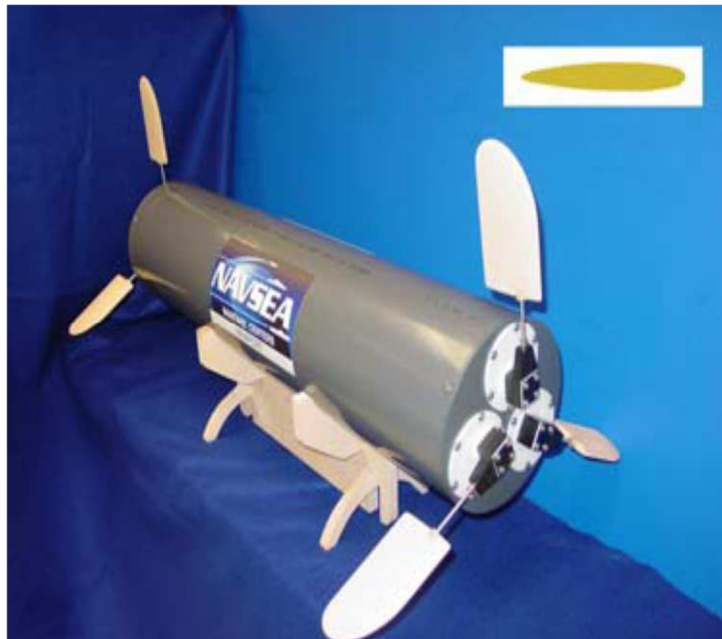


Fig 1.7 Biorobotic AUV (BAUV) developed by Naval Undersea Warfare Center (NUWC), Newport, RI [17]



Hydrodynamic maneuverability data of the flat fish type AUV, “MARIUS” is presented in [17]. “MARIUS” was developed under the EC MAST Programme as a vehicle for seabed inspection and environmental surveys in coastal water.

The rigid cylindrical hull [14] of the vehicle is attached with six strategically located fins to produce forces and moments in all orthogonal directions and axes with minimal redundancy. The fins are penguin-wing inspired and they implement the unsteady high-lift principle found widely in swimming and flying animals.

### ***Underwater Gliders***

They are battery-driven. They do not directly propel themselves but they work on induced propelling. By varying their buoyancy and trim, they repeatedly sink and ascend their wings and consequently utilize this up and down motion to convert to forward motion. Due to their low speed and use of low power electronics in them, the required energy for cycle trim states is far less than for conventional AUVs, and gliders have endurances of several months. The Slocum Glider [18] was used in 2008 in the Eastern Atlantic Ocean by a group of scientists and engineers of National Oceanography Centre, Southampton, England in collaboration with the Canary Institute of Marine Science, Canary Islands, Spain, with the objective of determining the relation between the different phenomena in oceans and climate change.

## ***1.2 Motivation behind the Research in AUV/Necessity of AUV/Application of AUV***

### **1.2.1 Mission**

The different emerging fields of applications/missions motivated to do AUV research. Basically missions are performed by AUV is categorized as survey mission and intervention mission. The

survey mission requires an energy efficient vehicle to cruise and follow designated way points whilst taking relevant oceanographic data. The intervention mission requires a vehicle capable of slow speed and even station keeping with thrusters and servo control to objects using vision, sonar, tactile sensors, or combinations thereof. Examples of survey vehicles include the ODYSSEY and the Ocean Voyager-II [20].

### **1.2.2 Application of AUVs**

AUVs are now routinely employed in a wide range of civilian and military mission/ applications as follows.

*Commercial Needs:* AUVs are used for different commercial needs such as tactical oceanography, communications through undersea environment, navigation in ocean water, continuous monitoring of coral-reef eco-system in shallow marine environment, under water pipeline inspection in oil and gas industry.

*Military Applications:* Several military applications in navy also depend on use of AUVs like anti-submarine warfare, surveillance in ocean, mine countermeasures /intelligence gathering in ocean, to obtain minefield reconnaissance data reconnaissance.

*Underwater Maintenance:* Different complicated underwater maintenance work like maintenance at oil platform in underwater oil mines, for underwater fiber optic communications line, under water construction using manipulators, under water repairing work.

*Environmental Monitoring:* AUVs are being used for recording salinity, oxygen content, temperature of water, forecasting of marine weather, monitoring of seismic phenomenon.

*Scientific Needs:* Almost eighty percent of this earth is full of ocean water. Still it is unknown. Therefore, planet exploration, to study dynamic behavior of ocean, to investigate the causes of

global warming, searching for mineral deposited zone in ocean, to detect hazardous substances in the ocean such as chemicals from an underwater vent or toxic algae such as red tide, to detect chemical, biological and radioactive threat, to study the ocean ecosystem, to investigate geological status of ocean, to explore the planet other than earth. *Exploration of Ocean Underwater*: Deep space or undersea exploration for oil and gas deposit, mapping bathymetry around an oil well head.

*Long Distance Long Duration Oceanographic Sampling Mission*: AUV has been used for oceanographic surveys such as the survey of sea bottom earthquake area and the research of global warming phenomena. Japan Agency for Marine-Earth Science and Technology (JAMSTEC) has developed a deep and *long-distance cruising* (high-speed) AUV (Autonomous Underwater Vehicle) “URASHIMA” in 2000.

*Detect and Localize Pollutant Sources*: AUV has also detected and localized pollutant sources. As an example, REMUS AUV was used [11] for the same purpose.

*Ocean Floor Mapping*: AUVs are also applied for collection of scientific and geographical data from ocean floor.

*Pipeline Inspection*: Small AUVs are used for inspection of inside wall of pipe in power plant or outside wall of pipelines in oil field.

### **1.3 Advantages of Multi-AUV System**

The concept of multiple Autonomous Underwater Vehicles (AUVs) cooperatively performing a mission offers several advantages over single heavily equipped vehicle working in a non-cooperative manner such as *Reliability*: In a cooperative application scenario, each vehicle may

only need to carry a single sensor (per environmental variable of interest) allowing each of the vehicles in the formation group less complex, thus increasing their reliability.

➤ *Increased work efficiency:* Through cooperation, AUV fleet could work together on tasks, coordinating, negotiating, and distributing the workload. Therefore, performance of a group is better than that of a single AUV. As an example, single vehicle needs to wander significantly to collect data over a large spatial domain in ocean.

➤ *Mission time:* Use of multiple AUVs increases the data collection rate for particular mission in a given area and therefore reduces mission time.

➤ *Complex Mission:* Relatively simple AUVs comparing to single heavily equipped AUV composed of many interconnected parts, can collectively perform complex tasks like minesweeping etc. which is quite impossible for the heavily equipped single vehicle.

➤ *Reconfigurability:* Team of AUVs has capability of reconfiguring its formation network. For example, if a vehicle is lost during minesweeping, the other vehicles could quickly change formation to cover the lost vehicle's area. Group can also reconfigure itself in response to environmental parameters in order to increase performance of mission and optimize the strategies for detection and measurement of vector or scalar fields and features of particular interest.

➤ *Robustness:* Desired task can not be finished by a single AUV system on the event of failure of its system, but group of multiple AUVs can complete the task even if few of them under their systems' failure. Therefore, for a particular task the system of single AUV suffers from lack of robustness.

- *Mutual support and protection*: In some cases, using formation flying, mutual support is obtained among multiple robotic vehicles in military application. Generally, leader robotic vehicle escorts the enemy, whereas other vehicles are engaged in protection and support of it.
- *Control strategy*: An AUV in group may need to adopt a simplified control strategy for performing a particular goal
- *Bandwidth availability*: The ability to exchange data at close proximity of number of AUVs can help to mitigate the low bandwidth availability of the underwater communications channel.

## **1.4 Challenges in AUV Research**

### ***1.4.1 The Control Issues and Autonomy***

The control issue of underwater vehicles is very challenging due to the following

- *Disturbances*: The nonlinear, time variance, unpredictable external disturbances, such as the sea current fluctuation against the motion of AUVs.
- *Dynamics*: Dynamics of AUV is inherently complex, nonlinear and time variant such that it can not be simply ignored or drastically simplified for control design. Also its mass and buoyancy change according to different working conditions.
- *Parametric uncertainties*: the difficulty in accurately modeling the hydrodynamic effect, Coriolis force is the important hindrance against providing autonomy to AUV.
- *Actuator saturation*: Actuators of AUV have finite torque generating capability. During operation of AUV, torque demand may become higher than AUV's torque limit. Hence, saturation of actuators is unavoidable. This indicates actuator saturation is an important problem in motion control of AUV.

- *Linear controller:* Conventional linear controllers may fail in satisfying performance requirements, especially when changes in the system and environment occur during the operation since it is almost impossible to manually retune the control parameters in water as linear controller works locally.
- *Formation Control:* In spite significant progress in the area of formation control, much works remains to be done to develop strategies capable of yielding robust performance of a fleet of vehicles in presence of complex vehicle dynamics, unmeasured vehicle states, severe communication constraints, and partial vehicle failure. These difficulties are specially challenging in the field of marine robotics for two main reasons: first one is the dynamics of marine vehicles are often complex and can not be simply ignored or drastically simplified for control design purposes, and second one is controller may depend on states that are not measured.
- *Communication:* Control of AUVs poses a difficult problem because traditional methods of communication and navigation, i.e. radio and GPS, are not effective due properties of seawater.
- *Underactuation:* AUVs present a challenging control problem since most of them are underactuated, i.e., they have fewer actuated inputs than degrees of freedom (DOF), imposing nonintegrable acceleration constraints.

#### **1.4.2 Communication**

Communication is the most important process in underwater technology. The process enables the data transfer between two or more groups/entities. These data are used for navigation, tactical strategies, monitoring, identification, etc. Two kinds of communication methods are used, wired and wireless. Recent trend is to use wireless communication.

Underwater wireless communication is not a straight forward process. Communication suffers from several problems like channel model of water, attenuation, transmission distance, power consumption, SNR ratio, bit error, symbol interference, error coding, modulation strategies, instrumentation and underwater interferences. It is very complicated task to deal with interferences under water due to dynamic behavior of water. Three major factors cause interferences are mentioned below

*Characterstics of signal carrier:* Most commonly used carrier waves are electromagnetic wave, optical wave and acoustic wave. Communication using electromagnetic wave has advantages of high frequency and bandwidth. Drawback is high absorption/attenuation that has adverse effect on transmitted signal. Requirement of big antenna is another drawback which affects directly the design complexity and cost of communication system.

Optical wave communication offers high rate data transmission. Drawbacks of this system are high rate absorption in water and scattering effect which affects data transmission accuracy. Acoustic communication has low absorption characteristic for underwater communication. Although having large data transmission time (delays in the range of seconds) compared to other carrier signal, low absorption characteristics enables the carrier to travel at longer range. The other drawbacks of underwater acoustic communication and positioning are limited communication bandwidth, data latency (feedback controller needs to compute control signal using less recent data at ocean surface), intermittent failures (lack of underwater communication restricted coordinating feedback to occur only while gliders were on the surface) [19] and multipath effects, near and far problem. The near and far problem occurs when an acoustic unit may not transmit and receive at same time because of local transmit power levels.

*Environment/propagation medium:* Water itself has become the main source of interference. The type of water (fresh water/sea water), depth, pressure, dissolved impurities, water composition and temperature affect the sound propagation. Common terrestrial phenomena like scattering, reflection, refraction also occurs underwater communication.

*Instrumentation system devices:* In ensuring effective underwater communication, the design of communication system plays a vital role. Factors such as transducer parameters (sensitivity, power consumption, noise immunity, transduction mechanism, directivity, resolution and properly matched impedance must be taken into account during the design process. In the present days, MEMS technology has several advantages to overcome sensor related problems. Communication requirements, especially regarding bandwidth limits, are often challenging obstacles to control system design of formation of AUVs.

## **1.5 Motivations of the Thesis**

Applications of Underwater Vehicles and challenges associated in control design of these vehicles motivate to undertake research on AUV. More specifically the applications and control challenges are as follows.

- AUVs find applications in defense, inspection of pipelines, mine counter measures and weather forecasting etc. Therefore AUV research is a motivating topic.
- AUV system dynamics is highly nonlinear and uncertain, for example, the hydrodynamics effects lead to uncertainty in the dynamics. From the viewpoint of development of control algorithms, the challenges to handle these kinds of complexities are major issues.



- Control of AUV is challenging due to the constraints in acoustic medium that hinders sensors signals necessary for control law generation.
- Deployment of a number of AUVs for performing a large mission necessitates design of co-operative control algorithms which involve coordination of participating AUV, heavy computational burden and constrained communication.

## 1.6 Objectives of this Research Work

(i) As parametric uncertainties lie in the dynamics of AUV are obvious, this thesis explores opportunities to develop a robust set-point control algorithm of a single AUV.

(ii) After having developed a robust set-point controller for an AUV, the thesis then intends to develop a robust tracking control algorithm.

(iii) Recognising the fact that cooperative control is essential for a number of oceanographic applications and challenges involved in designing the controllers this thesis intends to propose a coordination control scheme of multiple autonomous point agents participating in a minimally persistent formation.

(iv) To propose a set of decentralized control laws for point agents in the formation control and to extend the coordination control formulation for multiple point agents to multiple AUVs.

(v) To design a trajectory tracking control strategy for cooperative control of AUVs in a minimally persistent formation.

## 1.7 Organization of the Thesis

This thesis consists of seven chapters organised as follows.

**Chapter-1** describes briefly about the introduction, objectives and scopes of this thesis on AUV research. It briefly discusses different challenging issues on control, and motivation of pursuing research on control of AUVs.

**Chapter-2** reviews the reported control architecture and different control algorithms for set-point control, trajectory tracking etc. for single AUV. It also provides review on different control algorithms together with the implementation aspects for cooperative motion control of multiple AUVs. The chapter concludes with remarks on literature review pursued.

**Chapter-3** proposes development of a globally stable robust set point control algorithm for an AUV such that it would work effectively against parametric uncertainties and takes care of actuator saturation. The above controller is nonlinear PID (N-PID) with bounded integral (BI) and bounded derivative (BD). Performance of this control algorithm has been compared with that of a basic PID like controller i.e. PD and N-PID controller without BI and BD.

**Chapter-4** proposes a globally stable robust tracking control scheme exploiting ideas from both continuous time Sliding Mode Control (SMC) and nonlinear (N) PID control with BI and BD. Thus proposed controller is named as SM-N-PID with BI and BD. The proposed controller works successfully against parametric uncertainties and actuator saturation. Performance of the proposed algorithm has been compared with that of basic PID like tracking controller i.e. PD plus Feed Forward Compensation (PD plus FC) and SM-N-PID controller without BI and BD.

**Chapter-5** describes the concept of minimally persistence property of a directed graph. Two different methods namely Sequential Quadratic Programming (SQP) based optimization and

simple concept of geometry is proposed for providing coordination scheme for multiple non-holonomic point agents in a cycle free minimally persistent (CFMP) formation. Subsequently, it is shown how a set of decentralized control laws can be developed for this type of coordination considering four point agents in a quadrilateral formation. The proposed control strategy has been extended to CFMP formation of multiple AUVs.

**Chapter 6** extends the work described in chapter 5 and introduces the concept of tracking control of CFMP formation of multiple AUV for time-critical mission which is different from a non-time critical mission that has been developed in chapter 5. The Sliding Mode N-PID with BI and BD controller is applied to each AUV. Entire formation is formulated as the combination of several cascaded sub-systems. Stable motion of each AUV in the formation is analyzed in the framework of input-to-state stability while global leader tracks a predefined path.

**Chapter-7** presents the general conclusion of work described in this thesis. Further, suggestions for future work as an extension of the present work pursued in this thesis are provided. The chapter concludes with a list of contributions made in the thesis.



# Chapter-2

## Literature Review on Control Strategies of AUVs

### 2.1 Introduction

This chapter reviews the different control objectives and algorithms reported in literature of motion control for both a single and multiple AUVs. All the available techniques applied to AUVs can be categorized into three broad categories such as motion control, mission control and formation/cooperative motion control. Evolution of these control strategies is described in Fig. 2.1.

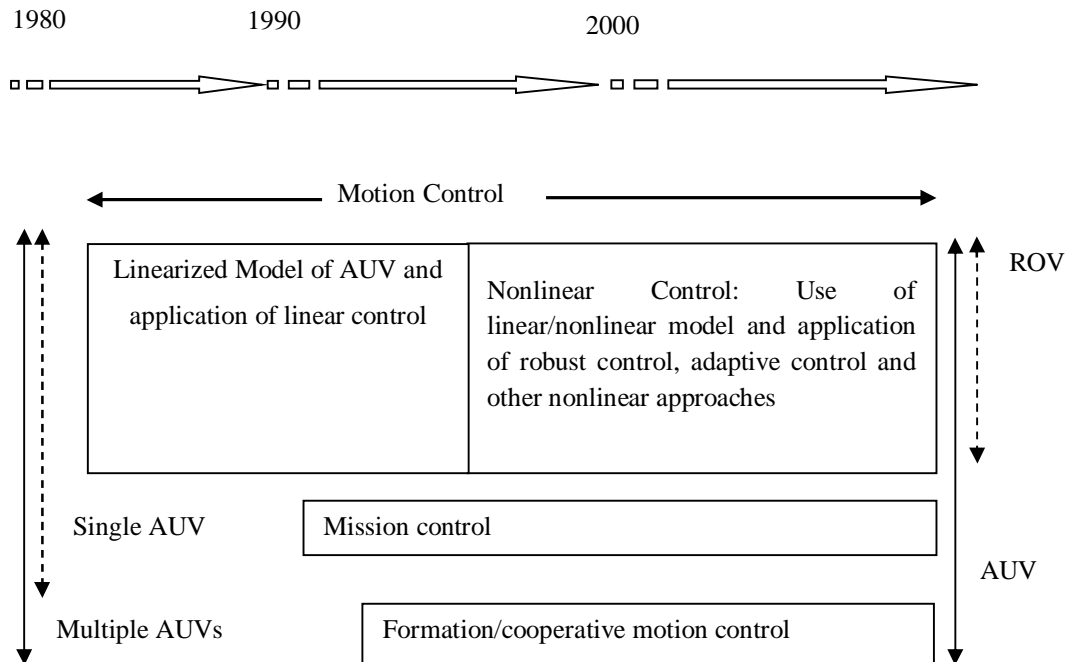


Fig. 2.1 Evolution of Motion Control of AUV

Motion control focuses on subjects such as the platform response to an input and stability of a remotely operated/autonomous underwater vehicle. Mission control focuses on the execution of

the behavioral modeling of an autonomous underwater platform, where this behavior is redefined parametrically. Formation control focuses on coordinated behavior of multiple AUVs (i.e. swarms, platoons, flocks). Categorically different motion planning strategies, control architectures and control algorithms to implement those strategies for single and multiple AUVs are discussed in this chapter.

## **2.2 Motion Control Objectives of an AUV**

Each mission has its own control objectives. To meet those control objectives a proper planning of motion of an AUV is needed. A number of such motion planning strategies are reported in literature which are described in the following subsections.

### **2.2.1 Navigation**

Navigation considers the movement of an AUV in a either a structured or unstructured (with obstacles) water environment without intervention of a human operator. During navigation, the AUV (frequently called inspection AUV) continuously localizes itself and plans its path based on estimation process with the help of onboard sensors and then sends information (as a feedback) to control room.

Navigation may be of two types such as, *cruising* and *maneuvering*. Cruising refers to high speed deep and long range sea navigation, whereas maneuvering refers to slow speed navigation. Currently used techniques [21] for position estimation process for AUV are Kalman filter, Particle filter, Simultaneous Localization and Mapping (SLAM) and Concurrent Mapping and Localization (CML) algorithms. The methods [21] of AUV navigation are categorized as inertial, acoustic, and geophysical. In inertial navigation, gyroscopic sensors (INS) are used to detect the acceleration of the AUV with Doppler velocity log (DVL) for relative velocity

measurement. Acoustic navigation uses acoustic transponder beacons to allow the AUV to determine its position. The most common methods for AUV navigation are long baseline (LBL) using at least two widely separated transponders and ultra-short baseline (USBL)/short base line (SBL) which generally uses Global Positioning System (GPS)-calibrated transponders on a single surface vessel. CML uses forward looking/side-scan SONAR to detect landmarks. Geophysical navigation uses physical features of the AUV's environment to produce an estimate of the location of it. Navigation of AUV typically finds application in mapping of sea floor. Elements of a typical navigation system of an AUV are shown in Fig. 2.2.

### ***2.2.2 Path Tracking/Trajectory Tracking***

In this objective, an AUV is forced to reach and follow a time parameterized reference i.e. a geometric path with an associated timing law. The vehicle may turn back in its attempt to reach the given reference point at a prescribed *time* as shown in Fig. 2.3(b). Problem of path tracking may be stated as: For an AUV system

$$\dot{x} = f(x, u) \text{ and } y = h(x, u) \quad \forall, t \geq 0, \quad (2.1)$$

where, state  $x \in \mathbb{R}^n$ , input  $u \in \mathbb{R}^k$ , output  $y \in \mathbb{R}^m$ , and  $r: [0, \infty) \rightarrow [0, \infty)$ , is continuously differentiable bounded time varying desired trajectory. Derive a feedback control law  $u$  such that the position of the vehicle converges to and remains inside a tube, centered around the desired path, which can be made arbitrarily thin, i.e., error  $\|e(t)\| = \|y(t) - r(t)\|$  converges to neighborhood of the origin that can be made arbitrarily small.

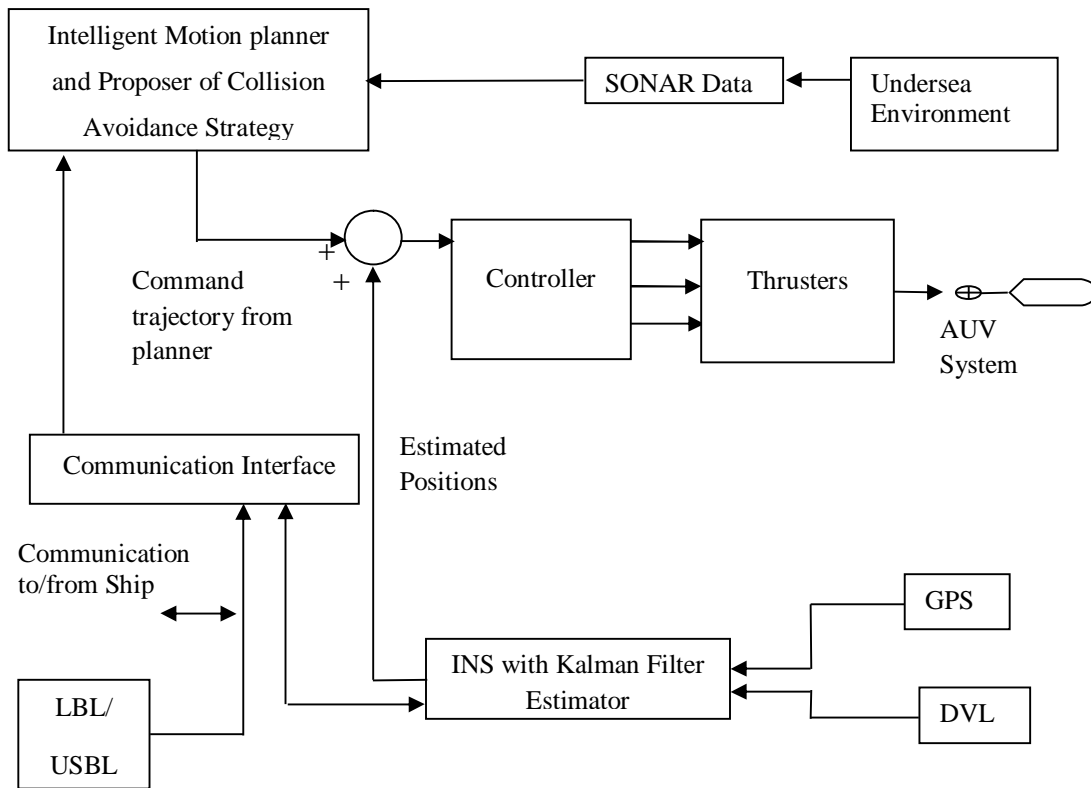


Fig 2.2 Typical Navigation System of AUV

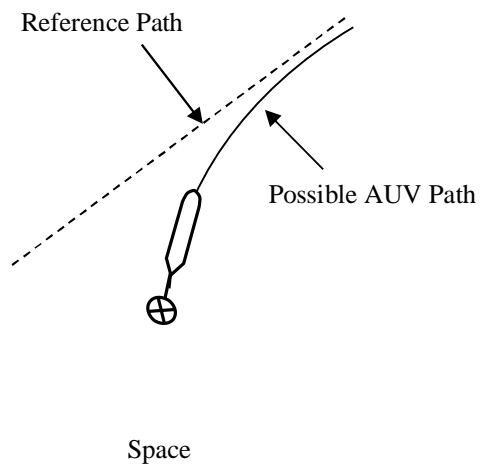


Fig 2.3(a) Path following

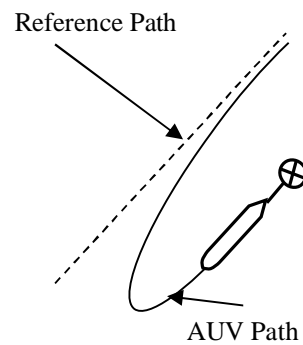


Fig 2.3(b) Path tracking



Position and attitude tracking algorithms are given in [22]. Strategy for simple trajectory tracking is proposed in [23], where trajectory tracking controller with path planning was reported in [24]. Both trajectory tracking and path-following problems can be tackled by decomposing the motion-control problem into an inner-loop dynamic task, which consists of making the vehicle move at a desired speed, and an outer-loop kinematic task, which assigns the reference speed so to achieve convergence to the path. Block diagram of a typical path tracking control is given in Fig 2.4.

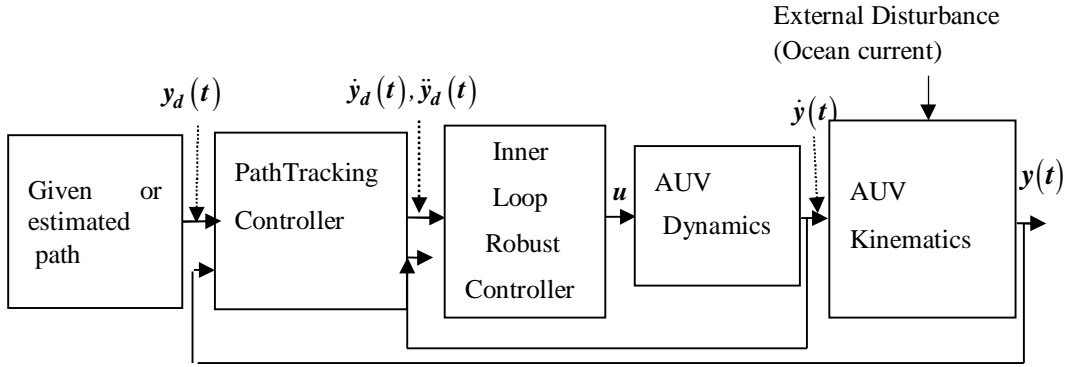


Fig 2.4 Path tracking control for an AUV

### 2.2.3 Path Following

*Path-following problems* [25] are concerned with the design of control laws that drive an object (robot arm, mobile robot, ship, aircraft, AUV etc.) to reach and follow a geometric *path without time constraint*. A secondary goal is to satisfy some additional dynamic specification such as to follow the path with some desired *speed assignment*.

Problem of path following may be stated as: for an AUV system as described in (2.1) where state  $x \in \mathfrak{R}^n$ , input  $u \in \mathfrak{R}^k$ , output  $y \in \mathfrak{R}^m$ , and a desired geometric path  $\{y_d(\theta) \in \mathfrak{R}^m, \theta \in [0, \infty)\}$ , defined as a function of continuous parameter  $\theta$  and  $\dot{y}_d(\theta) \in \mathfrak{R}^m$  is a desired speed assignment.

Suppose also that  $y_d(\theta)$  is sufficiently smooth and its derivative with respect to  $\theta$  are bounded.

Design a feedback control  $u$  such that position of the vehicle  $(i)$  converges to and remains inside a tube, centered around a desired path, which can be made arbitrarily thin i.e.  $e_p(t) = y(t) - y_d(\theta(t))$ , converges to a neighborhood of origin that can be made arbitrary small,  $(ii)$  satisfies a desired speed assignment  $\dot{y}_d$  along the path i.e.  $|\dot{\theta}(t) - \dot{y}_d(\theta)| \rightarrow 0$  as  $t \rightarrow \infty$ .

In [26], Breivik et.al proposed a nonlinear model based velocity and attitude controller, in order to fulfil the guidance-based path following task. Lapierre et al. [27] derived control law, based on Lyapunov and backstepping technique, to steer AUV along a desired path. The technique adopted for path following overcomes stringent initial condition constraints which describes the initial position of the vehicle is restricted to lie inside a tube around the path, the radius of which must be smaller than the smallest radius of curvature that is present in that path. Typical path following controller for an AUV is shown in Fig 2.5 where  $u$  represents control forces/torques.

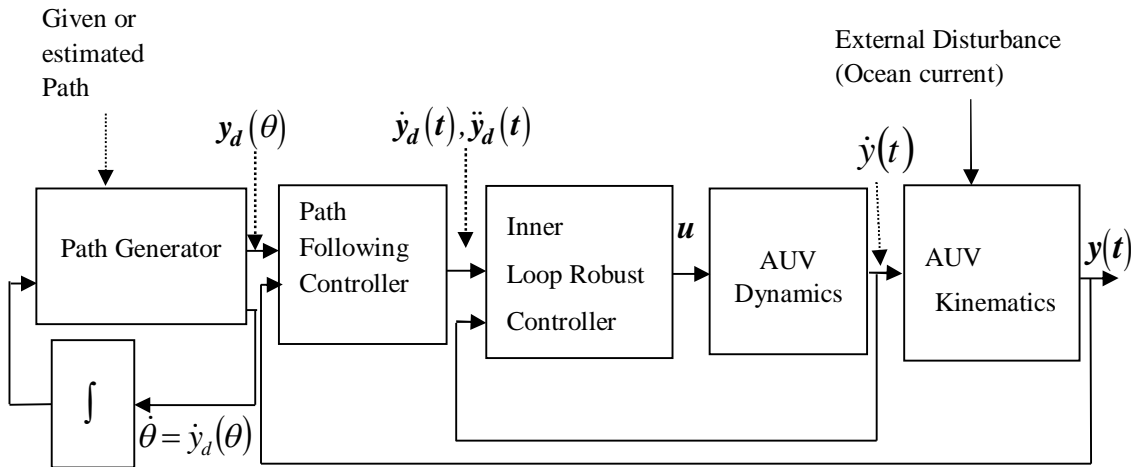


Fig 2.5 Path following control for an AUV

### 2.2.4 Set Point Stabilization and Regulatory Problem

In the control terminology it is fundamentally a regulation problem where the closed loop dynamics of the control law assumes the state vector  $\eta_i = \text{constant}$ , unlike smooth time varying trajectory  $\eta_i(t)$  of a trajectory tracking control. Regulatory problem for multiple AUVs is found in [28], where each AUV maintains their position from the average position of all AUVs such that a specified variance is maintained. The set point stabilization (Fig 2.6) refers to the problem of steering a vehicle to a final target point with a desired orientation, point stabilization [29]. Works in [169] are examples of regulatory control problems of multiple agents.

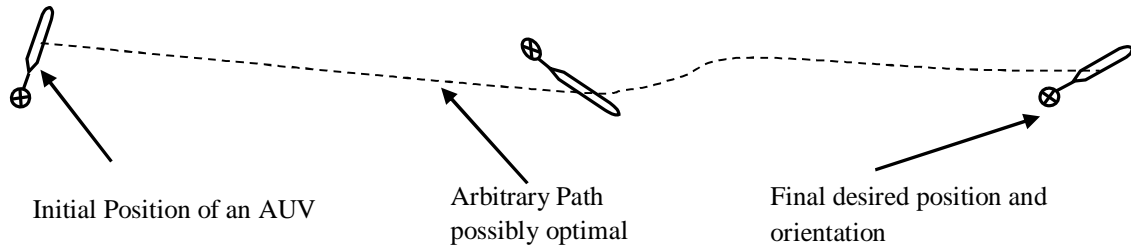


Fig 2.6 Set point control of an AUV

### 2.2.5 Line-of-sight (way-point) Guidance Based Path Following

Route of an AUV can be compactly described in terms of way-points, with the reference trajectory made up of the straight lines interconnecting the way-points [30]. Way point is usually a fixed point in the space, given in Cartesian coordinates in some inertial reference frame. The way point's description leads to an attractive decoupling between the geometric task of controlling the position and orientation of AUV and the dynamic task of controlling the speed of

the vehicle. In this strategy objective is to converge a set of way-points, in order they are given. A way-point guidance based path following strategy for a sinusoidal desired path is shown in Fig 2.7.

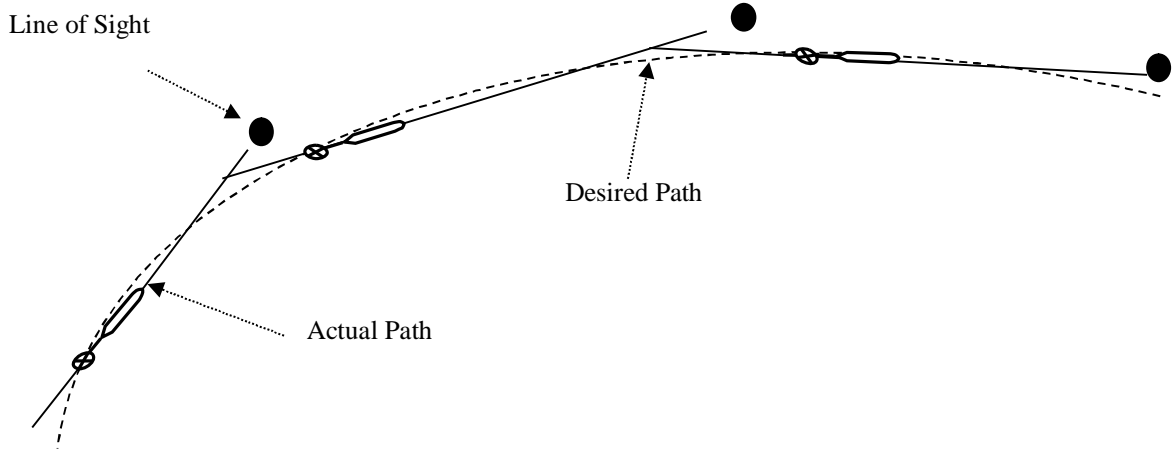


Fig. 2.7 Way-point guidance based tracking of a part of a sinusoidal path

### 2.2.6 Cross-Track Control

It is already stated route of an AUV can compactly be described in terms of way-points, with the reference trajectory made up of the straight lines interconnecting the way-points. For an AUV, choosing the earth-fixed coordinate system such its origin is at previous way-point and such that the  $x$  axis points towards the next way-point, the cross track error equals the sway position  $y$  of vehicle. The cross-track or path control thus implies controlling the sway position  $y$  to zero. Cross-track control of a slender underactuated AUV is reported in [31].

### 2.2.7 Region Based Tracking

In the region based tracking, the AUV is required to track a moving region (desired target) [32] rather than a point, to perform a given task such that control effort applied to track the region

(Fig 2.8) is minimal. When precision is important, high control effort is required. When the precision is not critical, low control effort is used to minimize the energy consumption. In presence of disturbance, the controller does not need to be activated to move the AUV out of region. In case of high precision requirement, the region is made in small to an extent such that the precision is lost. Therefore, the region based tracking is considered as the generalization of the conventional tracking control algorithm.

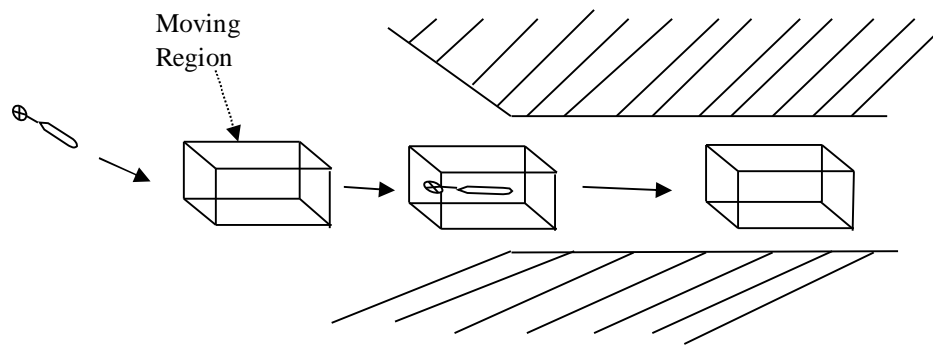


Fig 2.8 Dynamic moving region in region based tracking control

### 2.2.8 Homing and Docking

Homing refers to *point stabilization* and *dynamic positioning* of AUVs. A critical strategy to drive an AUV towards its base station/support vessel, which is basically considered as fixed target point. Homing allows a successful long-term autonomous operation of AUV since it allows the vehicle to approach a base station/support vessel, and then often offer capabilities and permission to sleep, recharge its batteries, transfer data, and download new mission parameters. This last stage of this process, usually termed as docking in the literature, may vary significantly depending on the vehicle itself, the location, and the type of docking station. Homing and docking [33], [34], [35] also usually requires extra aiding sensors, e.g., optical or electromagnetic aiding sensors. A sensor-based controller for homing of underactuated

AUVs is reported in [36] where, the problem of development of accurate control law is not affected by errors in the estimates of the attitude of the vehicle.

## 2.3 Control Architectures

With continuous significant advances in control, navigation, artificial intelligence, material science, computer, sensor and communication, AUVs have become very useful for various underwater tasks. The autonomy is one of the most critical issues for successful use of AUVs in a mission/application. Various control architectures have been studied to help increase the autonomy of AUVs [37]–[40] for successful desired motion. They could be classified into three groups namely deliberative architecture, behavior-based architecture, and hybrid architecture. Advantages and drawbacks of different approaches are provided in [41].

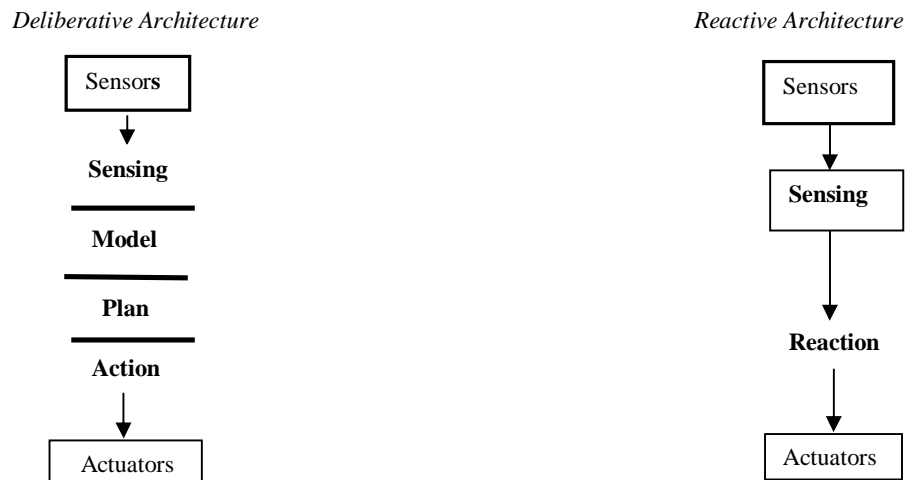


Fig 2.9 Difference between deliberative and reactive control architectures for AUVs

### 2.3.1 Deliberative Architectures

These are based on planning using a world model [42]. A mission is specified to achieve a set of goals and each goal is executed by a control system. They allow reasoning and making predictions concerning the environment. Data flows from sensors to the world model, which is

used to plan new actions to be undertaken by the actuator. When dealing with a highly dynamic environment, the delay in the response time is the main drawback. Algorithm of this architecture is shown in Fig.2.9.

### ***2.3.2 Behavioral Architectures***

These are also known as reactive architectures or hierarchies [43]. The decomposition is based on the desired behaviors for the vehicle and missions are normally described as a sequence of phases with a set of active behaviors. The behaviors continuously react to the situation sensed by the perception system. The vehicle's global behavior emerges from the combination of the elemental active behaviors. The real world acts as a model to which the vehicle reacts, based on the active behaviors. As active behaviors are based on the sense-react principle, they are suitable for dynamic environments. However, since each behavior pursues its own goal, reaction actions issued by one behavior may cause another behavior to deviate from its respective goal. As a result, the vehicle behavior is, at times, unpredictable. The algorithm of this architecture is shown in Fig 2.9.

### ***2.3.3 Hybrid Architectures***

This architecture takes advantage of the two previous architectures while minimizing their limitations [44], [45]. They usually consist of three layers: the deliberative layer, the behavior-based layer, and the control execution layer. The deliberative layer has the goal of breaking down the mission to be accomplished into a set of tasks. The behavior-based layer has the goal of carrying out each task. The deliberative layer also acts over the behavior-based layer by configuring the particular set of behaviors and the priorities among the behaviors. The deliberative layer determines if the task is being accomplished properly by monitoring sensor information and the output of the behavior-based layer. The behavior-based layer generates

outputs as inputs to the low-level controller which generates the actions to be followed in the control execution layer. These actions depend directly on the current perception (through sensors) of AUV since behaviors are very reactive.

## **2.4 Control Algorithms**

Single AUV/marine craft has been used for different missions for various needs. Different control objectives which may include path tracking, path following, way-point guidance based control strategies for an AUV. Different control algorithms have been developed for implementing these strategies. In order to achieve autonomy by an AUV its control algorithms must have adaptive and robustness properties for overcoming the problems arises due to the nonlinearity and time variance of AUV dynamics, unpredictable environmental uncertainties such as sea current fluctuation, and reaction force from the manipulator intervention, modeling difficulty in hydrodynamic and coriolis forces the changes in AUV configuration according to different missions. Although algorithms are broadly classified as adaptive and robust approaches, they are further categorized as traditional and hybrid controllers. Control algorithms of AUV are further categorized as controllers for linearized and nonlinear model, for fully actuated and underactuated systems. Categories based on traditional and hybrid control design methodologies are described as follows.

### **2.4.1 Traditional Controllers**

#### ***2.4.1.1. Proportional-Integral-Derivative (PID) Type Control***

A Proportional plus Integral plus Derivative i.e. PID controller refers to P, I, PD, PI or PID controller. Traditional PID controller with fixed gains cannot meet the requirements for control of underwater vehicles. Although it successfully deals the nonlinearities and uncertainties of



AUV dynamics; it can only ensure local stability of AUV system. Also it does not guarantee optimal control of the system or system stability, since the system to be controlled shows highly nonlinear behavior for the underwater vehicle.

Nevertheless, PD plus gravity and buoyancy compensation control technique was proposed for regulatory control of AUV by Fossen in [46]. Fossen [46] also proposed PID controller and proves the stability for regulatory control of AUV. Jalving [47] proposed a simple PD controller for AUV steering (Yaw) control. Chellabi [48] used a PD controller combined with an optimal error correcting terms. Here, the AUV dynamics has been linearized and decoupled into subsystems. A linear PD controller combined with LQR optimal controller is used for controlling each subsystem. Fjellstad and Fossen [49] defined a virtual velocity reference signal that is a linear combination of desired speed, tracking error and its integration, and formulated a controller that has two parts namely feed forward part and PID controller. First part is the multiplication of the AUV dynamic model and the virtual velocity and the second part is a PID controller. Its global convergence was proved by Barbalat's lemma. Ollennu [50] proposed a PD controller combined with the I/O linearization method. Linearized dynamics is obtained from I/O linearization with the application of Lie derivative and then state feedback control law has been exploited to achieve asymptotical regulating or tracking error. White [51] proposed a full state feedback controller that has the very classical observer-controller form. Koh [52] proposed a simple PID control in underwater vehicle control. Constraint optimization technique has been used for tuning parameters of PID controller. Fossen [46] proposed tracking controller using PD plus feedforward compensator (FC). Fossen [46] also used PID controller for reference trajectory tracking and proves its local stability conditions.

Limitations due to local stability, PID controllers are not used alone for an AUV, rather their benefits are exploited by combining with one or more advanced controllers such as  $H_\infty$  PID [53], model free SMC-PID [54].

In [56] controller is expressed in terms of quasi velocities (QV) in a transformed equation of motion with a diagonal inertia matrix and thus it is decoupled. A proportional and derivative control is applied on this new dynamic system and stability is studied using Lyapunov based argument. In contrast to the classical PD controller, the modified controller containing dynamic parameters of the under-water vehicle works very fast flexibility of selection of the regulator gain coefficients. Literature survey of use of PID group controllers such that PI, PD, or PID for AUVs clearly indicates that

- Most of the research works are based on linearized dynamics of AUV.
- These controllers have been verified for position control or motion control when hydrodynamic uncertainties are not involved in dynamics of AUV.
- Some research papers consider the uncertainties in the dynamics, but the assumption of availability of complete description (in linearization process) of AUV dynamics [48], [49] for development of control is the significant drawback. Because cancellation of dynamics, if not exact, may cause serious threat to robustness.
- PID group controllers for tracking such as PD plus FC and for regulation PD plus gravity or buoyancy compensation involve dynamic model parameters in their control law. This control law requires calculation of forward kinematics online which are often overhead for most cheap microprocessor.

- Last two points therefore assure, under real operating conditions where the dynamic parameters shifted from their nominal values, performance of these controllers deteriorates.

#### ***2.4.1.2 Robust Control***

Robustness of an AUV system means stability of the system against perturbation with respect to model parameter uncertainties (payload variation, change of hydrodynamic coefficients in different speeds and orientation) and uncertainties from external sources (wave and current variation). The uncertainties may be modeled as bounded constant valued (guaranteed stability bound), deterministic as a functional bound of parameters or stochastic based on probability distribution of uncertainties. Hence deterministic or stochastic robust controller are proposed based on the modeling behavior of the uncertain disturbances. In the robust control strategy, the performance of the system is verified for a family of plant models. Often, this family is defined by means of a nominal and a size of the uncertainty specified in parameter domain or in the frequency domain ( $H_\infty$  family of controller). The Smallwood and Whitcomb [58] gave information that no exact model of analytical form of dynamic equations of an AUV is available at present.

Robust control algorithm is best suitable as it requires only the information about the bound in uncertainty. But depending upon the amount of uncertainty the controller gain needs to be changed. Therefore, there is a chance for saturation of actuator due to requirement of higher values of gains for higher bounds of uncertainties. This is the limitation of robust control.

*Sliding Mode Control (SMC)*: It is a robust design technique that can withstand external disturbances and parameter uncertainties. It is a well-established approach for dealing with deterministic uncertainties in both linearized and nonlinear system of AUV. Uncertainties are assumed *norm-bounded*. This variable structure control alters the dynamics of a nonlinear system

by applying a high frequency switching control. The basic implementation of SMC involves selecting a hypersurface or a manifold for the whole state space such that system trajectory exhibits desirable behavior when confined to this space, and then finding appropriate feedback gains so that the system trajectory intersects and stays on the selected manifold. Yoerger and Slotine [59] proposed basic techniques of using SMC for trajectory tracking of AUV. Healy and Lienard [60] used discrete sliding modescheme for diving, steering and speed control separately of an AUV. In this scheme, sliding surface has been designed by pole placement technique or considering LQR optimal control to ensure global asymptotic convergence. Macro [61] and Riedel [62] used the same sliding mode controller in which the switching surface is defined by a Lyapunov function to guarantee the global stability of state variable errors and a boundary layer to reduce the chattering. Innoceti [63] used a cost functional to define the sliding surface and a ‘unit-vector control’ scheme as control law which has several parameters to smooth the discontinuity and determine the strength accordingly. Lee et.al [64] proposed a discrete-time sliding mode controller for AUV.

Even though SMC has been well known for its robustness to parameter variations, but this robustness is achieved at cost of considerable degradation of performances in controlling the complex AUV dynamics. These performance degradations are summarized as follows

- Control law involves lots of computation such differentiation of states (which may involve noise also), computation of matrix inverse. This results in delay in applying the control law which results in chattering.
- Dynamics compensating feature of control law in combination with chattering results in high control effort
- Reduction in life of actuator due to the rapid changing of discontinuous control action

- Possibility of actuator saturation due to high control effort i.e control action is achieved at the degradation of performance.
- Requirement of full state feedback for control action
- Lack of robustness during reaching phase and sensitivity to unmatched uncertainties [65].

*Time-Delay Control:* In [66], Kumar et al. proposed a robot control scheme for robust trajectory control based on direct estimation of system dynamics of AUV. The proposed controller can work satisfactorily under heavy uncertainty that is commonly encountered in the case of underwater vehicle control. The dynamics of the plant are approximately canceled through the feedback of delayed accelerations and control inputs. No knowledge of the bounds on uncertain terms is required. It is shown that only the rigid body inertia matrix is sufficient to design the controller. The control law is conceptually simple and computationally easy to implement.

### ***2.3.1.3 Robust/Optimal Control***

Principles of the robust/optimal control are based on calculus of variations, Pontryagin maximum principle, and Bellman dynamic programming. However, due to the difficulty of deriving an accurate model of AUV system, it is difficult to apply optimal control directly. Therefore, generally optimal control combined with system identification or robust control is used in AUV control. Among various optimal controls based robust control schemes such as classical approach Linear Quadratic Gaussian/Loop Transfer Recovery (LQG/LTR), and advanced approaches like  $H_\infty$ ,  $\mu$  syntheses methodology are most important.

Triantafyllu [67] proposed a robust control scheme based on Smith controller and the LQG/LTR methodology where Smith controller compensates for time delay in transferring signal through tether (in case of ROV) or through the acoustic link (in case of AUV). Conte [68] proposed a

robust controller based on Lyapunov method considering hydraulic disturbance and model uncertainties as bounded perturbation. Boskovic [69] introduced a Lyapunov function consisting of a quadratic term in velocity, quadratic term in position and a logarithmic term in the attitude, and based on this designed a controller that can achieve global asymptotic convergence to a given position and attitude setting. Mennozi [70] conducted experiments to obtain couple of nonlinear dynamics models near optimal operating conditions, and proposed LQR for gain calculation based on piecewise linearization. Wit [71] proposed a robust nonlinear control scheme that designs an additional control force to cope with the system state dependent disturbance.

*$H_\infty/H_2$  Control:*  $H_\infty$  controllers are synthesis approach based controllers for achieving robust performance or stabilization of a multi-variable linear system. The performance of the system is verified for a family of plant models. Often, this family is defined by means of a nominal and a size of the uncertainty specified in the frequency domain. It is very much appropriate for control of complex system like an AUV as its control problem can be divided into several interacting or non-interacting control subsystems such as speed control, steering control and diving control.  $H_\infty$  controllers in linear systems can be obtained in the state space by solving Riccati equation or Linear Matrix Inequality (LMI) technique. In the last case the solution is obtained by efficient convex optimization algorithms.

Kim [72] proposed  $H_2/H_\infty$  control scheme, in which robust stability problem against time delays and parameter uncertainties is transformed into  $H_\infty$  control problem and performance problem is transformed into  $H_2$  problem. For autopilot design Feng [73] proposed an  $H_\infty$  control scheme that was based on linearized model derived from the operating point of straight ahead motion with a fixed cruising speed. Moreira et.al.[74], proposed  $H_\infty$  and  $H_2$  controller for diving and course

control of AUV considering the presense of wave disturbances. Petrich et.al. [75], proposed a robust attitude controller which provides robustness against the cross-coupling due to roll motion. They proposed a linear model that captures the coupled pitch and yaw dynamics. A sensor and actuator allocation technique was used to minimize kinematic coupling. A fundamental concept of  $H_\infty$  control was introduced to provide robustness against the remaining coupling terms and ultimately a compromise exists between design criteria such as robustness, tracking performance and actuator bandwidth. Similar previous work for AUV attitude control using  $H_\infty$  method is reported in [76]. Loc et.al. [77] has designed a depth controller based on  $\mu$  sythesis methodology to compensate the effect of parametric uncertainties. Logan [78] has drawn a comparison between  $H_\infty/\mu$  Synthesis and SMC for heading and depth control of the Draper Laboratory/MIT Sea Grant Sea Squirt autonomous underwater vehicle (AUV). To avoid checking the performance measure for all frequencies "loop shaping" of performance transfer function is used with the help of frequency-domain weighting functions. In [79], a comparison have been drawn between LMI based  $H_\infty$  and SMC where control has been proposed based on unit vector control of SMC theory where parameter matrices are chosen based on a sliding surface which is achieved by optimizing a cost function. Advantages of  $H_\infty$  controller are as follows

- To use  $H_\infty$  methods, a control designer expresses the control problem as a mathematical optimization problem and then finds the controller that solves this.  $H_\infty$  techniques have the advantage over classical control techniques in that they are readily applicable to problems involving multivariable systems with cross-coupling between channels.
- In  $H_\infty$  control technique, parameter uncertainty is modeled as a disturbance system taking values in some range and modeled in a feedback setting. The  $H_\infty$  [80] arises when broader class

of input signals is considered, thus making  $H_\infty$  optimal control problem more robust to input uncertainty.

- To check the robust performance  $\mu$  –based test can be used.

Limitations of LQG/LTR,  $H_2$ ,  $H_\infty$  controller based on linearized dynamics of AUV are summarized as follows

- LQR control requires full state measurement for state feedback control.
- LQG control sticks to a particular power spectrum of disturbance signals. Performance of the systems designed with these criteria tends to be sensitive to the modest change in signal power spectrum and plant model.
- $H_\infty$  techniques include the level of mathematical understanding needed to apply them successfully and the need for a reasonably good model of the system to be controlled. Moreover, it works based on the assumption that the system is exactly modeled which is practically not possible.
- The linearization of AUV dynamics by Taylor series expansion suffers from serious drawbacks when body-fixed velocities take zero value in the quadratic part of hydrodynamic damping matrix where derivative does not exist as this part involve absolute value of these velocities.
- Consistent amount of uncertainties in both high and low frequency region due to approximations by linearization of nonlinear systems may exist in the process of applying  $H_\infty$  controller to linear system.
- Use of model parameters in the control law makes the stability analysis complicated.



- Robust stability of closed-loop system is the minimum requirement. However even though the closed-loop system is robustly stable, it will not be of any use if it does not deliver the required performance. Robust stability is achieved in these control methods but robust performance is still an open issue. In some cases  $\mu$  analysis technique is used to verify the robust performance of  $H_\infty$  controller.

- These controllers need to estimate desired acceleration for providing control law for tracking control of an AUV. This estimate always is contaminated with noise for trajectory which is not known in advance. Therefore, it adversely affects the control action applied to AUV.

#### ***2.4.1.4 Optimal Control***

There is little work reported in literature for applications of optimal control to AUV. Biggs et.al. [81], modeled the AUV as a nonholonomic system. Then an optimal kinematic control on the Euclidean group of motions  $SE(3)$ , where the costs function to be minimized is chosen as the integral of a quadratic function of velocity components. Maximum principle is used to get the Hamiltonian and corresponding vector field give the necessary conditions for optimality. In [82], a nonlinear optimal control using the method of successive approximations was designed for the purpose of station-keeping of an AUV. Kumar et al. [83] deal with real-time optimal motion planning for astable AUV, and present an approximate analytical solution for the optimal control problem of a symmetric astable AUV with symmetric thruster configuration. Yuan et al. [84] design an optimal real-time collision-free trajectory for autonomous underwatervehicles (AUVs) that move in a 3D unknown underwater space. A class of feasible trajectories is derived in a closed form by explicitly considering the kinematic model of AUVs. Class of trajectories is then expressed in terms of two adjustable parameters such as for the purpose of collision avoidance. A collision avoidance condition is developed to determine a class of collision-free trajectories.

One of the advantages of nonlinear optimal control is that it can handle robustness as well as optimality which are not available in optimal control based on linearized dynamics.

#### ***2.4.1.5 Adaptive Control***

Adaptive control can provide automating tuning of control gains in real time according to the uncertainties/nonlinearities in the process dynamics and the external disturbances. The uncertainties/disturbances may be of two types namely unknown constant or unpredictably changing in time. Three types of adaptive controller namely; model-based, regressor based and regressor-free based is reported in literature of AUV control. In model based adaptive control such as adaptive feedback linearization based adaptive control in [46], model reference adaptive control [85] researchers proposed the control law by estimating the system parameters since there are parameter uncertainties and unknown disturbances in the AUV's hydrodynamics. In regressor based adaptive system [46] controller parameters are adapted based on tracking/regulation error using an adaptation gain matrix; no information of AUV model is required. Only information required is the structural information of AUV dynamics, desired and actual position and velocities and desired accelerations. To avoid the use of noisy estimation of actual states in regressor based adaptive controller Fossen and Fjellestad [46] proposed desired compensation adaptive law (DCAL) which is actually modified version of DCAL proposed by Sadegh and Horowitz [87]. This strategy utilizes only the states of desired trajectory in the regressor.

Fossen and Sagatun [86] proposed adaptive control with online estimation of uncertainties in parameters. Antonelli et al. [88] used an adaptive control algorithm which considers the hydrodynamic damping parameters affecting the performance of tracking. Li et al. [89] proposed

adaptive region tracking controller for AUV where stability is studied based on Lyapunov function.

However model-structure based nonlinear controller such as regressor based adaptive control often fails to achieve desired performance in the presense of modeling error, parameter uncertainties and unknown disturbances. Values of parameters of AUV system depend on operational conditions and structure of AUV dynamics in regressor may not be precisely known in advance. On the other hand, the non-regressor controllers do not use model parameters/structure of AUV dynamics in them. An experimental study was done on underwater robotics using non-repressor-based adaptive control with bound estimation in [90]. Zhao et.al. [91] proposed adaptive disturbance observer based (DOB) controller to cope with the affects of both external disturbances and parameter uncertainties.

Disadvantages of this controller are mentioned as follows

- Feedback linearization based adaptive controllers are unable to achieve stability without restrictions on either nonlinearities or location of unknown parameters due to dependence on feedback linearization conditions and certainty equivalence implementations.
- All types of adaptive controllers namely model-based, regressor or regressor-free need to estimate desired acceleration for providing control law for tracking control of an AUV. This estimate always is contaminated with noise in the case when the desired trajectory is not known in advance. Therefore, it adversely affects the control action applied to AUV.
- In all the above controllers except DCAL, noise in estimation of actual state variables of AUV used in control law/ update law affects the actions of these laws.

- Model based adaptive controller may fail when the dynamics changing speed is beyond its adapting capability[92] and also it may be calculation burdensome because of the excessive endeavor in identification of highly nonlinear system of AUV.
- Computation of the regressor matrix in regressor based adaptive control is a time-consuming task (update rate is slower than update rate of desired velocities, accelerations and error in positions and velocities) since adaptation gain matrix is generally taken in such that adaptation process is slower than control bandwidth [92]. The computation time for parameter estimation will increase as number of unknown system parameters increase. Implementation also requires a precise knowledge of the structure of the entire/partial (e.g. PD plus gravity compensation) information of AUV dynamic model in the said control strategy.
- Update law based adaptive controllers suffers from poor transient response when adaptation is initiated. High control effort is required due to use of high control gains at this stage. Advantages of this control are mentioned as follows
- DCAL uses only the desired states only in its control and update law. Therefore, there is no scope of degradation of control law or update law due to noise in actual state estimation. Also significant amount of on-line computation is reduced in this kind of control/update law.
- The regressor-free adaptive controllers are computationally efficient as these controllers neither use the parameters nor the structure of AUV model.
- The advantage of all the controllers is that the control effort is applied in accordance with the requirement based on error in states and estimation of uncertainties (not the entire parameter/parametric matrix bound) at every instant of time. Therefore, unnecessary high control

effort can be avoided. It is just opposite to SMC where high control effort is inevitable owing to requirement of compensation of nonlinear dynamics.

#### ***2.4.1.6 Intelligent Control***

Intelligent control uses various Artificial Intelligence (AI) computing approaches like neural network (NN), Bayesian probability, fuzzy logic, and machine learning and evolutionary computation.

*Neural network (NN) control:* Neural networks attracted many researchers because they can achieve nonlinear mapping. Using NN in constructing controllers has the advantage that the dynamics of the controlled system need not be completely known. This facilitates NN to provide robustness to the controller [93] for underwater vehicle control with respect to non-uniform and unstructured seawater environment and highly nonlinear response of the vehicle where autonomy is difficult to achieve. However, NN-based controllers have the disadvantage that no formal mathematical characterization exists for the closed-loop system behavior. Yuh [94] exploits a multiple layer feed forward network in which each layer has 13 neurons, except the last layer that has 6 neurons. The input signals are six position errors, six velocity errors, and a constant. The output signals are six control forces. BP algorithm has been used for training the network. In applying NN to AUV Seube [95] compared the BP learning algorithm and continuous Hebbian learning rule. Venugopal [96] used a two hidden- layer feed forward neural network trained with BP algorithm to estimate the bounds AUV inverse Jacobian of the dynamics. Sutton [97] proposed a direct learning type neural networks controller that is trained with chemotaxis algorithm and compared with a tuned PID controller. Advantages and limitations of NN controllers from the perspective of AUV motion control are cited as follows

- Advantage is that these are non-model based controller. Therefore it is very advantageous from viewpoint of implementation.
- Real-time implementation of AUV control (e.g. defense application) is simply impossible using NN-based control.

*Fuzzy logic control:* In this control strategy, fuzzy inference system approximates any real continuous function over compact set to any degree of accuracy. For control engineering applications, researchers use fuzzy logic to form a smooth approximation of a nonlinear mapping from system input space to system output space. This makes it suitable for nonlinear system control. Kato [98] used a very basic fuzzy controller in an AQUA EXPLORER 100 cable's inspection. DeBietto [99] used a fuzzy logic controller for underwater vehicle's depth control. Guo [100] proposed a fuzzy logic controller that uses a genetic algorithm for membership function optimization. Lee [101] exploited a fuzzy logic controller that used the very basic TSK (Tagaki-Sugeno-Kang) models. Advantages and limitations of fuzzy logic based controllers from the perspective of AUV motion control are cited as follows

*Advantage:* (i) Uncertainties in communication network among multiple AUVs is easily handled using fuzzy logic formulation [147].

*Disadvantages:* (i) It is robust but not adaptive (ii) It is often complicated to make rule-base required for fuzzy-logic control for complex AUV system.

#### **2.4.1.7 Behavior Based Scheme**

A behavior-based (i.e. reactive) robotic system properly couples perception to action without the use of intervening abstract representations or time history. Behaviours can be expressed as a Stimulus-Response block. The global architecture is represented with behaviours (e.g. obstacle

avoidance, avoid trapping, go to) in parallel structure and outputs are channelled into a coordination mechanism that develops an appropriate response (Fig. 2.10). Two types of coordination mechanisms are found in literature [102] namely, competitive methods, cooperative methods. Also, behaviours can be expressed with a functional notation, like mathematical functions, by providing weights depending upon the preference of behaviors at a particular instant of time in underwater environment. A coordination function evaluates all the behaviours and gives the final response. Several behavior based scheme [102] like schema-based, subsumption architecture, process description language, action selection dynamics have been tested successfully. Few fundamental principles [103] which have been used by different researchers in behavior-based robotics are parallelism, modularity, situatedness/embeddedness, and emergence. Behavioral response is a functional mapping from the stimulus plane to the motor plane.

In [104] behavior-based control of an AUV for the purpose of inspection of coral reefs, a task which is performed by divers holding a video camera while following a rope. In [105] a set of core functions that allows an underwater robot to perform surveillance under operator control are used. Specifically, behaviors and interaction modes for a small underwater robot based on behaviors that facilitate the monitoring of organisms on a coral reef are presented.

#### ***2.4.1.8 Geometric Control***

There are many challenges to high performance control of AUV's. Notably underwater vehicle dynamics are basically nonlinear and hydrodynamic parameters are often poorly known. Mostly used nonlinear control for AUV is sliding mode control which renders robustness and avoids linearization of AUV model. It has two parts: first part attempts to cancel the nonlinear dynamics (akin to computed torque method) while the second part which is discontinuous across a sliding

surface makes up for uncertainty in the dynamic model. But geometric control is another *robust* control method which avoids both linearization of AUV model and cancellation of nonlinearities. The complete mechanical behavior of the AUV system can be well understood by this control technique. Since the theory is represented in differential geometric framework, the notion of the force is not obvious as when viewed from Newtonian point of view.

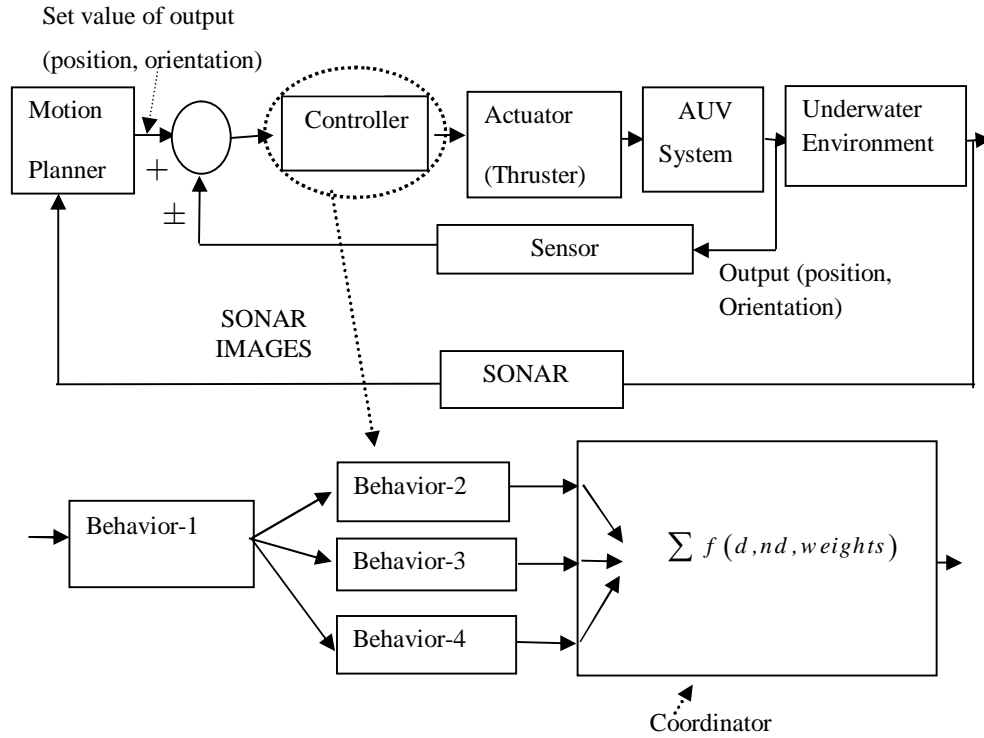


Fig 2.10 Behavior-Based Controller (motor-schema approach and cooperative coordination)  
Architecture for an AUV where ‘ $d$ ’ and ‘ $nd$ ’ denote dominant and non-dominant behaviors

In [106] geometric method referred to as energy-Casimir method has been used for stability studies of simple AUV dynamic model which does not consider the viscous effects. In [107] the dynamic equations of motion of a rigid body without considering external forces (potential and dissipative) are expressed as affine connection control system. This control system



introduces the notion of kinematic reduction and decoupling vector field. The equations of motions of AUV in a real fluid, subject to external potential and dissipative forces, are presented as forced affine control system (FACCS) [108]. Thus, the characterization of kinematic reduction and decoupling vector field has been extended to include the external forces in [108]. In [109] the underwater vehicle is modeled as a forced affine connection control system, and the control strategies are developed through the use of integral curves of rank one and kinematic reductions. Singh et al. [110] proposed a robust feedback trajectory algorithm of AUV on SE (3) under environmental disturbance. Stability is proved using Lyapunov type analysis.

#### ***2.4.1.9 Some Lyapunov Based Controller***

*Direct Lyapunov Method:* An output feedback controller is derived in [111] reconstructing the axial flow velocity from vehicle's speed measurement, using three state model of propeller shaft speed, forward (surge) speed of the vehicle, and axial flow velocity. Lyapunov stability theory is used to prove that a nonlinear observer combined with an output feedback integral controller providing exponential stability. Nakamura and Savant [112] used Lyapunov-like function to develop nonlinear tracking control scheme.

*Iterative Lyapunov Based Techniques:* Controller for trajectory tracking was proposed by Repoulas and Papadopoulos in [24]. They proved the stability of the proposed controller using recursive backstepping method, an iterative Lyapunov based technique.

Anguiar and Pascoal [30] proposed a nonlinear adaptive controller that steers an AUV to track a sequence of points consisting of desired positions, followed by positioning of vehicle at the final target. The controller is derived at the kinematic level with the assumption of the known ocean current disturbance. A closed-loop system is completed with an exponential observer. Integrator

backstepping and Lyapunov based techniques are then used to extend the kinematic level controller to dynamic case and to deal the parameter uncertainty.

- Advantages: (i) In contrast to feedback linearization based adaptive methods that required cancellation of all linearities, the back-stepping design avoids wasteful cancellation and retains useful nonlinearities. (ii) Back-stepping method is flexible and allows a choice of design tools for dominating or adapting to uncertain nonlinearities (iii) Backstepping is suitable for the system with unmatched uncertainty.
- Disadvantages: (i) Strong properties like global stability or regional stability are built into the nonlinear systems in multiple steps.

*Combination of Direct Lyapunov and Backstepping:* Do et al. [25] have proposed a nonlinear robust adaptive control strategy to force six degrees of freedom underactuated underwater vehicle with only four actuators to follow a prescribed path at a desired speed despite of the presence of environmental disturbances and vehicle's unknown physical parameters. The proposed controller is designed using Lyapunov's direct method, the popular backstepping and parameter projection techniques. The closed loop path following errors can be made arbitrarily small. The developed control strategy is easily extendible to situations of practical importance such as parking and point-to-point navigation. Lapierre et al. [27] proposed stringent initial condition constraints free path following control based on Lyapunov theory and backstepping technique.

#### ***2.4.1.10 Passivity-based Control***

It has been observed from the study of different controllers that most of them need to avail all the states by measurement or estimation for proposing the control law. To overcome the problems of measurement of all the states passivity based method was used by Fossen [46] for AUV. Passivity based formation control with consensus coordination has been proposed in [138].

Passivity is related to the property of stability in an input-output sense, that is, we mean the system is stable if bounded input energy supplied to the system, yields bounded output energy. This is in contrast to Lyapunov stability which concerns the internal stability of a system, that is, how far the state of a system is from a desired value. Passivity based control is a methodology which consists in controlling a system with the aim at making the closed loop system, passive. A system which can not store more energy than is supplied by some source with the difference stored and supplied energy being the dissipated energy, is referred as passive system. Advantages of this controller are

- *Advantages:* From implementation point of view (which refers to implementation cost) passivity based controller is favoured due to its low complexity and robustness.
- *Drawbacks:* Passivity control makes the system open-loop in speed tracking. The convergence rate of speed tracking error is bounded from below by mechanical time constant, relying on a positive damping of the system.

#### ***2.4.1.11 Energy Based Control***

Using energy based control, control system of AUV rigid body system are formulated and analysed as mechanical control system. The fundamental and most important feature of a mechanical system is notion of energy. Forces associated with energy are dissipative force and

gyroscopic force. A force which decreases the energy of the system is called dissipative force and the force which does not change the energy is termed as gyroscopic force. Gyroscopic forces add coupling to the dynamics. Two kinds of energy, involved with the AUV dynamics are kinetic and potential energy.

Energy based control basically refers to popularly known energy shaping control. Consider a mechanical system with unstable equilibria at  $q_0$ . The objective is to stabilize the system using feedback. One of the solutions is energy shaping procedure. The feedback so constructed for providing the closed-loop system to possess the structure of mechanical system is called *energy shaping feedback*. Two kinds of energy shaping are found in literature. Changing the potential energy is described as *potential energy shaping*. Shaping the kinetic energy is termed as *kinetic energy shaping*.

This kind of control is found in [113], where a Lagrange equation of motion for a bio-mimetic AUV (BAUV) is derived based on the notion of generalized coordinates, energy, and generalized forces. Then the Lagrangian function as the difference between the kinetic and potential energy is defined and problem of line-of-sight based tracking is solved.

#### ***2.4.1.12 Switched SeeSaw Control***

In [114], a switching controller, named switched seesaw control, has been developed for stabilization of an underactuated AUV in presence of input disturbances and measurement noise. Two classes of systems for control design have been proposed; stable/unstable switched system and seesaw systems. Two stable/unstable systems (when one is stable, the other one is unstable) are interconnected by switched seesaw system and conditions are provided such that interconnection is input-to-stable.

## 2.4.2 Hybrid Controller

AUV in recent days uses a combination or hybridization of different traditional control schemes adding the merits of traditional controllers to achieve robustness. Some of these hybrid control schemes reported in literature for AUV control are reviewed and presented below.

### 2.4.2.1 $H_\infty$ Optimal PID

To avoid the complex mathematical approximation of nonlinear  $H_\infty$  optimal control [115], [116], [117] a PID based nonlinear  $H_\infty$  is introduced in [53].

*Advantages:* (i) Nonlinear dynamics of AUV has been used instead of linearized dynamics as in case of traditional  $H_\infty$  controller, (ii) Effort to reduce the dependence on parameter matrices of dynamics of AUV in control law (iii) No approximation is adopted in solving Hamilton-Jacobi inequality. Complex inequalities have been reduced to simple set of inequalities.

*Disadvantages:* (i) Mass matrix has been used in control law (ii) Oscillations are observed in position and velocity tracking, (iii) Settling time of tracking performance is very high.

### 2.4.2.2 Adaptive Sliding Mode Control

Robust control design will benefit from the use of adaptive control in terms of performance improvements and extension of the range of operation. On the other hand, using an underlying robust controller design for building an adaptive control system may drastically improve the performance of the adaptive controller.

Estimation of the uncertainty bound is necessary to apply sliding mode control. For this reason, some researchers took the help of numerous adaptive mechanisms to tune bound estimation online. Fossen et.al. [86] proposed an adaptive sliding mode control of an AUV that compensates

for the uncertainties in the input matrix which arose due to thruster hydrodynamics. In adaptive SMC a discontinuous term has been added to an existing adaptive controller. Cristi et.al. [118] proposed an adaptive sliding mode control based on dominant linear model and bound on nonlinear perturbation of the dynamics. Robust controller can adjust to changing dynamics and operating conditions with consideration of both adaptive and non-adaptive techniques. Yoerger et. al. [119] used an adaptive sliding mode control for a nonlinear system model. Compensation for environmental changes is achieved by this controller by updating the nonlinear model parameters and control input.

*Advantages in AUV control* :(i) In sliding mode control performance degrades due to requirement of high control effort. But in adaptive sliding mode the performance does not degrade owing to adaptive implementation of controller (ii) indirectly it may be stated that the transient response of adaptive controller is improved by incorporating sliding mode control (SMC) to it.

#### **2.4.2.3 Adaptive Optimal Control**

In [120], adaptive control of a low speed bio-robotic autonomous underwater vehicle in dive plane using dorsal fins is considered. An indirect adaptive control system has been designed for the depth control using dorsal fins. The control system consists of a gradient based identifier for on-line parameter estimation, an observer for state estimation and an optimal criterion.

#### **2.4.2.4 Adaptive Supervisory Control**

In [121], an adaptive switching supervisory control has been combined with a nonlinear Lyapunov-based tracking control law for proposing the control law for an underactuated AUV.

This combination helps to achieve global boundedness and position tracking error converges to a neighborhood of the origin that can be made arbitrarily small.

#### **2.4.2.5 Fuzzy Sliding Mode Control**

In this control a switching layer instead of a not the switching surface is used to reduce the chattering. Fuzzy logic is used to generate a control command as a nonlinear function of  $S$  within the boundary layer. Chiu [122] proposed a fuzzy sliding mode control that uses a five fuzzy rule base to generate nonlinear control output in the sliding boundary layer. Guo et.al [123] designed a sliding mode fuzzy controller which offers a systematical means of constructing a set of shrinking-span and dilating-span membership functions for the controller. Stability and robustness of the control system are guaranteed by properly selecting the shrinking and dilating factorsof the fuzzy membership functions.

In Sliding Mode Fuzzy ControlIt includes the advantages of interpolation property of fuzzy logic control and robustness property of sliding mode control.Such kind of controller can be used for different optimization design: fuzzy logic can achieve very sophisticated switching surface functions. In [124],[125] a sliding mode fuzzy controller has been used which utilizes Pontryagin's maximum principle for switching surface design, and used a fuzzy logic to form this surface.

#### **2.4.2.6 Adaptive FuzzyLogic Control**

An daptive fuzzy logic based controller for the depth control of an AUV.has been described in [147]

#### **2.4.2.7 Adaptive Fuzzy Sliding Mode Control**

In the work of Balasurya et.al. [126], an adaptive fuzzy SMC has been developed where dynamics of AUV has been approximated. This strategy shows robustness against model uncertainties and external disturbances. Global asymptotic stability of proposed control system has been verified by Lyapunov criteria.

#### **2.4.2.8 Neural Sliding Mode Control**

Similar with adaptive sliding mode control scheme, in this scheme neural networks are used to set new SMC parameters for AUV. Lee [127] proposed a control scheme that uses a multilayer neural network trained with back propagation algorithm to compensate for the digression of the state from the sliding surface caused by unexpected large uncertainty.

#### **2.4.2.9 Neural Network (NN) Based Time Optimal Sliding Mode control**

Chatchanayuenyong [128] presented a combined controller using SMC as its main controller. The SMC follows switching according to Pontryagin's time optimal control principle, in which solution is obtained by applying neural network approach. Performance of the proposed controller is compared with various classical SMC and conventional linear control system. The controller shows effectiveness with respect to plant nonlinearity and parameter uncertainties.

#### **2.4.2.10 Neuro-Fuzzy Control**

Kim and Yuh [129] proposed a fuzzy membership function based on neural networks. Advantages of combining neural network with fuzzy logic control are given below

*Advantages:* (i) Neural networks have learning and optimization ability (ii) Neural network reduces the difficulties of determining the membership function of fuzzy controller (iii) Learning ability of NN scheme supplements adaptability and robustness to fuzzy logic controller.



#### **2.4.2.11 Adaptive Neuro-Fuzzy Control**

Lee et.al [130] presents a systematic approach for developing a concise self-adaptive neurofuzzy inference system (SANFIS) with a fast hybrid parameter learning algorithm for on-line learning of the control knowledge for autonomous underwater vehicle (AUV) control. Wang et. al. [131] proposed a self-adaptive recurrent neuro-fuzzy controller as an alternative to a feed forward controller and a proportional-plus-derivative controller (as a feedback controller) for an AUV in an unstructured environment.

#### **2.4.2.12 Adaptive Backstepping**

Hong et.al [132] presented a neural network based adaptive controller for autonomous diving control of an AUV using an adaptive back-stepping method.

#### **2.4.2.13 Adaptive-Behavior-based Control Strategy**

Adaptation is usually associated with the behavior-based robotics. To provide autonomy and robustness to an AUV with respect to changes in the environment control law must be adaptive [133]. In the case of AUV there is need of adaptation in control algorithms due to following situations

- (i) The control designer does not have information about all the parameters of behavior-based system
- (ii) the AUV needs to perform in changing environments under water.

Therefore, it must have adaptive mechanism. Adaptive system should have the features like tolerance to sensor noise, ability of learning during course of action and in all environments. Various level of adaption exists in behavior-based system namely sensory adaption, behavioral adaption, evolutionary adaption, learning as adaption.

In [134] a hybrid behavior-based schemes using reinforcement learning for high-level control of AUV is proposed. Two main features of the presented approach are hybrid behavior coordination and semi on-line neural-Q\_learning (SONQL). Hybrid behavior coordination takes advantages of robustness and modularity in the competitive approach as well as efficient trajectories in the cooperative approach. SONQL, a new continuous approach of the Q\_learning algorithm with a multilayer neural network is used to learn behavior state/action mapping online. [135] investigates a behavior-based control system for an AUV to adaptively map a deep-sea hydrothermal non-buoyant turbulent plume.

#### **2.4.2.14 Adaptive PD for Set Point Control**

In [136], controller is expressed in terms of quasi velocities (QV) in a transformed equation of motion with a diagonal inertia matrix and thus it is decoupled. A proportional and derivative control is applied on this new dynamic system and stability is studied using Lyapunov based argument. In contrast to the classical PD controller, the modified controller contains dynamic parameters of the AUV. One advantage of this controller is that it works fast because the dynamics of the underwater vehicle is included in the control law. The second advantage concerns the selection of the regulator gain coefficients. The proposed gain matrix arises from the decomposition of the inertia matrix and it is strictly related to the dynamics of the vehicle regulator.

Sun and Cheah proposed [137], an adaptive saturated proportional-derivative (SP-D) setpoint controller for autonomous underwater vehicles. In this controller no knowledge is required about the inertia matrix, Coriolis and centripetal force, hydrodynamic damping, and parameters of the gravity and buoyancy forces. The structure of this setpoint controller is based on the SP-D feedback, plus an adaptive update law for gravity and buoyancy forces. Simple explicit

conditions on the regulator gains are used by using Lyapunov's direct method and LaSalle's invariance principle such that global asymptotic stability is ensured. In [139], Hou et.al proposed an adaptive PD controller for region-based tracking for a formation control of multiple AUVs. Need of structure of gravity vector is the disadvantages of the controller used in this research work.

**2.4.2.15 Synthesis Method:** Synthesis method of control system for spatial motion of AUV is reported in [227]. In this paper, Filaretov et.al have divided the entire control design of AUV in six subsystems. They combine both adaptive (self tuning) and robust (sliding mode) for ensuring spatial motion of AUV.

## **2.5 Control of Multiple AUVs under Cooperative Motion**

### **2.5.1 Architecture of Cooperative Motion Control System of AUVs**

Basic building blocks of general framework of a cooperative control system of multiple AUVs are shown in Fig.2.11. Each AUV has an on-board sensory and computation system by which it gets its navigational information. The information refers to state of AUV such as linear position and angular position, linear and angular velocities. Each AUV gets information about state of subset of entire network of AUVs through communication system (e.g. acoustic modem). Due to action of prescribed coordination strategy based on the information available over the entire network, different AUV gets different commands for maintaining parameters for desired behaviors of formation during motion like speed synchronization command in case of cooperative path-following maneuver. In some specific cases coordination strategy includes local navigation data gained with the vehicle itself as well as by a subset of the other AUVs. This is especially required in situations where only some of the vehicles can carry accurate navigation

suites, whereas the others must rely on less precise sensor suites, supplemented with information that is exchanged over the network. Coordination strategy finds the way of using the sensory information among AUVs with the help of prescribed *decision making strategy*. In Fig 2.11, architecture is shown based on decentralized/distributed decision making strategy.

Different blocks are well coordinated to perform the tasks given to multi-AUV system. Desired state of an AUV depend upon particular *control objectives* (e.g. path planning, path following, LOS tracking etc.) to be performed by the network, relative state of each vehicle in network with respect to spatial formation structure (formation constraints) of network during navigation etc. Further relative state depends upon coordination strategy, decision making strategy,

*Communication topology*. Navigation data required for development of control law for a particular AUV includes its own data and data from neighbouring AUVs both. Flow of signals through controller, actuator and its system of individual AUV have also been shown in Fig 2.11.

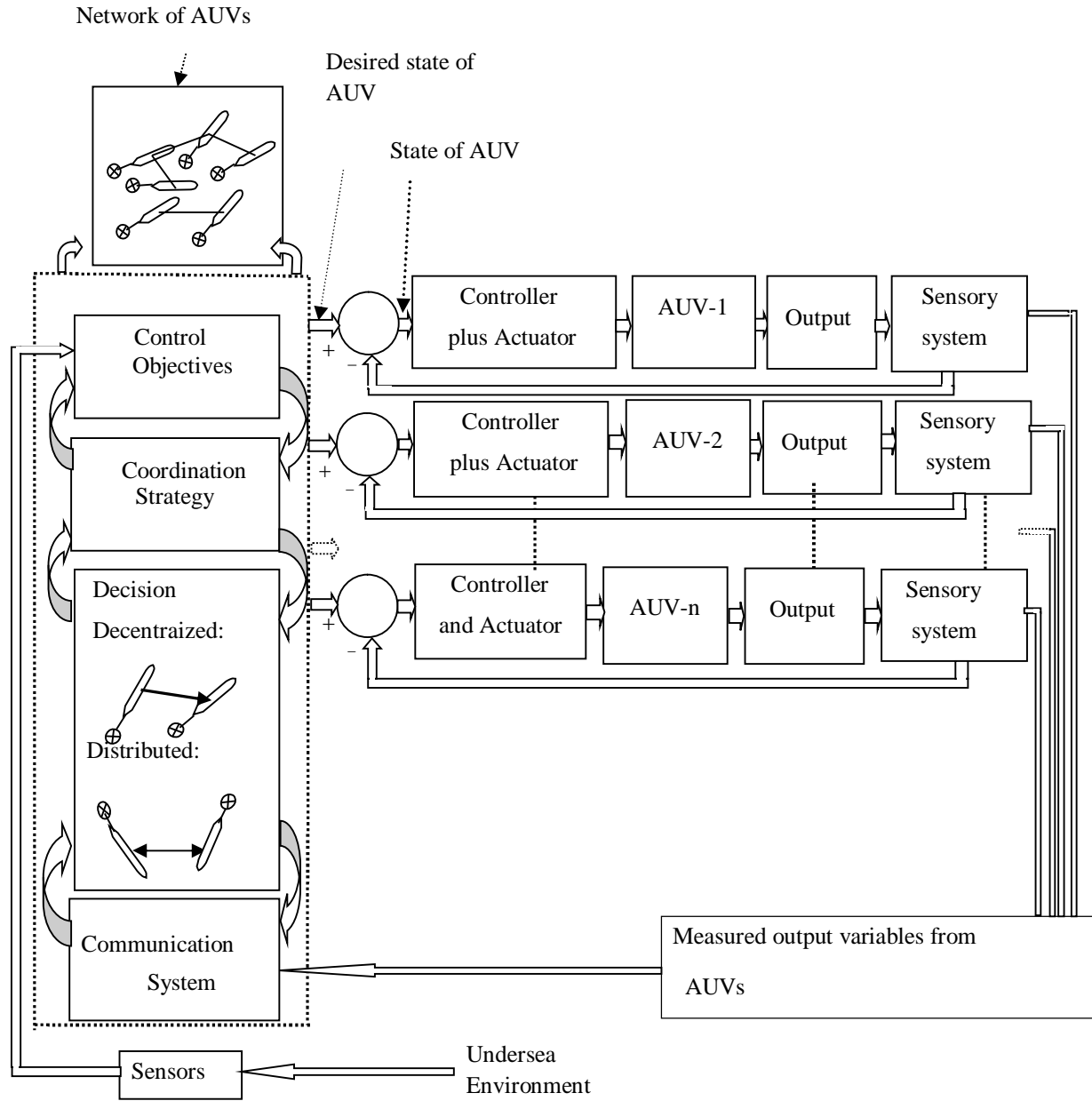


Fig 2.11 General framework of a cooperative control system of multiple AUVs

### 2.5.1.1 Decision Making Strategies

Three kinds of decision making strategies are reported in literature namely centralized [141], decentralized [142] and distributed [138]. Alternatively, decision making may be classified

as centralized and decentralized control. Decentralized control is further classified as hierarchical decentralized (or simply decentralized) or distributed decentralized (or simply distributed).

#### ***2.5.1.1.1 Centralized***

Each AUV gets control command from a central processor which may be placed in a leader [140] of the group or in a remote control room or in a guiding support vessel [141] using a parallel acoustic modem. During the motion, each AUV in the group maintains specific relative position in a fixed geometric formation with respect to the leader. Leader tracks the way points/path

(*Control objectives* of cooperative motion of group) and broadcasts its position to all follower AUVs. The thrusters of each AUV may get control command directly from central processor. All follower members of the network of AUVs know the desired shape and location of formation and position of way points or position of paths through communication from central processor using sensory system.

*Advantages:* (i) The centralized formation control could represent a good strategy (with respect to cost and complexity of whole system) for a small team of AUVs, when it is implemented with a single computer and a single sensor to monitor and control the whole team. (ii) No inter-vehicle communication is required. (iii) Human decision can override the automatic system in case of emergency.

• *Disadvantages:* (i) Global information requirement (ii) Communication burden restricts the use of this scheme for large number of AUVs (iii) Time delay is inevitable in communication (iv) Heavy computational burden.

A typical centralized cooperative motion control scheme for multi-AUV system is shown in Fig 2.12.

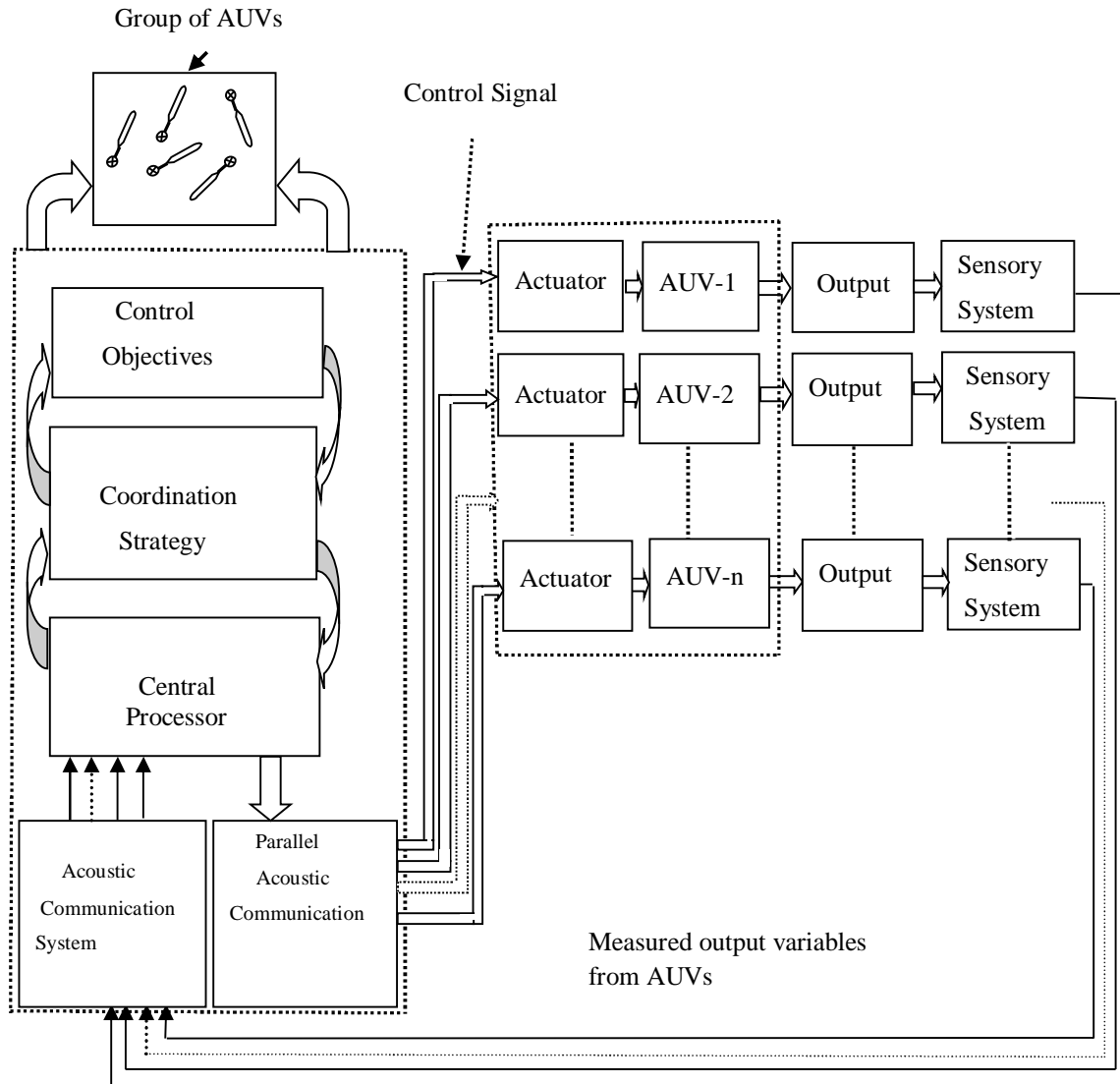


Fig 2.12 A typical centralized cooperative motion control scheme for multi-AUV system

#### 2.5.1.1.2 Decentralized

The control on each AUV only depends on measured or communicated information from neighbour. Decentralized control, also called hierarchical method, control is locally centralized.

Typical block diagram representation of decentralized control is shown in Fig 2.11. In typical decentralized control information flow is unidirectional between two AUVs. Two kinds of coordination are observed. An AUV may get information from only one [142] other AUV (Fig 2.13a) or from two [143] other AUVs (Fig 2.13b). Example in Fig.2.13a is sometimes called string type decentralized coordination.

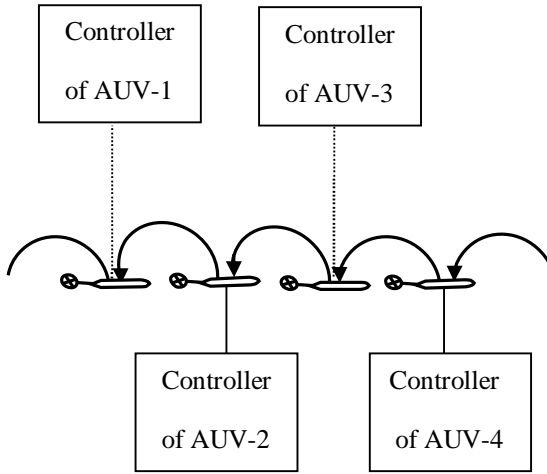


Fig 2.13(a) Decentralized Control with one to one unidirectional communication

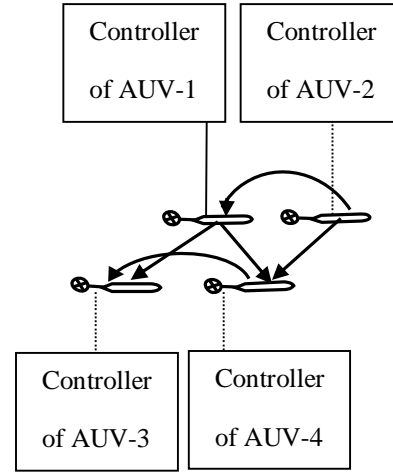


Fig 2.13(b) Decentralized Control with two to one unidirectional communication

- *Advantages:* (i) Decentralized control method is advantageous over centralized ones in that they are more fault tolerant, scalable, and reliable (ii) This control strategy is independent of geometry of formation. (iii) Each agent has its own separate controller (iv) No heavy communication burden (vi) Easy to synthesize.
- *Disadvantages:* (i) Lack of good design methods for decentralized architecture (ii) Stability margins become worse with increasing vehicle number (iii) Sensitive to external disturbances.



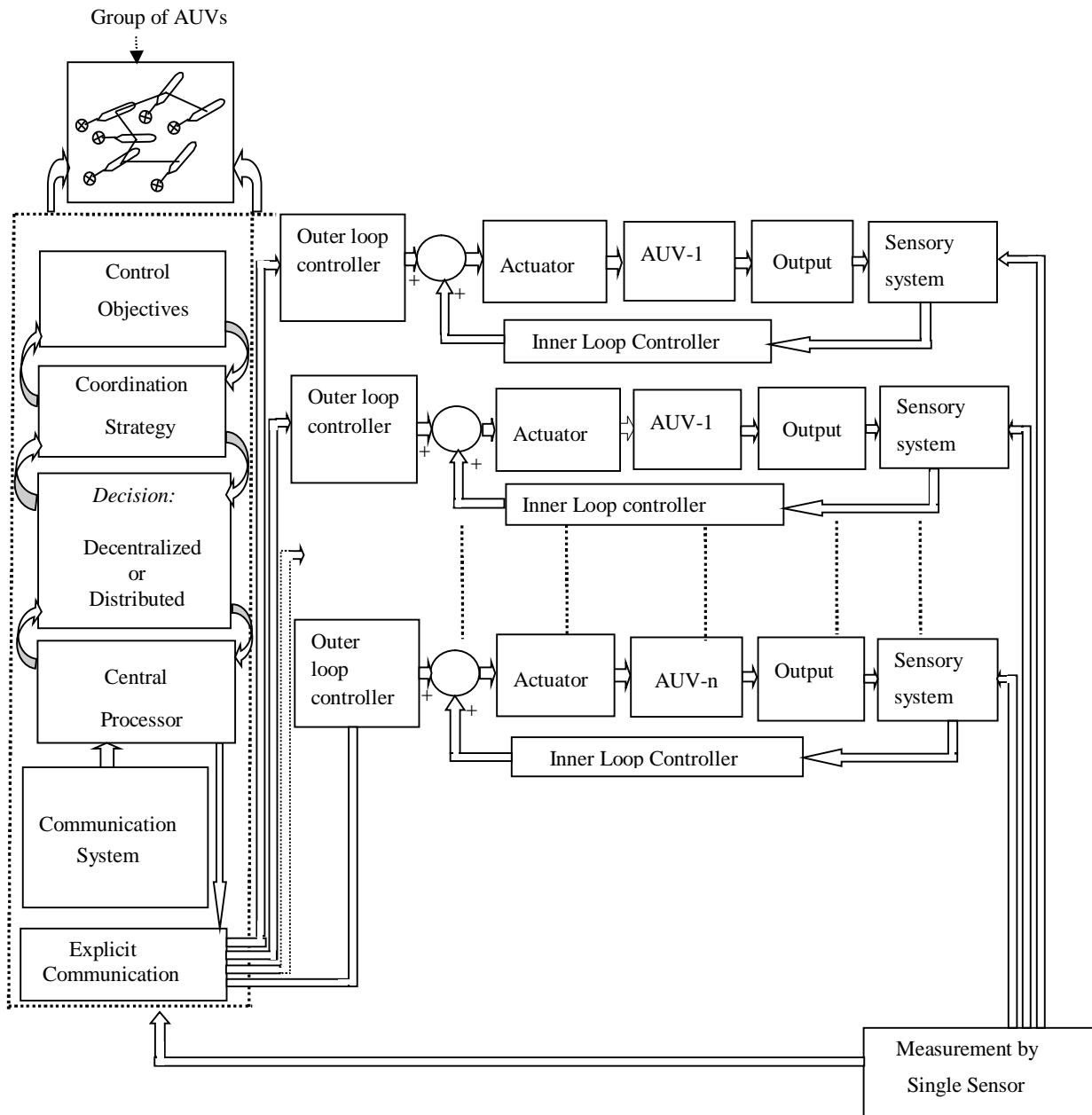


Fig 2.14 A typical combination of centralized and decentralized cooperative scheme of Multi-AUV system

#### ***2.5.1.1.3 Combination of Centralized and Decentralized***

In centralized control a single sensor is used from exogenous system. In centralized control a single sensor is used from exogenous system. A typical combination [144] of centralized and decentralized cooperative scheme of Multi-AUV system is shown in Fig.2.14.

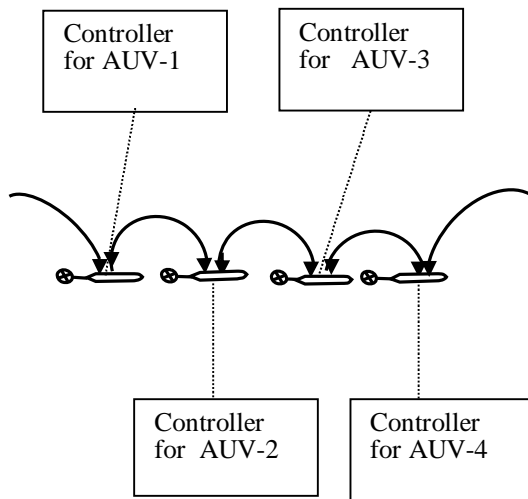
#### ***2.5.1.1.4 Distributed***

Distributed control, or distributed problem solving, involves the use of decentralized, loosely coupled controllers or problem solvers. Only neighbor to neighbor information (communicated or measured) is used to generate control inputs to each agent. Information must be shared to allow the group as a whole to solve the control problem; thus, a bidirectional communication protocol is defined for distributed control (Fig 2.11). A number of research papers on distributed control [138], [145] strategy are discussed in consensus, behavior based coordination. In distributed control systems, communication is usually asynchronous communication and locally transmitted, since bandwidth limitations make it impossible for all of the controllers to communicate with each other continuously all the time. Different types of distributed schemes are shown in Fig 2.15(a) and Fig.2.15 (b). Fig 2.15(a) indicates each AUV gets information from two neighbor AUVs and it also sends information to those AUVs. Fig 2.15(b) indicates each of three AUVs is in sharing information with other three AUVs.

- *Advantages:* (i) Distributed control method is advantageous over centralized ones in that they are more fault tolerant, scalable, and reliable (ii) No one AUV can become barrier for a solution (iii) In distributed control, all robots are equal with respect to control (iv) As only neighbor to neighbour communication is required i.e. light communication is required (v) Communication is

usually asynchronous communication and locally transmitted, therefore, one AUV is in share with other AUVs. This kind of strategy is observed in dynamic graph based coordination like flock of AUVs [145] (vi) Simple calculation (vii) Easy to synthesize

*Disadvantages:*(i) No one AUV of the distributed control system is capable of solving the entire problem (ii) Bandwidth is not so high



2.15(a) Distributed Control with one to one bidirectional communication

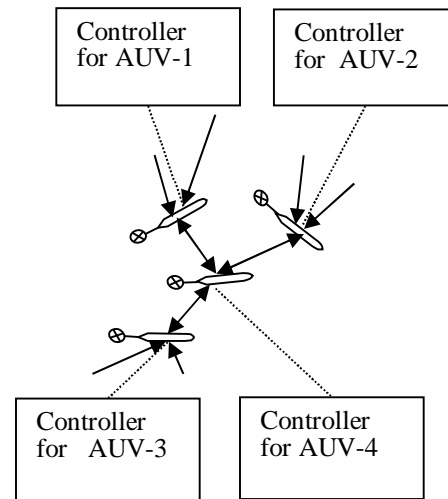


Fig. 2.15(b) Distributed Control with many to one bidirectional communication

### 2.5.1.2 Coordination Strategies

Six different coordination strategies are reported in literature. These are leader-follower, virtual leader, consensus, behavioral, potential field based, graph based. It is difficult to discuss these strategies separately as two or more strategies are frequently combined together to gain additional advantages.

### 2.5.1.2.1 Leader Follower

In this approach one AUV acts as a global leader which does not need to follow any other AUVs in the group. This leader tracks predefined path or planned path (estimated as per the structured or unstructured underwater environment) with its control based on path parameters and its states. Followers may follow the global leader in purely decentralized [146] or combination of centralized and decentralized [140] manner. In [146], directed graph based fixed topology has been used in two forms; as a network or as a string. Every case decomposes into numbers of leader-follower pairs as decentralized subsystems of the whole group, where each leader is in communication with maximum of two followers. Each follower has knowledge of position (position and orientation) state,  $q_{kL}$  of corresponding leader only; desired state in the need of fulfillment of formation constraints for desired formation. Leader state is defined as  $q_G$ . In [146], followers track their paths which are parallel to track of leader which tracks predefined way points. Each follower vehicle has knowledge of its own position state, global leader position state (through broadcast) and way points tracked by it. Each follower generates its trajectory using its achieved information and develops control law accordingly. A typical decentralized leader-follower control scheme is shown in Fig 2.16, where the complete controlled systems of a global leader and its follower are shown. There it is also mentioned how the output signal of a leader other than global is incorporated when the follower corresponds to any leader other than global leader.

- *Advantages:* (i) It is relatively easy to understand and implement (ii) Reference trajectory is clearly defined by leader (iii) Entire stability of the formation is implied by stability of control level of individual vehicle (iv) Complex dynamics like AUV is easily included.

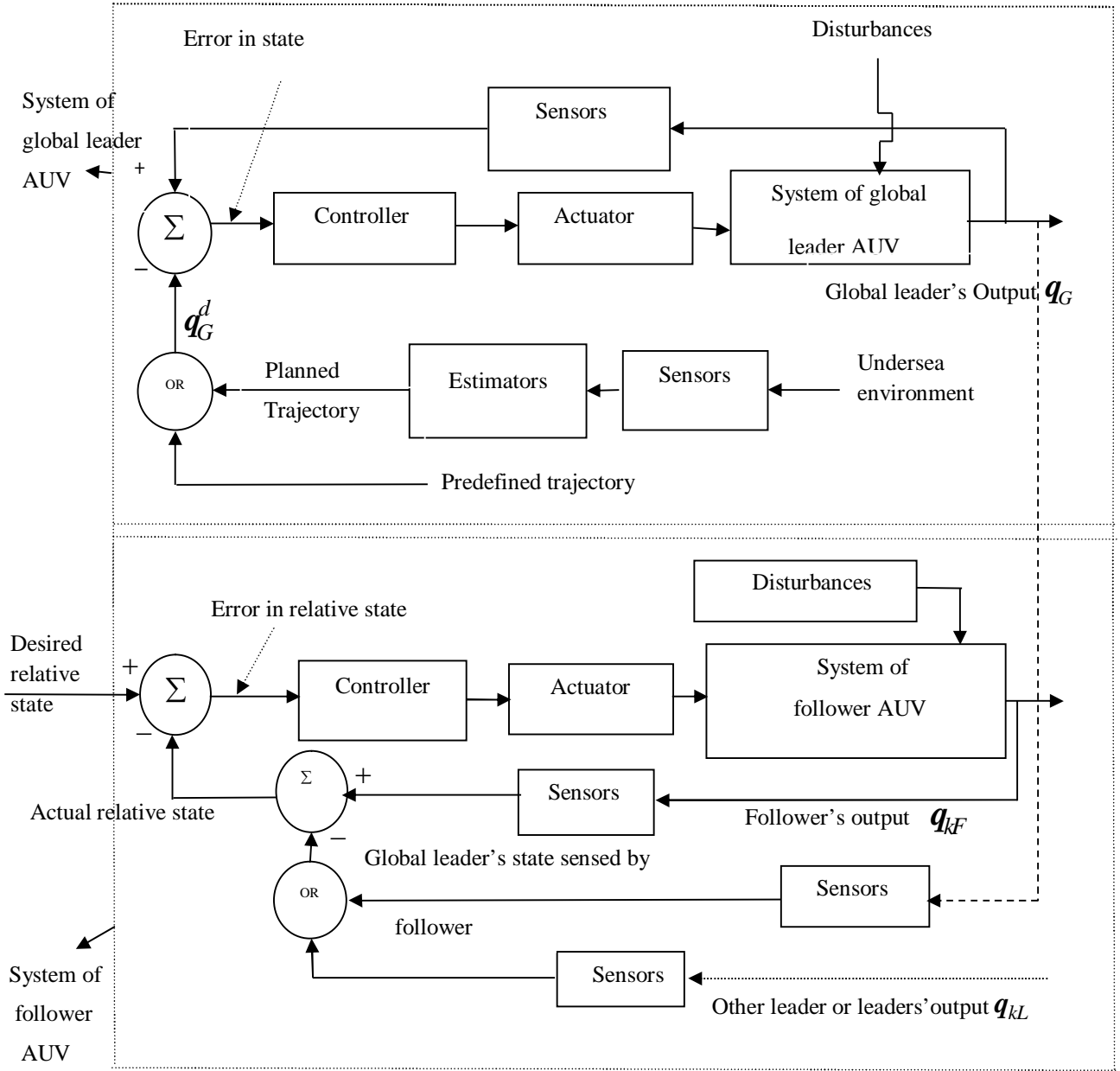


Fig 2.16 Control scheme based on a decentralized leader–follower approach

- *Disadvantages:* (i) There is no feedback from the followers to the leader. Due to lack of this feedback, formation can become disjoint and followers can be left behind if they are not able to track the motion of leader accurately. Therefore, such a formation control strategy lacks robustness in the face of such perturbations in followers (ii) In most cases, failure of leader

ensures collapsing of whole formation. This is termed as single point failure (iii) Most existing leader-follower formation control methods are model-based.

#### 2.5.1.2.2 Consensus

Consensus means to reach an agreement (by mutual decision and consent) regarding a certain quantity of interest (in most of the cases velocity) that depends on the instantaneous value of state, called *information state* of all agents. A "consensus algorithm" (or protocol) is an interaction rule that specifies the information exchange between an agent and all of neighbours on the network. Both for the decentralized or distributed cooperative control strategies, consensus algorithms focus on driving the information states of all agents to a common value. Consensus may be applied to both fixed [138] or dynamic topology [145] graph based network. Graph Laplacian ( $\mathbf{L}$ ), an important graph-related matrices and their spectral properties play a crucial role in convergence analysis of consensus [147] and alignment algorithm in these research papers. Basic building blocks of control scheme based on consensus coordination for a group of AUVs is shown in Fig. 2.17.

In the Fig.2.17,  $\mathbf{x}=[\mathbf{x}_1, \mathbf{x}_2, \dots, \mathbf{x}_k \dots \mathbf{x}_n] \in R^{(n \times m) \times 1}$  where,  $\mathbf{x} \in R^n$  is state of position (angular and/linear) and/velocity (angular and/linear) of  $n$ th AUV.  $n$  and  $m$  denote total number of AUVs in the group and the number of variables in state vector of each AUV respectively. In two dimensional motions, position state for  $k$ th AUV is  $\mathbf{x}_k \in (x_{kx}, x_{ky}, \theta_k) \in \mathfrak{R}^3$  that comprises of linear position and orientation in inertial coordinate frame. State may refer coordination state based on path parameters (like path length) in case of coordinated path following control [148].

In Fig.2.17,  $\mathbf{u}=[\mathbf{u}_1, \mathbf{u}_2, \dots, \mathbf{u}_k \dots \mathbf{u}_n] \in R^{(n \times m) \times 1}$  represents control input vector, where,  $\mathbf{x} \in R^m$ .  $\mathbf{u}_k$

includes surge force  $F_u$ , sway force  $F_v$ , and torque around inertial  $z$  axis, that is termed as  $F_\omega$ .

Feedback controller using consensus [149] may be implemented for both discrete-time or continuous time system. Mostly, network of group is configured as a dynamic [145] graph  $G(t) = (V, E(t))$  where,  $V$  is number of nodes whereas each node represents Centre of Mass (CoM) of each vehicle.  $E(t)$  is number of edges in that graph where each edge represents information flow between any two vehicles. In the analysis of consensus based coordination, a frequently used matrix, called adjacency matrix of graph is defined as,

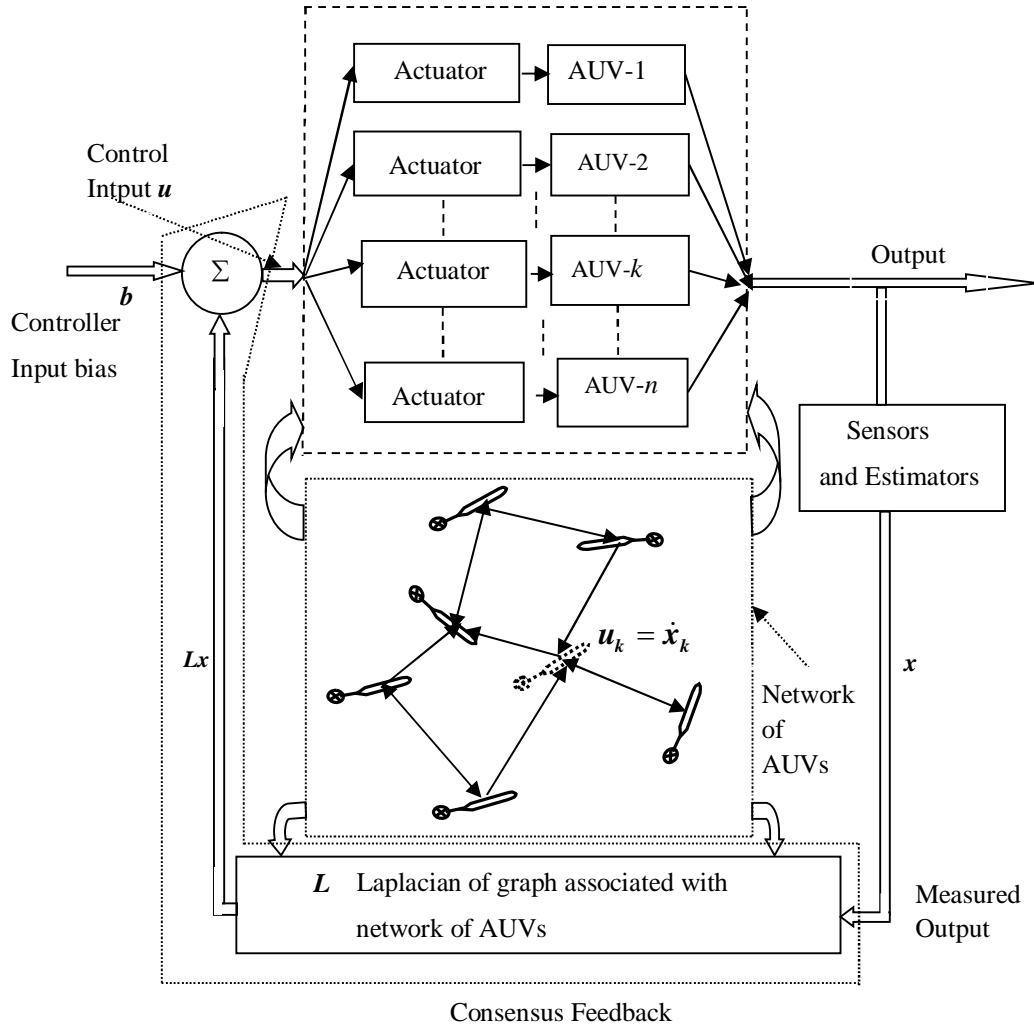


Fig. 2.17 Basic building blocks of control scheme based on consensus coordination for a group of AUVs, where, Dotted AUV represents  $k$ th AUV

$A = [a_{kj}]_{n \times n}$ , where,  $a_{ij} \neq 0$ , if  $k$ th AUV is in communication with  $j$ th AUV

otherwise  $a_{ij} = 0$ .

The sign and value of  $a_{ij}$  depends upon the orientation of graph (directed/undirected) and weight of the edge. Therefore,  $E(t)$  is characterized as  $E(t) = \{(k, j) \in V \times V : a_{kj} \neq 0\}$ . Assume,  $k$ th AUV takes communicated information states from its neighbor AUVs ( $N_k$ ); called neighbor set and is defined by  $N_k = \{j \in V : a_{ij} \neq 0\}$ ,  $V = \{1, \dots, n\}$ . Then it develops distributed control signal  $u_k$  as follows.

$$\dot{\mathbf{x}}_k = \gamma \sum_{j \in N_k} a_{kj}(t) (\mathbf{x}_j - \mathbf{x}_k) + \mathbf{b}_k = \mathbf{u}_k \quad (2.2)$$

where,  $\mathbf{b}_k$  is called *input bias* which decides the desired state as per the objective of  $k$ th AUV in the network. It may be different or same for each AUV. Considering control law given in eq.2.2 one can rewrite it for all AUVs in matrix form as given below.

$$\dot{\mathbf{x}} = -\mathbf{L}\mathbf{x} \quad (2.3)$$

where,  $\mathbf{L}$  has been used in [138] whereas,  $\mathbf{L}_p(t)$  an explicit dependence of graph Laplacian has been used in [148]. By reaching consensus for whole system of AUVs, means each AUVs asymptotically converges to agreement space characterized by

$$\mathbf{x}_1 = \mathbf{x}_2 = \mathbf{x}_3 = \dots = \mathbf{x}_n = \mathbf{x}_L \quad (2.4)$$

where,  $\mathbf{x}_1, \mathbf{x}_2, \dots, \mathbf{x}_n$  are the velocity states of all AUVs.  $\mathbf{x}_L$  is common reaching value (velocity of a fictitious leader called virtual leader or common speed assignment of fleet) of all AUVs.



Consensus based patrolling of a square path by a group of underwater swarm robots is observed in [150].

### 2.5.1.2.3 *Potential Field Approach*

An artificial potential field approach considers AUVs as a group of coupled dynamics of all the participants AUVs and virtual AUVs such that a desired group configurations (and subsequent formation) is obtained at a global minima of potential function and control of its motion of formation is achieved. Three types of potential fields namely, [151], [152] may be designed for this purpose. This approach is used for both two dimensional and three dimensional systems. For simplicity, analysis of this coordination method is briefed for 2D case. Let there are  $N$  number of AUVs in a group with simple double integrator model [151], [152].

First kind of potential function is proposed to maintain a desired distance between a vehicle and a vehicle of its neighbors. As an example, the potential function between  $j$ th and  $k$ th AUV may be formulated as

$$\Phi_{vv}^k(x_{kj}, d_0, d_1)$$

where,  $x_{kj}$  represents the actual distance between  $j$ th and  $k$ th AUVs and  $d_0, d_1 > 0$  are two constants. Control force for any AUV (e.g.  $k$ th AUV) is developed by taking negative gradient of

$\Phi_{vv}^k(x_{kj}, d_0, d_1)$  w.r.t  $x_k$  like  $(-\nabla_{x_k}(\Phi_{vv}^k))\hat{x}_{kj}$ .  $\hat{x}_{kj}$  indicates direction vector of produced force.  $\Phi_{vv}^k$  is designed in such a way that it produces repelling force when the vehicles are too close i.e. when  $\|x_{kj}\| < d_0$ ; attracting force when the vehicles are too far i.e. when  $\|x_{kj}\| > d_1$ ; and zero when the vehicles are very far apart i.e. when  $\|x_{kj}\| \geq d_1 > d_0$  or when  $\|x_{kj}\| = d_0$ , which is the global minimum condition of potential function. Variation of  $\Phi_{vv}^k$  w.r.t.  $x_{kj}$  is in Fig 2.18(a). Total

control force for  $k$ th AUV will be summation of individual forces produced separately with the AUVs in its neighbourhood zone bounded by  $d_1$ . Therefore, the total force is

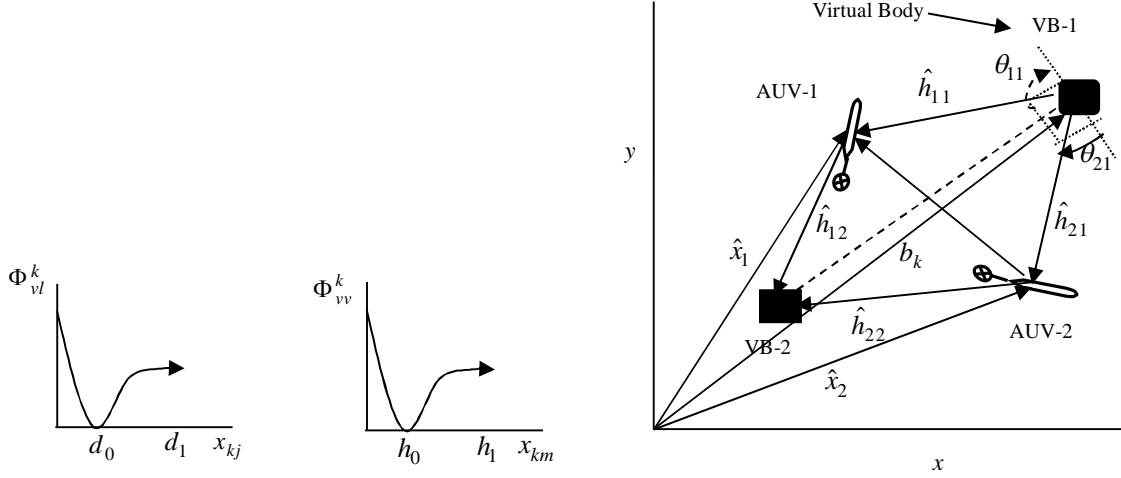


Fig.2.18(a):Potential function between  $j$ th and  $k$ th AUV

Fig.2.18(b):Potential function between  $k$ th AUV and  $m^{\text{th}}$  virtual

Fig 2.19: Potential field based coordination between two AUVs

body

$$\Phi_{vv}^{kT} = \left[ -\sum_{j \neq k}^N \nabla_{x_k} \Phi_{vv}^k(x_{kj}d_0, d_1) \right] \hat{x}_{kj}. \quad (2.5)$$

Similarly other AUVs also produce their control forces. Second kind of potential function provides a field to maintain a specific distance between a particular AUV and a virtual body. This is formulated in the same way as it was in case of vehicle to vehicle potential function and acts as guidance to provide specific shape of the formation. Let there be  $M$  number of virtual bodies numbered as  $1, 2, \dots, m, \dots, M$ . Potential function between  $k$ th AUV and  $m$ th virtual body is characterized as

$$\Phi_{vl}^k(x_{km}, h_{0m}, h_{1m})$$

Variation of  $\Phi_{vl}^k(x_{km}, h_{0m}, h_{1m})$  w.r.t  $x_{km}$  is shown in Fig 2.18 (b). In this case, control force is obtained taking the negative gradient of  $\Phi_{vl}^k$  w.r.t  $x_k$ . Therefore, the total force, for interaction  $k$ th AUV with  $m$  number of virtual bodies, is given by

$$\Phi_{vl}^{kT} = \left[ -\sum_{m=1}^M \nabla_{x_k} \Phi_{vl}^k(x_{km}, h_{0m}, h_{1m}) \right] \hat{x}_{km} \quad (2.6)$$

An artificial potential may also be designed to match each vehicle's orientation with the orientation of virtual body. The orientation of an AUV w.r.t virtual leader is expressed in terms of distance vector from virtual body to that particular AUV. Example of this type of orientation is  $\theta_{11}$ , which may be expressed in terms  $\hat{x}_1, b_1, \hat{h}_{11}$  between AUV-1 and VB-1 as shown in Fig 2.19. In general, it has been expressed for  $k$ th AUV in the previous mentioned group and  $m$ th virtual leader is given by  $\Phi_0^k(\theta_{km})$ . This potential function is designed so that it has isolated global minima at specified angles about the virtual leader. The control force is developed from this potential function by taking gradient w.r.t  $x_k$  and thus total force considering all virtual bodies is characterized as

$$-\nabla_{x_k} \sum_{m=1}^M (\Phi_o^k(\theta_{km})) \quad (2.7)$$

Sometimes velocity damping terms, as the part of control law based on difference between an AUV and virtual body under translational motion, are also added for asymptotic convergence of motional variables [151]. Total force  $u_k$  for  $k$ th AUV is obtained by adding all the forces in the

equations, (2.5), (2.6), (2.7) and damping terms. A typical control structure of an AUV under potential field coordination is shown in Fig 2.20.

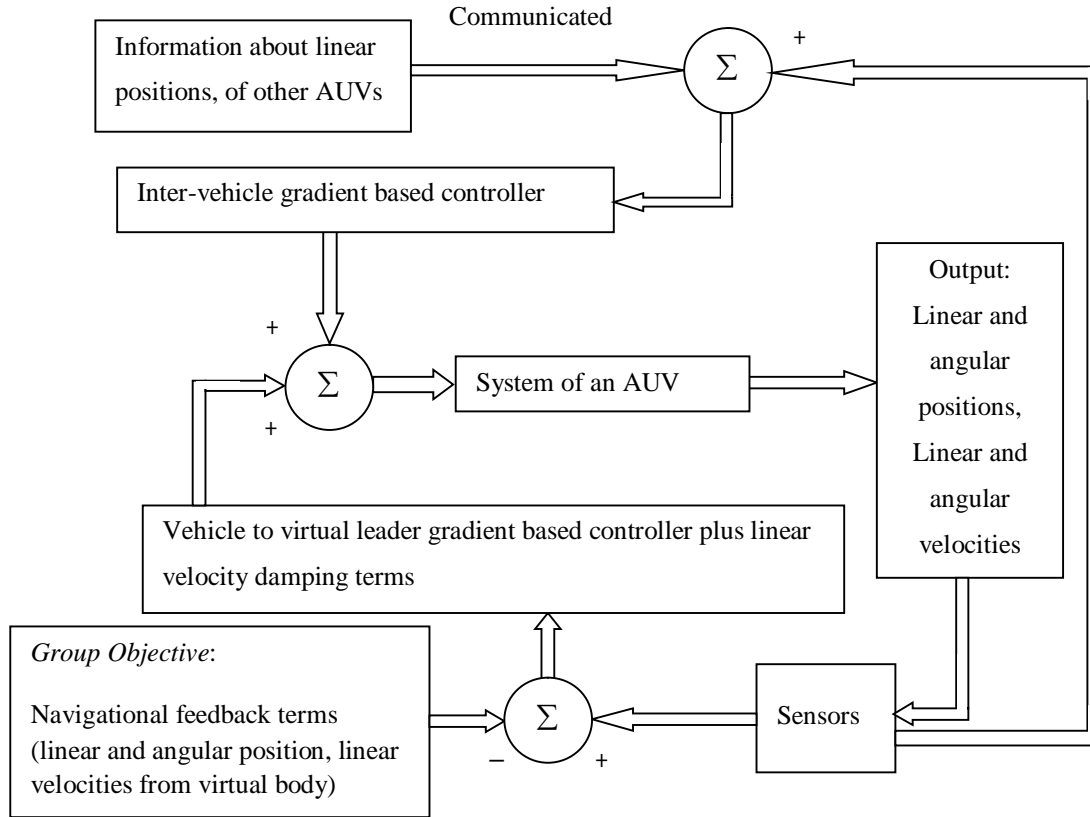


Fig 2.20 Controller structure for system of an AUV in potential field based coordination

Advantages of potential field based coordination are that stability analysis becomes easy due to easy formulation of Lyapunov function.

#### 2.5.1.2.4 Virtual Structure/Body/Leader:

In this approach, AUVs in the formation jointly synthesize a single, possibly fictitious, leader vehicle (called virtual leader/structure) whose trajectory acts as a leader for the group. Instead of a physical leader, a virtual leader is suggested to avoid the problems with disturbance rejection

inherent in the leader-follower approach. The virtual-structure-based approach deals with the entire formation members as a single individual and the geometric relationships are maintained during the maneuver. Virtual leader based coordination is frequently combined with potential field and consensus coordination.

#### **2.5.1.2.5 Behavioral**

Behavior-based coordination still has limited use in multi-AUV operation because cooperative control strategy using this approach suffers from lack of proper mathematical formulation between any two AUVs and consequently provides less guarantee of keeping desired formation structure/behavior during motion. According to this approach, several behaviors each of which corresponds to a sole objective of motion of formation have to be built up. These behaviors produce different decisions corresponding to the robot control parameters. These may be combined in some way to take the final decision such that desired formation motion is achieved.

- *Advantages:* Behavior-based approaches are decentralized and may be implemented with significantly less communication burden.
- *Disadvantages:* Behavior based coordination is difficult to analyze mathematically. Therefore, it is difficult to guarantee the convergence of formation to the desired configuration, or to guarantee formation keeping during a maneuver.

#### **2.5.1.2.6 Graph Based Coordination**

Coordination among AUVs are modeled using formation graph where each vertex represents individual agent kinematics and each edge represents inter-agent constraint (e.g. desired distance) that must be maintained during motion of formation. Depending upon the pattern of

information exchange in that coordination, two types of graphs are possible i.e. directed and undirected.

#### *Undirected graph based coordination*

In this coordination both of any pair of AUVs, constrained by an edge have equal responsibility to satisfy the constraint. As an example, distance between any pair of agents is sensed by both the agents i.e. information exchange is distributed. The structure of undirected graph have several advantages and disadvantages as mentioned below.

- *Advantages:* (i) Possibility of single point failure is reduced (ii) Time varying coordination can easily be handled.
- *Disadvantages:*(i) One of those disadvantages is information-based-instability [153], which happens due to possibility of difference in distances measured by noisy sensors of any pair of agents(ii) Communication requirement among agents is more. Therefore external observer based centralized control strategy is best suited for undirected formation graph (iii) Control law is mainly focused on rigidity property of formation(iv)Due to distributed coordination problem formulation and control analysis becomes complicated. Undirected graph based formation control problem is analysed using rigid graph theory [154] or graph Laplacian and its spectral properties.

#### *Directed graph based coordination*

Only one (called *follower*) of any pair of agents, constrained by an edge has responsibility to satisfy the constraint. Therefore decentralized control strategy is best suited for directed formation graph. A graph is *constraint consistent*[155] when all agents simultaneously satisfy their respective constraints. A formation that satisfies both rigidity and constraint consistency

property is termed as *persistent* graph. *Persistence* property plays key role in the analysis of directed graph based formation control. Stability analysis focuses on preservation of underlying rigidity of directed graph with the fulfillment of constraints.

## **2.5.2 Objectives of Cooperative Motion of Multiple AUVs**

Several objectives of collaborative motion control of multiple AUVs are discussed as follows.

### **2.5.2.1 Formation Acquisition**

In formation acquisition, the goal is for the AUVs to acquire and maintain a pre-defined, fixed geometric shape in the plane. The control objective for formation acquisition, which serves as the common, primary objective for the other problems elaborated in subsequent subsections.

### **2.5.2.2 Cooperative Path Planning and Navigation**

For large scale oceanographic surveys multiple AUVs need to navigate in a complex unstructured environment without following preplanned trajectory. In [156] a task allocation based cooperative algorithm has been designed for acoustic communication.

### **2.5.2.3 Co-operative Path Following**

In cooperative path following [157]/synchronized path following, a group of AUVs follow parallel paths collectively following a particular speed assignment. A group of three AUVs follow their straight-line parallel paths for a particular mission as shown in Fig.2.21.

### **2.5.2.4 Cooperative Target Following/ Target Tracking**

In this approach, a target AUV with sensor (INS/GPS) set-up is assumed as target to be tracked by an AUV (most of cases leader AUV) in the group. The leader follows the target [158] and estimate its future position. Followers are dragged on their generated path such that desired set

of constraints (required for desired formation structure) among them are satisfied. Smooth target following objective of a group of three AUVs is shown in Fig. 2.22 where targets moves on a circular path.

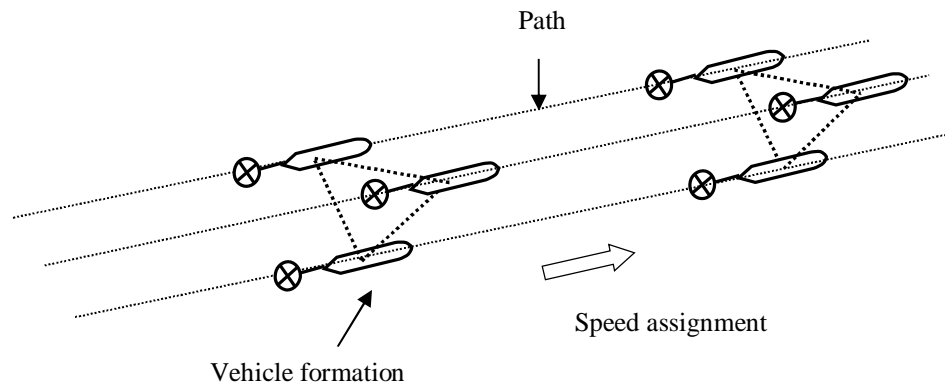


Fig 2.21 Cooperative path following of three AUVs

#### 2.5.2.5 Cooperative LOS/Way-point Target Tracking

In cooperative line of sight (LOS) tracking only leader or both [159] the leader and followers use the same steering controller which tries to look at a desired point. The desired point is a waypoint for the leader and a desired formation position for the followers. No sensor is put in way-point.

#### 2.5.2.6 Region-Based Tracking

Like a single AUV moves based on a moving region around the desired path in oceanic environment as discussed in subsection 2.2.7, a group of AUVs also may adopt same type control objectives [160] for a particular mission.

#### 2.5.2.7 Rendezvous

Rendezvous (Fig.2.25) problem of AUVs states that given a group of AUVs dispersed in a plane, how should they move together around a specific location? This is equivalent to reaching a



consensus in position by a number of AUVs with an interaction topology that is position induced (i.e., a proximity graph). Example of this kind of mission is flock of AUVs moves towards a target configuration.

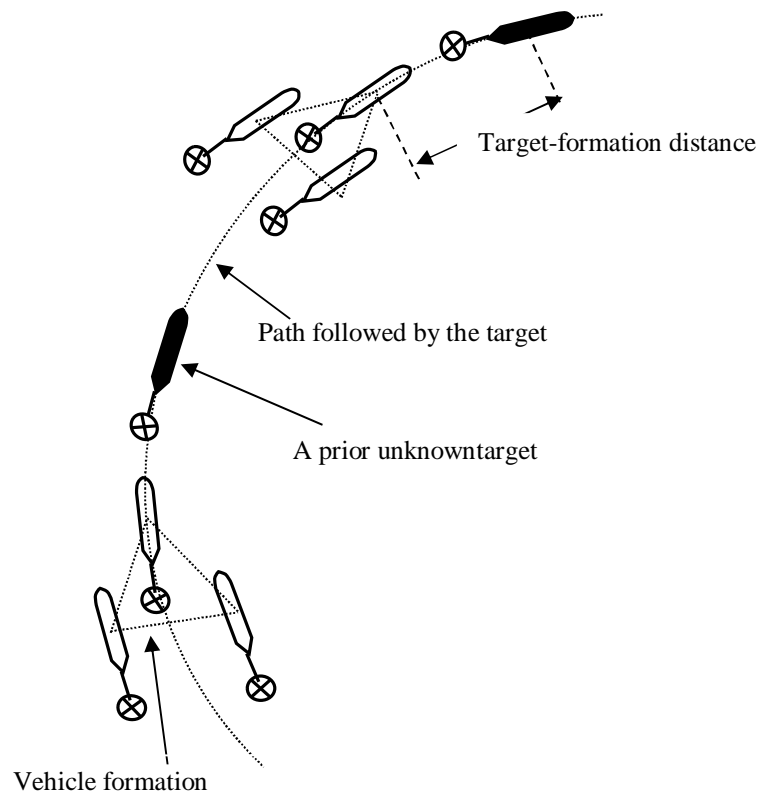


Fig 2.22 Cooperative target following of three AUVs

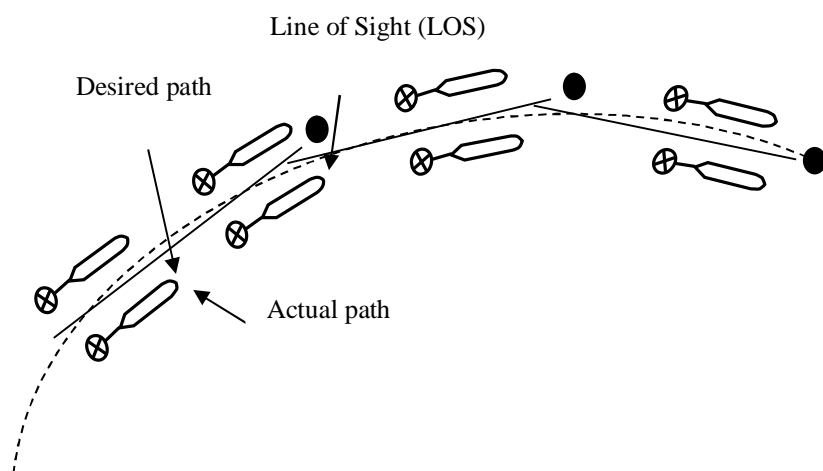


Fig 2.23 Cooperative Line of Sight (LOS) target tracking of two AUVs

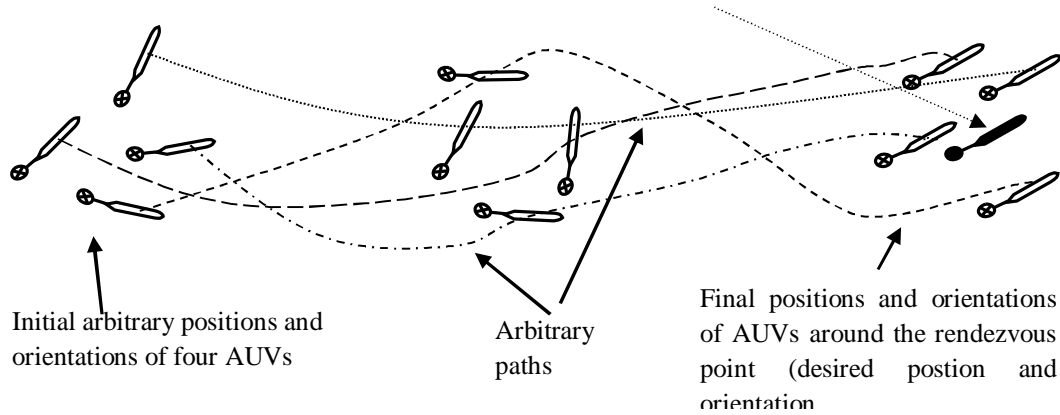


Fig. 2.24 Rendezvous of four AUVs

## 2.6 Remarks on Literature Review Conducted

The following observations are made from the literature review pursued on the control of AUVs. Dynamics of an AUV is nonlinear, time-varying and uncertain. Due to existence of highly nonlinear hydrodynamic and Coriolis effects it becomes impossible to get accurate model of an AUV. Moreover, actuators of AUV have limited output torques. If the controller commands actuators to deliver torques beyond their limited capacities, actuators saturate. Consequently, the motion is degraded. Therefore, a sophisticated control algorithm which is robust as well against actuator saturation is indispensable.

One of choices among the advanced control strategies reported in literature for motion control of single AUV or multiple AUVs in cooperative motion may be robust control. Use of different robust control strategies such that PID group controllers, SMC,  $H_\infty/\mu$  synthesis, passivity, geometric, intelligent controllers for control of AUVs indicate significant progress in the area of AUV research. These controllers, using their own methodologies, show very good behavior while treating uncertainties. Out of these controllers, PID group controllers, SMC,  $H_\infty/\mu$

synthesis are most commonly used.  $H_\infty/\mu$  synthesis controllers [73],[77],[161],[162] are not suitable in real time implementation because stability proof of most of the associated works follow the assumption of linearly approximated model where real underwater complexities are approximated. Also achievement of robust performance is still an open issue for these controllers. No significant development on application of nonlinear  $H_\infty$  for AUV is observed; rather it is in infancy stage. Among different robust strategies for tracking control of AUV traditional sliding mode SMC [163],[60] offers efficient control with respect to good disturbance rejection properties and compensation of model uncertainties. But one of the drawbacks of this control strategy wrt AUV dynamics is lacking of easy tuning of switching gain due to inclusion of parameters of complex and nonlinear dynamic model, estimated noisy states (e.g. acceleration), bound on uncertainty of constant mass property as these factors involve several approximations. Other drawbacks include high control activity at steady state due to unpleasant chattering phenomenon (discrete SMC [60]) and due to less significant equivalent control part. Reduction of chattering is possible by continuous approximation of SMC ([59],[60]). But there exists a trade off between accuracy and chattering. Owing to these drawbacks, SMC is harder to implement in complex underwater scenario. For the same reasons model-based LPID controller [22], tracking controller PD plus FC [46] suffer from implementation complexities although they ensures global asymptotic stability. Due to model-based implementation, these controllers exhibit poor transient and steady-state performances under parametric uncertainties.

Several model-free implementation of these controllers are also reported in the literature. But they have several drawbacks as follows. Simplest model-free controller for set-point control of an AUV under planar motion is PD control [47] which provides global asymptotic stability. But when the motion of AUV is considered under parametric uncertainties and within the actuators'

torque production limit, it shows poor transient and steady state performances, sometimes performances become unpredictable. Another choice of model free robust control techniques is traditional PID[46]. This controller is the simplest controller of this kind, which has adequate ability to deal with the nonlinearities and uncertainties of dynamics and can be used for both regulatory and tracking control. But LPID controller works locally[46],[55],[165],[164] domain of attraction w.r.t error in states is very narrow, when it needs to achieve certain level of precision coping with the model parameter uncertainties. Another crucial drawback of LPID is integrator wind-up [166], [167], which happens due to unlimited integral action. Due to this phenomenon, the robotic system with limited output torque of actuator suffers from large overshoot and long settling time for large initial error in states. This drawbacks prevents PID controller to be used as only controller rather they have been used in combination with other advanced controllers e.g. robust and optimal control strategies. A reparameterized PID control based on nonlinear  $H_\alpha$  control has been used in [53] to overcome the problems of slow control and measurement frequency, severe thrusters' saturation. Koh [52] proposed a simple PID control for simplified model of an underactuated AUV where parameters of controller is tuned based on constrained optimization. An exception exists in [165] where a linear PID controller with an easy to tune nonlinear PID loop has been proposed for both regulatory and tracking control in the aiming of improving transient response while satisfying an optimal energy criteria. But [53], [165] practically offer poor transient response in the form of overshoots or underdamped response with long settling time. Also control laws in [53], [165] are model-based. An improvement of [165] is available in [168] where an optimal response is obtained by tuning the slope of SMC switching surface based on principle of Pontryagin's time optimal control where neural network is used for achieving its solutions. PI control is provided at switching

phase to avoid high undesired control effort. This model free approach though offers good transient response but suffers from long settling time. Another disadvantage of these research works, similar to any other tracking controller, is that they need to estimate the acceleration as it is used in the control law.

## **2.7 Scope of Use of N-PID like Controllers for AUV**

In certain applications, accurate set point control and precision tracking of AUV are immensely expected under parametric uncertainties. Station-keeping (an example of set-point control) is one of such applications, where, an AUV needs to place itself with accurate desired position and orientation with regard to reference object (e.g. cable, underwater structure, sunken ship, and seabed), possibly with faster convergence to reduce time consumption. In unmanned docking system [169],[170] of an AUV the station-keeping[169] is also required during the first phase of docking, called homing[169],[170] where AUV needs to direct itself and dock into the seabed structure without tracking any reference path. But in the second phase of docking [169] precision (may be bounded) reference tracking is required with faster convergence to desired path to avoid collision with unmanned surface vessel (USV) guiding the AUV. AUV needs to recharge its battery during a mission in docking station at the end of a docking phase. Accurate positioning [170] is required between nose of AUV and socket/pole at docking station. Application of small AUV inside wall inspection of a pipeline in power plant requires maintaining safe distance from the wall to avoid collision with it. Therefore, this problem demands bounded tracking performance. It is also true that AUV can not be placed at the starting point of desired trajectory perfectly in these applications due to effect of ocean wave. Hence, large initial error in position state is unavoidable.

Hence, it is understood from the above discussion about several important applications of AUV that there is a requirement of special kind of robust controllers for regulation and tracking which should have ability to deal with the uncertainties in marine hydrodynamics, variations in mission payload and external disturbances and can render globally stable regulatory/globally bounded tracking performance. LPID may be the best choice due to its simplicity from the viewpoint of implementation. But from the discussion in subsection 2.5 it is clear that no significant development of LPID group controllers for AUV are observed for achieving integrator-wind-up free globally stable performance under massive parametric uncertainties and torque limits of actuators as comparing with other two robust strategies, namely SMC,  $H_\infty/\mu$ synthesis for the last several years. Several efforts are also reported for use of the combinations of LPID with nonlinear PID for regulation/tracking and optimal SMC with PI and NN [168],  $H_\infty$  with LPID for tracking. But these controllers suffer from prolonged settling time and/high overshoot and/oscillatory response which do not match with the necessary features of controllers for AUVs in the applications as mentioned in the first paragraph of this subsection.

On the other hand, several significant developments in this area of controller design to achieve better response are reported in [171], [172], [173] for regulatory and in [57], [174] for tracking for robotic manipulators. However, very little is reported on the use of these controllers in AUVs. Therefore, there is a gap between the ability of LPID and other advanced control strategies like SMC and  $H_\infty$  controllers for AUV. Hence, there is a scope of contributing in control design for AUV by improving the performance of LPID. Some modified versions of LPID controllers, called PID like controllers, are already reported for robotic manipulators as mentioned in the

next paragraph. In this work, essence of these control strategies are explored and compared for AUV.

Among recent developments of PID like controllers for regulation, the saturated-P and differential feedback with a I controller steered by a bounded nonlinear function of position errors (SP-D-N-I)[171], a linear PD feedback with an integral action of a nonlinear function of position errors (PD plus NI) [172] control, a linear PD feedback with an double integral action steered by the positions error and the filtered position ( $PI^2D$ )[173], are most important to achieve response with less overshoot and settling time with reasonable steady-state accuracy. Work in [171] [172], ensures global asymptotically stable system, whereas [173] offers semi-globally stable performance. Among the recent developments in tracking control of manipulators the work in [57] and [174] are most significant. Exponential semi-global stability for a robotic manipulator using terminal sliding mode for faster convergence has been proved in [57]. Absence of unpleasant reaching phase is the advantage of this strategy whereas functioning of terminal attractor within a limit, cumbersome tuning of different parameters, poor transient response (overshoot and oscillation) are number of drawbacks. In [174], variable structure PID control controller has been designed for robot manipulators where necessary equivalent control for SMC has not been used. Introducing integral term in sliding surface makes the control analysis problem complicated, although global stability has been proved. On the other hand, integral action of PID has capability to compensate [57] disturbance introduced by inertial and gravitational forces, which is basic requirement for any tracking controller. Also integral action increases steady state accuracy. No requirement of estimation of acceleration for controller is another advantage of the work in [57]. Some nonlinear filters have also been used to improve the performance of the proposed controllers. But all these N-PID like controllers, have efforts to

reduce the unlimited integral action but these did not focus the torque limit of actuator specifically.

The chapters 3 and 4 of this thesis address the set point regulation and tracking control problems respectively for planar motion of an AUV with the application of Nonlinear-PID (N-PID) like controllers and their combination with SMC (for tracking), keeping in mind about the torque production limit of actuators.

## **2.8 Advantages of Directed Graph Based Coordination Strategy**

In recent years, the procedure for solution of formation control problem changes from centralized [176] approach to decentralized/distributed [177], [178] one. In decentralized/distributed strategy each agent generates its control input depending upon only local measurements instead of global information requirement which is the reality in centralized scheme. But shortage of information about the entire formation makes control design of an agent complicated in decentralized scheme. However, in graph theoretic framework, decentralized coordination strategy may be implemented with any of two kinds of interaction topologies (based on information flow) namely undirected and directed graph model of formation. On the other hand, control strategies based on local information are of two kinds as found in literature. These are displacement related formation control and distance related formation control. In displacement related formation control [179], [180] each agent needs to maintain specific displacements (linear and/ angular both) from neighboring agents. This strategy allows the agents to have common directional sense. In distance based formation control [181], [182] each agent needs to maintain only specific distances from its neighbors without concerning about any directional criteria. Several graph theoretic tools like Laplacian [183], rigidity [184] for undirected graph and persistence [182] for directed graph have been used to describe structure of the formation, sensing pattern,



communication topology among agents for both these control strategies. Subsequently, these tools contribute in designing the decentralized control law for each agent in a formation. Two kinds of situation may arise in proposing control laws, namely when absolute positions [185], [182] of agents are known from their own measurement system or when each agent can measure its relative position [184],[186] w.r.t to a neighboring agent. First situation provides to achieve the control design in straightforward way by exploiting merely a position controller. Controller based on relative position measurement needs special planning. Commonly used controllers for distance based formation control depending on relative position measurements are gradient based controller derived from potential functions and direct distance dynamics based controllers. Two kinds of formulations using potential functions are found, directed graph model[186],[188],[189] and undirected graph model using rigidity property [184],[190]. Stability analysis of control algorithm in [186] exploits center manifold theorem which can not guarantee global asymptotic stability because there are various invariant sets of the robots dynamics other than the target formation. Control algorithm in [188] and [189], although ensures global exponential stability, are specific to triangular formation only. Moreover, algorithm is not extendable to higher order formation. Cai in his PhD thesis [184] has failed to provide globally asymptotically stable control algorithm due to limitation of possible occurrence of flip ambiguous realization during non-infinitesimal motion. Dörfler and Francis [190] introduced link dynamics for triangular formation and exploits differential geometric tool for global stability analysis. But Oh and Ahn in [187] have proved that there exists an unnecessary variation of already adjusted distances between agent 2 and 3 from their desired values [190]. A quite different design approach to gradient of artificial potential functions has been used in [187] to overcome the non-compactness of the equilibrium sets [188], [190]. Algorithm in [187] utilizes undirected inter-agent distance

dynamics of formation with the help of Euclidean Distance Dynamics Matrix (EDD Matrix) to formulate the problem of controlling distance based formation control. To analyze stability of this algorithm the properties of gradient systems has been exploited. Next, the concept of existence of neighborhood of a point in desired equilibrium set has been introduced such that the point is isolated from undesired equilibrium set in the neighbourhood. Consequently, local asymptotic convergence to the desired formation from an initial non-collinear formation is ensured. The work of [214] is based on measurement of absolute position of each agent where cycle free minimally persistent graph (CFMP) [155] has been used. Sandeep et.al. [214] designed a path following algorithm for multiple autonomous agents to accomplish a time-critical mission. This work has no stability proof.

From the above discussions it is observed that control strategy in the framework of undirected graph [187], [184], [194] suffers from heavy communication burden due to existence of two way communication along an edge between two agents. Therefore, it is harder to implement formation control of group of AUVs in underwater scenario using undirected framework. On the other hand, there are several advantages of directed graph model. In directed graph based formation control, only one of the two agents needs to sense the position of the other agent or receive the position information broadcast by the other agent and make decisions on its own. Advantages of directed graph based coordination are mentioned as follows,

- i) Both the overall communication complexity in terms of sensed or received information and the overall control complexity for the formation can be halved [191],[192] in contrast with the shared responsibility features of undirected graph model.
- ii) The reduction of number of communication links facilitates lower bit rates and reduced difficulties with interference.

*iii)* For rigidity maintaining problem of a formation, due to shared responsibility in undirected graph model, instability may occur. When position measurements are faulty or not communicated properly between the participating agents due to real underwater noisy environment, two agents may fail to share accurate estimated distance information. Instead, the agents use inconsistent estimates of the distance between each other [193], which may lead to generation of inaccurate control inputs. The problem is termed as information based instability. This problem cannot arise in the one sided responsibility by a single-agent where distance constraints are implemented unilaterally. Therefore, directed graph based control is more robust than its undirected counterpart.

*iv)* Many works on formation control conceive of using directed links; in the special case when the associated graph is acyclic, the control problem is more easily handled instinctively. From the existing literature on the graph based formation control mentioned above, it is noticeable that most of the distance based or displacement based techniques have been exploited only for formation acquisition of group of single integrator, double integrator, or nonholonomic point agents. A very little works are found for formation acquisition [184], tracking [183], using complex dynamics. Moreover, work in [184] has adopted centralized strategy which restricts the use of large number of AUVs in the formation due to heavy communication and computational burden. In addition, distance based control strategies only concern for maintaining the desired shape of the formation, does not care about the desired orientation of the formation. On the other hand, position-based formation control involves both desired shape as well as desired orientation of the formation.

In several applications such that surveillance for a specific area of ocean, ocean survey [152], mine sweeping [140], environmental tracking [219], a large number of AUVs are deployed to

reduce the time of collecting sufficient data. In these applications AUVs in a group are allowed to track different kinds of trajectories according to the necessity of mission. One good feature of these applications may be AUVs may need to maintain specific distances among them, maintaining the bounded permissible orientation error among the desired value.

In pipeline inspection [195] a group of AUVs cooperatively acquire 3D images. They need to move synchronously staying in a formation and track the fixed parallel paths dispersing over the actual track of the underwater pipeline. Centralized strategy has been used to reduce communication requirement to the followers from leader. But strategy suffers from single-point failure when leader fails to work. Also velocities of AUVs are needed to be synchronized to maintain desired formation which has several drawbacks discussed later. An alternative problem formulation may be adopted for the same mission, where only distances among AUVs may be maintained at their desired values to achieve desired formation. Explicitly the orientations of followers may be maintained to a bounded set around the orientation of leader. No velocity synchronization is required in this scheme.

Keeping in mind several advantages of directed formation graph and numerous possible applications of these, this thesis focuses on the distance based formation tracking control strategy based on CFMP directed graph. Fundamental works by author of this thesis towards this direction are found in [143], [182]. In [182] (in chapter five), continuous realization of CFMP formation on application of a simple model based control law for each AUV has been ensured during the desired motion of formation. In [143] (chapter 5), a position controller has been used to prove the same phenomenon. Global bounded stability of formation is ensured utilizing the information of absolute positions and orientations of AUVs. Several advantages of this kind of formation control includes

*i)* In underwater scenario, the flow of information among AUVs may be severely restricted due to security reasons (in defense applications), weak underwater communication and low bandwidth limitations. It is natural, under these circumstances, that no vehicle is able to communicate with the entire formation; furthermore, the amount of information that can be exchanged may be severely limited. Acknowledging these limitations proposed control strategy uses only linear positions and orientations as communicated data among AUVs.

*ii)* The key requirement is that all maneuvers must be collision-free as well as energy efficient. Implementation of minimally persistent formation based on gradient of artificial potential function, each AUV does not follow shortest path on its trajectory and energy requirement is more for its motion. But the proposed scheme follows shortest path method for trajectory generation of each AUV. Thus, the scheme allows each AUV to use less control effort.

*iii)* Ocean exploration by multiple AUVs involves several complexities like passing through unknown narrow region [220] or unstructured underwater environment especially where obstacles are present and AUVs need to avoid those with the generation of unknown trajectories. Merely, velocity synchronization [195] based fixed parallel path following of formation can not handle these situations. The proposed formation control strategy in this thesis does not need velocity synchronization among AUVs; rather velocities are merely maintained within their actuator limit with arbitrary trajectories followed by them. This kind of flexibility of the proposed strategy is useful in managing the problems mentioned above.

*(iv)* Although the absolute position based proposed control strategy may not be suitable for a mission in an unknown zone in ocean, because commonly used method of localization using INS suffers from large drift with the progress in motion. Therefore, control strategy of this kind of problem mostly use relative position measurement. But position based control is more

appropriate than relative measurement based formulation in a pre-specified zone e.g. in shallow water in the ocean, where localization [196] for accurate absolute coordinate is possible. Because, achievement of global stability is an advantage of position based formation control and still there is unavailability of distance preserving formation control based on relative position measurement, which can provide global stability. Pipeline inspection [195] in a specified zone in the ocean by a group of AUVs is a typical application of absolute position based strategy.

Although main objective is to control distances among agents, the orientations of AUVs are also synchronized explicitly with the orientation of leader during sufficiently smooth trajectory tracked by leader. Two different tracking control strategies are used for each AUV, namely a simple model based control law (in chapter 5) and Nonlinear-PID (N-PID) like controllers in combination with SMC (chapter 6).

Several applications of single AUV and multiple AUVs mentioned in section 2.6 and 2.7 mainly indicate their suitability in three dimensional motions. As preliminary works towards this direction this thesis focuses on development of control algorithms for planar motion.

## **2.9 Chapter Summary**

In this chapter, different motion control objectives, control architectures and their implementation algorithms for single AUV have been reviewed first. A comparative description of all the traditional and hybrid motion control algorithms based on linearized/nonlinear model of an AUV is presented. Subsequently, architecture of cooperative motion control of multiple AUVs has been described in detail which includes different decision making strategies, coordination strategies among multi-AUV system. Next, different motion control objectives of cooperative motion are briefly mentioned, which are followed by remarks on literature survey.

Thereafter, scope of use of N-PID like controllers for set-point and tracking control for AUV is elaborated. Finally, the chapter indicates benefits of directed graph based coordination strategy for multi-AUV tracking mission.





## Chapter-3

# Robust Set-Point Control of AUV using Nonlinear PID Controller with Bounded Integral and Bounded Derivative

### 3.1 Introduction

Motivated by several applications of AUV in accurate positioning, described in chapter 2, this chapter attempts to contribute some research towards set-point control of AUV. The regulation or set point stabilization refers to the problem of steering an underwater vehicle to a final target point with desired orientations from its initial configuration [28], [137]. This type of control may find application in position control system of AUV such as way-point guidance based system, station-keeping etc.

Uncertainties in hydro-dynamic parameters and torque limits of actuators restrict the operating range of AUV. It is reported that N-PID like controllers [171],[172] have robustness against bounded parametric uncertainties and actuator constraints, adopts simple controller structure which is easy for implementation, offers fast transient response and best steady state performance. On the other hand, Proportional plus Double Integral plus Derivative ( $PI^2D$ ) [173] controller further enhances the quality of transient response. Inspired by different position control applications of AUV, this chapter proposes a globally stable position control algorithm as

an improvement of aforesaid controllers [171],[172],[173]. The proposed controller which is actually a modified  $PI^2D$  controller combines a feedback action of two different nonlinear error functions e.g. one is for position error and another one is for derivative of position. Boundary values of these nonlinear functions are chosen such that summation of these boundary values when added to boundary value of nonlinear function shaping the integral action; never exceeds the input torque limit specified by actuator constraints. In the integral part of modified  $PI^2D$  controller a nonlinear function, the same function used for P-control part of proposed controller is used. Thus, the proposed set-point controller is termed as N-PID with BI (Bounded Integral) and BD (Bounded Derivative) as integral and derivative actions both remains bounded. Parameters of the nonlinear functions are set in accordance with gains of the controller. Gains of the controllers are tuned by developing several explicit conditions from the Lyapunov based analyses for achievement of global asymptotically stable system. The performance of the proposed controller is compared with a basic PID group globally stable set point controller i.e. PD controller and basic modified  $PI^2D$  controller with unbounded integral i.e. N-PID without BI and BD.

The chapter is organised as follows. Section 3.2 describes kinematics and dynamics of AUV. Section 3.3 formulates problem of this chapter. Section 3.4 describes properties of dynamic parameters of AUV. Section 3.5 provides mathematical preliminaries. Section 3.6 proposes control law. Section 3.7 derives the closed loop error dynamics whereas stability is analysed in section 3.8. Simulation results are discussed in section 3.9 whereas section 3.10 summarizes this chapter.

## 3.2. Kinematics and Dynamics of an AUV

In order to develop a robust set-point control algorithm for AUV one requires kinematics and dynamics of AUV. For describing the motion in two dimensional planes two reference frames [46] are defined for AUV, namely Inertial Reference Frame (IRF) and Body-Fixed Reference frame (BRF) which is attached with the body of it as shown in Fig.3.1. Center of mass (CoM) of AUV coincides with the origin of BRF.

### 3.2.1 Kinematic Equationsof AUV

Assume, position state  $\boldsymbol{\eta} = (x, y, \theta) \in \mathbb{R}^3$  combines the coordinate of the center of mass (CoM) of AUV with respect to inertial reference frame (IRF) and  $\theta$  which represents orientation of AUV measured from positive inertial  $x$  axis. Orientation varies from  $\theta_{min}=0$  to  $\theta_{max}=6.28$  rad [46].  $\dot{\boldsymbol{\eta}} = (\dot{x}, \dot{y}, \dot{\theta})$  represents velocity state in IRF.  $u$  and  $v$  are translational surge and sway velocities, described in body-fixed reference frame (BRF).  $\omega$  represents the angular velocity (yaw) with respect to  $z_b$  axis.  $\boldsymbol{v} = (u, v, \omega) \in \mathbb{R}^3$  represents velocity state in BRF. Thus the state  $\boldsymbol{\xi}$  of AUV is represented as

$$\boldsymbol{\xi} = (x, y, \theta, \dot{x}, \dot{y}, \dot{\theta}, u, v, \omega) = (\boldsymbol{\eta}(t), \dot{\boldsymbol{\eta}}(t), \boldsymbol{v}(t)) \in \mathbb{R}^9 \quad (3.1)$$

The kinematic relations of states (assuming anti-clock-wise rotation about positive  $Z_b$  axis) for a fully actuated AUV on the horizontal  $x$ - $y$  plane are described as follows [46]

(i) Position State in IRF:

$$\boldsymbol{\eta} = \begin{bmatrix} \boldsymbol{\eta}_1^T & \eta_2 \end{bmatrix}^T \in \mathbb{R}^3, \text{ where, } \boldsymbol{\eta}_1 = \begin{bmatrix} x & y \end{bmatrix}^T \text{ and } \eta_2 = \theta \quad (3.2a)$$

(ii) Velocity state in BRF:

$$\mathbf{v} = \begin{bmatrix} \mathbf{v}_1^T & v_2 \end{bmatrix}^T, \text{ where, } \mathbf{v}_1 = \begin{bmatrix} u & v \end{bmatrix}^T \text{ and } v_2 = \omega = \dot{\theta} = \dot{\eta}_2. \quad (3.2b)$$

(iii) Relation between quantities in IRF and BRF:

Considering the components of  $u$  and  $v$  shown in Fig.3.1 it may be written that

$$\dot{\boldsymbol{\eta}} = \begin{bmatrix} \dot{x} & \dot{y} & \dot{\theta} \end{bmatrix}^T = \mathbf{J} \mathbf{v} \quad (3.2c)$$

where,  $\mathbf{J}$  is the transformation matrix, given by  $\mathbf{J} = \begin{bmatrix} \cos\theta & -\sin\theta & 0 \\ \sin\theta & \cos\theta & 0 \\ 0 & 0 & 1 \end{bmatrix}$ .

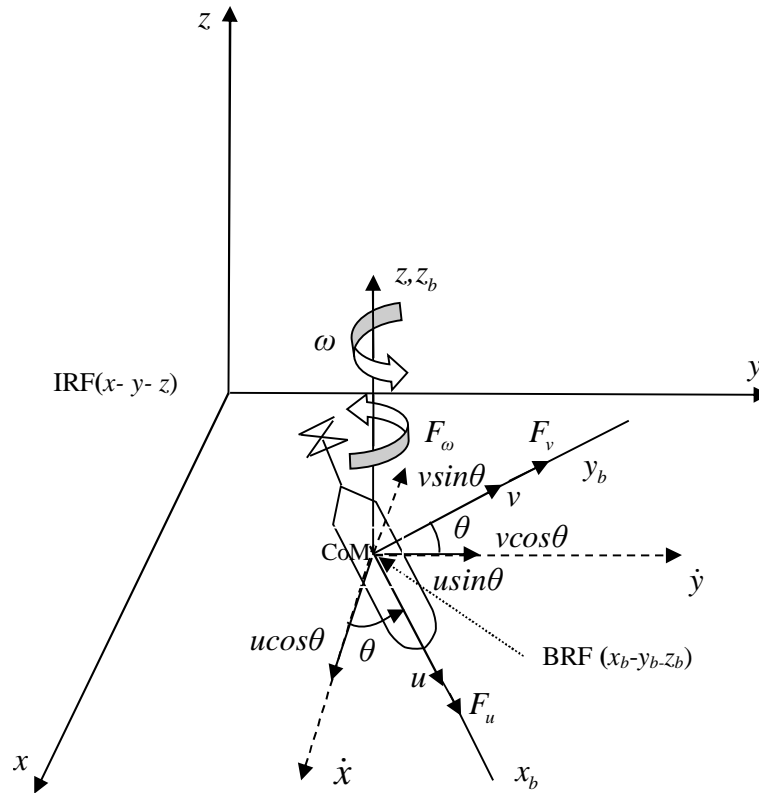


Fig.3.1 Kinematic description of an AUV

$$(iv) \dot{J}(\boldsymbol{\eta}) = J(\boldsymbol{\eta})[\boldsymbol{\omega}]^\wedge \text{ where, } [\boldsymbol{\omega}]^\wedge = \begin{bmatrix} 0 & -\omega & 0 \\ \omega & 0 & 0 \\ 0 & 0 & 0 \end{bmatrix} \quad (3.2d)$$

### 3.2.2 Dynamics of AUV

Before characterizing the motion of AUV by exploiting dynamic equations the following necessary assumptions are made [46], [24] under which these equations are valid.

*Assumptions 3.1:* i) CoM of AUV coincides with buoyancy center. ii) Distribution of mass is homogeneous. iii) The order of hydrodynamic terms is limited to two only. iv) Motions corresponding to heave, pitch and roll are neglected.

On the basis of Assumptions 3.1, the dynamics of a fully actuated neutrally buoyant AUV may be expressed in vector-matrix form as

$$M\dot{\mathbf{v}} + C(\mathbf{v})\mathbf{v} + D(\mathbf{v})\mathbf{v} = \mathbf{F} \quad (3.3)$$

where,  $M \in \mathbb{R}^{3 \times 3}$ , combines mass and inertia matrix  $M_{(RB)}$  and added mass matrix  $M_{(A)}$ . If  $m, I_z$ ,

$X_{\dot{u}}, Y_{\dot{v}}$  and  $N_{\dot{\omega}}$  stand for mass of AUV rigid body, rotational inertia, added mass in surge direction, added mass in sway direction and added mass due to rotation around  $z_b$  axis respectively, then  $M$  is expressed as

$$M = \text{diag}[m_{11} \quad m_{22} \quad m_{33}]$$

where,  $m_{11} = m - X_{\dot{u}}, m_{22} = m - Y_{\dot{v}}$  and  $m_{33} = I_z - N_{\dot{\omega}}$  are combined rigid body and added masses in surge and sway directions and combined rigid body and added inertia respectively. The Coriolis matrix  $C(\mathbf{v}) \in \mathbb{R}^{3 \times 3}$ , combines the rigid body Coriolis and Centripetal matrix  $C_{RB}(\mathbf{v})$

induced by  $M_{(A)}$  and  $C_A(\mathbf{v})$ , Coriolis-like matrix which is induced by  $M_{(AB)}$ .  $C(\mathbf{v})$  is expressed as follows

$$C(\mathbf{v}) = \begin{bmatrix} 0 & -m\omega & Y_v v \\ m\omega & 0 & -X_u u \\ -Y_v v & X_u u & 0 \end{bmatrix}$$

Hydrodynamic damping matrix with its parameters is given by

$$D(\mathbf{v}) = \begin{bmatrix} X_u + X_{u|u}|u| & 0 & 0 \\ 0 & Y_v + Y_{v|v}|v| & 0 \\ 0 & 0 & N_\omega + N_{\omega|\omega}|\omega| \end{bmatrix}$$

where,  $X_u, Y_v, N_\omega$ : linear drag coefficient and  $X_{u|u}, Y_{v|v}, N_{\omega|\omega}$ : quadratic drag coefficients. Control

input,  $\mathbf{F} = [\mathbf{F}_v^T \quad F_\omega]^T = [F_u \quad F_v \quad F_\omega]^T \in \mathbb{R}^3$ , where,  $\mathbf{F}_v$  and  $F_\omega$  represent control force vector and torque (to produce angular motion around  $Z_b$  axis) to be designed.  $F_u$  and  $F_v$  in  $\mathbf{F}_v$  represent control forces applied along surge and sway direction respectively.

*Assumptions 3.2:* Forces along surge and sway direction and torque for angular motion produced by actuators of AUV have known maximum limits. Thus, actuators satisfy following limits

$$|\mathbf{F}| \leq \mathbf{F}_{max} \quad (3.4)$$

where,  $|\mathbf{F}| = [|\mathbf{F}_v|^T \quad |F_\omega|]^T = [F_u \quad F_v \quad F_\omega]^T$  and  $\mathbf{F}_{max} = [\mathbf{F}_{vmax} \quad F_{\omega max}]^T = [F_{umax} \quad F_{vmax} \quad F_{\omega max}]^T$ .  $F_{umax}, F_{vmax}, F_{\omega max}$  are maximum forces in surge and sway direction and maximum torque around

$Z_b$ .

### 3.3 Problem Formulation

Consider an AUV with kinematics and dynamics as given in (3.2) and (3.3) respectively. It is intended to study the motion of AUV under following assumptions

*Assumptions 3.3:*

- i) Absolute linear position and orientation using navigation sensor[196] and magnetic compass are available to AUV. It is assumed that these measurements are free of noise.
- ii) AUV can measure/estimate its translational velocities, angular velocities in IRF. These measured values are assumed noise free.

For proposing the set-point control algorithm, the position regulation error of AUV is defined in IRF as

$$\boldsymbol{\eta}_e(t) = \boldsymbol{\eta}(t) - \boldsymbol{\eta}_r(t). \quad (3.5)$$

where,  $\boldsymbol{\eta}(t) \in \mathbb{R}^3$  and  $\boldsymbol{\eta}_r(t) \in \mathbb{R}^3$  are the instantaneous and desired position state of the AUV. Let,  $\boldsymbol{\xi}(0) = (\boldsymbol{\eta}(0), \dot{\boldsymbol{\eta}}(0), \boldsymbol{v}(0)) \in \mathbb{R}^9$  and  $\boldsymbol{\xi}_r(0) = (\boldsymbol{\eta}_r(0), \mathbf{0}, \mathbf{0}) \in \mathbb{R}^9$  are initial and constant desired state of the AUV respectively. Initial error is defined as  $\boldsymbol{\xi}_e(t) = (\boldsymbol{\eta}_e(t), \dot{\boldsymbol{\eta}}_e(t), \boldsymbol{v}_e(t)) \in \mathbb{R}^9$ . The objective is to design a  $\boldsymbol{F}$  for given AUV under the Assumption 3.3 such that  $\boldsymbol{\xi}_e(t)$  converges to  $[\mathbf{0}] \in \mathbb{R}^9, \forall t \geq 0$  in presence of bounded model parameter uncertainties as mentioned in Table 3.6 and under the actuator constraints of Assumptions 3.2.

### 3.4 Properties of Dynamic Parameters of AUV

To include robustness in the proposed control algorithm for achieving desired output, it is essential to explore the upper and lower bounds of the parameter matrices and their behavior in combination with states of AUV in its dynamics (3.3). These matrices are symmetric positive definite or skew-symmetric. Hence, properties of the matrices play crucial role in the design procedure of controller in terms setting of gains. Before discussing the properties of parameter matrices, an important property of an  $n$ -dimensional Euclidean vector and any square matrix should be mentioned.

*Notation:* The norm of any vector  $\mathbf{x} \in \mathbb{R}^n$  is defined as  $\|\mathbf{x}\| = \sqrt{\mathbf{x}^T \mathbf{x}}$ .  $\lambda_{\min}\{A\}$  and  $\lambda_{\max}\{A\}$  are

used to indicate its smallest and largest eigen values of any real square matrix  $A$ . The induced norm of  $A$

is  $\|A\| = \sqrt{\lambda_{\max}\{A^T A\}}$ .

The following properties are then defined for parameter matrices of (3.3)

*Property 3.1*[46]: The inertia matrix, including the added mass is symmetric and positive definite and constant such that  $M^T = M$  and  $\dot{M} = 0$ .

*Property 3.2*[46]: The Coriolis and centripetal matrices, is skew-symmetric matrices such that for all  $C(\mathbf{v}) = -C^T(\mathbf{v})$ ,  $\forall \mathbf{v} \in \mathbb{R}^3$ .

*Property 3.3* [46],[172]:  $C(m, X_u, Y_v, \mathbf{x})\mathbf{y} = C(m, X_u, Y_v, \mathbf{y})\mathbf{x}$ ,  $\forall \mathbf{x}, \mathbf{y} \in \mathbb{R}^3$

*Property 3.4*[46],[172]:  $\mathbf{x}^T C(m, X_u, Y_v, \mathbf{y})\mathbf{x} = 0$ ,  $\forall \mathbf{x}, \mathbf{y} \in \mathbb{R}^3$

*Property 3.5*[46]: The matrix  $D$  is strictly positive.



*Property 3.6[46]:* The matrix  $J(\boldsymbol{\eta})$  satisfies  $J^{-1}(\boldsymbol{\eta}) = J^T(\boldsymbol{\eta})$ . This implies  $J(\boldsymbol{\eta})$  is orthogonal i.e

$$J(\boldsymbol{\eta}) J^T(\boldsymbol{\eta}) = J^T(\boldsymbol{\eta}) J(\boldsymbol{\eta}) = I.$$

*Property 3.7:* A list of some useful structural properties of AUV dynamic model is given below.

These properties are supportive for stability analysis.

$$(i) \quad 0 < \lambda_{\min}\{M\} \leq \|M\| \leq \lambda_{\max}\{M\} \quad \text{where,} \quad \lambda_{\max}\{M\} = \left\{ \max_{\substack{i=1..3 \\ j=1..3}} |(M)_{ij}| \right\} \quad \text{and} \quad \lambda_{\min}\{M\} = \left\{ \min_{\substack{i=1..3 \\ j=1..3}} |(M)_{ij}| \right\}.$$

Procedure of finding out the  $\lambda_{\max}\{M\}$  and  $\lambda_{\min}\{M\}$  depends on the uncertainties in parameters of AUV dynamics. The procedure is elaborated in Appendix A.1.

(ii) A similar procedure of estimation of max/min of  $M$  matrix,  $\lambda_{\max}\{D(\mathbf{v})\}$  and  $\lambda_{\min}\{D(\mathbf{v})\}$  can be found out based on maximum and minimum values of hydrodynamic parameters and maximum and minimum of  $\mathbf{v}$ , as described in Appendix A.2.

(iii)  $\|C(m, X_u, Y_v, \mathbf{x})\mathbf{y}\| \leq C_m \|\mathbf{x}\| \|\mathbf{y}\|, \forall \mathbf{x}, \mathbf{y} \in \mathbb{R}^3$ . Procedure of obtaining the value of  $C_m$  is

described Appendix A.3.

### 3.5 Mathematical Preliminaries

Prior to development of control algorithm, a class of nonlinear functions are defined which have significant role in the development of control law. Their definitions and properties are given as

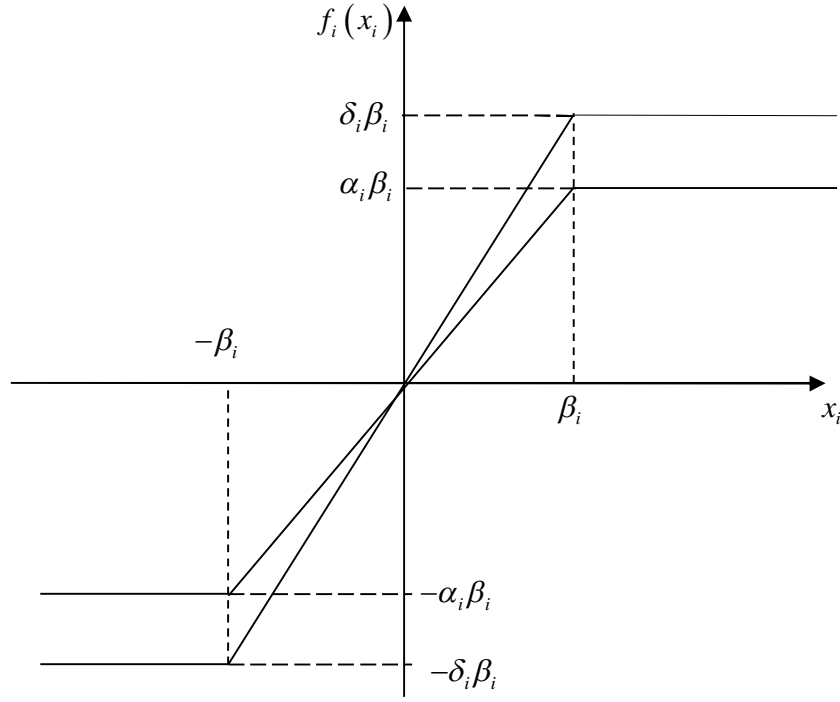


Fig 3.2 Element  $f_i(x_i)$  of function vectors  $\mathbf{f}(\mathbf{x})$

*Definition 3.1* [172], [197]:  $L(\boldsymbol{\alpha}, \boldsymbol{\beta}, \boldsymbol{\delta}, \mathbf{x})$  with  $\mathbf{x} \in \mathbb{R}^n$  and constant vectors  $\boldsymbol{\alpha}, \boldsymbol{\beta}, \boldsymbol{\delta} \in \mathbb{R}^n$  denotes the set of all *continuously piece-wise differentiable increasing (CPDI)* function vectors  $\mathbf{f}(\mathbf{x}) = [f_1(x_1) \ f_2(x_2) \ \dots \ f_n(x_n)]^T \in \mathbb{R}^n$ , and  $\mathbf{x} = [x_1 \ x_2 \ \dots \ x_n] \in \mathbb{R}^n$   $\delta_i > 0, \beta_i > 0, \delta_i \geq \alpha_i > 0, \forall i = 1, 2, 3, \dots, n$ , such that

$$\begin{aligned} & (i) \delta_i |x_i| \geq f_i(x_i) \geq \alpha_i |x_i|, \forall x_i \in \mathbb{R}, |x_i| < \beta_i; (ii) \delta_i \beta_i \geq |f_i(x_i)| \geq \alpha_i \beta_i, \forall x_i \in \mathbb{R}, |x_i| \geq \beta_i; \\ & (iii) \delta_i \geq (d/dx_i) f_i(\mathbf{x}) \geq 0, \forall x_i \in \mathbb{R} (iv) G_f(\mathbf{x}) = \frac{\partial \mathbf{f}(\mathbf{x})}{\partial \mathbf{x}^T} = \text{diag} \left\{ \frac{\partial f_i(\mathbf{x})}{\partial x_i}, i = 1, 2, \dots, n \right\} \end{aligned}$$

where,  $\|\cdot\|$  represents absolute value. Fig.3.2 depicts the region allowed for functions belonging to set  $L(\alpha, \beta, \delta, x)$

Following the similar observation [200], [172] the following Lemma is introduced.

*Lemma 3.1:* The Euclidean norm of  $f(x)$  has following properties

$$\begin{aligned}
 (i) \|f(x)\| &\leq \begin{cases} \delta_{\max} \|x\|, & \text{if } \|x\| < \|\beta\| \\ \sqrt{n} \delta_{\max} \beta_{\max} & \text{where, } \delta_{\max} = \max_i \{\delta_i\}, \beta_{\max} = \max_i \{\beta_i\}, \text{ if } \|x\| \geq \|\beta\| \end{cases} \\
 (ii) f^T(x)x &\geq \begin{cases} \alpha_{\min} \|x\|^2, & \text{where, } \alpha_{\min} = \min_i \{\alpha_i\}, \text{ if } \|x\| < \|\beta\| \\ \min_i \{\alpha_i \beta_i\} \|x\|, & \text{if } \|x\| \geq \|\beta\| \end{cases} \\
 (iii) \|f(x)\|^2 &\leq \begin{cases} \sigma_1 \|x\|^2, & \sigma_1 = \delta_{\max}^2, \text{ if } \|x\| < \|\beta\| \\ \sigma_2 \|x\|^2, & \text{if } \|x\| \geq \|\beta\| \text{ where, } \sigma_2 = \frac{\delta_{\max}^2 \beta_{\max}^2}{\beta_{\min}^2} \end{cases} \quad (iv) \delta_{\max} \geq \|G_f(x)\| \geq 0
 \end{aligned}$$

Proof: Results of Lemma 3.1(i), (ii), (iv) are direct consequences of Definition 3.1 (i), (ii) and (iv).

See Appendix A.4 proof for Lemma 3.1(iii)

Next lemma is proposed associated with the integral of  $f_i(x_i)$ .

*Lemma 3.2:* There exists a constant  $\wp_i > 0$ , such that,  $\int f_i(x_i) dx_i \geq \wp_i f^2(x_i)$ , for  $x \neq 0$ .

*Proof:* Proof of this Lemma is given in A.5 of Appendix.

### 3.6 N-PID with BI and BD Control Law

Motivated by the effective use of N-PID like controllers [197], [200] for set-point control and taking help of section 3.1, 3.2 and 3.3, a feedback controller is proposed for set-point control of AUV as follows

$$\mathbf{F} = -\mathbf{K}_d \mathbf{f}_d(\mathbf{v}) - \mathbf{J}^T(\boldsymbol{\eta}) \mathbf{K}_p \mathbf{f}_p(\boldsymbol{\eta}_e) - \mathbf{K}_w \mathbf{f}_w(\boldsymbol{\chi}) \quad (3.6)$$

where,  $\boldsymbol{\chi}_e = \int_0^t [\mathbf{v}(\xi) + \rho \mathbf{J}^T(\boldsymbol{\eta}) \mathbf{f}_p^T(\boldsymbol{\eta}_e(\xi))] d\xi$  and  $\mathbf{f}_d \in L(\boldsymbol{\alpha}_d, \boldsymbol{\beta}_d, \boldsymbol{\delta}_d, \cdot), \mathbf{f}_p \in L(\boldsymbol{\alpha}_p, \boldsymbol{\beta}_p, \boldsymbol{\delta}_p, \cdot),$

$\mathbf{f}_w \in L(\boldsymbol{\alpha}_w, \boldsymbol{\beta}_w, \boldsymbol{\delta}_w, \cdot)$  are all CPDI functions. Parameters of these functions are made directly associated with the controllers' gains to limit the total surge and sway forces and torque demand from the controller. Descriptions of the parameters of nonlinear functions used in control law 3.6 are given below.

$$\left. \begin{aligned} &f_{di} : \beta_{di} = \frac{B_{di}}{K_{di}}, \text{ where, } \delta_{di} B_{di} = \emptyset_{\delta_{\max}(i)} = \emptyset_{\delta_{\max}(l)}, \forall i=1,2; \delta_{d3} B_{d3} = \emptyset_{\delta_{\max}(3)} = \emptyset_{\delta_{\max}(w)}; \emptyset_{\delta_{\max}(w)} \leq \emptyset_{\delta_{\max}(l)} \\ &\text{and, } \alpha_{di} B_{di} = \emptyset_{\alpha_{\max}(i)} = \emptyset_{\alpha_{\max}(l)}, \forall i=1,2; \alpha_{d3} B_{d3} = \emptyset_{\alpha_{\max}(3)} = \emptyset_{\alpha_{\max}(w)}; \emptyset_{\alpha_{\max}(w)} \leq \emptyset_{\alpha_{\max}(l)}. \\ &f_{pi} : \beta_{pi} = \frac{B_{pi}}{K_{pi}}, \text{ where, } \delta_{pi} B_{pi} = \emptyset'_{\delta_{\max}(i)} = \frac{\emptyset'_{\delta_{\max}(l)}}{\sqrt{2}}, \forall i=1,2; \delta_{p3} B_{p3} = \emptyset'_{\delta_{\max}(3)} = \emptyset'_{\delta_{\max}(w)}; \emptyset'_{\delta_{\max}(w)} \leq \frac{\emptyset'_{\delta_{\max}(l)}}{\sqrt{2}} \\ &\text{and, } \alpha_{pi} B_{pi} = \emptyset'_{\alpha_{\max}(i)} = \frac{\emptyset'_{\alpha_{\max}(l)}}{\sqrt{2}}, \forall i=1,2; \alpha_{p3} B_{p3} = \emptyset'_{\alpha_{\max}(3)} = \emptyset'_{\alpha_{\max}(w)}; \emptyset'_{\alpha_{\max}(w)} \leq \frac{\emptyset'_{\alpha_{\max}(l)}}{\sqrt{2}}. \\ &f_{wi} : \beta_{wi} = \frac{B_{wi}}{K_{wi}}, \text{ where, } \delta_{wi} B_{wi} = \emptyset''_{\delta_{\max}(i)} = \emptyset''_{\delta_{\max}(l)}, \forall i=1,2; \delta_{w3} B_{w3} = \emptyset''_{\delta_{\max}(3)} = \emptyset''_{\delta_{\max}(w)}; \emptyset''_{\delta_{\max}(w)} \leq \emptyset''_{\delta_{\max}(l)}, \\ &\text{and, } \alpha_{wi} B_{wi} = \emptyset''_{\alpha_{\max}(i)} = \emptyset''_{\alpha_{\max}(l)}, \forall i=1,2; \alpha_{w3} B_{w3} = \emptyset''_{\alpha_{\max}(3)} = \emptyset''_{\alpha_{\max}(w)}; \emptyset''_{\alpha_{\max}(w)} \leq \emptyset''_{\alpha_{\max}(l)}. \end{aligned} \right\} \quad (3.7)$$

where,  $\mathbf{K}_d, \mathbf{K}_r, \mathbf{K}_w$  are  $3 \times 3$  order diagonal positive definite feedback gain matrices,  $\rho$ , all  $\emptyset$  and all  $B$  in (3.7) are a positive constants.  $\mathbf{J}^T(\boldsymbol{\eta})$  is used to convert the error quantity of control law to BRF of AUV.  $\mathbf{v}$  can be estimated from the estimated states  $(\dot{\boldsymbol{\eta}})$  in IRF with help of transformation matrix. First part of this controller is the velocity damping term, which is bounded through  $\mathbf{f}_d(\cdot)$  and facilitates to provide asymptotic stability of the closed loop system of AUV under actuators' torque limit. Second part uses a filtered position error feedback using  $\mathbf{f}_p(\cdot)$  to enhance the global stability. Last term of (3.6) includes an integral of combination of filtered position error plus a differential feedback term, which is further shaped by  $\mathbf{f}_w(\cdot)$ . Hence,

the controller is named as N-PID controller with Bounded Integral (BI) and Bounded Derivative(BD). Typical structure of proposed controller is given in Fig 3.3.

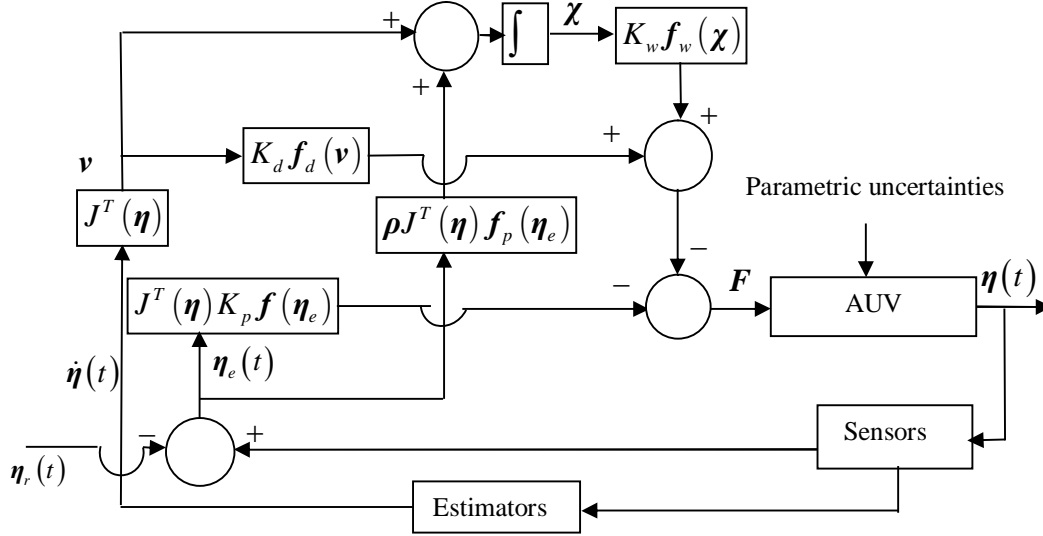


Fig. 3.3 Controller structure for set-point control of AUV using N-PID

### 3.7 Closed-Loop Set-Point Error Dynamics of AUV

The closed-loop dynamics of system of AUVs can be obtained by substituting (3.5) into (3.3),

$$M\dot{v} + C(v)v + D(v)v + K_d f_d(v) + J^T(\eta) K_p f_p(\eta_e) = -K_w f_w(\chi_e) \quad (3.8)$$

An integral action can define a zero state observable passive mapping with a radially unbounded and positive definite storage function [200]. In the line of this concept, a scalar potential function is defined corresponding to the expression of integral control action using bounded integrator in (3.6). In section 3.8, this function typically acts as a storage function for passivity based stability analysis of regulatory control of AUV.

Value of integral of a CPDI function over a region of independent variable is always positive or equal to zero. Hence, following *Lemma* holds.

*Lemma 3.4:* If integral of  $f_w(\chi_e)$ , is defined as

$$W = \int f_w(\chi_e) K_w d\chi_e, \chi_e \in \mathbb{R}^3 \quad (3.9)$$

Then, following two statements can be made for  $W$ .

(i)  $W$  is positive definite, as  $W(\chi_e) > 0$  when  $\chi_e \neq 0$  and  $W(0) = 0$

(ii)  $W$  is radially unbounded as  $W(\chi_e) \rightarrow \infty$  when  $|\chi_e| \rightarrow \infty$

In section 3.8,  $W$  is typically considered as a storage function for passivity based stability analysis of regulatory control of AUV.

### 3.8 Stability Analysis

To ensure the global asymptotic stability of the closed-loop system (3.8), conditions are provided on gain matrices. This is established in the form of the following theorem.

*Theorem 3.1:* Consider the dynamics (3.3) together with control law (3.6), such that following LMI based inequalities

$$\lambda_{\min} \{K_p\} \rho_{\min} > \rho^2 \lambda_{\max} \{M\} \quad (3.10a)$$

$$\lambda_{\min} \{K_d\} \alpha_{d\min} - \rho \frac{\lambda_{\max} \{K_d\}}{2} \sigma_{1d} > \rho \Gamma_1 - \lambda_{\min} (D(\mathbf{v})) \quad (3.10b)$$

$$\text{where, } \Gamma_1 = \left\{ \sqrt{3} \delta_{p\max} \beta_{p\max} C_{\max} + \frac{1}{2} \lambda_{\max} \{D(\mathbf{v})\} + \delta_{p\max} \lambda_{\max} \{M\} + \frac{1}{2} \lambda_{\max} \{M\} \omega_{\max} \right\}$$

$$\text{For } \rho \neq 0, \lambda_{\min} \{K_p\} > \Gamma_2 \quad (3.10c)$$

$$\text{where, } \Gamma_2 = \frac{1}{2} \left[ \lambda_{\max} \{D(\mathbf{v})\} + \lambda_{\max} \{K_d\} + \lambda_{\max} \{M\} \omega_{\max} \right]$$

$$\left(\rho\Gamma_1 - \lambda_{\min}(D(\mathbf{v}))\right) \geq \frac{\lambda_{\min}\{K_d\} \min_i \{\alpha_{di} \beta_{di}\}}{V_{\max}} - \rho \frac{\lambda_{\max}\{K_d\}}{2} \sigma_{2d} \quad (3.10d)$$

are satisfied, then the closed-loop system (3.8) is globally asymptotically stable i.e.  $\lim_{t \rightarrow \infty} \boldsymbol{\eta}_e(t) = 0$  and  $\lim_{t \rightarrow \infty} \mathbf{v}(t) = 0$ , under parametric uncertainties.

In addition, if parameter values of nonlinear functions based on (3.7), satisfy (3.11a) and (3.11b)

$$\varnothing_{\delta \max(l)} + \varnothing'_{\delta \max(l)} + \varnothing''_{\delta \max(l)} \leq F_{u \max}, \varnothing_{\delta \max(l)} + \varnothing'_{\delta \max(l)} + \varnothing''_{\delta \max(l)} \leq F_{v \max} \quad (3.11a)$$

$$\varnothing_{\delta \max(\omega)} + \varnothing'_{\delta \max(\omega)} + \varnothing''_{\delta \max(\omega)} \leq F_{\omega \max} \quad (3.11b)$$

then the forces and torque hold the actuator constraints i.e.  $|F_u| \leq F_{u \max}$ ,  $|F_v| \leq F_{v \max}$  and  $|F_\omega| \leq F_{\omega \max}$ .

*Proof:* To examine passivity [218],[200],[198],[199] for the input-output relationship of system of AUV corresponding to regulatory control, let us define an output vector

$$\boldsymbol{\gamma} = \mathbf{v} + \rho \mathbf{J}^T(\boldsymbol{\eta}) \mathbf{f}_p(\boldsymbol{\eta}_e) \quad (3.12a)$$

Hence, the following relation holds true from the expression of  $\boldsymbol{\chi}$ .

$$\dot{\boldsymbol{\chi}} = \boldsymbol{\gamma} \quad (3.12b)$$

Consider the integral action of (3.6) as an extra input to the system of AUV. To carry out stability for the closed-loop system (3.8), the inner product of (3.12a) and (3.8), is taken as

$$\boldsymbol{\gamma}^T (-K_w \mathbf{f}_w(\boldsymbol{\chi})) = \boldsymbol{\gamma}^T (M\dot{\mathbf{v}} + C(\mathbf{v})\mathbf{v} + D(\mathbf{v})\mathbf{v} + K_d \mathbf{f}_p(\mathbf{v}) + K_p \mathbf{J}^T(\boldsymbol{\eta}) \mathbf{f}_p(\boldsymbol{\eta}_e)) \quad (3.13)$$

Considering the *Property 3.4*, eq.(3.13) can expressed as follows

$$\frac{dV}{dt}(\boldsymbol{\chi}_e, \mathbf{f}_p(\boldsymbol{\eta}_e), \mathbf{v}) + Q(\mathbf{f}_p(\boldsymbol{\eta}_e), \mathbf{v}, \mathbf{f}_d(\mathbf{v})) = 0 \quad (3.14)$$

$$\text{for } V = V_1 + V_2 \quad (3.15)$$

where,

$$V_1(\mathbf{v}, \mathbf{f}_p(\boldsymbol{\eta}_e), \boldsymbol{\eta}) = \frac{1}{2} \mathbf{v}^T \mathbf{M} \mathbf{v} + \rho \mathbf{f}_p^T(\boldsymbol{\eta}_e) J(\boldsymbol{\eta}) \mathbf{M} \mathbf{v} + \sum_{i=1}^3 \int_0^{\boldsymbol{\eta}_e(i)} \mathbf{f}_{pi}^T(\boldsymbol{\eta}_e(i)) K_{pi} d\boldsymbol{\eta}_e(i) \quad (3.16a)$$

$$\text{and } V_2 = W(\boldsymbol{\chi}). \quad (3.16b)$$

where,  $W$  is defined in (3.9) and the dissipation rate  $Q$  is combination of two parts i.e.

$$Q = Q_1 + Q_2 \quad (3.17)$$

where,

$$Q_1 = \mathbf{v}^T K_d \mathbf{f}_d(\mathbf{v}) + \mathbf{v}^T D(\mathbf{v}) \mathbf{v} + \rho \mathbf{f}_p^T(\boldsymbol{\eta}_e) K_p \mathbf{f}_p(\boldsymbol{\eta}_e) \quad (3.18a)$$

$$\begin{aligned} Q_2 = & \rho \left\{ \mathbf{f}_p^T(\boldsymbol{\eta}_e) J(\boldsymbol{\eta}) C(\mathbf{v}) \mathbf{v} + \mathbf{f}_p^T(\boldsymbol{\eta}_e) J(\boldsymbol{\eta}) D(\mathbf{v}) \mathbf{v} + \mathbf{f}_p^T(\boldsymbol{\eta}_e) J(\boldsymbol{\eta}) K_d \mathbf{f}_d(\mathbf{v}) \right. \\ & \left. - \dot{\mathbf{f}}_p^T(\boldsymbol{\eta}_e) J(\boldsymbol{\eta}) \mathbf{M} \mathbf{v} - \mathbf{f}_p^T(\boldsymbol{\eta}_e) \dot{J}(\boldsymbol{\eta}) \mathbf{M} \mathbf{v} \right\} \end{aligned} \quad (3.18b)$$

It can be proved that  $V$  is positive definite in  $\mathbf{f}_d(\mathbf{v}), \mathbf{f}_p(\boldsymbol{\eta}_e)$  and  $\mathbf{v}$ . Hence,  $V$  eventually becomes a Lyapunov function for stability analysis of set-point control of AUV. With respect to  $V_1$  of (3.15) following inequality holds true based on an established condition.

$$\begin{aligned} H = & \frac{1}{4} \left( \mathbf{v} + 2\rho J^T(\boldsymbol{\eta}) \mathbf{f}_p(\boldsymbol{\eta}_e) \right)^T \mathbf{M} \left( \mathbf{v} + 2\rho J^T(\boldsymbol{\eta}) \mathbf{f}_p(\boldsymbol{\eta}_e) \right) - \rho^2 \mathbf{f}_p^T(\boldsymbol{\eta}_e) J(\boldsymbol{\eta}) \mathbf{M} J^T(\boldsymbol{\eta}) \mathbf{f}_p(\boldsymbol{\eta}_e) \\ & + \sum_{i=1}^3 \int_0^{\boldsymbol{\eta}_e(i)} \mathbf{f}_{pi}^T(\boldsymbol{\eta}_e(i)) K_{pi} d\boldsymbol{\eta}_e(i) \end{aligned} \quad (3.19a)$$



In(3.19a),  $J(\boldsymbol{\eta})MJ^T(\boldsymbol{\eta})$  is a symmetric matrix and  $J(\boldsymbol{\eta})$  is orthogonal. Thus,  $\lambda_{\max}\{J(\boldsymbol{\eta})MJ^T(\boldsymbol{\eta})\} = \lambda_{\max}\{M\}$ . With the help of *Lemma 3.2*, following inequality can be obtained from(3.19a), if (3.10a) is satisfied,

$$H \geq \lambda_{\min}\{K_p\} \wp_{\min} \|\mathbf{f}_p(\boldsymbol{\eta}_e)\|^2 - \rho^2 \lambda_{\max}\{M\} \|\mathbf{f}_p(\boldsymbol{\eta}_e)\|^2 \quad (3.19b)$$

where,  $\wp_{\min} = \min_i \{\wp_i\}$ . Substituting (3.19b) in (3.16a), one gets

$$V_1 \geq \frac{1}{4} \mathbf{v}^T M \mathbf{v} + (\lambda_{\min}\{K_p\} \wp_{\min} - \rho^2 \lambda_{\max}\{M\}) \|\mathbf{f}_p(\boldsymbol{\eta}_e)\|^2 \geq 0 \quad (3.20)$$

if (3.10a) is satisfied.  $V_2$  is radially unbounded positive definite function according to *Lemma 3.4*. Hence,  $V$  is a radially unbounded globally positive definite function according to (3.15). Next, the time derivative of  $V$  is proved negative semidefinite. According to (3.14), showing negative semi-definiteness of  $V$  is equivalent to showing positive semidefiniteness of  $Q$ .

As  $\mathbf{f}_p^T(\boldsymbol{\eta}_e)$  is bounded, lower bound of  $Q_2$  is derived from below mentioned four inequalities.

Using *Property 3.7(iii)*, *Lemma 3.1(iii)*, eq.(3.7) and putting  $n=3$  and  $\|J(\boldsymbol{\eta})\| = 1$ , one may write for the first part of  $Q_2$

$$\rho \mathbf{f}_p^T(\boldsymbol{\eta}_e) J(\boldsymbol{\eta}) C(\mathbf{v}) \mathbf{v} \geq -\rho \delta_{p_{\max}} \beta_{p_{\max}} \sqrt{3} C_{\max} \|\mathbf{v}\|^2 \quad (3.21a)$$

Using *Property 3.7(ii)*, and noting the fact [199]

$$-\left(\|\mathbf{f}_p(\boldsymbol{\eta}_e)\|^2 + \|\mathbf{v}\|^2\right) \leq 2\|\mathbf{f}_p(\boldsymbol{\eta}_e)\| \|\mathbf{v}\| \leq \|\mathbf{f}_p(\boldsymbol{\eta}_e)\|^2 + \|\mathbf{v}\|^2$$

following inequality can be obtained from the second part of  $Q_2$

$$\rho \mathbf{f}_p^T(\boldsymbol{\eta}_e) J(\boldsymbol{\eta}) D(\mathbf{v}) \mathbf{v} \geq \rho \|J(\boldsymbol{\eta}) D(\mathbf{v})\| \frac{1}{2} (\|\mathbf{f}_p(\boldsymbol{\eta}_e)\|^2 + \|\mathbf{v}\|^2) \geq -\rho \lambda_{\max}\{D(\mathbf{v})\} \frac{1}{2} (\|\mathbf{f}_p(\boldsymbol{\eta}_e)\|^2 + \|\mathbf{v}\|^2) \quad (3.21b)$$

For the third part of  $Q_2$ , one may get following inequality with the help of *Lemma 3.1(i)*

$$\begin{aligned} \rho \mathbf{f}_p^T(\boldsymbol{\eta}_e) J(\boldsymbol{\eta}) K_D \mathbf{f}_D(\mathbf{v}) &\geq -\rho \|J(\boldsymbol{\eta}) K_D\| \frac{1}{2} (\|\mathbf{f}_p(\boldsymbol{\eta}_e)\|^2 + \|\mathbf{f}_D(\mathbf{v})\|^2) \\ &\geq \begin{cases} -\rho \lambda_{\max}\{K_D\} \frac{1}{2} (\|\mathbf{f}_p(\boldsymbol{\eta}_e)\|^2 + \sigma_{1d} \|\mathbf{v}\|^2), & \text{if } \|\mathbf{v}\| < \|\boldsymbol{\beta}_d\|, \text{ where, } \sigma_{1d} = \delta_{d\max}^2 \\ -\rho \lambda_{\max}\{K_D\} \frac{1}{2} (\|\mathbf{f}_p(\boldsymbol{\eta}_e)\|^2 + \sigma_{2d} \|\mathbf{v}\|^2), & \text{if } \|\mathbf{v}\| \geq \|\boldsymbol{\beta}_d\|, \text{ where, } \sigma_{2d} = \frac{\delta_{d\max}^2 \beta_{d\max}^2}{\beta_{d\min}^2} \end{cases} \end{aligned} \quad (3.21c)$$

Using *Property 3.7 (i)*, *Lemma 3.1 (iii)* and (3.7), the following inequality holds good for fourth part of  $Q_2$

$$\begin{aligned} \rho \mathbf{f}_p^T(\boldsymbol{\eta}_e) J(\boldsymbol{\eta}) M \mathbf{v} &= \rho \dot{\boldsymbol{\eta}}_e^T G_{pf}(\boldsymbol{\eta}_e) J(\boldsymbol{\eta}) M \mathbf{v} = \rho \mathbf{v}^T J^T(\boldsymbol{\eta}) G_{pf}(\boldsymbol{\eta}_e) J(\boldsymbol{\eta}) \mathbf{v} \\ &\leq \rho \|J^T(\boldsymbol{\eta}) G_{pf}(\boldsymbol{\eta}_e) J(\boldsymbol{\eta}) M\| \leq \rho \delta_{p\max} \lambda_{\max}\{M\} \|\mathbf{v}\|^2 \end{aligned} \quad (3.21d)$$

Using 3.2(d) and *Property 3.7 (i)*, for fifth part of  $Q_2$ , one gets

$$\begin{aligned} \rho \mathbf{f}_p^T(\boldsymbol{\eta}_e) J(\boldsymbol{\eta}) M \mathbf{v} &= \rho \mathbf{f}_p^T(\boldsymbol{\eta}_e) ([\omega]^\wedge M) \mathbf{v} \leq \rho \|J(\boldsymbol{\eta}) [\omega]^\wedge M\| \|\mathbf{f}_p(\boldsymbol{\eta}_e)\| \|\mathbf{v}\| \\ &\leq \rho \|J(\boldsymbol{\eta}) [\omega]^\wedge M\| \frac{1}{2} (\|\mathbf{f}_p(\boldsymbol{\eta}_e)\|^2 + \|\mathbf{v}\|^2) \leq \rho \lambda_{\max}\{M\} \omega_{\max} \frac{1}{2} (\|\mathbf{f}_p(\boldsymbol{\eta}_e)\|^2 + \|\mathbf{v}\|^2) \end{aligned} \quad (3.21e)$$

Hence,  $Q_2$  can be expressed using inequalities of (3.20) as

$$\text{for } \|\mathbf{v}\| < \|\boldsymbol{\beta}_d\|$$

$$Q_2 \geq \rho \left\{ -\sqrt{3} \delta_{p\max} \beta_{p\max} C_{\max} \|\mathbf{v}\|^2 - \frac{1}{2} \lambda_{\max}\{D(\mathbf{v})\} (\|\mathbf{f}_p(\boldsymbol{\eta}_e)\|^2 + \|\mathbf{v}\|^2) \right\}$$

$$\begin{aligned}
& -\lambda_{\max}\{K_D\}\frac{1}{2}\left(\|\mathbf{f}_p(\boldsymbol{\eta}_e)\|^2 + \sigma_{1d}\|\mathbf{v}\|^2\right) - \delta_{p\max}\lambda_{\max}\{M\}\|\mathbf{v}\|^2 - \frac{1}{2}\lambda_{\max}\{M\}\omega_{\max}\left(\|\mathbf{f}_p(\boldsymbol{\eta}_e)\|^2 + \|\mathbf{v}\|^2\right)\Big\} \\
& \Rightarrow Q_2 \geq -\rho\left(\Gamma_1 + \frac{\lambda_{\max}\{K_d\}}{2}\sigma_{1d}\right)\|\mathbf{v}\|^2 - \rho\Gamma_2\|\mathbf{f}_p(\boldsymbol{\eta}_e)\|^2
\end{aligned} \tag{3.22a}$$

for  $\|\mathbf{v}\| \geq \|\boldsymbol{\beta}_d\|$ ,

$$\Rightarrow Q_2 \geq -\rho\left(\Gamma_1 + \frac{\lambda_{\max}\{K_d\}}{2}\sigma_{2d}\right)\|\mathbf{v}\|^2 - \rho\Gamma_2\|\mathbf{f}_p(\boldsymbol{\eta}_e)\|^2 \tag{3.22b}$$

where,  $\Gamma_1, \Gamma_2$  are three positive constants mentioned in Theorem 3.1.

Using *Lemma 3.1 (i)* the first term of  $Q_1$  satisfies following inequality

$$\begin{aligned}
& \mathbf{v}^T K_d \mathbf{f}_d(\mathbf{v}) \geq \lambda_{\min}\{K_d\}\alpha_{d\min}\|\mathbf{v}\|^2, \text{ for } \|\mathbf{v}\| < \|\boldsymbol{\beta}_d\| \\
& \mathbf{v}^T K_d \mathbf{f}_d(\mathbf{v}) \geq \lambda_{\min}\{K_d\}\min_i\{\alpha_{di}\beta_{di}\}\|\mathbf{v}\|, \text{ for } \|\mathbf{v}\| \geq \|\boldsymbol{\beta}_d\|
\end{aligned} \tag{3.23a}$$

Second term of  $Q_1$  satisfies following inequality

$$\mathbf{v}^T D(\mathbf{v})\mathbf{v} \geq \lambda_{\min}\{D(\mathbf{v})\}\|\mathbf{v}\|^2 \tag{3.23b}$$

Next, Third term of  $Q_1$  satisfies following inequality

$$\rho\mathbf{f}_p^T(\boldsymbol{\eta}_e)K_p\mathbf{f}_p(\boldsymbol{\eta}_e) \geq \rho\lambda_{\min}\{K_p\}\|\mathbf{f}_p(\boldsymbol{\eta}_e)\|^2 \tag{3.23c}$$

Therefore, substituting (3.22) in (3.15) yields

for  $\|\mathbf{v}\| < \|\boldsymbol{\beta}_d\|$ ,

$$Q \geq \left(\lambda_{\min}\{K_d\}\alpha_{d\min} - \rho\frac{\lambda_{\max}\{K_d\}}{2}\sigma_{1d} - (\rho\Gamma_1 - \lambda_{\min}(D(\mathbf{v})))\right)\|\mathbf{v}\|^2 + \rho(\lambda_{\min}\{K_p\} - \Gamma_2)\|\mathbf{f}_p(\boldsymbol{\eta}_e)\|^2 \tag{3.24a}$$

$$\begin{aligned}
\text{for } \|\mathbf{v}\| \geq \|\boldsymbol{\beta}_d\|, Q \geq & \left( \lambda_{\min} \{K_d\} \min_i \{\alpha_{di} \beta_{di}\} - \left\{ \rho \left( \Gamma_1 + \frac{\lambda_{\max} \{K_d\}}{2} \sigma_{2d} \right) - \lambda_{\min} (D(\mathbf{v})) \right\} \|\mathbf{v}\| \right) \|\mathbf{v}\| \\
& + \rho \left( \lambda_{\min} \{K_p\} - \Gamma_2 \right) \|\mathbf{f}_p(\boldsymbol{\eta}_e)\|^2
\end{aligned} \tag{3.24b}$$

From (3.24), it can be concluded that  $Q$  is positive semi-definite function if following three conditions are satisfied i.e.

$$\lambda_{\min} \{K_d\} \alpha_{dmin} + \rho \frac{\lambda_{\max} \{K_d\}}{2} \sigma_{1d} > \rho \Gamma_1 - \lambda_{\min} (D(\mathbf{v})), \rho \left( \lambda_{\min} \{K_p\} - \Gamma_2 \right) > 0$$

and

$$\begin{aligned}
\frac{\lambda_{\min} \{K_d\} \min_i \{\alpha_{di} \beta_{di}\}}{\left\{ \rho \left( \Gamma_1 + \frac{\lambda_{\max} \{K_d\}}{2} \sigma_{2d} \right) - \lambda_{\min} (D(\mathbf{v})) \right\}} > \|\mathbf{v}\| \Rightarrow V_{\max} \geq \frac{\lambda_{\min} \{K_d\} \min_i \{\alpha_{di} \beta_{di}\}}{\left\{ \rho \left( \Gamma_1 + \frac{\lambda_{\max} \{K_d\}}{2} \sigma_{2d} \right) - \lambda_{\min} (D(\mathbf{v})) \right\}} \Rightarrow \\
\left( \rho \Gamma_1 - \lambda_{\min} (D(\mathbf{v})) \right) \geq \frac{\lambda_{\min} \{K_d\} \min_i \{\alpha_{di} \beta_{di}\}}{V_{\max}} - \rho \frac{\lambda_{\max} \{K_d\}}{2} \sigma_{2d}
\end{aligned}$$

i.e. (3.10b), (3.10c) and (10.3d) are satisfied. Eq.(3.24) using (3.14), implies  $\dot{V}$  is negetative semidefinite i.e.

$$\dot{V} = -Q \leq 0 \tag{3.25}$$

Hence, using La Salle's invariance principle,  $\dot{V}=0$  means

$$\mathbf{v} \rightarrow 0, \mathbf{f}_p(\boldsymbol{\eta}_e) \rightarrow 0 \text{ when } t \rightarrow \infty \tag{3.26}$$

$$\text{Hence, } \boldsymbol{\eta}_e = 0 \text{ for } t \rightarrow \infty \tag{3.27a}$$

$$\text{Consequently, } \dot{\boldsymbol{\eta}}_e \rightarrow \mathbf{0} \Rightarrow \dot{\boldsymbol{\eta}} \rightarrow \mathbf{0} \text{ as } \boldsymbol{\eta}_r(t) \text{ is a constant vector} \tag{3.27b}$$

Therefore, closed-loop system (3.8) is globally asymptotically stable and initial state  $\xi(0)$  converges to final state  $\xi_r, \forall t \geq 0$ .

Under (3.11), the forces and torque produced by control law (3.6) satisfy the actuator constraints (3.4). Moreover, it is feasible to find the values of  $\varnothing_{\delta_{max}(l)}, \varnothing_{\delta_{max}(l)}, \varnothing''_{\delta_{max}(l)}, \varnothing_{\delta_{max}(\omega)}, \varnothing'_{\delta_{max}(\omega)}, \varnothing''_{\delta_{max}(\omega)}$  in reconciliation with (3.11). Hence, properly chosen values of parameters of  $f_D(\cdot), f_p(\cdot), f_w(\cdot)$  can maintain the actuator constraints i.e.  $|F_u| \leq F_{umax}, |F_v| \leq F_{vmax}$  and  $|F_\omega| \leq F_{\omega max}$ .

*Remarks 3.1:*  $K_w$  is a free controller gain which can be chosen arbitrarily. Generally it should be very low to make integral action within a limit.

### 3.9 Results and Discussion

In this section, the efficacy of the proposed N-PID with BI and BD controller has been investigated for regulatory control of AUV with kinematics and dynamics of (3.2) and (3.3) respectively in presence of bounded parametric uncertainties and under the actuator constraints (3.4). A list of parameters of AUV dynamics and their nominal values are given in Table 3.6. In this table, deviation of  $\pm 10\%$  from their nominal values for the parameters are also depicted. MATLAB of version 2012a has been used as the software environment for simulation of the control algorithms for an AUV. To compare the effectiveness of the proposed controller, two other model-independent globally stable set-point controllers PD and basic N-PID without BI and BD have been selected for the same dynamics of AUV. The structures of these controllers are given below.

$$\text{PD Controller: } F = -J^T(\eta) K_p \eta_e - K_d \dot{\eta} \quad (3.29)$$

$$\text{N-PID: } \mathbf{F} = -K_d \mathbf{v} - J^T(\boldsymbol{\eta}) K_p \mathbf{f}_p(\boldsymbol{\eta}_e) - K_w \int_0^t [\mathbf{v}(\zeta) + \rho J^T(\boldsymbol{\eta}) \mathbf{f}_p^T(\boldsymbol{\eta}_e)] d\zeta \quad (3.30)$$

Bounded function used in both derivative and integral action make the difference between (3.6) and (3.30). Similar to (3.6),  $K_w$  in (3.30) is a free controller gain which can be chosen arbitrarily. Normally it should be very low to make integral action within a limit. Following similar kind of stability analysis of [199], the matrix inequalities to be satisfied for achieving global asymptotic stability of (3.3), with parametric uncertainties and actuator constraints (3.4), under action of control law (3.29) are same as it is for (3.6). Values of common parameters of both controllers, such as maximum limits of forces and torque produced by the actuators of AUV, initial and final values of states of AUV etc. have been chosen according to Table 3.1 and Table 3.2.

Table 3.1: Force and torque limits [24] of actuator

Maximum limit of force(Newton) in surge direction	Maximum limit of force(Newton) in sway direction	Maximum limit of Torque(N-m) around $z_b$ axis
400	400	50

Ranges of velocities[24] are chosen as  $\mathbf{v}_{max} = [\pm 0.5 \quad \pm 0.5 \quad \pm 0.42]$ . Time step for simulation is considered as 0.03 s. For simulation of all set-point controllers, values of initial and final state are depicted in Table 3.2. Large initial error in states have been selected to verify properly the differences in effects of all controllers on AUV dynamics.

Observations from simulation of different set-point controllers are compared on the basis of three performance specifications depending upon both transient and steady state response of state

obtained on application of the control input generated by these controllers. These specifications are amplitude ( $M$ ) of peak overshoot/undershoot, settling time/converging time( $t_s$ ), steady-state-error( $e_{ss}(t)$ ) of state. State includes linear position, orientation, linear and angular velocities. Observations are shown in the form of a table as given in Table 3.5. In this observation table, force and torque required for reaching to a final state from an initial state are also recorded for each controller.

Table 3.2:Information about initial and final state

State	x- position	y- position	orientation	Surge velocity(m/s)	Sway velocity(m/s)	Angular Velocity(rad/s)
Initial state	-5	-6	0.09	$\pm 0.4259$	$\pm 0.5$	$\pm 0.35$
Final state	20	20	2	0	0	0

### 3.9.1. Simulation Results with Analysis

Performances of the proposed controller N-PID with BI and BD is compared with two other globally stable controllers PD, a basic PID group controller and N-PID without BI and BD, a basic nonlinear PID controller.

#### 3.9.1.1 PD (roughly tuned gains) on AUV dynamics with and without uncertainties

Initially PD with roughly tuned gains is applied for AUV with and without (nominal dynamics) uncertainties and performances are compared in Fig 3.4-Fig 3.9. Simulation studies in Fig 3.4-Fig 3.9, under the constraints depicted in Table 3.1 and given velocity range, indicate a lots of conclusions. Comparing the data of first row and second row of Table 3.5, it is clear that due to effect of parametric uncertainties especially in hydrodynamic damping parameters the settling

time for regulatory control of linear position and orientation in PD control increases. Or, in other words, it can be concluded that at the desired settling time corresponding to the application of PD control with the same gain setting applied on uncertain AUV dynamics results in steady state error. Another significant observation is the peaks of all states have decreased due to uncertainties as mentioned in second row of Table 3.5.

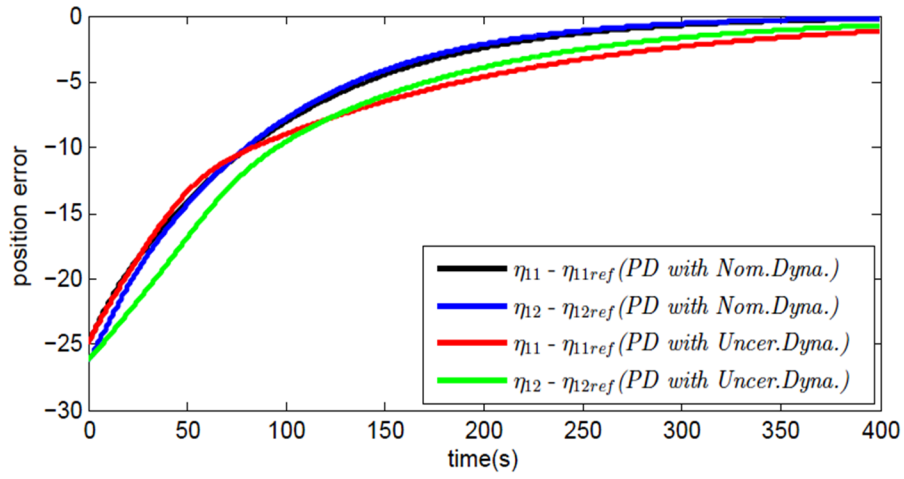


Fig.3.4: Position error vs. time

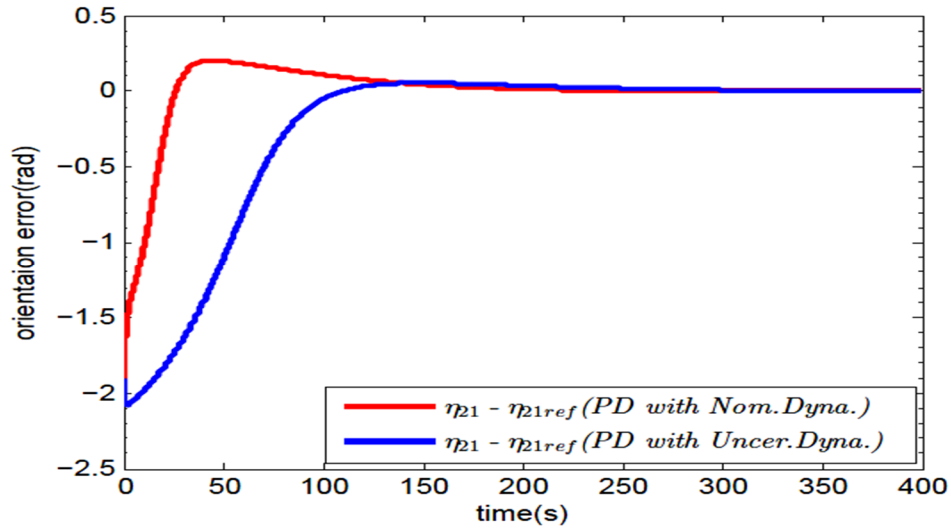


Fig.3.5: Error in orientation vs. time



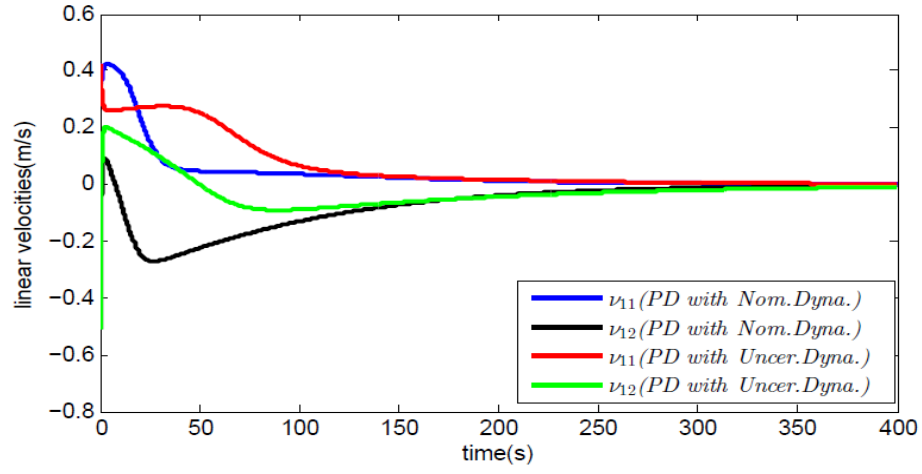


Fig.3.6: Error in linear velocities vs. time

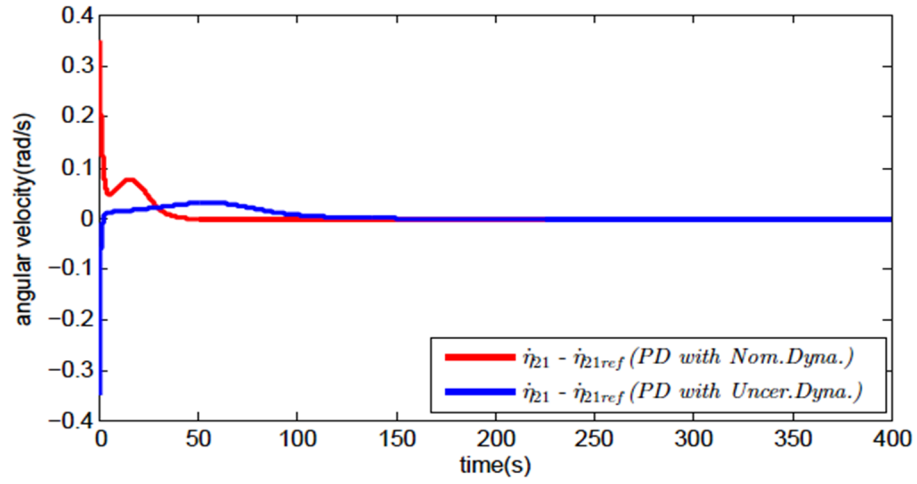


Fig.3.7: Error in angular velocities vs. time

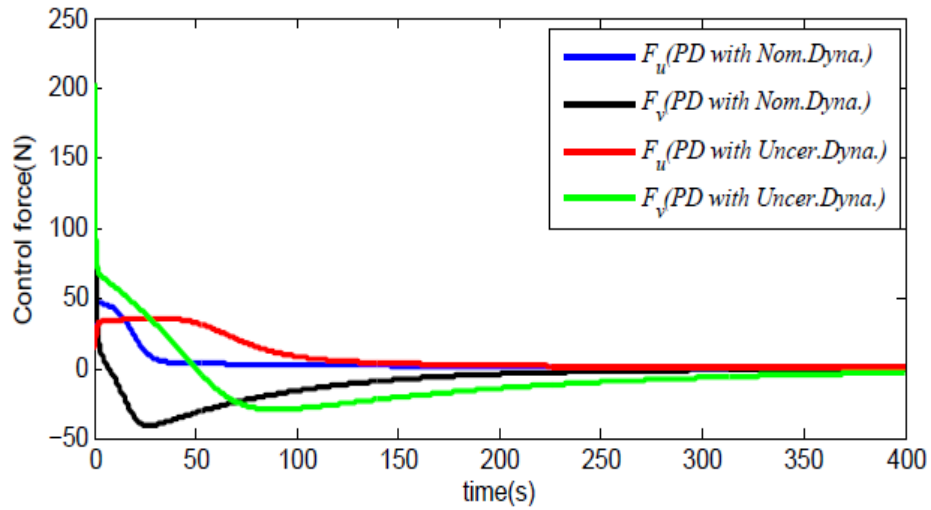


Fig.3.8: Control Forces vs. time

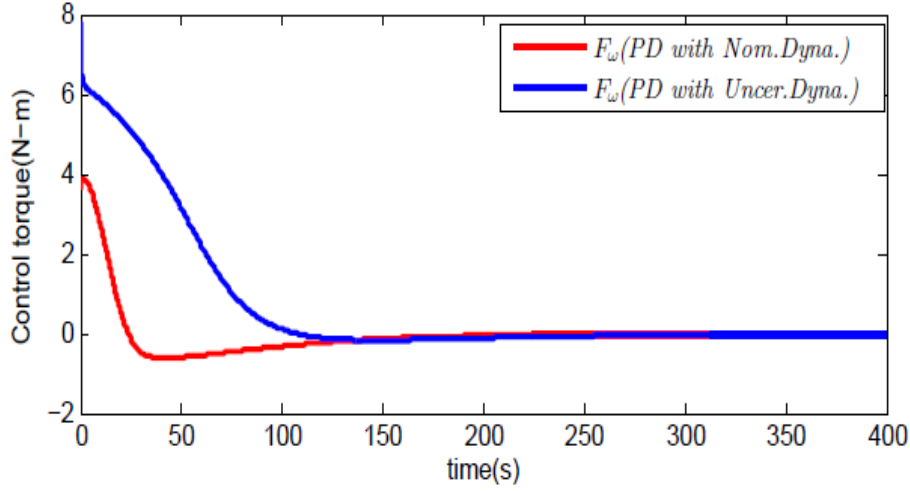


Fig.3.9: Control Torque vs. time

### 3.9.1.2 PD (roughly tuned gains) on AUV dynamics with uncertainties

If it is required to decrease the settling time, the values of the controller parameters need to be adjusted. If  $K_d$  is increased keeping  $K_p$  constant then up to a certain limit derivative control works well. From (Fig.3.10-Fig.3.13) it is seen that there is an increase (or maintaining of same value) in settling time and rise time, decrease in peak for all states than the previous setting of PD controller (Fig.3.4-Fig.3.7). Increasing  $K_p$ , keeping  $K_d$  constant yields overshoots with reduction of rise time and settling time (Fig.3.10-Fig.3.13). Observing the record of 3<sup>rd</sup>. and 4<sup>th</sup>. row of Table 3.5, it is concluded that large P case envisages increase in demand of velocities (Fig.3.12 and Fig.3.13) than large D case. Large D case demands less control inputs (Fig.3.14 and Fig.3.15) than large P case. But both large D and P cases demand more control inputs than those in previous setting (Fig.3.8 and Fig.3.9) of the PD controller.

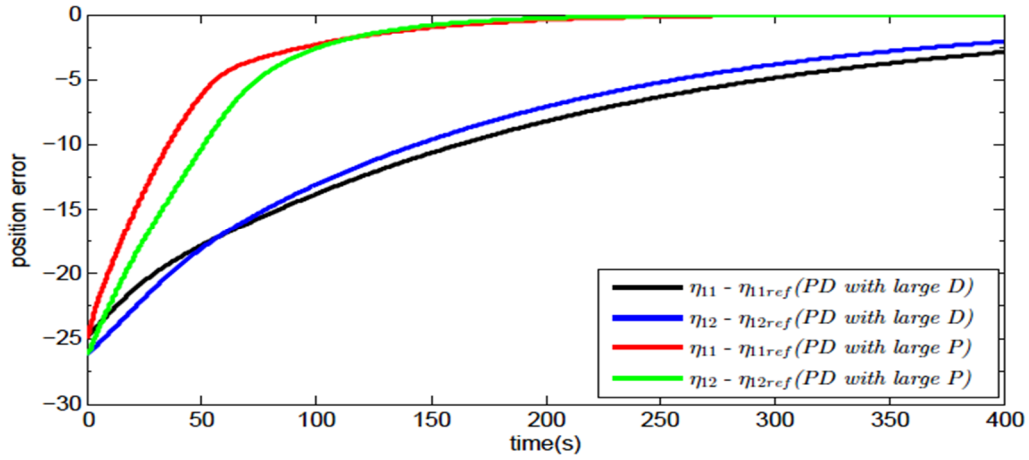


Fig. 3.10: Position error(large P & D) vs. time

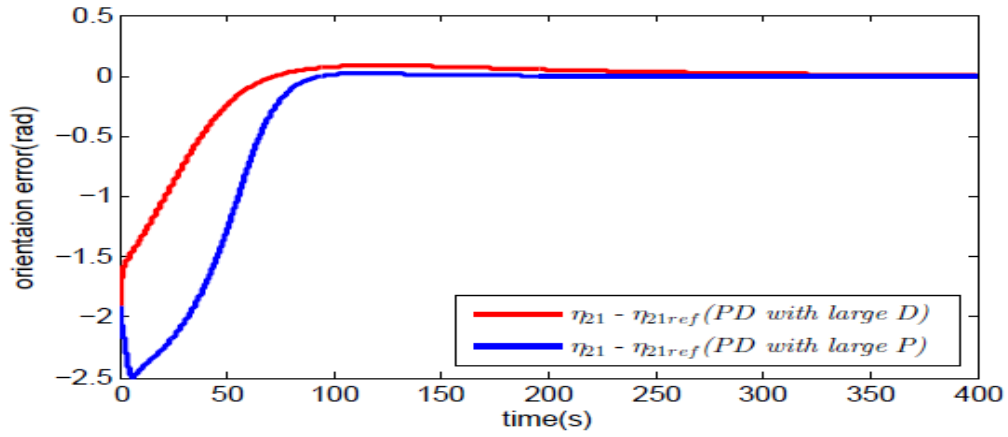


Fig.3.11: Error in orientation(large P & D) vs. time

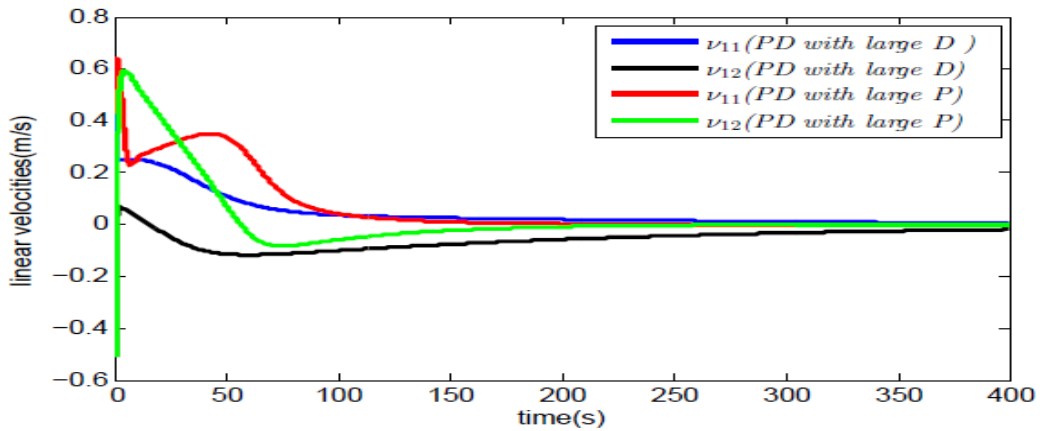


Fig.3.12: Error in linear velocities(large P &D) vs. time

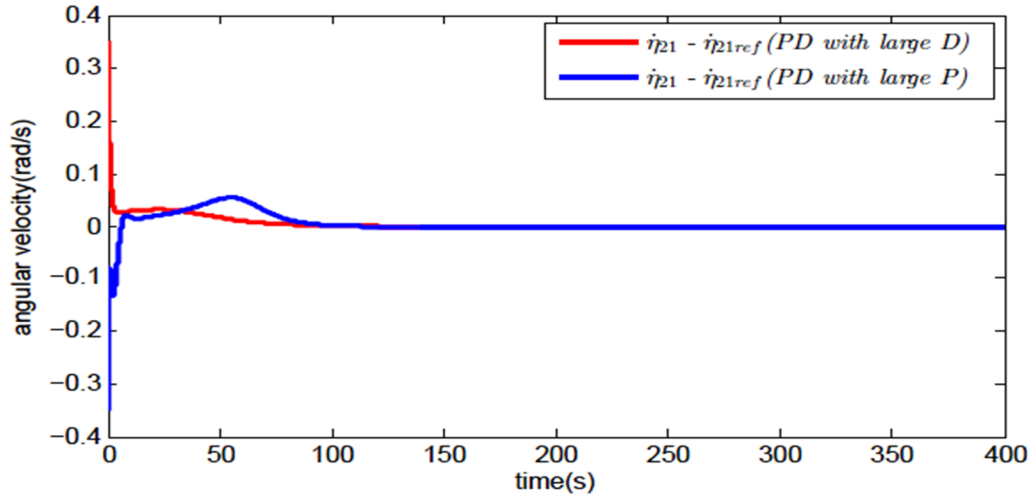


Fig.3.13: Error in angular velocities (large P & D) time

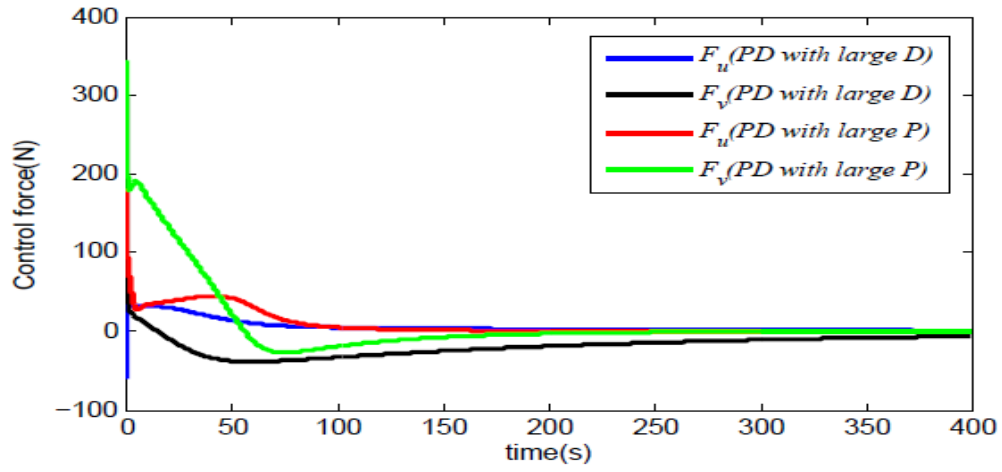


Fig.3.14: Control force (large P & D) vs. time

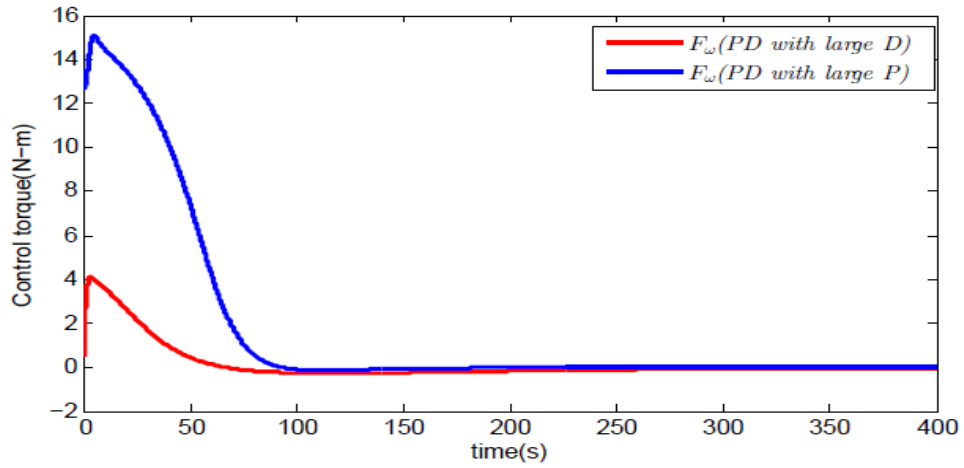


Fig.3.15: Control Torque (large P & D) time

### 3.9.1.3 PD (sufficiently tuned gains) on AUV dynamics with uncertainties:

Thus, proper adjustment between  $K_p$  and  $K_d$  for tuning (Fig.3.16-Fig.3.21) of the gains is very important to achieve desired transient and steady-state performance. It is cumbersome and also varies for different percentage of deviation in parameters from their nominal values. The reason is that controller gains of PD does not include information about upper bounds of parameter variation. Thus, for large initial error in state and huge parametric uncertainties, PD controller may not ensure stable output from an AUV system. It generally brings steady state error in linear position (Fig. 3.16). Thus, PD controller has a limitation for providing best transient and steady state responses from a system of AUV in a set-point control objective.

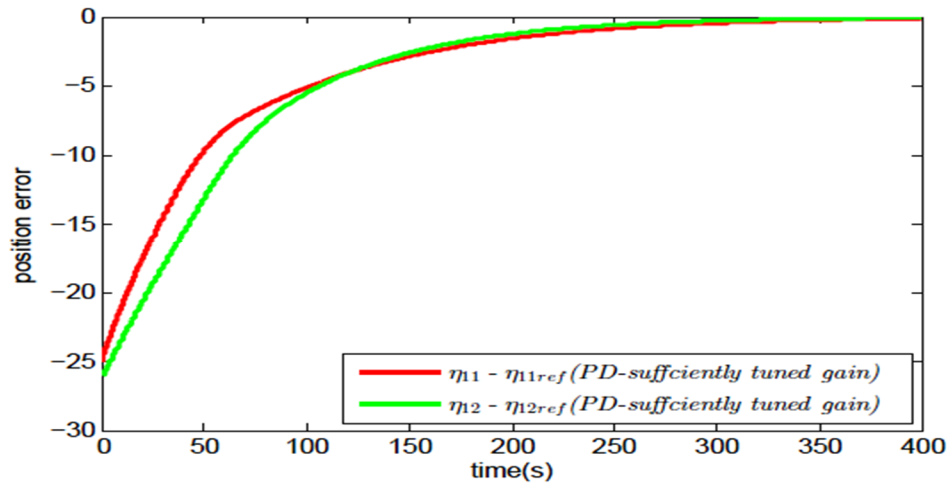


Fig.3.16: Position error(suff. tuned gain) vs. time

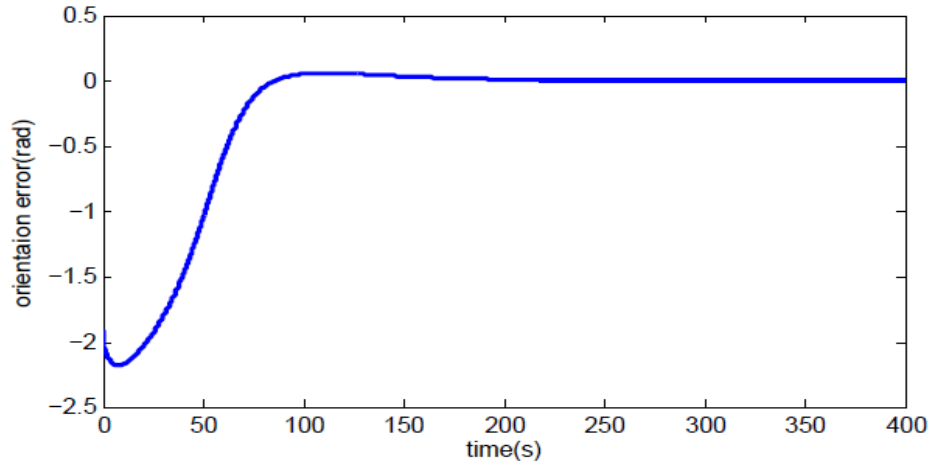


Fig.3.17: Error in orientation(suff. tuned gain) vs. time

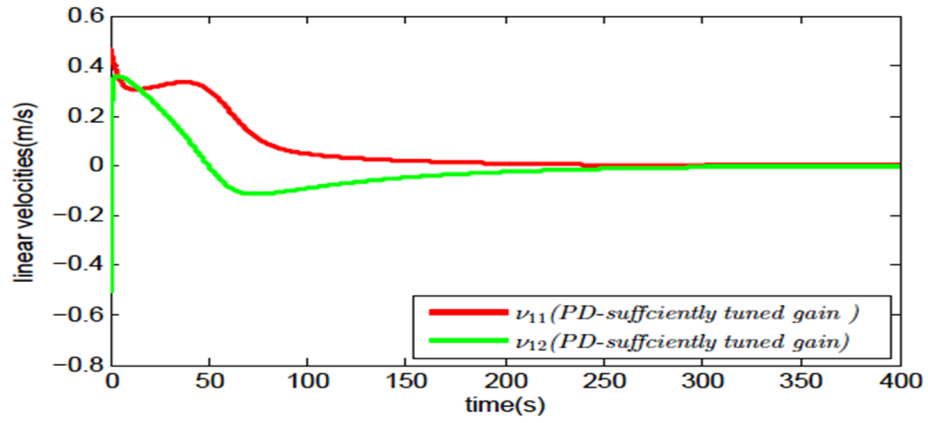


Fig.3.18: Error in linear velocities(suff. tuned gain) vs. time

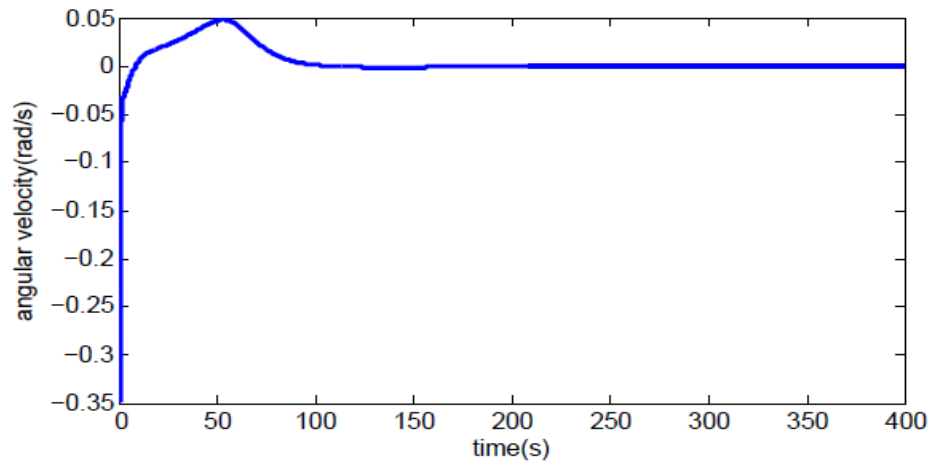


Fig.3.19: Error in angular velocities (suff. tuned gain) time

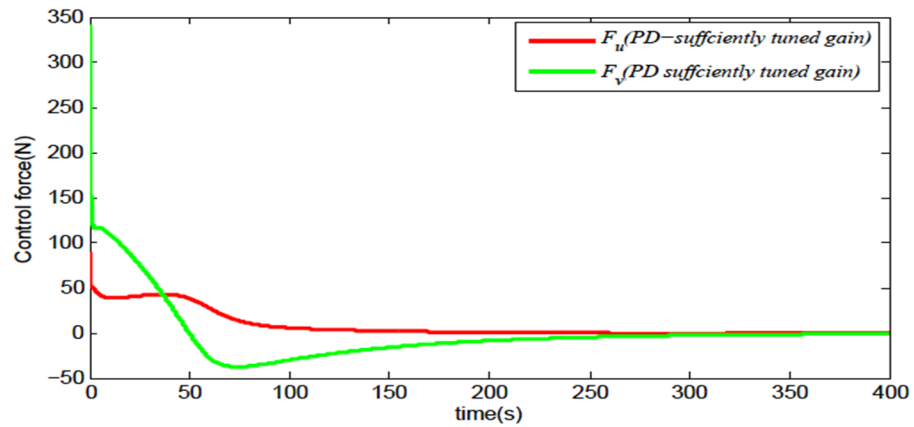


Fig.3.20: Control force (suff. tuned gain) vs. time

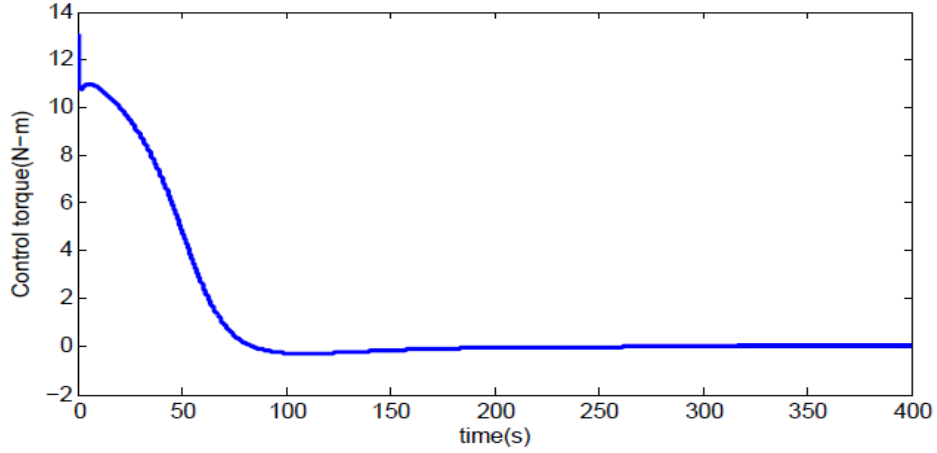


Fig.3.21: Control Torque (suff. tuned) vs.time

Therefore, to improve the performances by compensating the uncertainties in a system, LPID may be used, because LPID has inherent capability of compensation of uncertainties. But its drawback is it works locally i.e. it can not accommodate large initial error in state.

**3.9.1.4 NPID with BI and BD Control:** As a remedy of all the drawbacks of PD and PID, this thesis exploits Nonlinear PID like controller namely N-PID with BI and BD, which is further compared with its close controller N-PID without BI and BD.

Values of gains of both these controllers are depicted in Table 3.4. Values of parameters of nonlinear functions for different controllers are tabulated in Table 3.3.

Table 3.3: Values of parameters of nonlinear functions for different controllers

Controllers $\longrightarrow$	N-PID without BI and BD	N-PID with BI and BD
Parameters of nonlinear functions $\downarrow$		
$\Phi_{max}(l)$	-----	82
$\delta_{di}, \alpha_{di}, \beta_{di}, \forall i=1,2$	-----	0.6, 0.4, 0.3253968

$\Phi_{max(\omega)}$	-----	10
$\delta_{di}, \alpha_{di}, \beta_{di}, \forall i=3$	-----	0.4, 0.2, 0.0625
$\Phi'_{max(l)}$	140	140
$\delta_{pi}, \alpha_{pi}, \beta_{pi}, \forall i=1,2$	7,4.5.0.03488	7,4.5.0.03488
$\Phi'_{max(\omega)}$	25	25
$\delta_{pi}, \alpha_{pi}, \beta_{pi}, \forall i=3$	1,0.8,0.0556	1,0.8,0.0556
$\Phi''_{max(l)}$	—	4
$\delta_{wi}, \alpha_{wi}, \beta_{wi}, \forall i=1,2$	—	3,1,0.4
$\Phi''_{max(\omega)}$	—	2
$\delta_{wi}, \alpha_{wi}, \beta_{wi}, \forall i=3$	—	0.9, 0.7, 1.38

Fig.3.26 and Fig. 3.27 indicate integrator wind up occurs under application of N-PID without BI and BD as the saturation of force and torque occurs at the initial stage due to large initial error in linear and angular position and velocities. Consequently, linear position error (Fig. 3.22) has longer settling time due to saturation in control force (as shown in Fig.3.28). Similar kind of phenomenon occurs for orientation error (Fig.3.23), where error appears in overshoot and long settling time as saturation occurs in control torque (Fig.3.29). But for N-PID with BI and BD, linear position error (Fig.3.22) has lesser settling time than that in N-PID without BI and BD. Orientation error (Fig. 3.23) reaches to zero steady state with lesser overshoot and settling time. These phenomenon happen as there is no possibility of integrator wind-up and therefore no consequences (saturation in force or torque as shown in Fig.3.26 and Fig. 3.27) take place.



Table 3.4: Values of gains for different controllers

Gains →	$K_p$	$K_d$	$K_w$	$\rho$
Controller ↓				
PD without uncertainties	$diag [4, 4, 3]$	$diag [212, 212, 6]$	-----	-----
PD with uncertainties	$diag [4, 4, 3]$	$diag [212, 212, 6]$	-----	-----
PD with large D and uncertainties	$diag [4, 4, 3]$	$diag [400, 400, 15]$	-----	-----
PD with large P and uncertainties	$diag [10, 10, 6]$	$diag [212, 212, 6]$	-----	-----
PD with sufficiently tuned gain with uncertainties	$diag [8, 8, 5]$	$diag [300, 300, 10]$	-----	-----
N-PID without BI and BD With uncertainties	$diag [565, 565, 455]$	$diag [625, 625, 305]$	$diag [2.4, 2.4, 0.8]$	0.09
N-PID with BI and BD with uncertainties	$diag [570, 570, 470]$	$diag [425, 425, 405]$	$diag [2.7, 2.1, 0.7]$	0.1

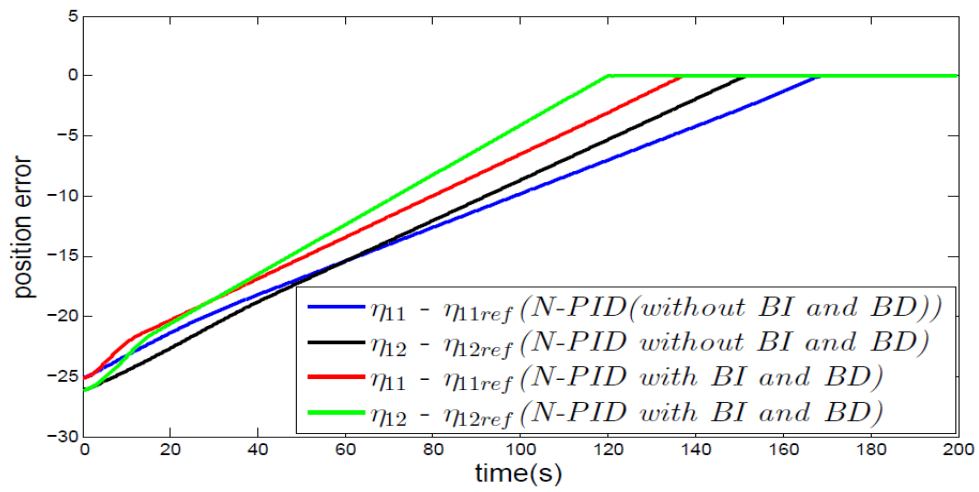


Fig. 3.22 Position errors vs. time

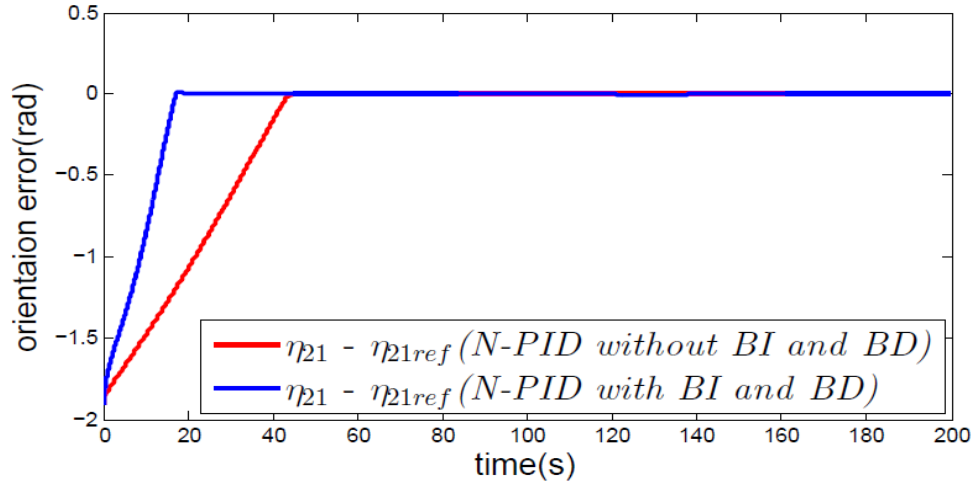


Fig.3.23 Orientation error vs. time

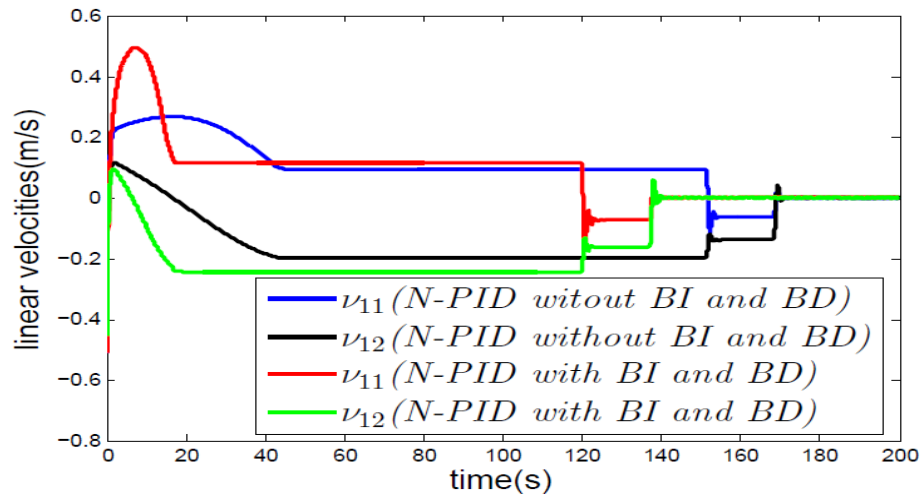


Fig. 3.24 Linear velocities vs. time

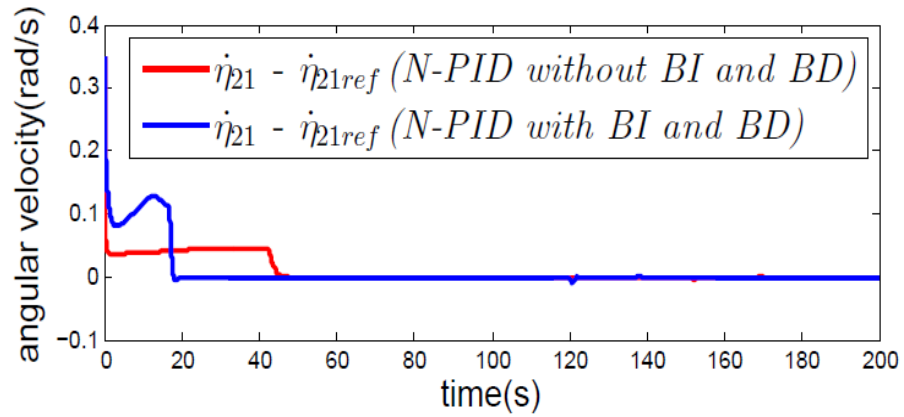


Fig. 3.25 Angular velocity vs.time

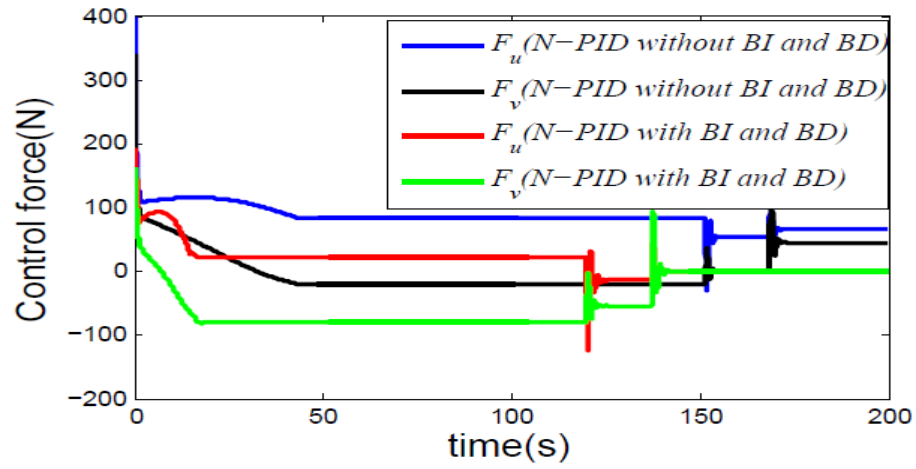


Fig.3.26 Control force vs. time

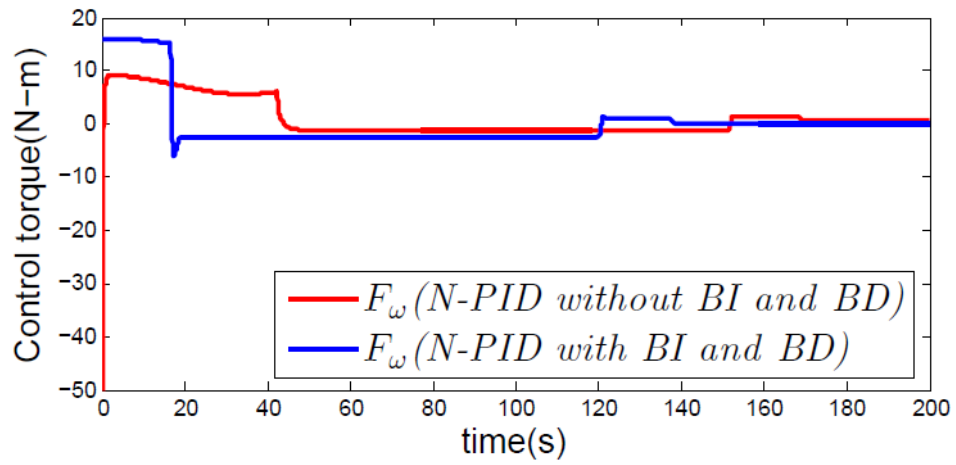


Fig. 3.27 Control torque vs. time

Table 3.5: Observations from the simulation of application of different regulatory controllers on AUV dynamics

States Control inputs	Position ( $\eta_{11}, \eta_{12}$ )		Orientatation (rad)		Linear velocities ( $v_{11}, v_{12}$ ) (m/s)		Angular velocity (rad/s)		Max. force (N)		Max. torque (N-m)
Performance → Specifications	M <sub>p</sub>	$t_s$ and $e_{ss}$	M <sub>o</sub>	$t_s$ and $e_{ss}$	M <sub>v</sub>	$t_s$ and $e_{ss}$	M <sub>a</sub>	$t_s$ and $e_{ss}$	F <sub>u</sub>	F <sub>v</sub>	F <sub>w</sub>
Controller ↓											
PD for Nom. Dynamics	No	375,375 and 0,0	0.2	225 and 0	0.42, 0.2	300, 350 And 0,0	0.35	110 And 0	50	200	6.5
PD for Uncertain Dynamics	No	$e_{ss}$ : 3,-2 at 400s	0.09	325 And 0	0.42, 0.09	$e_{ss}$ : 0.04,- 0.04 at 400s	-0.35	160 And 0	35	200	4
PD with large D	No	$e_{ss}$ : -2.5,-1.7 at 400s	0.1	350 and 0	0.4,0.06	$e_{ss}$ : 0.017, -0.025 at 400s	0.35	120 and 0	-52	300	4.2
PD with large P	No	275,270and 0,0	0.05	198 and 0	0.64,- 0.6	200,280 and 0,0	0.05	148 and 0	198	350	15
PD with sufficiently tuned P & D	No	370,350 and 0,0	0.1	250 and 0	0.42,- 0.5	275,370 and 0,0	0.05	175 and 0	350	350	13
N-PID without BI and BD	No	165,150 and 0,0	No	42 and 0	0.25 and 0.2	170 and 0	0.35	45 and 0	Saturated at 400	Saturated at 400	Saturated at -50

<i>States Control inputs</i>	<i>Position</i> ( $\eta_1, \eta_2$ )		<i>Orientatation</i> (rad)		<i>Linear velocities</i> ( $v_1, v_2$ ) (m/s)		<i>Angular velocity</i> (rad/s)		<i>Max. force</i> (N)		<i>Max. torque</i> (N-m)
N-PID with BI and BD	No	130, 118 and 0,0	No	18 and 0	0.5 and 0.2	140 and 0	0.34	20 and 0	200	180	15

### 3.10 Chapter Summary

In this chapter, Nonlinear PID controller with Bounded Integral and Bounded Derivative has been deployed for set-point control of an Autonomous Underwater Vehicle. The stability of the uncertain AUV dynamics under the application of this controller has been analyzed by applying Direct Lyapunov Method. The performances of this controller have been compared with other two controllers in the area of PID like controllers namely Proportional plus Derivative controller and Nonlinear PID controller without Bounded Integral and Bounded Derivative by simulating these for the same large initial error, specified uncertainties and specified torque limitation of actuators used in Nonlinear PID controller with Bounded Integral and Bounded Derivative. It is found that Nonlinear PID controller with Bounded Integral and Bounded Derivative is the most efficient controller to provide superior performance for achieving the desired configuration from an initial configuration for a given task of set-point control.

Table 3.6: List of parameters of AUV [24] and  $\pm 10\%$  variation in their nominal values

Parameters	Nominal	Maximum	Minimum	Unit
Mass ( $m$ )	185	203.5	169.5	Kg
Rotational Inertia ( $I_z$ )	50	55	45	kg-m <sup>2</sup>
Added mass ( $X_{\dot{u}}$ )	-30	-27	-33	Kg
Added mass ( $Y_{\dot{v}}$ )	-80	-72	-88	Kg
Added mass ( $N_{\dot{w}}$ )	-30	-27	-33	Kg
Surge linear drag ( $X_u$ )	70	77	63	kg/s
Surge quadratic drag ( $X_{u u }$ )	100	110	90	kg/m
Sway linear drag ( $Y_v$ )	100	110	90	kg/s
Sway quadratic drag ( $Y_{v v }$ )	200	220	180	kg/m
Yaw linear drag ( $N_w$ )	50	55	45	kg-m <sup>2</sup> /s
Quadratic yaw drag ( $N_{w w }$ )	100	110	90	kg-m <sup>2</sup>
$m_{11}$	215	236.5	196.5	Kg
$m_{22}$	265	291.5	241.5	Kg
$m_{33}$	80	88	72	kg-m <sup>2</sup>

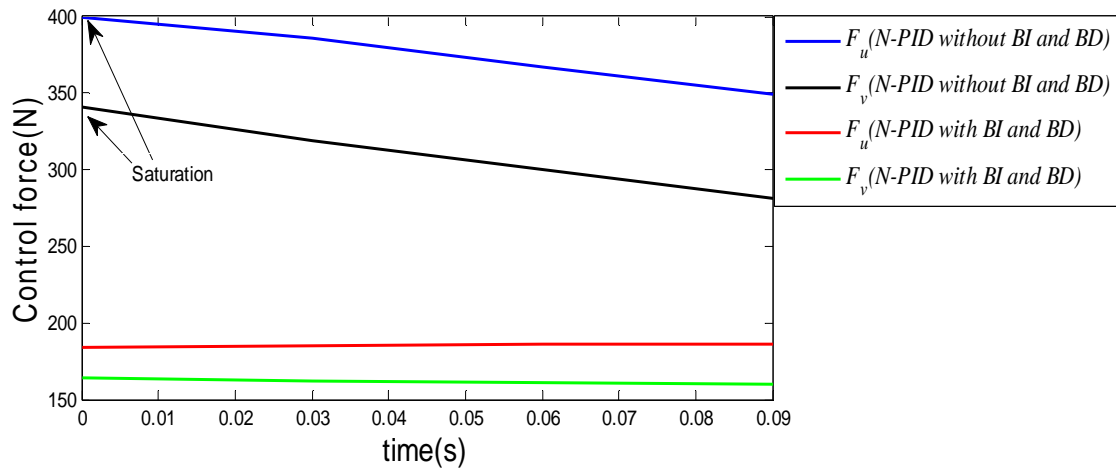


Fig 3.28 Saturation of actuator w.r.t. control force

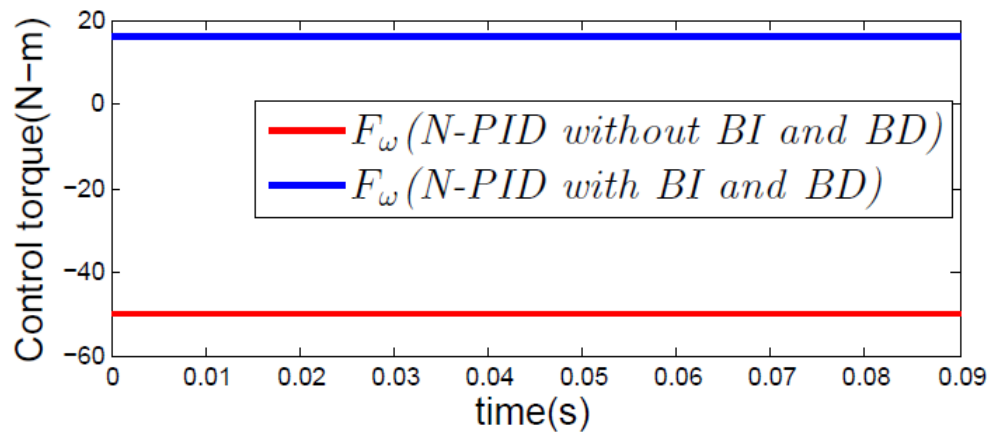


Fig 3.29 Saturation of actuator w.r.t. control torque

# Set Point Control of an Autonomous Underwater Vehicle using N-PID with BI and BD Control Strategy

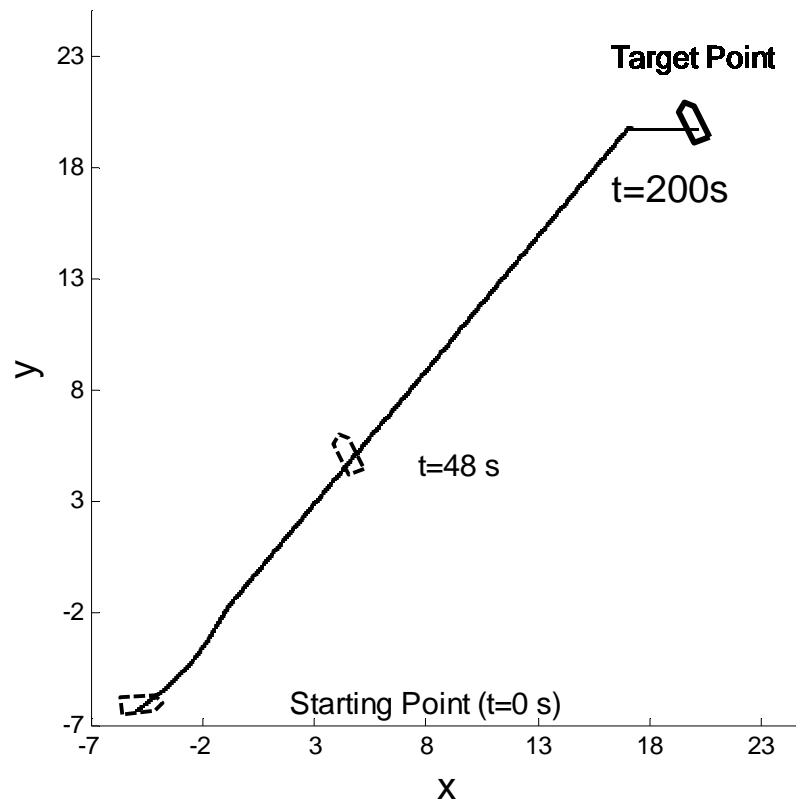


Fig .3.30 Set-Point Control of Autonomous Underwater Vehicle using N-PID with BI and BD Controller



# Chapter 4

## Robust Tracking of AUV Using Sliding Mode- Nonlinear PID Controller with Bounded Integral and Bounded Derivative

### 4.1 Introduction

In the chapter 3, a robust set-point control of AUV is proposed. The contribution of this chapter focuses on the development of robust tracking control of an AUV under uncertainties in hydrodynamics and limited torque produced by actuator. Motivated by reviewed literature in chapter 2, this chapter combines the advantages of the continuous approximation of SMC and N-PID and proposes a new model-independent globally stable tracking control algorithm. To get faster convergence and for achievement of better control performance in wide range of tracking error, a nonlinear sliding surface, using nonlinear function of position error [201], [202], is chosen in place of linear surface.

There is no significance of the use of equivalent control part [204] of a traditional SMC as it does not involve parameter uncertainties. Therefore, equivalent control action does not have capability to compensate instantaneous nonlinearities and uncertainties in AUV dynamics. Instead of equivalent control, an integral (I) action of position error can be used for compensating [57] nonlinearities and uncertainties. In place of linear position error, nonlinear function [172] of position error has been used like its use in the set-point control of AUV to restrict unlimited integral action and to achieve globally asymptotically stable system. The use of this kind of integral action is termed as nonlinear integral (N-I) control.

Ideally an SMC needs to generate high frequency discontinuous control in its switching control part. But practically it is not implementable by the digital controller. Thus, discretization chatter [203] occurs. Also chattering occurs due to fast unmodeled dynamics which are neglected in the design process. A nonlinear saturation function like tangent hyperbolic[60] can be used to avoid chattering by smoothing out the control discontinuity in a thin boundary layer. This kind of controller is called continuous SMC. As this controller leaves steady state error, addition of integral action with this controller has advantage in reduction of steady state error to certain extent. Therefore, integral action can be used for both increasing accuracy in tracking and handling of nonlinearities and uncertainties in the dynamics of AUV.

Combination of continuous SMC with N-I still requires improvement wrt its features of transient performance. Due to integrator wind-up effect [166],[167] of integral part of these controllers, performances deteriorate. A velocity damping term[205] is injected in integrator part to enhance globally stable response which always converges to zero. In this technique, although bounded function is used inside the expression of integral part, very large error can still yields a possibility of integrator wind-up which further deteriorates the transient response. To further improve the response the integral action can be bounded by passing it through another nonlinear function. Then the controller is called SM-N-I with bounded integrator (BI). To further stabilize the closed loop tracking dynamics against actuator saturation, a nonlinear derivative (D) control action in place of linear one can be provided with a nonlinear (same as used in integral action) of position error. The overall controller, combination of different controlling actions discussed above, is termed as SM-N-PID with BI and BD. Boundary values of the nonlinear functions of P,D,I controller are chosen such that summation of these boundary values in addition with switching gain of SMC; never exceeds the input torque limit specified by actuator.

The chapter is organised as follows. Section 4.2 provide mathematical preliminaries. Section 4.3 describes kinematics and dynamics of reference AUV. Section 4.4 formulates the problem of trajectory tracking. Section 4.5 proposes SM-NPID based tracking controller for AUV. Section 4.6 derives the closed-loop tracking error dynamics of AUV system under the action of proposed control law. In section 4.7, stability of the closed-loop system is proved, whereas in section 4.8 simulation results are presented to show the performances of proposed tracking controller. Section 4.9 draws the conclusion and points to immediate future work for improvement of the proposed controller.

## 4.2 Mathematical Preliminaries

*Definition 4.1:* A Saturation function  $\tanh$  is defined as follows

$$\left. \begin{aligned} \tanh(x) &= x, \text{ if } |x| \leq 1 \\ \tanh(x) &= \text{sgn}(x), \text{ if } |x| > 1 \end{aligned} \right\} \quad (4.1)$$

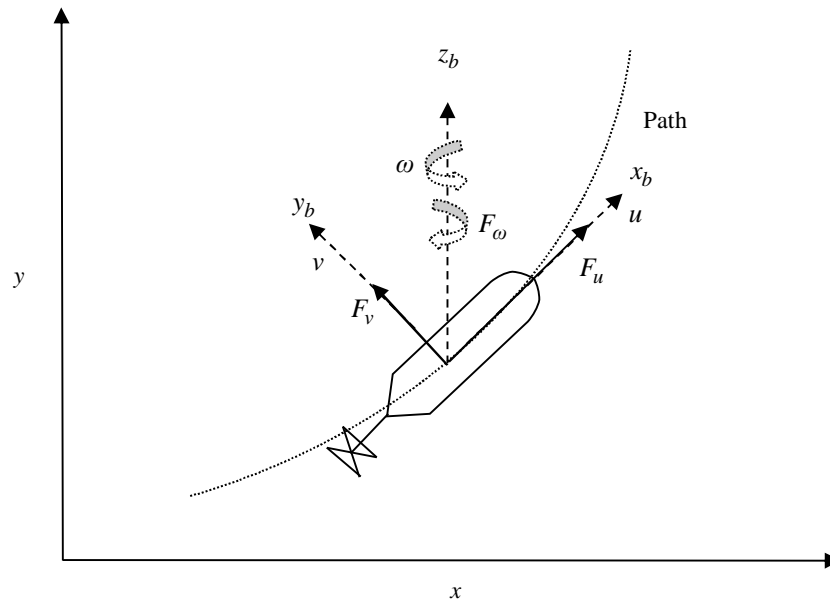


Fig. 4.1 Motion of an AUV on a planar path

### 4.3 Definition of Reference AUV

In trajectory tracking, an AUV is assumed to track the position state of a reference AUV (RA)[208] moving along a sufficiently smooth predefined/planned path (navigation). It is also assumed that AUV may be used for low to moderate speed tracking/maneuvering [206]. The state of reference AUV is the desired state of the AUV. A reference trajectory  $\eta_{lr}(t): \mathbb{R} \rightarrow \mathbb{R}^2$  of RA is assumed. Then, the following definitions hold for the state of RA. Assume, during a time interval  $\tau < t < \tau + \Delta\tau, \Delta\tau \rightarrow 0$ , linear position of RA changes from  $\eta_{lr}(\tau)$  to  $\eta_{lr}(\tau + \Delta\tau)$ .

Hence, instantaneous linear velocity of RA in IRF can be expressed as

$$\begin{aligned} \dot{\eta}_{lr}(t) \Big|_{t=\tau+\Delta\tau} &= \lim_{\Delta\tau \rightarrow 0} \frac{\Delta \eta_{lr}(\tau + \Delta\tau)}{\Delta\tau} = \lim_{\Delta\tau \rightarrow 0} \left\{ \frac{x_r(\tau + \Delta\tau) - x_r(\tau)}{\Delta\tau} \hat{i} + \frac{y_r(\tau + \Delta\tau) - y_r(\tau)}{\Delta\tau} \hat{j} \right\} \\ &= \left( \frac{dx_r(t)}{dt} \hat{i} + \frac{dy_r(t)}{dt} \hat{j} \right) \Big|_{t=\tau+\Delta\tau} \end{aligned} \quad (4.2)$$

where,  $\hat{i}$  and  $\hat{j}$  represent the unit vector along  $x$  and  $y$  direction in 2D space. If  $\theta_r$  represents the orientation of RA wrt  $x$ -axis in IRF during this interval, it can be defined as

$$\theta_r(t) \Big|_{t=\tau+\Delta\tau} = \tan^{-1} \left\{ \lim_{\Delta\tau \rightarrow 0} \frac{y_r(\tau + \Delta\tau) - y_r(\tau)}{x_r(\tau + \Delta\tau) - x_r(\tau)} \right\} = \tan^{-1} \left( \frac{dy_r(t)}{dx_r(t)} \right) \Big|_{t=\tau+\Delta\tau} = \eta_{2r}(t) \Big|_{t=\tau+\Delta\tau}. \quad (4.3)$$

Hence, assuming orientation at  $t=\tau$  and at the end of  $t=\tau+\Delta\tau$  are  $\theta_r(\tau)$  and  $\theta_r(\tau+\Delta\tau)$  respectively, then at the end of  $\tau + \Delta\tau$  angular velocity is then defined as follows

$$\omega_r(t) \Big|_{t=\tau+\Delta\tau} = \lim_{\Delta\tau \rightarrow 0} \frac{\Delta \theta_r(\tau + \Delta\tau)}{\Delta\tau} = \frac{\theta_r(\tau + \Delta\tau) - \theta_r(\tau)}{\Delta\tau} = \frac{d\theta_r(t)}{dt} \Big|_{t=\tau+\Delta\tau} = \dot{\eta}_{2r}(t) \Big|_{t=\tau+\Delta\tau} \quad (4.4)$$

All the quantities above can be transformed to BRF of RA similar to (3.2c)

$$\dot{\boldsymbol{\eta}}_r(t) = J(\boldsymbol{\eta}_r) \mathbf{v}_r(t) \quad (4.5)$$

where,  $\mathbf{v}_r(t)$  is velocities in BRF of RA. Thus, the state of the reference AUV is defined as

$$\boldsymbol{\xi}_r = (x_r, y_r, \theta_r, \dot{x}_r, \dot{y}_r, \dot{\theta}_r = \omega_r, u_r, v_r) \in \mathfrak{R}^8 \quad (4.6)$$

The tracking control law proposed in this chapter does not need information about acceleration state of the RA. Boundary value of acceleration is only necessary. Feasible values of state of RA-GB is restricted by constraints on dynamics of GB. These constraints are specified bounds on velocities and accelerations

$$\|\mathbf{v}_{1r}\| \leq V_{1max} \text{ and } |\dot{v}_{21r}| \leq V_{2max}, \|\dot{\mathbf{v}}_{1r}\| \leq A_{1max}, |\dot{v}_{21r}| \leq A_{2max}, \quad (4.7)$$

where,  $V_{1max}, V_{2max}, A_{1max}$  and  $A_{2max}$  are positive constants.

*Remarks 4.1:* To control a reference point on a planned path, the reference point with its associated dynamics was conceptualized as a virtual vehicle in [207]. Similarly, the concept of referenceAUV has been considered in this work, to generate the complete state (4.6) of the desired trajectory. From this state the tracking control law can be designed.

#### 4.4 Problem Formulation

Consider an AUV with kinematics and dynamics as given in (3.2) and (3.3) respectively. Its motion is studied under the Assumptions 3.2. The position tracking error of the AUV wrt to its reference AUV is defined in IRF as

$$\boldsymbol{\eta}_e(t) = \boldsymbol{\eta}(t) - \boldsymbol{\eta}_r(t) \quad (4.8)$$

where,  $\boldsymbol{\eta}(t) \in \mathbb{R}^3$  and  $\boldsymbol{\eta}_r(t) \in \mathbb{R}^3$  are the actual and desired state of the AUV.

*Problem statement:* Let,  $\boldsymbol{\eta}_r(t): \mathbb{R} \rightarrow \mathbb{R}^3$  is a sufficiently smooth time-varying given trajectory, definition of which is provided in section 4.2. The objective is to design  $\mathbf{F}$  for a given AUV under the Assumption 3.3 such that  $\boldsymbol{\eta}_e(t)$  reaches and remains in the neighbourhood of  $[\mathbf{0}] \in \mathbb{R}^3, \forall t \geq 0$  in presence of bounded model parameter uncertainties mentioned in Table 3.6 and under (4.6).

#### 4.5 SM-N-PID Control Law with Bounded Integral and Bounded Derivative

In this section, on the basis of formulaion of problem in section 4.4, a trajectory tracking controller is proposed for an AUV using the combination of N-PID and continuous SMC. In fact, a desired tracking error dynamics is specified in SMC[59],[60] and this dynamics is considered as a restriction on the system. The objective is to propose a control law such that these dynamics are attained by closed-loop dynamics of AUV in presence of model parameter uncertainties. Considering the trajecory tracking error defined in eq (4.8) the error dynamics are defined as

$$\mathbf{s}(t) = [s_1 \quad s_2 \quad s_3]^T = \rho \mathbf{J}^T(\boldsymbol{\eta}) \mathbf{f}_p(\boldsymbol{\eta}_e) + \mathbf{v}_e \quad (4.9)$$

where,  $\mathbf{f}_p \in L(\boldsymbol{\alpha}_p, \boldsymbol{\beta}_p, \boldsymbol{\delta}_p, \cdot)$  and  $\rho > 0$  is used to vary the control bandwidth of the system of AUV.  $\boldsymbol{\eta}_e = (x_e, y_e, \theta_e) \in \mathbb{R}^3$  and  $\mathbf{v}_e = (u_e, v_e, \omega_e) \in \mathbb{R}^3$  are errors in position vector in IRF and velocity vector in BRF of AUV respectively. Nonlinear function [201], [202] of position error instead of linear position error has been used in robot manipulators to get faster convergence of actual state to desired state.  $\mathbf{s}(t) = \mathbf{0}$  represents a surface (nonlinear switching surface) in the state space of order one (as AUV dynamics is a second order system). A thin boundary layer

$B_i(t)$  is assumed neighboring each surface  $s_i(t)=0$  and all boundary layers are represented by the following set

$$\mathbf{B}(t) = \{(\boldsymbol{\eta}_e, \mathbf{v}_e) : |x_e| \leq \mu_1, |y_e| \leq \mu_2, |\theta_e| \leq \mu_3, |s_i| \leq \varphi_i, \forall i=1,2,3\} \in \mathbb{R}^3 \quad (4.10)$$

where,  $\mu_i$  and  $\varphi_i, \forall i=1,2,3$  are strictly positive constants. Outside each boundary layer, a control law has to be chosen such that it satisfies  $\eta$ -reaching condition [209]. This condition ensures that boundary layer  $\mathbf{B}(t)$  always remain attractive. Consequently, this attractiveness guarantees that any trajectory starts inside  $\mathbf{B}(t=0)$ , always remain in it for  $t \geq 0$ . With this objective and based on the discussion in the introduction section, a tracking control law which is a combination of N-PID and continuous SMC is proposed as follows

$$\mathbf{F} = -K_d \mathbf{f}_d(\mathbf{v}_e) - J^T(\boldsymbol{\eta}) K_p \mathbf{f}_p(\boldsymbol{\eta}_e) - K_s \mathbf{f}_s(\cdot) - K_w \mathbf{f}_w(\boldsymbol{\chi}_e) \quad (4.11)$$

where,  $\boldsymbol{\chi}_e = \int_0^t [\mathbf{v}_e(\xi) + \rho J^T(\boldsymbol{\eta}) \mathbf{f}_p(\boldsymbol{\eta}_e)] d\xi$ , and parameters of different nonlinear CPDI function

vectors  $\mathbf{f}_d(\mathbf{v}_e), \mathbf{f}_p(\boldsymbol{\eta}_e), \mathbf{f}_w(\boldsymbol{\chi}_e)$  are set following similar procedure as described in (3.7). Switching

functions are defined as  $\mathbf{f}_s(\cdot) = \left[ \tanh\left(\frac{s_1}{\varphi_1}\right) \quad \tanh\left(\frac{s_2}{\varphi_2}\right) \quad \tanh\left(\frac{s_3}{\varphi_3}\right) \right]^T$ .  $K_s, K_w, K_d, K_p$  are  $3 \times 3$  order

diagonal positive definite gain matrices.  $J^T(\boldsymbol{\eta})$  is used to convert the error quantity of control law

to BRF of AUV. Every moment  $\mathbf{v}_e$  can be estimated from the estimated states  $(\dot{\boldsymbol{\eta}}_e)$  in IRF with

help of  $J(\boldsymbol{\eta})$ . First part of this controller is the velocity damping term, which is bounded through

a nonlinear function  $\mathbf{f}_d(\cdot)$  and facilitates to provide asymptotic stability of the closed loop

system of AUV. Second part uses a filtered position error feedback using  $\mathbf{f}_p(\cdot)$  to enhance the

global stability. Third part involving  $\mathbf{f}_s(\cdot)$  is the switching control part of SMC which uses  $\tanh(\cdot)$  function defined in (4.1) to reduce chattering. Last part contributes a bounded output from an integral action similar to 3.6. A differentiable potential function and its gradient like defined in (3.9) may also defined for tracking control.

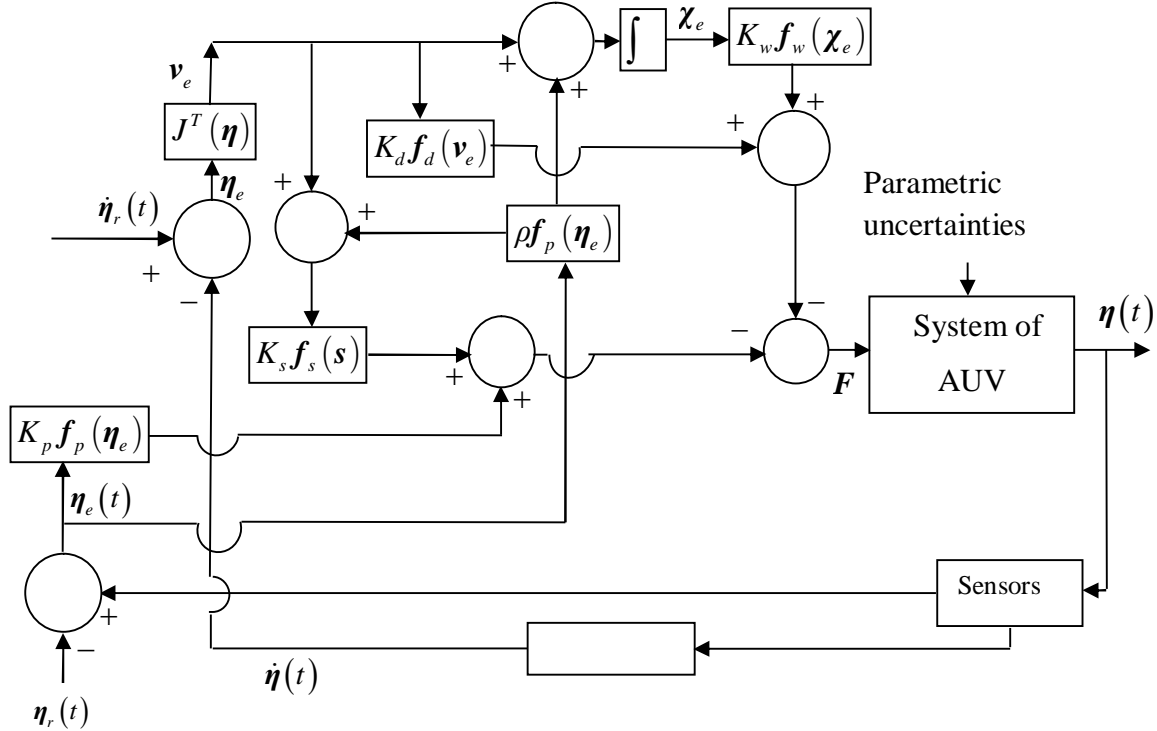


Fig. 4.2 Tracking Controller structure of AUV using SM-N-PID with BI and BD

A CPDI function integrated over any range of independent variable always gives positive or zero. value. Hence, following Lemma holds.

*Lemma4.1:* If integral of  $\mathbf{f}_w(\chi_e)$ , is defined as

$$W = \int K_w \mathbf{f}_w(\chi_e) d\chi_e, \chi_e \in \mathbb{R}^3 \quad (4.12)$$

Then, it is (i) is positive definite as  $W(\chi_e) > 0$  when  $\chi_e \neq 0$  and  $W(0) = 0$



(ii) is radially unbounded as  $W(\boldsymbol{\chi}_e) \rightarrow \infty$  when  $|\boldsymbol{\chi}_e| \rightarrow \infty$

In section 4.7,  $W$  is typically considered as a storage function for passivity based stability analysis of tracking control of AUV.

#### 4.6 Dynamics of AUV in Terms of Trajectory Tracking Error

The closed-loop system dynamics can be obtained by substituting (4.11) into (3.3) as follows,

$$M\dot{\mathbf{v}}_e + C(\mathbf{v})\mathbf{v}_e + D(\mathbf{v})\mathbf{v}_e + K_d \mathbf{f}_d(\mathbf{v}_e) + J^T(\boldsymbol{\eta})K_p \mathbf{f}_p(\boldsymbol{\eta}_e) + K_s \mathbf{f}_s(\mathbf{s}) - \mathbf{h} = -K_w \mathbf{f}_w(\boldsymbol{\chi}_e) \quad (4.13)$$

where,  $\mathbf{h} = -M \frac{d}{dt} (J^T(\boldsymbol{\eta})J_r(\boldsymbol{\eta}_r)\mathbf{v}_r) - C(\mathbf{v})J^T(\boldsymbol{\eta})J_r(\boldsymbol{\eta}_r)\mathbf{v}_r - D(\mathbf{v})J^T(\boldsymbol{\eta})J_r(\boldsymbol{\eta}_r)\mathbf{v}_r$

To get the expression of  $\mathbf{h}$  in terms of only  $\mathbf{v}_e$  and  $\mathbf{v}_r$ , put  $\mathbf{v} = \mathbf{v}_e + J^T(\boldsymbol{\eta})J_r(\boldsymbol{\eta}_r)\mathbf{v}_r$ . Thus,

with the help of *Property 3.3*,  $\mathbf{h}$  can be written as,

$$\begin{aligned} \Rightarrow \mathbf{h} &= -M \left( \dot{J}^T(\boldsymbol{\eta})J_r(\boldsymbol{\eta}_r) + J^T(\boldsymbol{\eta})\dot{J}_r(\boldsymbol{\eta}_r) \right) \mathbf{v}_r - MJ^T(\boldsymbol{\eta})J(\boldsymbol{\eta}_r)\dot{\mathbf{v}}_r \\ &\quad - C \left( J^T(\boldsymbol{\eta})J_r(\boldsymbol{\eta}_r)\mathbf{v}_r \right) (\mathbf{v}_e + J^T(\boldsymbol{\eta})J_r(\boldsymbol{\eta}_r)\mathbf{v}_r) - D(\mathbf{v})J^T(\boldsymbol{\eta})J_r(\boldsymbol{\eta}_r)\mathbf{v}_r \\ &= - \left\{ MJ^T(\boldsymbol{\eta})J(\boldsymbol{\eta}_r)\dot{\mathbf{v}}_r + C \left( J^T(\boldsymbol{\eta})J_r(\boldsymbol{\eta}_r)\mathbf{v}_r \right) J^T(\boldsymbol{\eta})J_r(\boldsymbol{\eta}_r)\mathbf{v}_r + D(\mathbf{v})J^T(\boldsymbol{\eta})J_r(\boldsymbol{\eta}_r)\mathbf{v}_r \right\} \\ &\quad - \left\{ M \left( \dot{J}^T(\boldsymbol{\eta})J(\boldsymbol{\eta}_r) + J^T(\boldsymbol{\eta})\dot{J}_r(\boldsymbol{\eta}_r) \right) \mathbf{v}_r + C \left( J^T(\boldsymbol{\eta})J_r(\boldsymbol{\eta}_r)\mathbf{v}_r \right) \mathbf{v}_e \right\} = \mathbf{h}_1 + \mathbf{h}_2 \end{aligned} \quad (4.14a)$$

where, in  $\mathbf{h}_2$ ,

$$\left\| \dot{J}^T(\boldsymbol{\eta})J_r(\boldsymbol{\eta}_r) + J^T(\boldsymbol{\eta})\dot{J}_r(\boldsymbol{\eta}_r) \right\| = \left\| J^T(\boldsymbol{\eta})[\omega]^\wedge J_r(\boldsymbol{\eta}_r) + J^T(\boldsymbol{\eta})J_r^T(\boldsymbol{\eta}_r)[\omega_r]^\wedge \right\| \leq |\omega - \omega_r| = |\omega_e| = |\mathbf{v}_{2e}|.$$

Using  $\left\| J^T(\boldsymbol{\eta})J(\boldsymbol{\eta}_r) \right\| = 1$  and following A.2, upper bound of  $\mathbf{h}_2$  can be expressed as

$$\begin{aligned} \|\mathbf{h}_2\| &\leq \lambda_{\max}\{M\}\|\mathbf{v}_r\|\|\mathbf{v}_{2e}\| + C_{\max}\|\mathbf{v}_r\|\|\mathbf{v}_e\| \leq \lambda_{\max}\{M\}\|\mathbf{v}_r\|\|\mathbf{v}_e\| + C_{\max}\|\mathbf{v}_r\|\|\mathbf{v}_e\| \text{ as } |\mathbf{v}_{2e}| < \|\mathbf{v}_e\| \\ \|\mathbf{h}_2\| &\leq \lambda_{\max}\{M\}\|\mathbf{v}_r\|\|\mathbf{v}_{2e}\| + C_{\max}\|\mathbf{v}_r\|\|\mathbf{v}_e\| \leq (\lambda_{\max}\{M\}\|\mathbf{v}_r\| + C_{\max}\|\mathbf{v}_r\|)\|\mathbf{v}_e\| = c_1\|\mathbf{v}_e\| \end{aligned} \quad (4.14b)$$

where,  $c_1 = (\lambda_{\max}\{M\} + C_{\max})V_{\max}$  assuming  $\|\mathbf{v}_r\| = V_{\max}$ . With help of (4.7), the maximum value of each element of  $\mathbf{h}_1$  vector can be determined as described in A.6. From A.6, the following is obtained.

$$\mathbf{h}_1 \leq \begin{bmatrix} h_{11\max} \\ h_{12\max} \\ h_{13\max} \end{bmatrix} \quad (4.14c)$$

*Remarks 4.2:* As mentioned in section 4.1, in designing a tracking controller using traditional SMC, tuning of gain for switching control part is not straightforward rather it involves several approximations and complexities [211]. But closed-loop system involving proposed control law with AUV dynamics and subsequently stability proof of proposed tracking control shows that switching gain only depends upon the upper bounds on velocity and acceleration, structural bound of parameter matrices of dynamics of AUV in a straightforward way. Another advantage of the proposed tracking controller over other tracking controller is that this controller does not require instantaneous acceleration of desired path in control law, only its boundary value is utilized.

## 4.7 Stability Analysis

### 4.7.1 Development of Global Reachability and Global Bounded Stability Conditions

In continuous SMC, the control law should be designed such that the trajectories tend towards the bounded set [209] in state-space and reach it in finite time and remain in it for future time. Reaching phase is prone to nonlinearities, model uncertainties. Moreover, actuator constraints must affect the characteristics of this phase. Controller must be robust such that stable reaching motion is generated overcoming these effects. Thus, it is required to develop some conditions which must be satisfied by the gains of the controllers to ensure stable reaching phase for the

states of closed-loop dynamics of AUV under these constraints. These sufficient conditions for global reachability and global bounded stability to the desired bounded set are derived in the form of a set of inequalities. The establishment of these conditions is presented in the form of the following lemma and theorem.

*Lemma 4.2 :* A stable global reachability to boundary layer  $\mathbf{B}(t)$  of (4.10) in the dynamics (3.3) driven by control law (4.11) is always achieved if the following sufficient conditions are satisfied:

$$\text{for } V_{\max} \geq \|\mathbf{v}_e\| \geq 0, R - \lambda_{\min} \{D(\mathbf{v})\} > \frac{C_2 - H}{V_{\max}} - C_4 \quad (4.15a)$$

$$\text{for } \frac{1}{\rho} \left[ \varphi_{\max} - \frac{H}{(C_1 - C_3) - (R - \lambda_{\min} \{D(\mathbf{v})\})} \right] > \|\mathbf{f}_p(\boldsymbol{\eta}_e)\|_{(\max)} \quad (4.15b)$$

$$\text{where, } C_1 = \lambda_{\min} \{K_d\} \alpha_{d\min}, C_2 = \lambda_{\min} \{K_d\} \min \{\alpha_{di} \beta_{di}\}, C_3 = \frac{\rho \lambda_{\max} \{K_d\}}{2} \sigma_{1d}, C_4 = \frac{\rho \lambda_{\max} \{K_d\}}{2} \sigma_{2d},$$

$$\sigma_{1d} = \delta_{d\max}^2, \sigma_{2d} = \frac{\delta_{d\max}^2 \beta_{d\max}^2}{\beta_{d\min}^2}, H = \lambda_{\max} \{K_p\} \sqrt{3} \delta_{p\max} \beta_{p\max}, \|\mathbf{f}_p(\boldsymbol{\eta}_e)\|_{(\min)} \in \{\|\mathbf{f}_p(\boldsymbol{\eta}_e)\| : \|\mathbf{s}\| = \|\boldsymbol{\varphi}\|\}.$$

$$R = \left[ \left\{ \rho \sqrt{3} \delta_{p\max} \beta_{p\max} C_{\max} + \frac{\rho}{2} C_{\max} V_{\max} + \frac{\rho}{2} \lambda_{\max} \{D(\mathbf{v})\} + \frac{1}{2} \rho \lambda_{\max} \{M\} \omega_{\max} \right. \right. \\ \left. \left. + \rho \delta_{p\max} \lambda_{\max} \{M\} + \frac{\rho^2}{2} \delta_{p\max} \lambda_{\max} \{M\} + c_1 \left( 1 + \frac{\rho}{2} \right) \right\} \right]$$

$$S > 0 \quad (4.15c)$$

$$\text{where, } S = \rho \left[ \lambda_{\min} \{K_p\} - \left\{ \frac{1}{2} C_{\max} V_{\max} + \frac{\lambda_{\max} \{K_d\}}{2} + \frac{1}{2} \lambda_{\max} \{D(\mathbf{v})\} + \frac{1}{2} \lambda_{\max} \{M\} \omega_{\max} \right. \right. \\ \left. \left. + \rho \lambda_{\max} \{M\} + \frac{\rho}{2} \lambda_{\max} \{M\} + \frac{c_1}{2} \right\} \right]$$

$$\text{For } i=1,2,3; K_{si} \geq (K_{wi} |f_{wi}(\chi_{ei})| + h_{1imax}) \quad (4.15d)$$

In addition, if parameter values of nonlinear functions based on (3.7), satisfy (4.16a) and (4.16b) and (4.16b)

$$\varnothing_{\delta \max(l)} + \varnothing'_{\delta \max(l)} + \varnothing''_{\delta \max(l)} \leq F_{u \max} - K_{s1}, \varnothing_{\delta \max(l)} + \varnothing'_{\delta \max(l)} + \varnothing''_{\delta \max(l)} \leq F_{v \max} - K_{s2} \quad (4.16a)$$

$$\varnothing_{\delta \max(\omega)} + \varnothing'_{\delta \max(\omega)} + \varnothing''_{\delta \max(\omega)} \leq F_{\omega \max} - K_{s3} \quad (4.16b)$$

then the forces and torque hold the actuator constraints i.e.  $|F_u| \leq F_{u \max}, |F_v| \leq F_{v \max}$  and  $F_\omega \leq F_{\omega \max}$ .

*Proof:* To derive reaching condition, consider a quadratic Lyapunov candidate function inspired by [210] as

$$V_g = \frac{1}{2} \mathbf{s}^T M \mathbf{s} \quad (4.17)$$

Global sliding reachability is established based on conditions for achievement of negative-definiteness of first derivative of  $V_g$  along the state error trajectory corresponding to closed-loop dynamics (4.13). Therefore,

$$\dot{V}_g = \mathbf{s}^T M \dot{\mathbf{s}} = \mathbf{s}^T M \dot{\mathbf{v}}_e + \rho \mathbf{s}^T M \dot{J}^T(\boldsymbol{\eta}) \mathbf{f}_p(\boldsymbol{\eta}_e) + \rho \mathbf{s}^T M J^T(\boldsymbol{\eta}) \dot{\mathbf{f}}_p(\boldsymbol{\eta}_e) \quad (4.18)$$

Substituting  $M \dot{\mathbf{v}}_e$  from (4.13), using *Property 3.4*, (4.18) can be written as follows

$$\begin{aligned} \dot{V}_g = & -\mathbf{v}_e^T C(\mathbf{v}) \mathbf{v}_e - \mathbf{v}_e^T D(\mathbf{v}) \mathbf{v}_e - \mathbf{v}_e^T K_d \mathbf{f}_d(\mathbf{v}_e) - \mathbf{v}_e^T J^T(\boldsymbol{\eta}) K_p \mathbf{f}_p(\boldsymbol{\eta}_e) \\ & - \rho (\mathbf{f}_p^T(\boldsymbol{\eta}_e) J(\boldsymbol{\eta}) C(\mathbf{v}) \mathbf{v}_e + \mathbf{f}_p^T(\boldsymbol{\eta}_e) J(\boldsymbol{\eta}) D(\mathbf{v}) \mathbf{v}_e + \mathbf{f}_p^T(\boldsymbol{\eta}_e) J(\boldsymbol{\eta}) K_d \mathbf{f}_d(\mathbf{v}_e) \\ & + \mathbf{f}_p^T(\boldsymbol{\eta}_e) J(\boldsymbol{\eta}) J^T(\boldsymbol{\eta}) K_p \mathbf{f}_p(\boldsymbol{\eta}_e)) + \rho (\mathbf{v}_e^T M \dot{J}(\boldsymbol{\eta}) \mathbf{f}_p(\boldsymbol{\eta}_e) + \rho \mathbf{f}_p^T(\boldsymbol{\eta}_e) J(\boldsymbol{\eta}) M \dot{J}(\boldsymbol{\eta}) \mathbf{f}_p(\boldsymbol{\eta}_e) + \\ & \mathbf{v}_e^T M J^T(\boldsymbol{\eta}) \dot{\mathbf{f}}_p(\boldsymbol{\eta}_e) + \rho \mathbf{f}_p^T(\boldsymbol{\eta}_e) J(\boldsymbol{\eta}) M J^T(\boldsymbol{\eta}) \dot{\mathbf{f}}_p(\boldsymbol{\eta}_e)) - \mathbf{s}^T (K_w \mathbf{f}_w(\boldsymbol{\chi}_e) + K_s \mathbf{f}_s(\mathbf{s}) - \mathbf{h}) \\ \dot{V}_g = & -\left\{ \mathbf{v}_e^T D(\mathbf{v}) \mathbf{v}_e + \mathbf{v}_e^T K_d \mathbf{f}_d(\mathbf{v}_e) + \mathbf{v}_e^T J^T(\boldsymbol{\eta}) K_p \mathbf{f}_p(\boldsymbol{\eta}_e) + \rho (\mathbf{f}_p^T(\boldsymbol{\eta}_e) J(\boldsymbol{\eta}) C(\mathbf{v}) \mathbf{v}_e \right. \\ & + \mathbf{f}_p^T(\boldsymbol{\eta}_e) J(\boldsymbol{\eta}) K_d \mathbf{f}_d(\mathbf{v}_e) + \mathbf{f}_p^T(\boldsymbol{\eta}_e) J(\boldsymbol{\eta}) D(\mathbf{v}) \mathbf{v}_e + \mathbf{f}_p^T(\boldsymbol{\eta}_e) K_p \mathbf{f}_p(\boldsymbol{\eta}_e)) \\ & - \rho (\mathbf{v}_e^T M \dot{J}^T(\boldsymbol{\eta}) \mathbf{f}_p(\boldsymbol{\eta}_e) + \mathbf{v}_e^T M J(\boldsymbol{\eta}) \dot{\mathbf{f}}_p(\boldsymbol{\eta}_e) + \rho \mathbf{f}_p^T(\boldsymbol{\eta}_e) J(\boldsymbol{\eta}) M \dot{J}^T(\boldsymbol{\eta}) \mathbf{f}_p(\boldsymbol{\eta}_e) \\ & \left. \rho \mathbf{f}_p^T(\boldsymbol{\eta}_e) J(\boldsymbol{\eta}) M J^T(\boldsymbol{\eta}) \dot{\mathbf{f}}_p(\boldsymbol{\eta}_e)) \right\} - \mathbf{s}^T (K_w \mathbf{f}_w(\boldsymbol{\chi}_e) + K_s \mathbf{f}_s(\mathbf{s}) - \mathbf{h}) \end{aligned} \quad (4.19)$$

From first term of (4.19), following inequality may be obtained

$$\mathbf{v}_e^T D(\mathbf{v}) \mathbf{v}_e \geq \lambda_{\min} \{D(\mathbf{v})\} \|\mathbf{v}_e\|^2 \quad (4.20)$$

Using Lemma 3.1 (i), from second term of (4.19), one gets

$$\begin{aligned} \mathbf{v}_e^T K_d \mathbf{f}_d(\mathbf{v}_e) &\geq C_1 \|\mathbf{v}_e\|^2, \text{ for } \|\mathbf{v}_e\| < \|\boldsymbol{\beta}_d\| \\ \mathbf{v}_e^T K_d \mathbf{f}_d(\mathbf{v}_e) &\geq C_2 \|\mathbf{v}_e\|, \text{ for } \|\mathbf{v}_e\| \geq \|\boldsymbol{\beta}_d\| \end{aligned} \quad (4.21)$$

For the third term of (4.19) one may write noting,  $2\|\mathbf{v}_e\| \|\mathbf{f}_p(\boldsymbol{\eta}_e)\| \leq (\|\mathbf{v}_e\|^2 + \|\mathbf{f}_p(\boldsymbol{\eta}_e)\|^2)$

$$\mathbf{v}_e^T J^T(\boldsymbol{\eta}) K_p \mathbf{f}_p(\boldsymbol{\eta}_e) \geq -\lambda_{\max} \{J^T(\boldsymbol{\eta}) K_p\} \|\mathbf{v}_e\| \|\mathbf{f}_p(\boldsymbol{\eta}_e)\| \geq -\lambda_{\max} \{K_p\} \sqrt{3} \delta_{p\max} \beta_{p\max} \|\mathbf{v}_e\| \quad (4.22)$$

Using Property 3.3, and putting  $\mathbf{v} = \mathbf{v}_e + J^T(\boldsymbol{\eta}) J_r(\boldsymbol{\eta}_r) \mathbf{v}_r$  in the fourth term of (4.19),

$$\rho \mathbf{f}_p^T(\boldsymbol{\eta}_e) J(\boldsymbol{\eta}) C(\mathbf{v}) \mathbf{v}_e = \rho (\mathbf{f}_p^T(\boldsymbol{\eta}_e) J(\boldsymbol{\eta}) C(\mathbf{v}_e) \mathbf{v}_e + \mathbf{f}_p^T(\boldsymbol{\eta}_e) J(\boldsymbol{\eta}) C(\mathbf{v}_e) J^T(\boldsymbol{\eta}) J(\boldsymbol{\eta}_r) \mathbf{v}_r)$$

Using Property 3.7 (iii) and Lemma 3.1(iii) and noting,  $2\|\mathbf{v}_e\| \|\mathbf{f}_p(\boldsymbol{\eta}_e)\| \leq (\|\mathbf{v}_e\|^2 + \|\mathbf{f}_p(\boldsymbol{\eta}_e)\|^2)$

$$\begin{aligned} \rho \mathbf{f}_p^T(\boldsymbol{\eta}_e) J(\boldsymbol{\eta}) C(\mathbf{v}) \mathbf{v}_e &\geq -\rho \left( \sqrt{3} \delta_{p\max} \beta_{p\max} C_{\max} \|\mathbf{v}_e\|^2 + C_{\max} V_{\max} \|\mathbf{v}_e\| \|\mathbf{f}_p(\boldsymbol{\eta}_e)\| \right) \\ &\geq -\rho \left( \sqrt{3} \delta_{p\max} \beta_{p\max} C_{\max} \|\mathbf{v}_e\|^2 + \frac{1}{2} C_{\max} V_{\max} (\|\mathbf{v}_e\|^2 + \|\mathbf{f}_p(\boldsymbol{\eta}_e)\|^2) \right) \end{aligned} \quad (4.23)$$

Next, following inequality is derived from fifth term of (4.19) with the help of Lemma 3.1(i) and

(4.15a)

$$\begin{aligned} \rho \mathbf{f}_p^T(\boldsymbol{\eta}_e) J(\boldsymbol{\eta}) K_d \mathbf{f}_d(\mathbf{v}_e) &\geq -\rho \|J(\boldsymbol{\eta}) K_d\| \frac{1}{2} (\|\mathbf{f}_p(\boldsymbol{\eta}_e)\|^2 + \|\mathbf{f}_d(\mathbf{v}_e)\|^2) \\ &\geq \begin{cases} -\rho \lambda_{\max} \{K_d\} \frac{1}{2} (\|\mathbf{f}_p(\boldsymbol{\eta}_e)\|^2 + \sigma_{1d} \|\mathbf{v}_e\|^2), & \text{if } \|\mathbf{x}\| < \|\boldsymbol{\beta}_d\|, \\ -\rho \lambda_{\max} \{K_d\} \frac{1}{2} (\|\mathbf{f}_p(\boldsymbol{\eta}_e)\|^2 + \sigma_{2d} \|\mathbf{v}_e\|^2), & \text{if } \|\mathbf{x}\| \geq \|\boldsymbol{\beta}_d\| \end{cases} \end{aligned} \quad (4.24)$$

From the sixth term of (4.19), following inequality is obtained using *Property 3.7(ii)*

$$\rho \mathbf{f}_p^T(\boldsymbol{\eta}_e) J(\boldsymbol{\eta}) D(\mathbf{v}) \mathbf{v}_e \geq -\rho \|J(\boldsymbol{\eta}) D(\mathbf{v})\| \frac{1}{2} (\|\mathbf{f}_p(\boldsymbol{\eta}_e)\|^2 + \|\mathbf{v}_e\|^2) \geq -\rho \lambda_{\max} \{D(\mathbf{v})\} \frac{1}{2} (\|\mathbf{f}_p(\boldsymbol{\eta}_e)\|^2 + \|\mathbf{v}_e\|^2) \quad (4.25)$$

From seventh term of (4.19) one may get

$$\rho \mathbf{f}_p^T(\boldsymbol{\eta}_e) K_p \mathbf{f}_p(\boldsymbol{\eta}_e) \geq \rho \lambda_{\min} \{K_p\} \|\mathbf{f}_p(\boldsymbol{\eta}_e)\|^2 \quad (4.26)$$

With the help of 3.2(d), *Property 3.7(i)*, eighth term of (4.19) gives following inequality

$$\begin{aligned} \rho \mathbf{v}_e^T M \dot{J}^T(\boldsymbol{\eta}) \mathbf{f}_p(\boldsymbol{\eta}_e) &\leq \rho \|M \dot{J}^T(\boldsymbol{\eta})\| \|\mathbf{v}_e\| \|\mathbf{f}_p(\boldsymbol{\eta}_e)\| \leq \rho \frac{1}{2} \|M [\omega]^\wedge\|^T J^T(\boldsymbol{\eta}) (2 \|\mathbf{v}_e\| \|\mathbf{f}_p(\boldsymbol{\eta}_e)\|) \\ &\leq \rho \frac{1}{2} \|M [\omega]^\wedge\|^T J^T(\boldsymbol{\eta}) (\|\mathbf{v}_e\|^2 + \|\mathbf{f}_p(\boldsymbol{\eta}_e)\|^2) \leq \rho \frac{1}{2} \lambda_{\max} \{M\} \omega_{\max} (\|\mathbf{f}_p(\boldsymbol{\eta}_e)\|^2 + \|\mathbf{v}_e\|^2) \end{aligned} \quad (4.27)$$

With the help of *Lemma 3.1(ii)*, *Property 3.7(i)*, next inequality results from ninth term of (4.19)

$$\rho \mathbf{v}_e^T M J(\boldsymbol{\eta}) \dot{\mathbf{f}}_p(\boldsymbol{\eta}_e) = \rho \mathbf{v}_e^T M J(\boldsymbol{\eta}) G_{pf}(\boldsymbol{\eta}_e) J(\boldsymbol{\eta}) \mathbf{v}_e \leq \rho \delta_{p\max} \lambda_{\max} \{M\} \|\mathbf{v}_e\|^2 \quad (4.28)$$

Subsequently, using 3.2(d) from 10<sup>th</sup>. term of (4.19) following inequality is developed

$$\rho^2 \mathbf{f}_p^T(\boldsymbol{\eta}_e) J(\boldsymbol{\eta}) M \dot{J}^T(\boldsymbol{\eta}) \mathbf{f}_p(\boldsymbol{\eta}_e) \leq \rho^2 \|J(\boldsymbol{\eta}) M \dot{J}^T(\boldsymbol{\eta})\| \|\mathbf{f}_p(\boldsymbol{\eta}_e)\|^2 \leq \rho^2 \lambda_{\max} \{M\} \|\mathbf{f}_p(\boldsymbol{\eta}_e)\|^2 \quad (4.29)$$

Next, from 11<sup>th</sup>. term of (4.19), one gets

$$\begin{aligned} \rho^2 \mathbf{f}_p^T(\boldsymbol{\eta}_e) J(\boldsymbol{\eta}) M \dot{J}^T(\boldsymbol{\eta}) \dot{\mathbf{f}}_p(\boldsymbol{\eta}_e) &= \rho^2 \mathbf{f}_p^T(\boldsymbol{\eta}_e) J(\boldsymbol{\eta}) M \dot{J}^T(\boldsymbol{\eta}) G_{pf}(\boldsymbol{\eta}_e) \dot{\boldsymbol{\eta}}_e = \rho^2 \mathbf{f}_p^T(\boldsymbol{\eta}_e) J(\boldsymbol{\eta}) M \dot{J}^T(\boldsymbol{\eta}) \\ G_{pf}(\boldsymbol{\eta}_e) J(\boldsymbol{\eta}) \mathbf{v}_e &\leq \rho^2 \|J(\boldsymbol{\eta}) M \dot{J}^T(\boldsymbol{\eta}) G_{pf}(\boldsymbol{\eta}_e) J(\boldsymbol{\eta})\| \|\mathbf{f}_p(\boldsymbol{\eta}_e)\| \|\mathbf{v}_e\| \leq \frac{\rho^2}{2} \delta_{p\max} \lambda_{\max} \{M\} (\|\mathbf{f}_p(\boldsymbol{\eta}_e)\|^2 + \|\mathbf{v}_e\|^2) \end{aligned} \quad (4.30)$$

Using *Lemma 3.1(i)*,

$$\mathbf{s}^T K_w \mathbf{f}_w(\boldsymbol{\chi}_e) = \sum_{i=1}^3 K_{wi} f_{wi}(\boldsymbol{\chi}_{ei}) s_i \leq \sum_{i=1}^3 K_{wi} |f_{wi}(\boldsymbol{\chi}_{ei})| |s_i| \quad (4.31)$$

Using(4.14a),  $s^T \mathbf{h} = s^T \mathbf{h}_1 + s^T \mathbf{h}_2$

$$\text{With the help of (4.14c), } s^T \mathbf{h}_1 = \sum_{i=1}^3 s_i h_{1i} \leq \sum_{i=1}^3 h_{1imax} |s_i| \quad (4.32a)$$

$$\text{Since, } \|\mathbf{v}_e^T + \rho \mathbf{f}_p^T(\boldsymbol{\eta}_e) J(\boldsymbol{\eta})\| \leq \|\mathbf{v}_e\| + \rho \|\mathbf{f}_p(\boldsymbol{\eta}_e)\|$$

$$s^T \mathbf{h}_2 \leq \|s\| \|\mathbf{h}_2\| \leq c_1 \|s\| \|\mathbf{v}_e\| \leq c_1 \left(1 + \frac{\rho}{2}\right) \|\mathbf{v}_e\|^2 + \frac{\rho c_1}{2} \|\mathbf{f}_p(\boldsymbol{\eta}_e)\|^2 \quad (4.32b)$$

when  $\left|\frac{s_i}{\varphi_i}\right| \geq 1, \forall i = 1, 2, 3$  i.e. outside the boundary layer  $B_i(t)$ , note the fact

$$s^T K_s \mathbf{f}_s(\cdot) = \sum_{i=1}^n K_{si} |s_i| \quad (4.33)$$

Incorporating (4.15a), (4.20)-(4.33) in (4.19),one obtains for the velocity set  $\mathcal{A}_1 = \{\mathbf{v}_e : \|\mathbf{v}_e\| < \|\boldsymbol{\beta}_d\|\}$ ,

$$\dot{V}_g \leq -\{\Theta_1 + C_1 \|\mathbf{v}_e\|^2 - C_3 \|\mathbf{v}_e\|^2\} - \Theta_2 \quad (4.34a)$$

For the velocity set,  $\mathcal{A}_2 = \{\mathbf{v}_e : \|\mathbf{v}_e\| \geq \|\boldsymbol{\beta}_d\|\}$ ,

$$\dot{V}_g \leq -\{\Theta_1 + C_2 \|\mathbf{v}_e\| - C_4 \|\mathbf{v}_e\|^2\} - \Theta_2 \quad (4.34b)$$

$$\begin{aligned} \text{where, } \Theta_1 = & \left\{ \lambda_{\min} \{D(\mathbf{v})\} \|\mathbf{v}_e\|^2 - \lambda_{\max} \{K_p\} \sqrt{3} \delta_{pmax} \beta_{pmax} \|\mathbf{v}_e\| - \rho \left( \sqrt{3} \delta_{pmax} \beta_{pmax} C_{max} \|\mathbf{v}_e\|^2 \right. \right. \\ & \left. \left. + \frac{1}{2} C_{max} V_{max} \left( \|\mathbf{v}_e\|^2 + \|\mathbf{f}_p(\boldsymbol{\eta}_e)\|^2 \right) \right) - \frac{\rho \lambda_{\max} \{K_D\}}{2} \|\mathbf{f}_p(\boldsymbol{\eta}_e)\|^2 - \frac{\rho}{2} \lambda_{\max} \{D(\mathbf{v})\} \left( \|\mathbf{f}_p(\boldsymbol{\eta}_e)\|^2 + \|\mathbf{v}_e\|^2 \right) \right. \\ & \left. + \rho \lambda_{\min} \{K_p\} \|\mathbf{f}_p(\boldsymbol{\eta}_e)\|^2 - \frac{1}{2} \rho \lambda_{\max} \{M\} \omega_{max} \left( \|\mathbf{f}_p(\boldsymbol{\eta}_e)\|^2 + \|\mathbf{v}_e\|^2 \right) - \rho \lambda_{\max} \{M\} \|\mathbf{v}_e\|^2 \right. \\ & \left. - \rho^2 \lambda_{max} \{M\} \|\mathbf{f}_p(\boldsymbol{\eta}_e)\|^2 - \frac{\rho^2}{2} \lambda_{max} \{M\} \left( \|\mathbf{f}_p(\boldsymbol{\eta}_e)\|^2 + \|\mathbf{v}_e\|^2 \right) \right\} \text{ and} \\ \Theta_2 = & \left( \sum_{i=1}^3 K_{si} |s_i| - \sum_{i=1}^3 K_{wi} |f_{wi}(\chi_{ei})| |s_i| - \sum_{i=1}^3 h_{1imax} |s_i| - c_1 \left(1 + \frac{\rho}{2}\right) \|\mathbf{v}_e\|^2 - \frac{\rho c_1}{2} \|\mathbf{f}_p(\boldsymbol{\eta}_e)\|^2 \right) \end{aligned}$$

Thus,for the set,  $\mathcal{A}_1 = \{\mathbf{v}_e : \|\mathbf{v}_e\| < \|\boldsymbol{\beta}_d\|\}$ ,

$$\dot{V}_g \leq -\left[\left\{(C_1 - C_3) - (R - \lambda_{\min}\{D(\mathbf{v})\})\right\}\|\mathbf{v}_e\| - H\right]\|\mathbf{v}_e\| - S\|\mathbf{f}_p(\boldsymbol{\eta}_e)\|^2 - \sum_{i=1}^3 \gamma_i |s_i|, \quad (4.35a)$$

where,  $\gamma_i = K_{si} - K_{wi} |f_{wi}(\chi_{ei})| - h_{imax}$ .

and for  $\mathcal{A}_2 = \{\mathbf{v}_e : \|\mathbf{v}_e\| \geq \|\boldsymbol{\beta}_d\|\}$ ,

$$\dot{V}_g \leq -\left[(C_2 - H) - (R + C_4 - \lambda_{\min}\{D(\mathbf{v})\})\|\mathbf{v}_e\|\right]\|\mathbf{v}_e\| - S\|\mathbf{f}_p(\boldsymbol{\eta}_e)\|^2 - \gamma\|\mathbf{s}\| \quad (4.35b)$$

Hence, in (4.35a), for  $\mathcal{A}_1 = \{\mathbf{v}_e : \|\mathbf{v}_e\| < \|\boldsymbol{\beta}_d\|\}$ ,

$$(C_1 - C_3) - (R - \lambda_{\min}\{D(\mathbf{v})\}) > \frac{H}{\|\mathbf{v}_{e(min)}\|} \Rightarrow (C_1 - C_3) - \frac{H}{\|\mathbf{v}_{e(min)}\|} > R - \lambda_{\min}\{D(\mathbf{v})\} \quad (4.36a)$$

where,  $\|\mathbf{v}_e\|_{min} = \{\|\mathbf{v}_e\| : \|\mathbf{s}\| = \|\boldsymbol{\varphi}\|\}$ . As,  $\|\mathbf{v}_e\|_{min} = \|\mathbf{s} - \rho J^T(\boldsymbol{\eta}) \mathbf{f}_p(\boldsymbol{\eta}_e)\|_{min} \geq \|\mathbf{s}\|_{min} - \rho\|\mathbf{f}_p(\boldsymbol{\eta})\|_{max}$  and

outside the boundary layer, i.e.  $\|\mathbf{s}\| \geq \varphi_{max}$ , where,  $\varphi_{max} = \sqrt{\sum_{i=1}^3 \varphi_i^2}$ ; (4.36a) can be written as,

$$(C_1 - C_3) - \frac{H}{\|\mathbf{s}\| - \rho\|\mathbf{f}_p(\boldsymbol{\eta}_e)\|_{max}} > R - \lambda_{\min}\{D(\mathbf{v})\} \Rightarrow \frac{1}{\rho} \left[ \varphi_{max} - \frac{H}{(C_1 - C_3) - (R - \lambda_{\min}\{D(\mathbf{v})\})} \right] > \|\mathbf{f}_p(\boldsymbol{\eta}_e)\|_{max} \quad (4.36b)$$

In (4.35b), for  $\mathcal{A}_2 = \{\mathbf{v}_e : \|\mathbf{v}_e\| \geq \|\boldsymbol{\beta}_d\|\}$

$$(C_2 - H) - (R + C_4 - \lambda_{\min}\{D(\mathbf{v})\})\|\mathbf{v}_e\| > 0 \Rightarrow V_{max} \geq \frac{C_2 - H}{R + C_4 - \lambda_{\min}\{D(\mathbf{v})\}}$$

$$\Rightarrow R - \lambda_{\min}\{D(\mathbf{v})\} \geq \frac{C_2 - H}{V_{max}} - C_4 \quad (4.36c)$$



as maximum possible value of  $\|\mathbf{v}_e\|$  is  $V_{max}$ . Therefore, for  $V_{max} \geq \|\mathbf{v}_e\| \geq 0$ , if inequality of (4.15a), (4.15b) are satisfied; (4.35) may lead to

$$\dot{V}_g \leq -\sum_{i=1}^3 \gamma_i |s_i| \quad (4.37)$$

for  $\left| \frac{s_i}{\varphi_i} \right| \geq 1, \forall i = 1, 2, 3$ . Hence, whenever  $\{s(0) : |s_i(0)| > \varphi_i, \forall i = 1, 2, 3\}$ ; the squared distance to each boundary layer  $B_i(t)$ , as measured by  $s_i^2(t)$  is strictly decreasing until  $s_i(t)$  reaches to it in finite time and remains inside it thereafter if  $\gamma_i$  is strictly positive i.e. (4.15c) is satisfied. So, a stable reaching phase [210] corresponding to each switching surface always exists in finite time which is estimated from  $t_{ri} = \frac{s_i(0)}{\gamma_i}, \forall i = 1, 2, 3$ . Once, the system of AUV reaches  $\mathbf{B}(t)$ , it becomes robust to parameter uncertainties. Therefore, robustness to parameter uncertainties depends upon the thickness of boundary layer. Generally, the output can not reach desired value, rather it remains inside a bounded set around the desired one. Therefore, origin corresponding to tracking error is not stabilized, rather ultimate boundedness is established.

Under the condition (4.16), the forces and torque produced by control law (4.11) satisfy the actuator constraints (3.4). Moreover, it is feasible to find the values of  $\varnothing_{\delta \max(l)}, \varnothing'_{\delta \max(l)}, \varnothing''_{\delta \max(l)}, \varnothing_{\delta \max(\omega)}, \varnothing'_{\delta \max(\omega)}, \varnothing''_{\delta \max(\omega)}$  in reconciliation with (4.16) and depending upon the elements chosen for  $K_s$ . Hence, properly chosen values of parameters for functions  $f_d(\cdot), f(\cdot), f_w(\cdot)$  can maintain the actuator constraints i.e.  $|F_u| \leq F_{umax}, |F_v| \leq F_{vmax}$  and  $|F_\omega| \leq F_{\omega max}$ .

Next, conditions for global bounded stability for a tracking controller are developed based on the behaviour of trajectory inside the boundary layer. Conditions are cited in the following theorem.

*Remarks 4.4:*  $K_w$  should be selected carefully to make integral action within a limit. To reduce the level of integral output on occurrence of integrator-wind-up, usually low value for  $K_w$  is chosen.

*Theorem 4.1:* Consider the dynamics (3.3) together with the control law (4.11), switching manifold (4.9) and boundary layer (4.10). There exists gain matrices  $K_d, K_p, K_w, K_s$  such that

*Lemma 4.1* holds and following five inequalities are satisfied

$$\lambda_{\min} \{K_p\} \delta_{\min} > \rho^2 \lambda_{\max} \{M\} \quad (4.38a)$$

$$K_{si} > \frac{h_{imax} \phi_i}{|\phi_i|}, \forall i = 1, 2, 3 \quad (4.38b)$$

$$(C_1 - C_3) > A \quad (4.38c)$$

where,  $A = c_1 \left(1 + \frac{\rho}{2}\right) + \rho \Gamma_1 - \lambda_{\min} \{D(\mathbf{v})\}$  and positive constant  $\Gamma_1$  is expressed as

$$\Gamma_1 = \sqrt{3} \delta_{pmax} \beta_{pmax} C_{max} + \frac{1}{2} C_{max} V_{max} + \frac{1}{2} \lambda_{\max} \{D(\mathbf{v})\} + \lambda_{\max} \{M\} + \frac{1}{2} \lambda_{\max} \{M\} \omega_{max}$$

$$\text{For, } V_{max} \geq \|\mathbf{v}_e\| \geq 0; \left( \frac{C_2}{V_{max}} - C_4 \right) > A \quad (4.38d)$$

$$B > 0 \quad (4.38e)$$

where,  $B = \rho \left( \lambda_{\min} \{K_p\} - \frac{c_1}{2} - \Gamma_2 \right)$  and positive constant  $\Gamma_2$  is expressed as

$$\Gamma_2 = \frac{1}{2} [C_{max} V_{max} + \lambda_{\max} \{D(\mathbf{v})\} + \lambda_{\max} \{M\} \omega_{max} + \lambda_{\max} \{K_d\}]$$

and for a set  $\Omega_{\varphi>} = \{(\boldsymbol{\eta}_e, \mathbf{v}_e) : \forall |x_e| \geq \mu_1, |y_e| \geq \mu_2, |\theta_e| \geq \mu_3, |s_i| \geq \varphi_i, \forall i=1,2,3\}$  corresponding to outside of boundary layer  $\mathbf{B}(t)$ , following two inequalities are satisfied

$$\|\mathbf{f}_p(\boldsymbol{\eta}_e)\|_{\min} \geq \frac{2\rho(C_1 - (A + C_3))\varphi_{\max}}{\left\{\left((C_1 - (A + C_3))\rho^2 + B\right)\right\}} \quad (4.38f)$$

where,  $\|\mathbf{f}_p(\boldsymbol{\eta}_e)\|_{(max)} \in \{\|\mathbf{f}_p(\boldsymbol{\eta}_e)\| : \|s\| = \|\varphi\|\}$ . Then the trajectory reaches to a bounded set

$\Omega_{\varphi<} = \{(\boldsymbol{\eta}_e, \mathbf{v}_e) : |x_e| \leq \mu_1, |y_e| \leq \mu_2, |\theta_e| \leq \mu_3, |s_i| \leq \varphi_i, \forall i=1,2,3\}$ , corresponding to  $\mathbf{B}(t)$ , globally in

finite time and remain inside it for  $t \geq 0$ . Or, if the trajectory starts inside  $\Omega_{\varphi<}$ , it remains inside it for  $t \geq 0$ .

*Proof:* To examine passivity [200] for input-output relationship of (4.13), let us define the output vector for desired trajectory tracking by the system of AUV

$$\boldsymbol{\gamma} = \mathbf{v}_e + \rho J^T(\boldsymbol{\eta}) \mathbf{f}_p(\boldsymbol{\eta}_e) = \mathbf{s} \quad (4.39a)$$

Hence, the following relation holds true from the expression of  $\boldsymbol{\chi}_e$

$$\dot{\boldsymbol{\chi}}_e = \mathbf{s} \quad (4.39b)$$

To verify stability [199] for the closed-loop system (4.13), the inner product of (4.39a) and (4.13) is taken as

$$\begin{aligned} \boldsymbol{\gamma}^T (-K_w \mathbf{f}_w(\boldsymbol{\chi}_e)) &\geq \mathbf{s}^T (M\dot{\mathbf{v}}_e + C(\mathbf{v})\mathbf{v}_e + D(\mathbf{v})\mathbf{v}_e + K_d \mathbf{f}_d(\mathbf{v}_e) + J^T(\boldsymbol{\eta}) K_r \mathbf{f}_p(\boldsymbol{\eta}_e) + K_s \mathbf{f}_s(\mathbf{s}) - \mathbf{h}) \\ &\Rightarrow (\mathbf{v}_e + \rho J^T(\boldsymbol{\eta}) \mathbf{f}_p(\boldsymbol{\eta}_e))^T (M\dot{\mathbf{v}}_e + C(\mathbf{v})\mathbf{v}_e + D(\mathbf{v})\mathbf{v}_e + K_d \mathbf{f}_d(\mathbf{v}_e) + K_p J^T(\boldsymbol{\eta}) \mathbf{f}_p(\boldsymbol{\eta}_e) + K_s \mathbf{f}_s(\mathbf{s}) - \mathbf{h}) \\ &\quad + \mathbf{s}^T K_w \mathbf{f}_w(\boldsymbol{\chi}_e) \leq 0 \end{aligned} \quad (4.40)$$

Considering the *Property* 3.4, (4.40) is expressed as follows

$$\frac{dV}{dt}(\mathbf{v}_e, \mathbf{f}_p(\boldsymbol{\eta}_e), \boldsymbol{\eta}) + Q(\mathbf{f}_p(\boldsymbol{\eta}_e), \mathbf{v}_e, \mathbf{f}_d(\mathbf{v}_e)) = 0 \quad (4.41)$$

for  $V = V_1 + V_2$  (4.42) where,

$$V_1(\mathbf{v}_e, \mathbf{f}_p(\boldsymbol{\eta}_e), \boldsymbol{\eta}) = \frac{1}{2} \mathbf{v}_e^T M \mathbf{v}_e + \rho \mathbf{f}_p^T(\boldsymbol{\eta}_e) J(\boldsymbol{\eta}) M \mathbf{v}_e + \sum_{i=1}^3 \int_0^{\boldsymbol{\eta}_e(i)} \mathbf{f}_{pi}^T(\boldsymbol{\eta}_e(i)) K_{pi} d\boldsymbol{\eta}_e(i) \quad (4.43a)$$

$$\text{and } V_2 = W(\boldsymbol{\chi}_e) \quad (4.43b)$$

$$\text{and for } Q = Q_1 + Q_2 \quad (4.44)$$

$$\text{where, } Q_1 = \mathbf{v}_e^T D(\mathbf{v}) \mathbf{v}_e + \mathbf{v}_e^T K_d \mathbf{f}_d(\mathbf{v}_e) + \rho \mathbf{f}_p^T(\boldsymbol{\eta}_e) K_p \mathbf{f}_p(\boldsymbol{\eta}_e) + \mathbf{s}^T (K_s \mathbf{f}_s(\mathbf{s}) - \mathbf{h}) \quad (4.45a)$$

$$\begin{aligned} Q_2 = & \rho \left\{ \mathbf{f}_p^T(\boldsymbol{\eta}_e) J(\boldsymbol{\eta}) C(\mathbf{v}) \mathbf{v}_e + \mathbf{f}_p^T(\boldsymbol{\eta}_e) J(\boldsymbol{\eta}) D(\mathbf{v}) \mathbf{v}_e + \mathbf{f}_p^T(\boldsymbol{\eta}_e) J(\boldsymbol{\eta}) K_d \mathbf{f}_d(\mathbf{v}_e) \right. \\ & \left. - \dot{\mathbf{f}}_p^T(\boldsymbol{\eta}_e) J(\boldsymbol{\eta}) M \mathbf{v}_e - \mathbf{f}_p^T(\boldsymbol{\eta}_e) \dot{J}(\boldsymbol{\eta}) M \mathbf{v}_e \right\} \end{aligned} \quad (4.45b)$$

as  $\boldsymbol{\gamma} = \mathbf{s}$ . It can be proved that  $V$  is positive definite in  $\mathbf{f}_p(\boldsymbol{\eta}_e)$  and  $\mathbf{v}_e$ . Hence,  $V$  eventually becomes a Lyapunov function [199] for stability analysis of tracking control of AUV. According to Lyapunov theory it is necessary to prove positive definiteness of  $V$ . In association with  $V_1$  of (4.43a) following inequality holds true based on an established condition.

$$\begin{aligned} H = & \frac{1}{4} \left( \mathbf{v}_e + 2\rho J^T(\boldsymbol{\eta}) \mathbf{f}_p(\boldsymbol{\eta}_e) \right)^T M \left( \mathbf{v}_e + 2\rho J^T(\boldsymbol{\eta}) \mathbf{f}_p(\boldsymbol{\eta}_e) \right) - \rho^2 \mathbf{f}_p^T(\boldsymbol{\eta}_e) J(\boldsymbol{\eta}) M J^T(\boldsymbol{\eta}) \mathbf{f}_p(\boldsymbol{\eta}_e) \\ & \sum_{i=1}^3 \int_0^{\boldsymbol{\eta}_e(i)} \mathbf{f}_{pi}^T(\boldsymbol{\eta}_e(i)) K_{pi} d\boldsymbol{\eta}_e(i) \end{aligned} \quad (4.46a)$$

In (4.46a),  $J(\boldsymbol{\eta}) M J^T(\boldsymbol{\eta})$  is a symmetric matrix and  $J(\boldsymbol{\eta})$  is orthogonal. Thus,  $\lambda_{\max} \{J(\boldsymbol{\eta}) M J^T(\boldsymbol{\eta})\}$

$= \lambda_{\max} \{M\}$ . With the help of Lemma 3.2, following inequality can be obtained from (4.46a), if (4.38a) is satisfied

$$H \geq \lambda_{\min} \{K_p\} \wp_{\min} \|\mathbf{f}_p(\boldsymbol{\eta}_e)\|^2 - \rho^2 \lambda_{\max} \{M\} \|\mathbf{f}_p(\boldsymbol{\eta}_e)\|^2 \quad (4.46b)$$

where,  $\wp_{\min} = \min_i \{\wp_i\}$ . Substituting eq.(4.46b) in Eq.(4.43a), following may be obtained

$$V_1 \geq \frac{1}{4} \mathbf{v}_e^T \mathbf{M} \mathbf{v}_e + \left( \lambda_{\min} \{K_p\} \wp_{\min} - \rho^2 \lambda_{\max} \{M\} \right) \|\mathbf{f}_p(\boldsymbol{\eta}_e)\|^2 \geq 0 \quad (4.47)$$

If (4.38a) is satisfied. Since,  $V_2$  is radially unbounded positive definite function according to (4.12), therefore,  $V$  is a radially unbounded globally positive definite function according to (4.37).

Next, the time derivative of  $V$  is to be proved negative definite. According to (4.36), showing negative definiteness of  $V$  is equivalent to showing positive definiteness of  $Q$ . As  $\mathbf{f}_p^T(\boldsymbol{\eta}_e)$  is bounded, the lower bound of  $Q_2$  is derived with the help of inequalities (4.23),(4.24),(4.25) and the inequalities corresponding to last two terms of  $Q_2$ , developed following same procedure of developing (4.27) and (4.28). Thus, using (4.38b), (4.38c) and getting the expression of  $\sigma_{1d}$  and  $\sigma_{2d}$  from (4.15a)

if  $\|\mathbf{x}\| < \|\boldsymbol{\beta}_d\|$ ,

$$\begin{aligned} Q_2 &\geq -\rho \left\{ \sqrt{3} \delta_{pmax} \beta_{pmax} C_{max} \|\mathbf{v}_e\|^2 + \frac{1}{2} C_{max} V_{max} \left( \|\mathbf{v}_e\|^2 + \|\mathbf{f}_p(\boldsymbol{\eta}_e)\|^2 \right) + \frac{1}{2} \lambda_{\max} \{D(\mathbf{v})\} \left( \|\mathbf{f}_p(\boldsymbol{\eta}_e)\|^2 + \|\mathbf{v}_e\|^2 \right) \right. \\ &\quad \left. + \lambda_{\max} \{K_D\} \frac{1}{2} \left( \|\mathbf{f}_p(\boldsymbol{\eta}_e)\|^2 + \sigma_{1d} \|\mathbf{v}_e\|^2 \right) + \lambda_{\max} \{M\} \|\mathbf{v}_e\|^2 + \frac{1}{2} \lambda_{\max} \{M\} \omega_{max} \left( \|\mathbf{f}_p(\boldsymbol{\eta}_e)\|^2 + \|\mathbf{v}_e\|^2 \right) \right\} \\ &\Rightarrow Q_2 \geq -\rho \left( \Gamma_1 + \frac{C_3}{\rho} \right) \|\mathbf{v}_e\|^2 - \rho \Gamma_2 \|\mathbf{f}_p(\boldsymbol{\eta}_e)\|^2 \end{aligned} \quad (4.48a)$$

$$\text{if } \|\mathbf{x}\| \geq \|\boldsymbol{\beta}_d\|, Q_2 \geq -\rho \left( \Gamma_1 + \frac{C_4}{\rho} \right) \|\mathbf{v}_e\|^2 - \rho \Gamma_2 \|\mathbf{f}_p(\boldsymbol{\eta}_e)\|^2 \quad (4.48b)$$

$$\text{For, } \left| \frac{s_i}{\varphi_i} \right| \leq 1, \forall i = 1, 2, 3;$$

$$s^T K_s \mathbf{f}_s(.) = \sum_{i=1}^3 \left( \frac{K_{si}}{\varphi_i} \right) |s_i|^2 \quad (4.49)$$

$$\text{With the help of results of (4.20), (4.21), (4.26), (4.32) and since, } \lambda_{\min} \{J(\boldsymbol{\eta}) J^T(\boldsymbol{\eta})\} = 1, \quad (4.41)$$

an be written as

$$\begin{aligned} \text{For, } \mathcal{A}_1 &= \left\{ \mathbf{v}_e : \|\mathbf{v}_e\|_{\min} \leq \|\mathbf{v}_e\| < \|\boldsymbol{\beta}_d\| \right\}, \\ Q &\geq \sum_{i=1}^3 \left\{ K_{si} - h_{imax} \right\} |s_i| + \left( C_1 - \left( c_1 \left( 1 + \frac{\rho}{2} \right) + \rho \Gamma_1 + C_3 - \lambda_{\min} \{D(\mathbf{v})\} \right) \right) \|\mathbf{v}_e\|^2 \\ &+ \rho \left( \lambda_{\min} \{K_p\} - \frac{c_1}{2} - \Gamma_2 \right) \|\mathbf{f}_p(\boldsymbol{\eta}_e)\|^2 \end{aligned} \quad (4.50a)$$

$$\begin{aligned} \text{For, } \mathcal{A}_2 &= \left\{ \mathbf{v}_e : \|\mathbf{v}_e\| < \|\mathbf{v}_e\|_{\min} \right\}, \\ Q &\geq \sum_{i=1}^3 \left\{ \left( \frac{|s_i|}{\varphi_i} \right) K_{si} - h_{imax} \right\} |s_i| + \left( C_1 - \left( c_1 \left( 1 + \frac{\rho}{2} \right) + \rho \Gamma_1 + C_3 - \lambda_{\min} \{D(\mathbf{v})\} \right) \right) \|\mathbf{v}_e\|^2 \\ &+ \rho \left( \lambda_{\min} \{K_p\} - \frac{c_1}{2} - \Gamma_2 \right) \|\mathbf{f}_p(\boldsymbol{\eta}_e)\|^2 \end{aligned} \quad \dots(4.50b)$$

$$\begin{aligned} \text{For } \mathcal{A}_3 &= \left\{ \mathbf{v}_e : \|\mathbf{v}_e\| \geq \|\boldsymbol{\beta}_d\| \right\}, Q \geq \sum_{i=1}^3 \left\{ K_{si} - h_{imax} \right\} |s_i| + \left( C_2 - \left( c_1 \left( 1 + \frac{\rho}{2} \right) + \rho \Gamma_1 + C_4 - \lambda_{\min} \{D(\mathbf{v})\} \right) \right) \|\mathbf{v}_e\| \|\mathbf{v}_e\| \\ &+ \rho \left( \lambda_{\min} \{K_p\} - \frac{c_1}{2} - \Gamma_2 \right) \|\mathbf{f}_p(\boldsymbol{\eta}_e)\|^2 \end{aligned} \quad (4.50c)$$

$$\text{Assume, } A = c_1 \left( 1 + \frac{\rho}{2} \right) + \rho \Gamma_1 - \lambda_{\min} \{D(\mathbf{v})\}, B = \rho \left( \lambda_{\min} \{K_p\} - \frac{c_1}{2} - \Gamma_2 \right)$$

$$\text{For, } \mathcal{A}_1 = \left\{ \mathbf{v}_e : \|\mathbf{v}_e\|_{\min} \leq \|\mathbf{v}_e\| < \|\boldsymbol{\beta}_d\| \right\},$$

following (50a),

$$Q \geq \sum_{i=1}^3 \{K_{si} - h_{imax}\} |s_i| + (C_1 - (A + C_3)) \|\mathbf{v}_e\|^2 + B \|\mathbf{f}_p(\boldsymbol{\eta}_e)\|^2 \quad (4.51a)$$

For,  $\Delta_2 = \{\mathbf{v}_e : \|\mathbf{v}_e\| < \|\mathbf{v}_e\|_{min}\}$ ,

$$Q \geq \sum_{i=1}^3 \left\{ \left( \frac{K_{si}}{\varphi_i} \right) |s_i| - h_{imax} \right\} |s_i| + \left( C_1 - \left( c_1 \left( 1 + \frac{\rho}{2} \right) + \rho \Gamma_1 + C_3 - \lambda_{min} \{D(\mathbf{v})\} \right) \right) \|\mathbf{v}_e\|^2 \\ + \rho \left( \lambda_{min} \{K_p\} - \frac{c_1}{2} - \Gamma_2 \right) \|\mathbf{f}_p(\boldsymbol{\eta}_e)\|^2 \quad (4.51b)$$

For  $\Delta_3 = \{\mathbf{v}_e : \|\mathbf{v}_e\| \geq \|\boldsymbol{\beta}_d\|\}$ ,

$$Q \geq \sum_{i=1}^3 \{K_{si} - h_{imax}\} |s_i| + \{C_2 - (A + C_4) V_{max}\} \|\mathbf{v}_e\| + B \|\mathbf{f}_p(\boldsymbol{\eta}_e)\|^2 \quad (4.51c)$$

as  $V_{max} \geq \|\mathbf{v}_e\|$ . Inside the boundary layer  $\mathbf{B}(t)$ , one has

$$\mathbf{v}_e = -\rho \mathbf{J}^T(\boldsymbol{\eta}) \mathbf{f}_p(\boldsymbol{\eta}_e) + \mathbf{s} \quad (4.52)$$

Substituting  $\mathbf{v}_e$  of (4.52) and replacing  $A, B$  in (4.51b) one gets for  $\Delta_3 = \{\mathbf{v}_e : \|\mathbf{v}_e\| \leq \|\mathbf{v}_e\|_{min}\}$ ,

$$\|\mathbf{v}_e\|_{min} < \|\boldsymbol{\beta}_d\|,$$

$$Q \geq \sum_{i=1}^3 \left\{ \left( \frac{K_{si}}{\varphi_i} \right) |s_i| - h_{imax} \right\} |s_i| + (C_1 - (A + C_3)) \|\mathbf{s}\|^2 \\ + \left\{ (C_1 - (A + C_3)) \rho^2 + B \right\} \|\mathbf{f}_p(\boldsymbol{\eta}_e)\|_{min}^2 - 2\rho (C_1 - (A + C_3)) \|\mathbf{f}_p(\boldsymbol{\eta}_e)\|_{min} \varphi_{max} \} \quad (4.53)$$

since,  $\|\mathbf{v}_e\|_{max} = \|\mathbf{s} - \rho \mathbf{J}^T(\boldsymbol{\eta}) \mathbf{f}_p(\boldsymbol{\eta}_e)\|_{max} \geq \|\mathbf{s}\|_{max} - \rho \|\mathbf{f}_p(\boldsymbol{\eta}_e)\|_{min}$  and  $\|\mathbf{s}\| \leq \varphi_{max}$ , where,  $\varphi_{max} =$

$\sqrt{\sum_{i=1}^3 \varphi_i^2}$ . Conditions for achieving positive definiteness of  $Q$  may be derived from (4.51) and

(4.53). Thus, it may be concluded that  $Q$  is positive definite i.e.  $Q > 0$ , in the set

$$\Omega_{\varphi>} = \{(\boldsymbol{\eta}_e, \mathbf{v}_e) : \|\mathbf{s}\| \geq \varphi_{\max}\}, \text{ if}$$

i) For the first term of (4.51a) and (4.51b); (4.38b) is satisfied.

ii) for the second term of (4.51a); (4.38c) is satisfied.

iii) for the second term of (4.51b); (4.38d) is satisfied.

iv) for third term of (4.51a) and (4.51b);  $B > 0$  i.e. (4.38e) is satisfied.

v) for third term of (4.53), following inequality is satisfied i.e.

$$\left\{ \left( (C_1 - (A + C_3))\rho^2 + B \right) \|\mathbf{f}_p(\boldsymbol{\eta}_e)\|_{\min}^2 \geq 2\rho(C_1 - (A + C_3)) \|\mathbf{f}_p(\boldsymbol{\eta}_e)\|_{\min} \varphi_{\max} \right\} \Rightarrow$$

$$\left\{ \left( (C_1 - (A + C_3))\rho^2 + B \right) \|\mathbf{f}_p(\boldsymbol{\eta}_e)\|_{\min} \geq 2\rho(C_1 - (A + C_3)) \varphi_{\max} \Rightarrow \|\mathbf{f}_p(\boldsymbol{\eta}_e)\|_{\min} \geq \frac{2\rho(C_1 - (A + C_3))\varphi_{\max}}{\left( (C_1 - (A + C_3))\rho^2 + B \right)} = X \right.$$

is satisfied i.e. (4.38f) is satisfied. Thus,  $Q$  is positive definite in the set  $\Omega_{\varphi>} = \{(\boldsymbol{\eta}_e, \mathbf{v}_e) : \|\mathbf{f}_p(\boldsymbol{\eta}_e)\| \geq X,$

$\|\mathbf{s}\| \geq \varphi_{\max}\}$ . Since,  $V$  and  $Q$  are both positive definite, one may have, from (4.41)

$$\dot{V} \leq -Q(\mathbf{f}_p(\boldsymbol{\eta}_e), \mathbf{v}_e) < 0 \quad (4.54)$$

Therefore,  $\dot{V}$  remains negative definite in the set  $\Omega_{\varphi>} = \{(\boldsymbol{\eta}_e, \mathbf{v}_e) : \|\mathbf{f}_p(\boldsymbol{\eta}_e)\| \geq X, \|\mathbf{s}\| \geq \varphi_{\max}\}$ . Thus, if

$\Omega_{0>} = \{s(0) : \|\mathbf{f}_p(\boldsymbol{\eta}_e(0))\| \geq X(0), |s(0)| \geq \varphi_{\max}\}$  the trajectory reaches to  $\mathbf{B}(t)$ , globally in finite time and remains inside it thereafter or if  $\Omega_{0<} = \{s(0) : \|\mathbf{f}_p(\boldsymbol{\eta}_e(0))\| \leq X(0), |s(0)| \leq \varphi_{\max}\}$  it remains inside  $\mathbf{B}(t)$  for  $t \geq 0$ .

*Remarks 4.5:* It is true that both  $\|\mathbf{f}_p(\boldsymbol{\eta}_e)\|_{\max}$  and  $\|\mathbf{f}_p(\boldsymbol{\eta}_e)\|_{\min}$  are same as they both correspond to boundary layer.



## 4.8 Simulation Results and Discussion

In this section, the efficacy of the proposed SM-N-PID controller with BI and BD has been investigated for tracking control of AUV with kinematics and dynamics of an AUV as mentioned on (3.2) and (3.3) respectively in presence of bounded parametric uncertainties and actuator constraints. A list of parameters of AUV dynamics and their nominal values are given in Table 3.6. In this table, deviation of  $\pm 10\%$  from their nominal values for the parameters are also depicted. Simulation uses MATLAB of version 2012a as the software environment.

To compare the effectiveness of the proposed controller, a basic PID group controller for tracking namely PD plus Feedforward Compensation (PD plus FC) and one existing model-independent tracking controllers namely SM-N-PID controller without BI and BD have been selected for the same dynamics of AUV. SM-N-PID without BI and BD controller is based on its regulatory version [173]. Only Sliding Mode part makes the difference between tracking and set-point controller. The control laws of these controllers are given below.

i) PD plus Feedward Compensation:

$$\mathbf{F} = -K_p \mathbf{J}^T(\boldsymbol{\eta}) \boldsymbol{\eta}_e - K_d \mathbf{v}_e - M(\mathbf{v}) \frac{d}{dt} \left( \mathbf{J}^T(\boldsymbol{\eta}) \mathbf{v}_r \right) - C(\mathbf{v}) \mathbf{J}^T(\boldsymbol{\eta}) \mathbf{v}_r - D(\mathbf{v}) \mathbf{J}^T(\boldsymbol{\eta}) \mathbf{v}_r \quad (4.55a)$$

ii) SM-N-PID without BI and BD:

$$\mathbf{F} = -K_p \mathbf{J}^T(\boldsymbol{\eta}) \mathbf{f}_p(\boldsymbol{\eta}_e) - K_d \mathbf{v}_e - K_s \mathbf{f}_s(s) - K_w \int_0^t \left( \rho \mathbf{f}_p(\boldsymbol{\eta}_e(\xi)) + \mathbf{v}_e(\xi) \right) d\xi \quad (4.55b)$$

Values of common parameters of all controllers, such as maximum limit of velocity and acceleration provided by the actuator of AUV have been chosen as mentioned in Table 4.1. Actuator specifications according to requirement of given path is given in the Table 4.2. Time step for simulation is considered as 0.03 s. Simulation time is first 200 sec of tracking of desired

path. For simulation of all tracking controllers, values of initial state and initial error are depicted in Table 4.3. Large initial error in states have been selected to verify properly the differences in effects of all controllers on AUV dynamics.

AUV is intended to follow a sinusoidal path. Definition of sinusoidal path is given below:

$$\left. \begin{aligned} x(t) &= 0.03t \\ y(t) &= \sin(0.03t) \end{aligned} \right\} \quad (4.56)$$

Table 4.1: Velocity and acceleration limits [24] of actuators

Limit of Linear velocity (m/s) in BRF ( $v_{lmax}$ ):	Limit of Linear acceleration(m/s <sup>2</sup> ) in BRF( $a_{lmax}$ ):	Angular velocity (rad/s) ( $v_{2max}$ ):	Angular acceleration (rad/s <sup>2</sup> )( $a_{2max}$ ):
$\pm 0.5$	$\pm 0.005$	$\pm 0.42$	0.0008

Table 4.2: Force and torque limits [24] of actuator

Maximum limit of force(Newton) in surge direction	Maximum limit of force(Newton) in sway direction	Maximum limit of Torque(N-m) around $z_b$ axis
600	600	100

Table 4.3 Information about initial and final state

	$x$ -position	$y$ -position	Orientation	Surge velocity	Sway velocity	Angular velocity
Initial state	2	1	1.4720	0.1044	-0.0399	-0.0172
Initial error in state	12.02	12.985	0.003	0.1454	0.0547	0.0341

Gain selection The parameters of the nonlinear functions for SM-NPID with BI and BD are given in Table 4.4. Observations from simulation of different tracking controllers are compared on the basis of three performance specifications depending upon both transient and steady state response of state obtained on application of the control input generated by these controllers. These specifications are amplitude ( $M$ ) of peakovershoot/undershoot, settling time/convergence time( $t_s$ ), steady-state-error( $e_{ss}(t)$ ) of state. State includes linear position, orientation, linear and angular velocities. Observations are shown in the form of a table as given in Table 4.4. The

observation table keeps records of force and torque required for each controller for first 200 sec of tracking from an initial state.

Table 4.4 Values of parameters of nonlinear functions for SM-N-PID controller with BI and BD

Parameters of nonlinear functions	SM-N-PID without BI and BD	SM-N-PID with BI and BD
$\Phi_{max}(l)$	-----	200
$\delta_{di}, \alpha_{di}, \beta_{di}, \forall i = 1, 2$	-----	6, 4.5, 0.035714
$\Phi_{max}(\omega)$	-----	20
$\delta_{di}, \alpha_{di}, \beta_{di}, \forall i = 3$	-----	6, 5, 0.00735
$\Phi'_{max}(l)$	100	100
$\delta_{pi}, \alpha_{pi}, \beta_{pi}, \forall i = 1, 2$	12, 12, 0.00786	12, 12, 0.00786
$\Phi'_{max}(\omega)$	5	5
$\delta_{pi}, \alpha_{pi}, \beta_{pi}, \forall i = 3$	2, 2, 0.00235849	2, 2, 0.00235849
$\Phi''_{max}(l)$	-----	3
$\delta_{wi}, \alpha_{wi}, \beta_{wi}, \forall i = 1, 2$	-----	5, 3, 0.24
$\Phi''_{max}(\omega)$	-----	1
$\delta_{wi}, \alpha_{wi}, \beta_{wi}, \forall i = 3$	-----	0.9, 0.7, 0.740740

Table 4.5 Values of parameters for different controllers

Gains →	$K_p$	$K_d$	$K_s$	$K_w$
Controller ↓				
PD plus FC without uncertainties	<i>diag</i> [7, 7, 3]	<i>diag</i> [0.5, 0.5, 0.4]	-----	-----
PD plus FC with uncertainties	<i>diag</i> [7, 7, 3]	<i>diag</i> [0.5, 0.5, 0.4]	-----	-----
PD plus FC with uncertainties(suff. tuned P & D)	<i>diag</i> [70, 80,300]	<i>diag</i> [1500, 1400, 1500]	-----	-----
SM-N-PID without BI and BD	<i>diag</i> [1080,1050,1050]	<i>diag</i> [ $10^3$ , $10^3$ , $10^3$ ]	<i>diag</i> [210,210,80]	<i>diag</i> [1.2,1.2,0.5]
SM-N-PID with BI and BD	<i>diag</i> [ $10^3$ , $10^3$ , $10^3$ ]	<i>diag</i> [1200,1200,1200]	<i>diag</i> [260,260,90]	<i>diag</i> [1.5,1.5,0.7]
The value of $\rho$ is taken 0.09 for both the SM-N-PID controller with BI and and SM-N-PID Controller without BI and BD				

#### **4.8.1. Simulation Results with Analysis**

Performances of the proposed controller SM-N-PID with BI and BD is compared with two other globally stable controllers PD plus FC, a basic PID group controller and SM-N-PID without BI and BD, a basic nonlinear PID tracking controller. The setting of controller gains follows the Table 4.5.

##### ***4.8.1.1 PD plus FC (roughly tuned gains) on AUV dynamics with and without uncertainties***

Initially PD plus FC with roughly tuned gains is applied on AUV with and without (nominal dynamics) uncertainties for tracking the desired sinusoidal path under the constraints in Table 4.1 and Table 4.2 approximately. Performances are then compared in Fig 4.3-Fig 4.8. It is observed from simulations that while PD plus FC is applied on AUV without uncertainties errors in linear (Fig.4.3) and angular position (Fig. 4.4), linear (Fig.4.5) and angular velocities (Fig.4.6) converge to zero after certain intervals of time from their large initial value (Table 4.3). But when uncertainties (Table 3.6) exist especially in hydrodynamic parameters of dynamics of AUV, responses deteriorate. This happens as PD plus FC controller does not have required the structure to exactly compensate the dynamics of AUV when uncertainties involved in dynamics. The simulation envisages that errors in linear (Fig.4.3) and angular position (Fig.4.4), linear (Fig.4.5) and angular velocities (Fig.4.6) remains oscillatory with high peaks during the entire simulation period. Another observation is that the peaks of velocities are reduced in uncertainties case (Fig.4.5, Fig.4.6). Peak of control force is more in surge (Fig.4.7) and less in sway (Fig.4.7) motion in case of nominal dynamics than the values of these forces for uncertain dynamics. Peak of control torque in the case of uncertainties is more compared to its value for nominal dynamics. All observations above are recorded in 1<sup>st</sup>. and 2<sup>nd</sup>. rows of Table 4.4.

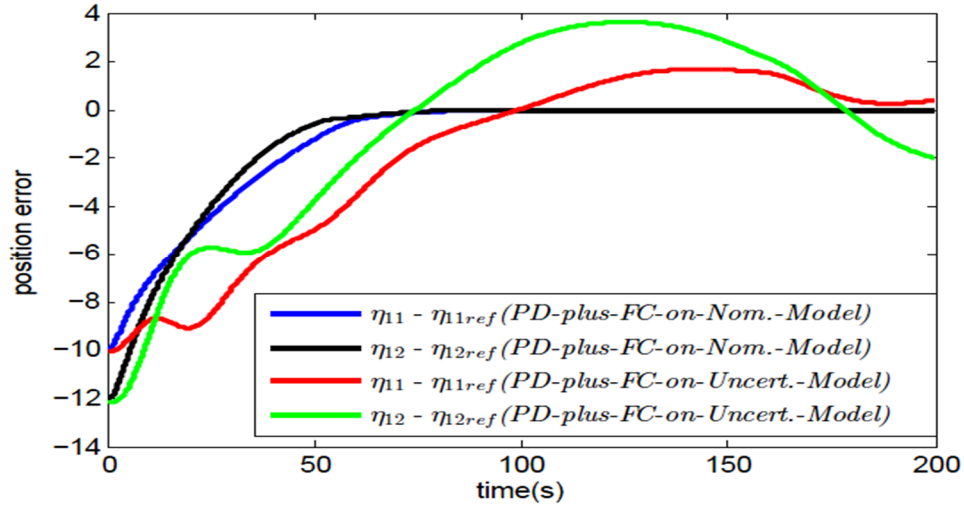


Fig. 4.3 Position errors vs. time

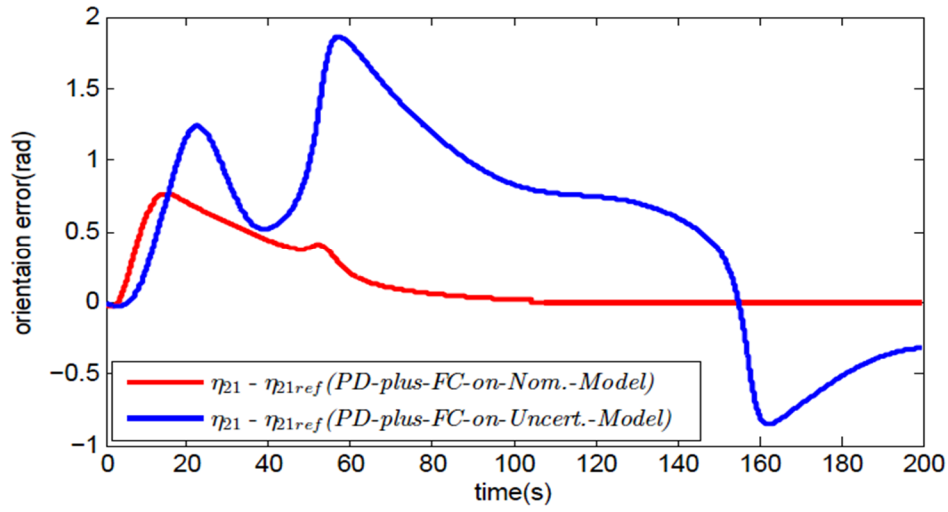


Fig.4.4 Orientation(rad) error vs. time

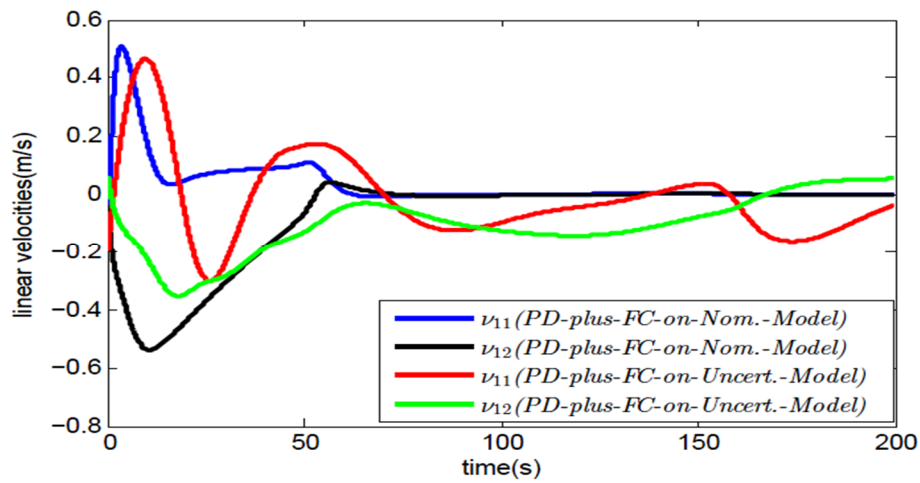


Fig.4.5:Error in linear velocities(m/s) vs. time

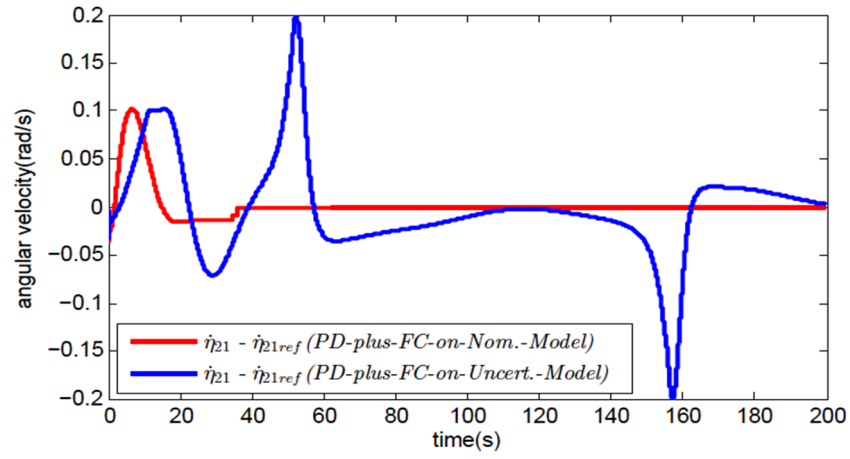


Fig.4.6 Error in angular velocity(rad/s) vs. time

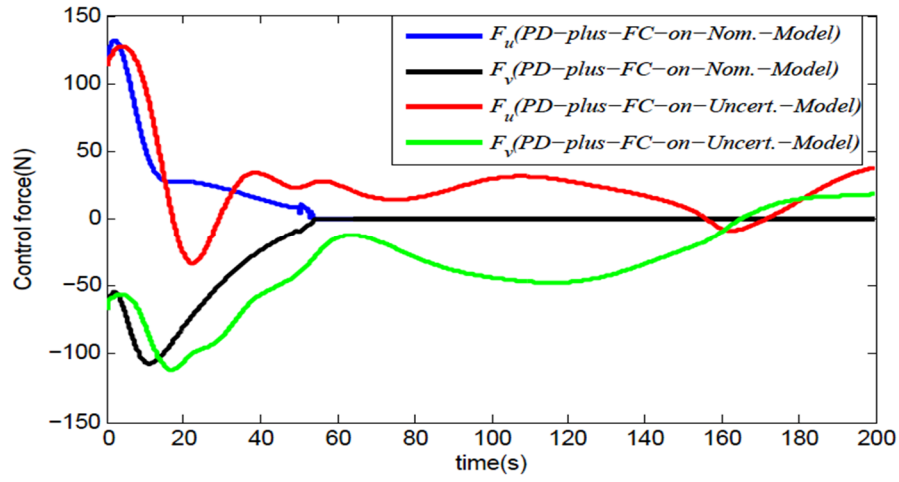


Fig. 4.7:Control forces (N) vs. time

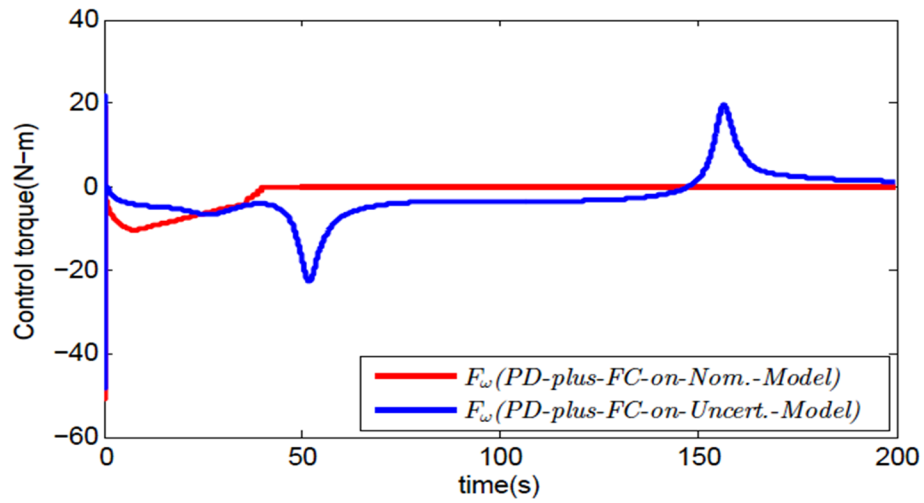


Fig. 4.8:Control torque (N-m) vs. time



#### 4.8.1.2 PD plus FC (sufficiently tuned gains) on AUV dynamics with uncertainties

If it is required to decrease the settling time by reducing the oscillation in responses, the values of the controller parameters need to be adjusted. If  $K_d$  is increased keeping  $K_p$  constant then up to a certain limit derivative control works well. But after a certain limit this gain setting generally deteriorates the responses. Moreover, it requires high control effort. If a high value of  $K_p$  is used, keeping  $K_d$  constant, the setting generally yields overshoots with reduction of rise time and settling time. Thus, proper adjustment between  $K_p$  and  $K_d$  for tuning (Fig.3.9-Fig.3.14) of the gains is very important to achieve desired transient and steady-state performance. It is cumbersome and also varies for different percentage of deviation in parameters from their nominal values. The reason is that controller gains of PD plus FC does not include information about upper bounds of parameter variation. Thus, for large initial error in state and huge parametric uncertainties, PD plus FC controller may not ensure desired output from an AUV system. It generally provides steady state error in linear position (Fig.3.9) and orientation (Fig.3.10). Demand in control forces (Fig.4.13) is very high which does not follow Table 4.2. Therefore, PD plus FC controller has a limitation for providing best transient and steady state responses from a system of AUV in tracking a reference trajectory.

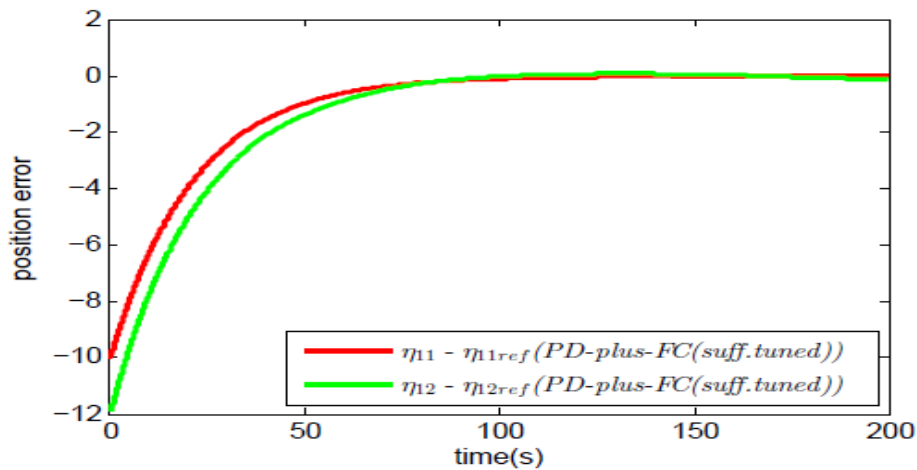


Fig. 4.9 Position errors vs. time

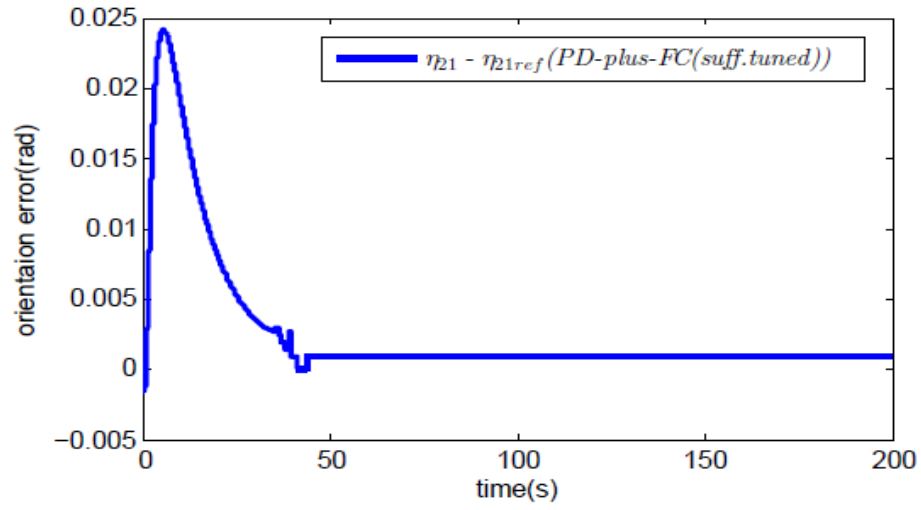


Fig.4.10 Orientation(rad) error vs. time

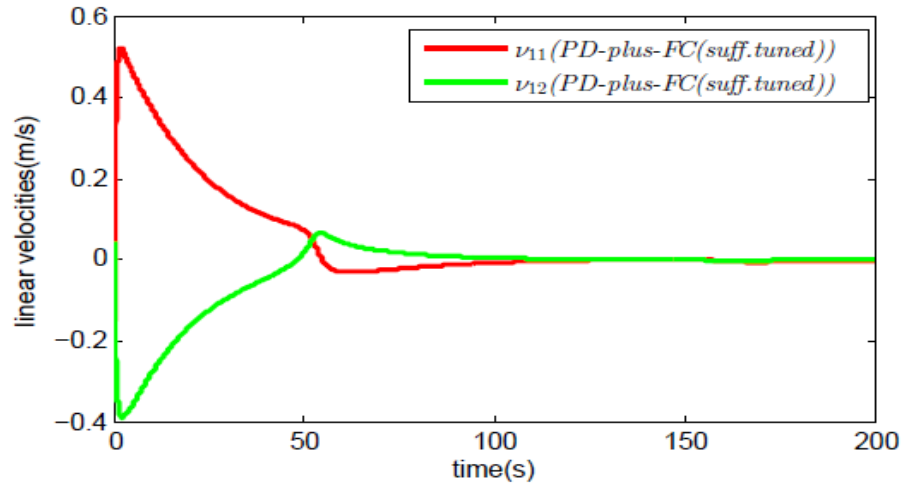


Fig. 4.11: Error in linear velocities (m/s) vs. time

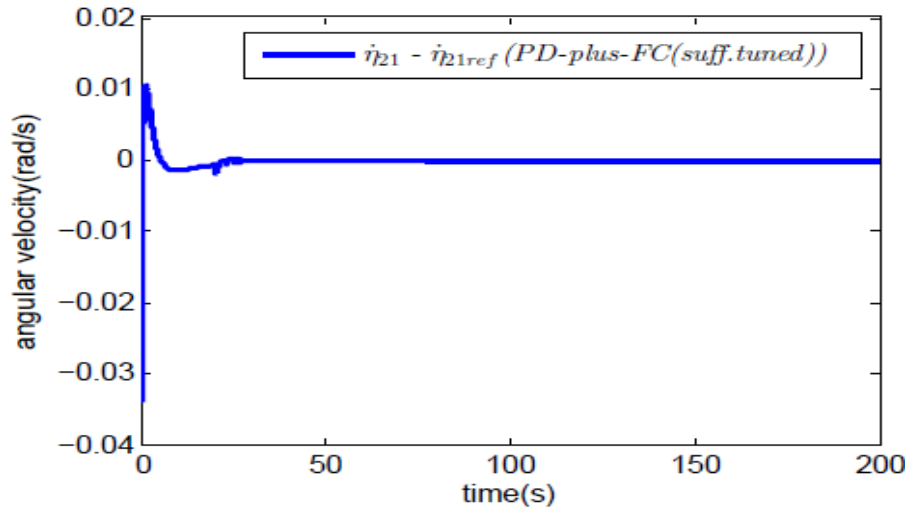


Fig.4.12 Error in Angular velocity (rad/s) vs. time

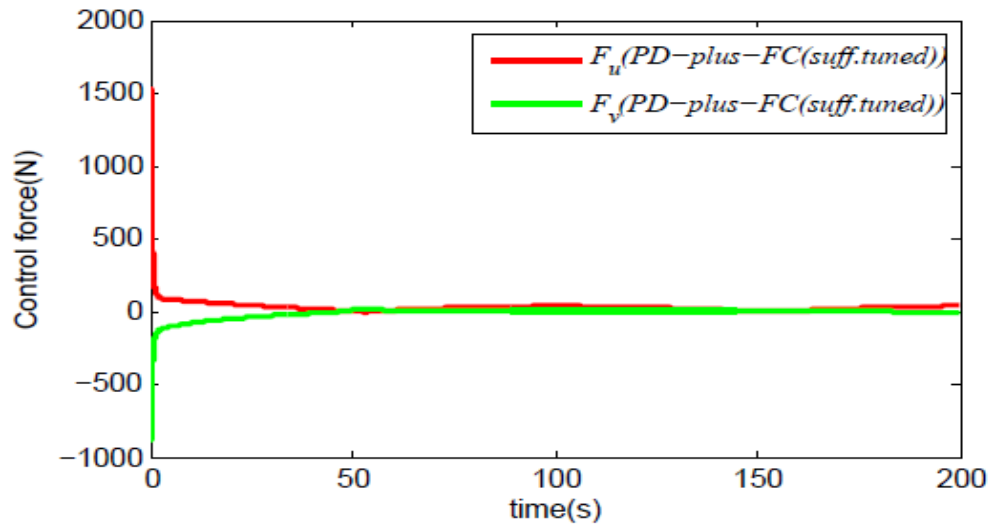


Fig. 4.13: Control forces (N) vs. time

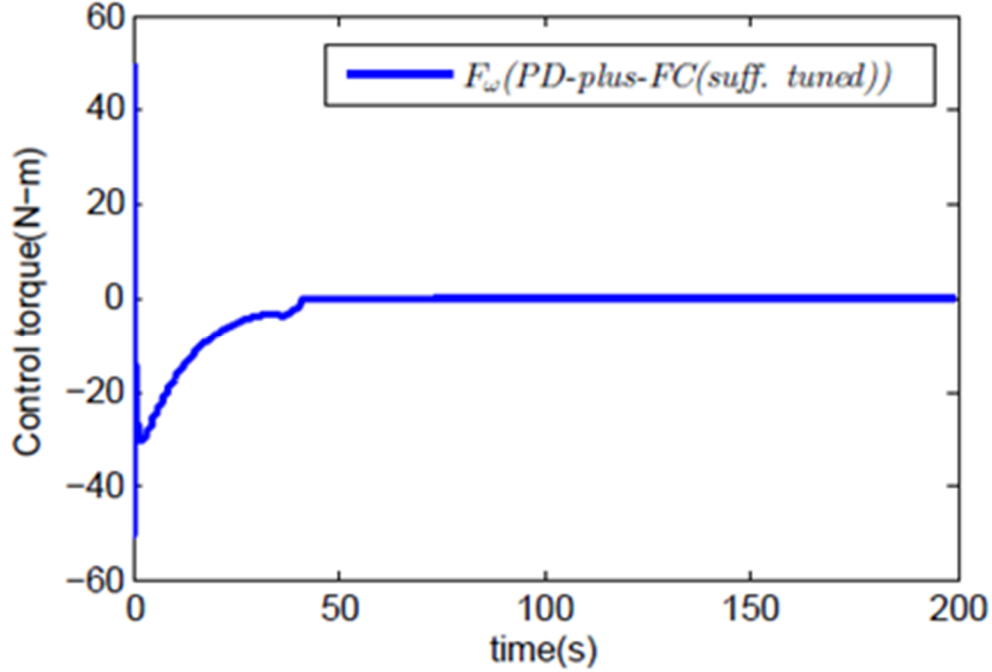


Fig.4.14 Control torque (N-m) vs. time

Next, choice is to use the other robust controllers like SMC or  $H_\infty$ . But as discussed in section 2.6 that these controllers are not preferred in application of AUVs as there lie a number of implementation difficulties such as tuning of gains and chattering in SMC and implementation of controller in complex and uncertain underwater scenario based on linearised model of AUV in case of  $H_\infty$ . Alternatively, in view of simplicity in its implementation, a PID controller can be easily chosen with introduction of some additional robustness features for applications in AUV. It has capability to compensate nonlinearities and uncertainties in dynamics, but it suffers from its narrow convergence domain. Therefore, the best choice may be Nonlinear-PID like controllers which have capability to provide convergence of large initial error to zero i.e. it can provide globally stable motion of AUV. Motivated by features of N-PID like controllers, Sliding Mode Nonlinear PID controller with Bounded Integral and Bounded Derivative has been proposed as tracking controller for AUV in subsection 4.8.1. In the next subsection, the performances of this

controller is compared with another robust controller SM-N-PID without BI and BD controller. Its performanes on application to AUV has been compared to application of SM-N-PID controller without BI and BD on the same uncertain dynamics of AUV.

#### 4.8.1.3 Tracking of sinusoidal path by application of SM-N-PID Controller with BI and BD and SM-N-PID Controller without BI and BD on AUV with uncertain dynamics

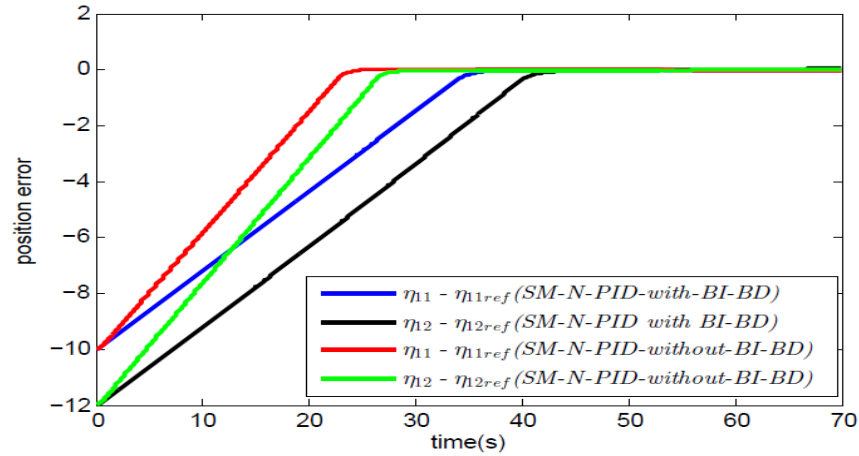


Fig.4.15 Position errors vs. time(s)

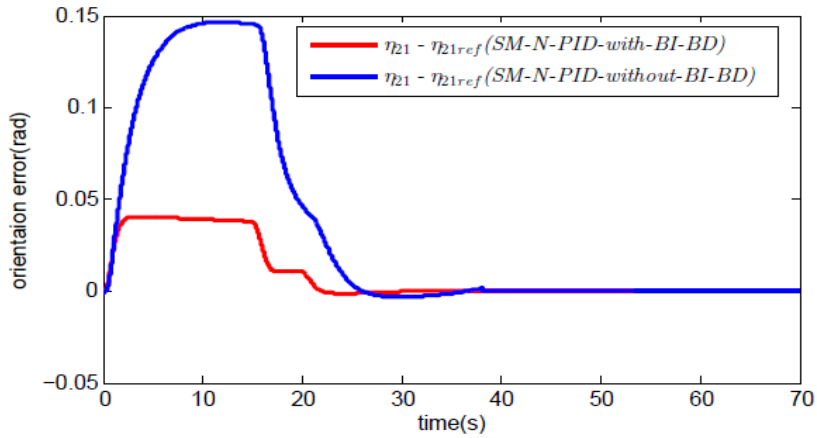


Fig.4.16 Orientation error(rad) vs.time(s)

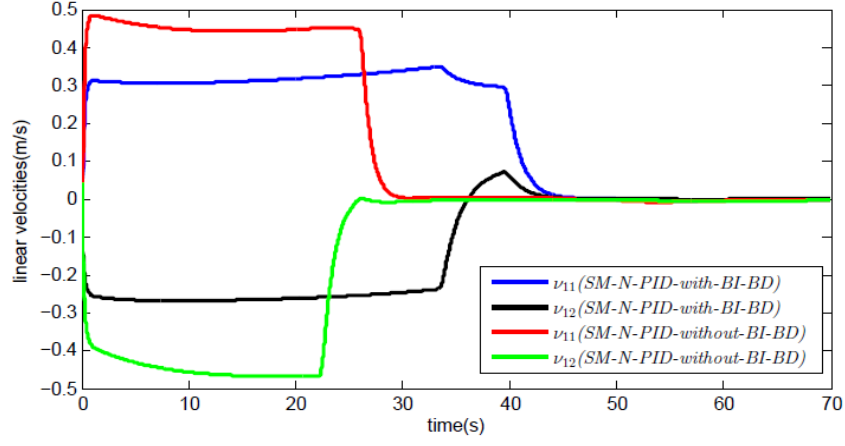


Fig.4.17 Error in linear velocities (m/s) vs.time

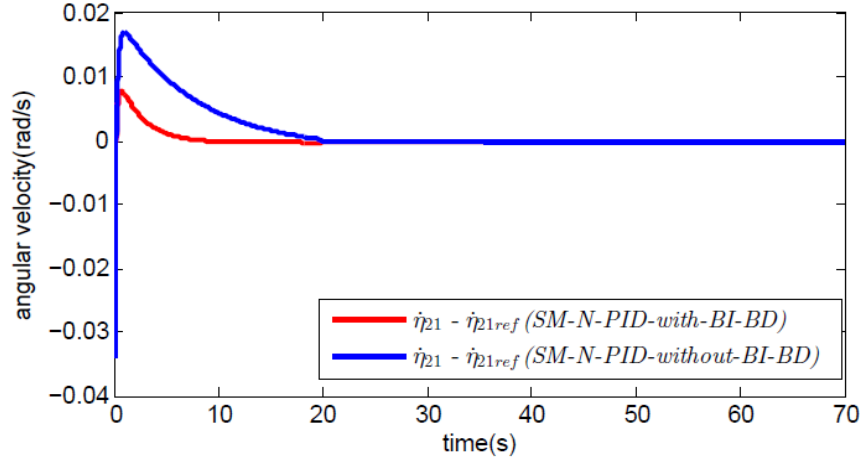


Fig.4.18 Error in angular velocity(rad/s) vs. time

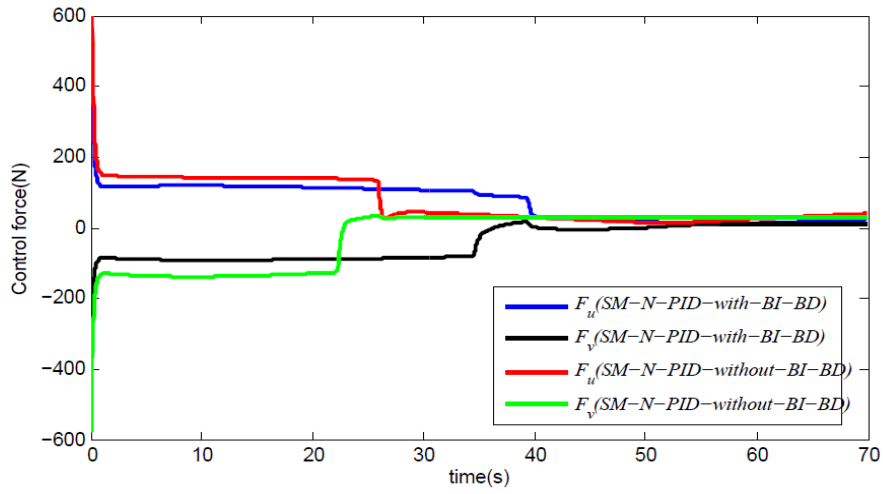


Fig.4.19 Control forces (N) vs time

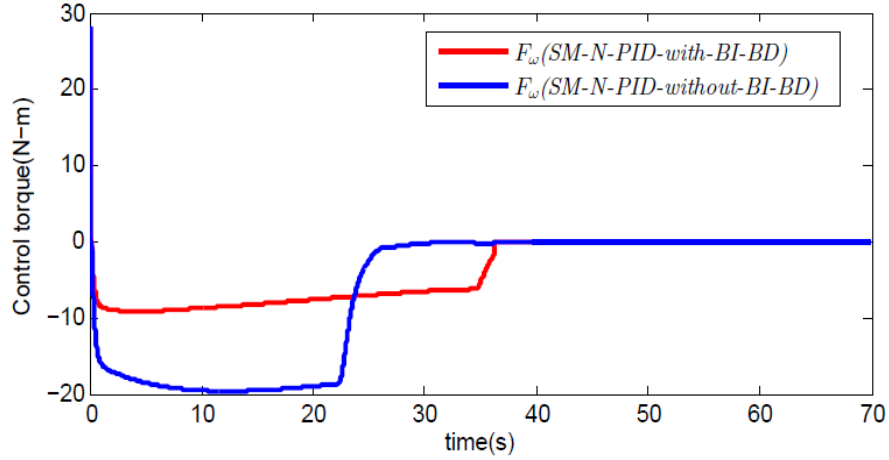


Fig.4.20 Control torque(N-m) vs. time

Comparing Fig.4.15- Fig.4.16 it is observed that that SM-N-PID with BI exhibits less overshoot and less settling time than SM-N-PID without BI and BD for position errors and orientation error respectively. Fig 4.17 and Fig 4.18 envisage similar kind observations where error in linear velocities in body fixed reference frame(Fig 4.17) and angular velocity(Fig 4.18) converge faster in case of SM-N-PID with BI and BD than SM-N-PID without BI and BD. Moreover,high peak is observed in SM-N-PID without BI and BD. Control forces required are more for SM-NPID without BI and BD than those of SM-N-PID with BI and BD. Similarly control torque demand is high for SM-N-PID without BI and BD. All the above observations are tabulated in Table 4.4.

Table 4.6: Observations from the simulation of application of different tracking controllers on AUV dynamics.

States/ Control Inputs	Linear Position ( $\eta_1, \eta_2$ )		Orientation (rad)		Linear velocities ( $v_1, v_2$ ) (m/s)		Angular velocity (rad/s)		Max. Force (N)		Max. Torque (N-m)
Performance Specifications →	$M_p$	$t_s$ and $e_{ss}$	$M_o$	$t_s$ and $e_{ss}$	$M_v$	$t_s$ and $e_{ss}$	$M_a$	$t_s$ and $e_{ss}$	$F_u$	$F_v$	$F_w$
Controller Types ↓											
PD plus FC for nom. dynamics	No	75	0.7 5	105	(0.46,- 0.52)	80	0.1	38	13 0	12 0	9
PD plus FC for uncertain dynamics	1.5, 3.5	$t_s$ : <i>Infinite</i>	1.9	$t_s$ : <i>Infinite</i>	0.36,- 0.35	$t_s$ : <i>Infinite</i>	0.2	$t_s$ : <i>Infinite</i>	12 5	12 5	25
PD plus FC with suff. tuned P & D	No	125,200 and 0,0	0.0 24	45	0.5,-0.4	125,12 0 and 0,0	0.0 35	25	15 00	10 00	40
SM-N-PID without BI and BD	No	22	0.0 025	25	0.8	24	0.0 25	21	45 0	60 0	16
SM-N-PID with BI and BD	No	17	0	20	0.6	17	0.0 32 5	5	50 0	50 0	17

It is concluded from the recorded observations that as no bounded functions are used for derivative and integral part of SM-N-PID without BI and BD, integral action goes high due to high initial error. Consequently, control forces and torque becomes high and actuators become saturated. As a result integrator wind-up happens all the error in states of AUV exhibit high peak and settling time before reaching to specified steady state values. But, due to use of nonlinear



bounded function for integral part of SM-N-PID with BI and BD, the integrator action remain restricted and integrator wind-up does not happen. Therefore SM-N-PID controller with BI and BD shows better transient and steady state performances than SM-N-PID without BI and BD as observed above in different simulations.

#### 4.9 Chapter Summary

This chapter describes the performances of Sliding Mode Nonlinear PID controller with Bounded Integral and Bounded Derivative as a robust tracking controller for AUV. Simulation results show the algorithm works excellent with respect to transient and steady state performances when parametric uncertainties are included in the dynamics and applied for large initial error. This algorithm has been compared with other two tracking controllers namely Proportional plus Derivative Controller with Feedforward Compensation and Sliding Mode Nonlinear PID

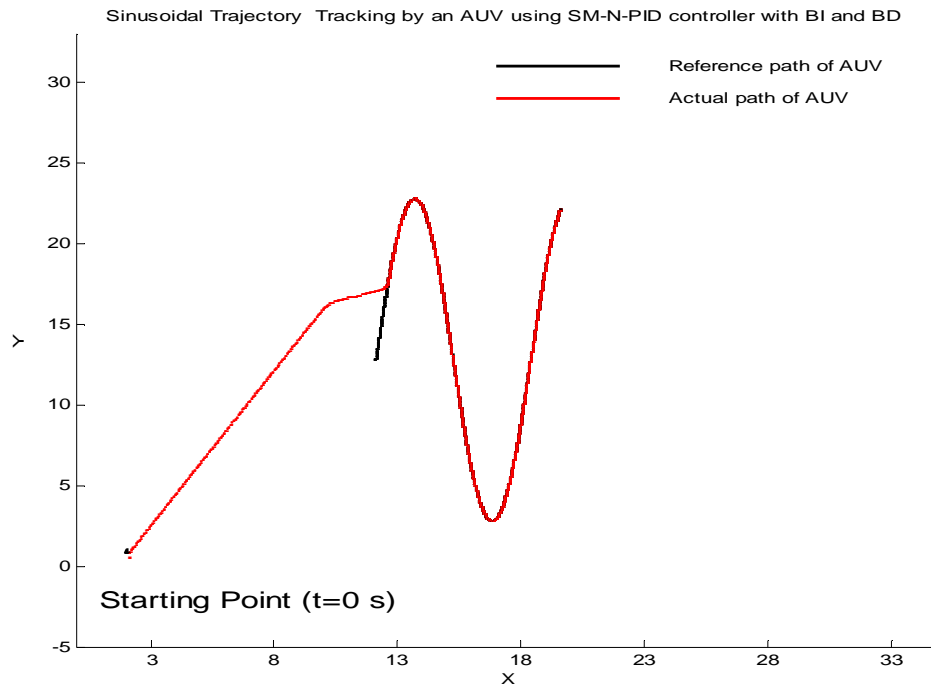


Fig 4.21: Tracking of sinusoidal trajectory by AUV with SM-N-PID controller with BI and BD.

controller without Bounded Integral and Bounded Derivative. It has been verified that the Sliding Mode Controller with Bounded Integral and Bounded Derivative is more efficient than both the controllers Proportional plus Derivative Controller with Feedforward Compensation and Sliding Mode Nonlinear PID controller without Bounded Integral and Bounded Derivative .

# **Chapter-5**

## **Directed Graph Based Formation Control of Multiple Autonomous Point Agents and Extension to AUVs**

### **5.1 Introduction**

This chapter discusses some basic properties of directed graph, which are useful for tracking control of group of cooperative AUVs to be described in chapter-6. Main focus of this chapter is to propose implementation procedure of minimally persistence property of a directed graph. This properties are useful for proposing distance-based collision free cooperative motion control algorithm for multiple agents based on CFMP formation. Two techniques namely Sequential Quadratic Programming(SQP) based optimization and simple geometric approach have been used for this purpose. First one utilizes an optimization technique to generate possible trajectory of each follower agent taking only information from the specified neighbours of that particular agent. Next, in this process, a set of decentralized control algorithm for formation motion is proposed based on those estimated trajectories to move along those trajectories. Second technique has been exploited for generation of trajectories of group of cooperative AUVs in a CMFP formation and subsequently the set of decentralized control laws is proposed from the estimated trajectories.

The chapter begins with the background of point agent based formation control, detailed application of graph theory in formation control. Next, problem statement for control of CMFP formation of multiple autonomous point agents, development of control law for the system of

agents, simulation and results are presented. In the middle of this chapter, problem statement for motion control of CMFP formation of  $n$  multiple AUVs, generation of their trajectories, control algorithm for verification of motion control of said formation are discussed. Chapter completes with a brief summary of this chapter.

## 5.2 Background

In some particular applications, autonomous agents (e.g. robots, vehicles, etc.) in cooperative motion need to maintain a particular geometrical shape, with maintaining of cohesive motion, called *formation* which satisfies some constraints like desired distance between two agents, desired angle between two lines joining two agents each. Examples of these types of formations are found in collective attack by a group of combat aircraft, search/rescue/surveillance/cooperative transportation by a troop of robots, under water exploration /under water inspection (like pipeline inspection) by a group of AUVs, etc.

Formations are modeled using *formation graph* whose each vertex represents individual agent kinematics and each edge represents inter-agent constraint (e.g. desired distance) that must be maintained during motion of formation. Specifically graph is used to represent coordinated behavior among agents.

Formation graph is *rigid* [155] if distance between any pair of agents remains constant during any continuous motion of formation. A graph is said to be *minimally rigid* if it is rigid and if there is no rigid graph having the same vertices but fewer edges.

In directed formation graph, only one (called *follower*) of any pair of agents, constrained by an edge has responsibility to satisfy the constraint. Therefore, decentralized control strategy is best suited for directed formation graph.

A graph is *constraint consistent* [155] if every agent is able to satisfy all the constraints on it provided all others are trying to do so. A formation that both rigid and constraint consistent is termed as *persistent* graph. *Persistence* is a generalization to directed graphs of the undirected notion of rigidity. A persistent graph is *minimally persistent* if it is persistent and if no edge can be removed without losing persistence.

However focus in this chapter is in development of control strategy for directed graph based formation. Basics of directed formation graph related issues are discussed in [155],[211],[192]. A closed directed path, with no repeated vertices other than the starting and ending vertices, is called a (directed) cycle. Digraph is called cycle free i.e *acyclic* [154] when no cycle is present in its sensing pattern. Control scheme for cyclic formation is more complicated than acyclic formation. Minimally persistent formation of autonomous agents may be formed in two ways. First one is *leader-follower* graph architecture constructed from an initial leader-follower seed by Henneberg Sequence with standard vertex additions or edge splitting [212]. Leader-follower type minimally persistent graph is always acyclic. In this chapter control strategies for only leader-follower type formation constructed from sequence of vertex addition is described.

Although a number of research works have been directed in the area of cyclic formation graph, but still there remains scope of further work. In the work [213] Anderson et. al. have proposed a distance preservation based control law when cycles contain in the formation graph. Control of leader-follower structure in continuous domain is discussed assuming linearized system for small motion and stability aspects are also discussed.

In [214], formation control strategy of leader-follower and three coleader structures is set up based on discrete-time motion equations considering decentralized approach. This work proposed the set-point control of multiple agents with the strategy of path planning. However, in

this chapter, tracking control strategy of leader-follower formation of multiple point agents is discussed in subsequent sections.

### 5.3 Application of Graph Theory in Formation Control

The graph theory described in section 5.2, is the best means for presenting of information flow among agents in a formation which can be used to design an efficient control scheme for the motion control of formation. In this chapter, formation of leader-follower structure has been considered and it may be extended to any number of agents. In this section, some definitions and theorems given in [155], [211], [192] about the rigidity and persistence are reviewed and subsequently the procedure of developing a leader-follower formation for a case of four numbers of autonomous agents is described.

#### 5.3.1. Definitions and Lemma and Criteria associated with Rigid Graph

*Definition 5.1 (Infinitesimally rigid graph):* A representation  $\mathbf{p}$  of an undirected graph  $G(V, E)$  with vertex set  $V$  and edge set  $E$  is a function  $\mathbf{p}: V \rightarrow \mathbb{R}^d$  where  $d$  (2, 3...) is the dimension of Euclidean space. Representation  $\mathbf{p}$  is rigid if there exists  $\sigma > 0$  such that for all realizations due to continuous deformations  $\mathbf{p}'$  of distance set induced by  $\mathbf{p}$  and satisfying,  $dist(\mathbf{p}, \mathbf{p}') < \sigma$  (where,  $dist(\mathbf{p}, \mathbf{p}') = \max \|\mathbf{p}(i) - \mathbf{p}'(i)\|$  for  $i \in V$ ), there holds  $\|\mathbf{p}'(i) - \mathbf{p}'(j)\| = \|\mathbf{p}(i) - \mathbf{p}(j)\|$  for all  $i, j \in V$ . This phenomenon as congruence relationship between  $\mathbf{p}$  and  $\mathbf{p}'$ .

*Definition 5.2 (Generically rigid graph):* A graph is said to be generically rigid if almost all realizations due to continuous deformations are rigid. This definition of rigidity is to exclude some undesirable situations like certain collections of vertices are collinear during continuous deformations, superposed vertices.

*Definition 5.3(Minimally rigid graph):* A rigid graph is minimally rigid when no single edge can be removed without losing its rigidity.

*Criteria 5.1(Laman's Criteria[192]):* If an undirected graph  $G(V, E)$  in  $\mathbb{R}^2$  with at least two vertices is rigid, then there exists a subset  $E'$  of edges such that  $|E'| = 2|V| - 3$  and any subgraph  $G'' = (V'', E'')$  of  $G'$  with at least two vertices satisfies  $|E''| \leq 2|V(E'')| - 3$ , where  $|V(E'')|$  is number of vertices that are end-vertices of the edges in  $E''$ .

*Lemma 5.1[155]:* Let  $G = (V, E)$  be a minimally rigid graph in  $\mathbb{R}^2$  and  $G(V', E')$  a subgraph of  $G$  such that  $|E'| = 2|V'| - 3$ . Then,  $G'$  is minimally rigid.

### 5.3.2. Definitions associated with Persistent Graph

Suppose, for a directed graph  $G$ , desired distances  $dist_{ij}$  for  $\forall (i, j) \in E$ , edge set where  $i, j \in V$ , vertex set and a realization  $\mathbf{p}$ , then the following definitions are described.

*Definition 5.4 (Active edge):* The edge  $(i, j) \in E$  is *active* if  $\|\mathbf{p}(i) - \mathbf{p}(j)\| = dist_{ij}$  i. e. if the corresponding distance constraint is satisfied.

*Definition 5.5 (Fitting position of a vertex):* The position of a vertex  $i \in V$  is *fitting* for any desired distance set  $\{dist\}$  of  $G$  if it is not possible to increase the set of active edges leaving  $i$  by changing the position of  $i$  while maintaining the positions of other vertices unchanged. Specifically, the position of vertex  $i$ , for a given realization  $\mathbf{p}$ , is fitting if there is no  $\mathbf{p}' \in \mathbb{R}^2$  for which the condition elaborated below is strictly satisfied

$$\{(i, j) \in E : \|\mathbf{p}(i) - \mathbf{p}(j)\| = dist_{ij}\} \subset \{(i, j) \in E : \|\mathbf{p}'(i) - \mathbf{p}(j)\| = dist_{ij}\} \quad (5.1)$$

*Definition 5.6(Fitting realization of a graph):* A realization of a graph is a fitting realization for a certain distance set  $\{\bar{dist}\}$  if all the vertices are at *fitting* positions for  $\{\bar{dist}\}$

*Definition 5.7(Constraint consistent graph):* A realization  $\mathbf{p}$  of digraph  $G$  is constraint consistent if there exists  $\sigma > 0$  such that any realization  $\mathbf{p}'$  fitting for the distance set  $\{\bar{dist}\}$  induced by  $\mathbf{p}$  and satisfying  $dist(\mathbf{p}, \mathbf{p}') < \sigma$  is a realization of  $\{\bar{dist}\}$ .

A graph is generically constraint consistent if almost all realizations are constraint consistent

*Definition 5.8 (Persistent graph):* Realization  $p$  of the digraph  $G$  having desired distances  $dist_{ij} > 0$  for all  $\{i, j\}$  is *persistent* if there exists  $\sigma > 0$  such that every realization due to continuous deformation,  $\mathbf{p}'$  fitting for the distance set induced by  $p$  and satisfying  $dist(\mathbf{p}, \mathbf{p}') < \sigma$  is congruent to  $p$ .

*Definition 5.8 (Generically persistent graph):* A graph is generically persistent if almost all possible realizations are persistent (same as in case of generically rigid).

*Theorem 5.1[154]:* A realization is persistent if and only if it is rigid and constraint consistent.

A graph is generically persistent if and only if it is generically rigid and constraint consistent.

*Minimally persistent graph:* A persistent graph is minimally persistent if it is persistent and if no edge can be removed without losing persistence.

*Theorem 5.2[154]:* A rigid graph is minimally persistent if and only if either of the two conditions given below is satisfied i.e.



(i) Out of all vertices, each of three vertices has one outgoing edge and each of the rest vertices has two outgoing edges

(ii) Out of all vertices, one vertex has no outgoing edge; another one vertex has one outgoing edge and each of the rest vertices has two outgoing edges

*Theorem 5.3[154]:*An acyclic digraph is persistent if all the conditions given below are satisfied:

Out of all vertices, (i) one vertex has one outgoing edge. This vertex represents Leader.

(ii) Another one vertex has one outgoing edge which must be incident to the Leader. This vertex represents first follower.

(iii) Each of rest vertices must have two or more number of outgoing edges.

### **5.3.3. Construction of cycle free minimally persistent (CFMP) graph**

Acyclic minimally persistent graph is always constructed starting from a combination of two vertices, one is called leader and the other one is first follower, and an edge directed towards leader using Henneberg Sequence with only vertex additions.

#### **5.3.3.1. Henneberg construction (directed case) containing vertex addition**

It describes the sequence of graphs  $G_2, G_3, \dots, G_{|V|}$ , such that each graph  $G_{i+1}$  ( $i \geq 2$ ) can be obtained by a vertex addition starting from  $G_i$ , where  $i$  is the number of vertices and  $|V|$  is cardinality of vertex set of desired graph. Hence, the procedure of drawing the graph using Henneberg sequence is described as follows

(i) Start with a directed edge between two vertices. The vertex towards which edge is directed is called leader and remaining vertex is called first follower. The combination of these two vertices with a directed edge is called initial leader-follower seed.

(ii) At each step of growing graph, add a new vertex

(iii) Join the new vertex to two old vertices (corresponding to leader and first follower) via two new edges, directed towards old vertices.

Fig.5.1 shows the construction procedure of Henneberg Sequence based minimally persistent formation of four agents.

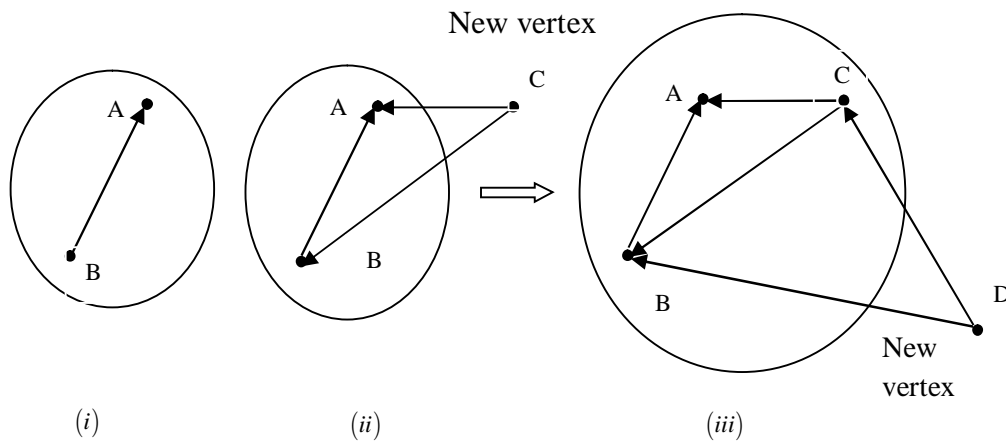


Fig.5.1.Henneberg construction for making leader-follower type formation from four agents 'A', 'B', 'C', 'D'

Fig.5.1.Henneberg construction for making leader-follower type formation from four agents 'A', 'B', 'C', 'D'

(i) 'A', 'B' are initial vertices with one edge directed towards 'A' (leader) from 'B' (first follower). (ii) 'C' is new vertex added to Fig. 5.1(i). (iii) 'D' is new vertex added to Fig 5.1(ii).

#### 5.4. Problem Formulation

For simplicity, only a leader-follower type quadrilateral CFMP formation with four mobile autonomous point agents is considered. This formation structure is shown in Fig.5.2. One among them is leader which has no outgoing edge i.e. it is free to move along a specified path and does not have any responsibility to maintain any distance constraint from other agents, the second one as the first follower which has one outgoing edge i.e. it requires to maintain only one desired distance constraint from the leader, third one as ordinary follower- 1 which has two outgoing edges i.e. it requires to maintain two distance constraints, one of which is directed towards leader and other one towards first follower, fourth one as ordinary follower-2 which has two outgoing edges i.e. it is required to maintain two distance constraints, one of which is directed towards the first follower and other one towards ordinary follower-1. In this figure the notations are as follows. R-1 denotes the leader and R-2 denotes the first follower, R-3 represents for the ordinary follower-1 and R-4 denotes the ordinary follower-2.

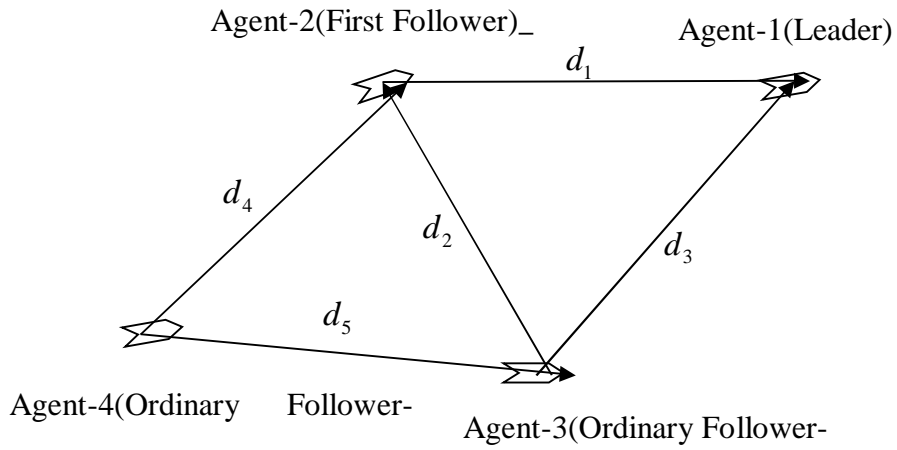


Fig. 5.2 Quadrilateral formation of four point agents with leader-follower type CFMP formation

The different instantaneous distances and distance constraints among agents are mentioned in Table 5.1.

Table 5.1: Instantaneous and desired distance constraints among different agents

Names of associated agents →	First follower to leader	Ordinary follower-1 to First follower	Ordinary follower-1 to leader	ordinary follower-2 to Ordinary follower-3	ordinary follower-2 to First follower
Distances between two agents ↓					
Instantaneous	$d_1$	$d_2$	$d_3$	$d_4$	$d_5$
Desired	$l_{1d}$	$l_{2d}$	$l_{3d}$	$l_{4d}$	$l_{5d}$

### 5.4.1 Agent Kinematics

Assume each agent represents a nonholonomic unicycle point agent. The kinematic model [214] of an agent is considered as

$$\left. \begin{aligned} (\dot{x}_i, \dot{y}_i) &= (\mathbf{v}_i \cos \theta_i, \mathbf{v}_i \sin \theta_i) \\ \omega_i &= \dot{\theta}_i \end{aligned} \right\} \quad (5.2)$$

where,  $\gamma_i(t) = (\mathbf{p}_i(t), \theta_i(t)) = (x_i(t), y_i(t), \theta_i(t)) \in \mathbb{R}^3$  with  $i = 1, 2, 3$  denotes, the position state of  $i$ th agent.  $\mathbf{p}_i(t) = (x_i(t), y_i(t))$  and  $\theta_i(t)$  represent the linear position and orientation respectively.

$\mathbf{v}_i(t)$  and  $\omega_i(t)$  stand for translational and angular velocities respectively. Position state of system of agents is  $\lambda = (\gamma_1, \gamma_2, \gamma_3, \gamma_4) = (\mathbf{p}_1, \theta_1, \mathbf{p}_2, \theta_2, \mathbf{p}_3, \theta_3, \mathbf{p}_4, \theta_4) \in \mathbb{R}^{3 \times 4}$ . Before stating the the main problem following assumptions are made.

*Assumption 5.1:*

(i) The desired distances among the agents for their initial positions satisfy non-collinear condition such that at least three point agents do not form a straight line.

$$\left. \begin{aligned} d_1(0) + d_2(0) &> d_3(0) \\ d_2(0) + d_3(0) &> d_1(0) \\ d_3(0) + d_1(0) &> d_2(0) \\ d_2(0) + d_5(0) &> d_4(0) \\ d_5(0) + d_4(0) &> d_2(0) \\ d_4(0) + d_2(0) &> d_5(0) \end{aligned} \right\} \quad (5.3)$$

(ii) Each agent can measure its linear position with respect to global coordinate system by proper sensor arrangement

(iii) First follower has global position information of leader. Ordinary follower gets global linear position information of leader & first follower by direct communication or by using an active sensor e.g. sonar. When sonar is used, an agent initially calculates its linear position w.r.t coordinate frame fixed to its body and next converts this position wrt to global coordinate system with the help of its own global linear position.

#### **5.4.2 Problem Statement**

Consider a quadrilateral formation of four agents with kinematics of eq(5.2) under Assumption 5.1. Assume initial structure of formation satisfies condition of eq(5.3). It is also assumed that initial formation preserves the desired inter-agent distances. It is intended to develop a set of decentralized [214] control laws for agents of this formation such that desired inter-agent distances (under motion of entire formation) are preserved after every fixed interval of time corresponding to desired tracking of leader for any mission.

### **5.5 Development of Formation Control Strategy for the System of Point Agents**

It is intended to develop a set of decentralized control laws for all agents in leader-follower type quadrilateral formation. Therefore, for each agent a separate control law on local knowledge only of direction of its neighbours is proposed. Control law is developed on the assumption that each agent accurately tracks its desired position state i.e stable trajectory tracking occurs. Control Law for each agent is derived from the desired and current position state  $\lambda_{ln} = (p_{1ln}, \theta_{1ln}, p_{2ln}, \theta_{2ln}, p_{3ln}, \theta_{3ln}, p_{4ln}, \theta_{4ln})$ . The desired state of an agent is obtained from solution of optimization problem involving corresponding objective function with given distance constraints to its neighbors in the formation. The desired state of system of agents is denoted as

$$\lambda_f = (p_{1f}, \theta_{1f}, p_{2f}, \theta_{2f}, p_{3f}, \theta_{3f}, p_{4f}, \theta_{4f}).$$

### Assumptions 5.2

- (i) Inter-agent distances are sufficiently large so that initial collision among robots can be avoided
- (ii) During motion of formation, failure of sensors do not occur
- (iii) There is no time delay in receiving data from neighbours
- (iv) Control input in the form of translational velocity and angular velocity (discussed later in this section) calculated from final and initial position state of any agent should be necessarily generated by controller of each agent.

*Definition 5.9:* Let, all the agents in a specified CFMP formation are placed to a new set of position state  $\lambda_f$  from an old set  $\lambda_{in}$  during certain period of time in a course of motion of entire formation. Desired distances among agents are preserved for both set of positions and all agents have achieved their final orientations. If no any other distance preserving position set is available in between these two sets during a course of motion, then the movement of formation from  $\lambda_{in}$  to  $\lambda_f$  is called one complete movement of formation. Before proceeding to develop the control laws for all agents, it is assumed that at any time  $t$  system of agents has reached a distance preserving state  $\lambda_f$  i.e. one complete displacement has been achieved. Then how these agents move to their new positions and what amount of control inputs are required for another complete displacement is discussed below.

### 5.5.1 Development of Control Law for the Leader

Leader does not need to maintain any distance constraint from any other agent in formation. A specified control action is generated such that it moves along a specified trajectory. Suppose, at time  $t$  linear position for leader is  $\mathbf{p}_1(t) = \mathbf{p}_{1ln} = (x_{1ln}, y_{1ln}) \in \lambda_{ln}(t)$ . Let, the leader moves to a new position  $\mathbf{p}_1(t + \Delta t) = \mathbf{p}_{1f} = (x_{1f}, y_{1f}) \in \lambda_f$  i.e. the final position, in very small period of time  $\Delta t \rightarrow 0$ . Using this assumption, all through this chapter,  $\lim_{\Delta t \rightarrow 0} L\Delta t = dt$  is used.  $dt$  is such that continuity preserves between  $\mathbf{p}_{1ln}$  and  $\mathbf{p}_{1f}$  i.e. the distance between these two positions is sufficiently small. Therefore,  $\mathbf{p}_1\left(t + \lim_{\Delta t \rightarrow 0} L(\Delta t)\right) = \mathbf{p}_1(t + dt) = \mathbf{p}_{1f} = (x_{1f}, y_{1f}) \in \lambda_f$ . This motion of the leader and corresponding to the movement of the first follower is shown in Fig5.3. According to Fig5.3,  $d\vec{s}_1 = dx_1\hat{i} + dy_1\hat{j}$  where,  $\vec{s}_1$  is a vector field along the trajectory of the leader.  $\hat{i}$  and  $\hat{j}$  are unit vectors along  $x$  and  $y$  direction of the global coordinate system.  $dx_1 = x_{1f} - x_{1ln}$  and  $dy_1 = y_{1f} - y_{1ln}$ . It should be noted that  $(x_{1ln}, y_{1ln})$  and  $(x_{1f}, y_{1f})$  are always on  $\vec{s}_1$ . Therefore, linear velocity control input, which is calculated from position error, to reach its final position is

$$\mathbf{v}_1(t + dt) = \mathbf{v}_{1f} = \frac{d\vec{s}_1}{dt} = \frac{dx_1}{dt}\hat{i} + \frac{dy_1}{dt}\hat{j} = v_{1xf}\hat{i} + v_{1yf}\hat{j} \quad (5.4)$$

where,  $v_{1xf} = \frac{dx_1}{dt}$  and  $v_{1yf} = \frac{dy_1}{dt}$ . The translational velocity control input during  $dt =$

$$\|\mathbf{v}_{1f}\| = \sqrt{v_{1xf}^2 + v_{1yf}^2} \text{ m/s.}$$

Following eq (5.2) and considering the fact that change in orientation happens during the time period  $dt$ , the angular velocity control input (rad/s) is given by



$$\left. \begin{aligned}
\omega_1(t+dt) &= \omega_{1f} = \tan^{-1} \left| \frac{dy_1}{dx_1} \right|, \text{ when both } dx_1 \text{ and } dy_1 \text{ are + ve} \\
&= \left( \pi - \tan^{-1} \left| \frac{dy_1}{dx_1} \right| \right), \text{ when } dx_1 \text{ is - ve and } dy_1 \text{ + ve} \\
&= - \left( \pi - \tan^{-1} \left| \frac{dy_1}{dx_1} \right| \right), \text{ when both } dx_1 \text{ and } dy_1 \text{ are - ve} \\
&= \left( \pi - \tan^{-1} \left| \frac{dy_1}{dx_1} \right| \right), \text{ when } dx_1 \text{ is + ve and } dy_1 \text{ is - ve} \\
&= -\frac{\pi}{2} \text{ or } \frac{\pi}{2}, \text{ when } dx_1 = 0 \text{ and } dy_1 \text{ is + ve or - ve}
\end{aligned} \right\} \quad (5.5)$$

### 5.5.2 Development of Control Law for the First Follower

It may be noted that first follower has one outgoing edge i.e. it has to maintain a distance constraint  $d_1$  from leader. Initial and final position coordinates for the leader are  $\mathbf{p}_{1In}$  and  $\mathbf{p}_{1f}$  respectively. Due to motion of leader the instantaneous distance between leader and first follower deviates from  $l_{1d}$ . First follower senses error between actual and desired distance by sensing  $\mathbf{p}_{1f}$  staying at its initial position  $\mathbf{p}_2(t) = \mathbf{p}_2(t+dt) = \mathbf{p}_{2In} = (x_{2In}, y_{2In})$ . It attempts to satisfy this distance constraint to leader. Suppose, it moves to its final position at the next instant of time  $dt$  after the instant during which the leader moves to its final position. Thus,  $\mathbf{p}_2(t+2dt) = \mathbf{p}_{2f} = (x_{2f}, y_{2f}) \in \lambda_f$ . During this movement of first follower, leader is assumed to be stationary at the position  $\mathbf{p}_1(t+2dt) = \mathbf{p}_{1f}$ . A condition is given to first follower such that only due to change in position of leader; first follower changes its position. To maintain the distance preserving motion with the leader distance of the first follower from the leader must be at final position of both the agents. It can be formulated as follows:

$$(x_{1f} - x_{2f})^2 + (y_{1f} - y_{2f})^2 - l_{1d}^2 = 0 \quad (5.6)$$

where the values of  $(x_{1f}, y_{1f}, l_{1d})$  are known to computational system of first follower. But it is clear from eq(5.6) that locus of the position of first follower is a circle. Hence, its final position may exist anywhere on this circle. The solution of eq (5.6) may be such that first follower may cross over the leader's final position and may collide with leader. Undesirable consequence of this phenomenon is ordinary follower may collide with leader and first follower both for maintaining the distant constraints from both of them. Hence, to provide a control input avoiding this unsafe situation, a restriction to the motion of first follower must be imposed, such that it reaches to its final point on the circle so that distance between the new and initial position becomes minimum. In Fig. 5.3,  $\|\vec{ds}_2\|$  is defined as the distance between the final and initial position of first follower.  $\vec{s}_2$  is a vector field along the trajectory of first follower. It should be noted that  $(x_{2ln}, y_{2ln})$  and  $(x_{2f}, y_{2f})$  are always on  $\vec{s}_2$ . Then,  $\|\vec{ds}_2\|$  can be determined as follows

$$\|\vec{ds}_2\|^2 = (x_{2f} - x_{2ln})^2 + (y_{2f} - y_{2ln})^2 \quad (5.7)$$

Therefore,  $\|\vec{ds}_2\|$  must be minimum such that first follower moves along the shortest path to its final position. Hence, the first follower follows the leader maintaining safe motion. Now it is intended to propose a control law for motion of first follower satisfying aforesaid conditions. Actually the whole problem can be treated as an optimization problem where minimization of objective function eq (5.7) under equality constraint eq (5.6) should be performed. Control law based on this optimization can be generated as

$$\mathbf{v}_2(t+2dt) = \mathbf{v}_{2f} = \frac{d\vec{s}_2}{dt} = \frac{dx_2}{dt} \hat{i} + \frac{dy_2}{dt} \hat{j} = v_{2xf} \hat{i} + v_{2yf} \hat{j} \quad (5.8)$$

where,  $v_{2xf} = \frac{dx_2}{dt}$  and  $v_{2yf} = \frac{dy_2}{dt}$  and  $\hat{i}$  and  $\hat{j}$  are unit vectors along  $x$  and  $y$  direction of the global

coordinate system. The translational velocity control input  $\|\mathbf{v}_{2f}\| = \sqrt{v_{2xf}^2 + v_{2yf}^2}$  m/s.

Following eq (5.2) and considering the fact that change in orientation happens during the time period  $dt$ , the angular velocity control input (rad/s) is given by

$$\left. \begin{aligned} \omega_2(t+dt) &= \omega_{2f} = \tan^{-1} \left| \frac{dy_2}{dx_2} \right|, \text{ when both } dx_2 \text{ and } dy_2 \text{ are +ve} \\ &= \left( \pi - \tan^{-1} \left| \frac{dy_2}{dx_2} \right| \right), \text{ when } dx_2 \text{ is -ve and } dy_2 \text{ +ve} \\ &= - \left( \pi - \tan^{-1} \left| \frac{dy_2}{dx_2} \right| \right), \text{ when both } dx_2 \text{ and } dy_2 \text{ are -ve} \\ &= \left( \pi - \tan^{-1} \left| \frac{dy_2}{dx_2} \right| \right), \text{ when } dx_2 \text{ is +ve and } dy_2 \text{ is -ve} \\ &= -\frac{\pi}{2} \text{ or } \frac{\pi}{2}, \text{ when } dx_2 = 0 \text{ and } dy_2 \text{ is -ve or +ve} \end{aligned} \right\} \quad (5.9)$$

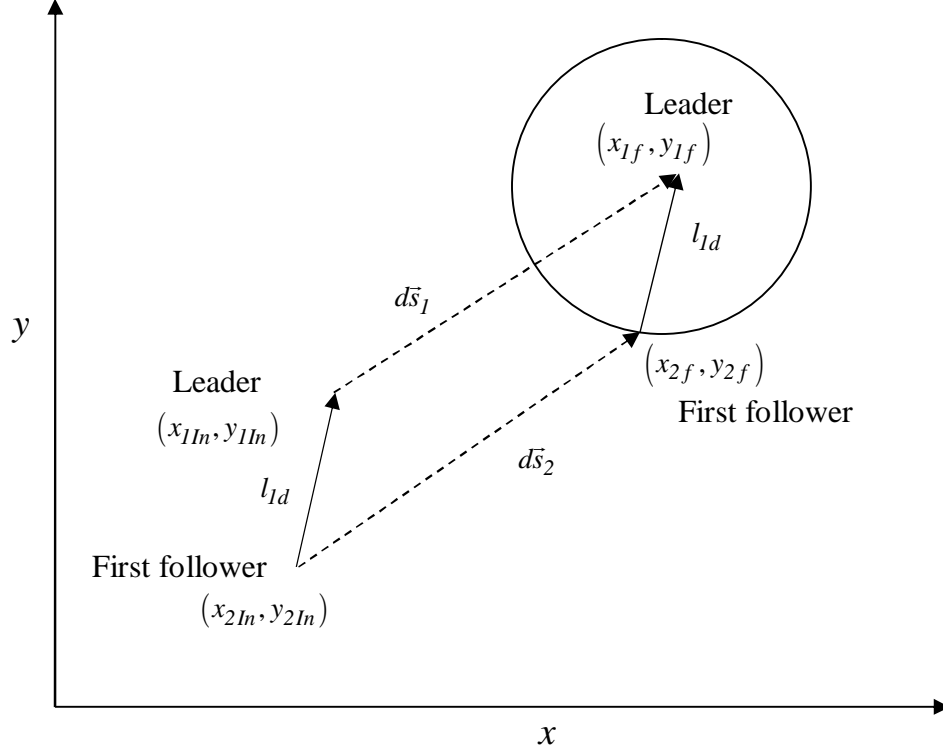


Fig 5.3. Motion of leader and first follower for a very small duration of time

### 5.5.3 Control Law for Ordinary Follower-1

Ordinary follower-1 tries to satisfy two distance constraints i.e. it has two outgoing edges, first one  $l_{2d}$  is directed towards first follower and second one  $l_{3d}$  is directed towards leader. Let, the leader and first follower have been placed at their corresponding final positions. The ordinary follower-1 senses the variation in position of leader and first follower i.e. it senses error between actual and desired distances by sensing the final position of the first follower and leader respectively remaining at its initial position  $\mathbf{p}_3(t) = \mathbf{p}_3(t + dt) = \mathbf{p}_3(t + 2dt) = \mathbf{p}_{3ln} = (x_{3ln}, y_{3ln})$ . It tries to satisfy these distance constraints to first follower and leader as shown in Fig.5.4. Assume, the ordinary follower moves to its final position at the next time instant of the time ( $dt$ ) after the instant during which first follower moves to its final position. During this movement leader and first follower are assumed to be stationary at the position  $\mathbf{p}_{1f}(t)$  and  $\mathbf{p}_{2f}(t)$  respectively. At the

final position ordinary follower-1 satisfies its distance constraints. A condition is given to the ordinary follower-1 such that only when changes in positions of both leader as well as first follower (not merely leader) occur; ordinary follower-1 changes its position to final one. This final position is assumed  $\mathbf{p}_3(t+3dt)=\mathbf{p}_{3f}=(x_{3f},y_{3f})\in\lambda_f$ . Thus, according to the above discussions two desire distance constraints  $l_{3d}$  and  $l_{2d}$  are to be satisfied for final state. They can be formulated as follows

$$\left. \begin{aligned} (x_{1f}-x_{3f})^2 + (y_{1f}-y_{3f})^2 - l_{3d}^2 &= 0 \\ (x_{2f}-x_{3f})^2 + (y_{2f}-y_{3f})^2 - l_{2d}^2 &= 0 \end{aligned} \right\} \quad (5.10)$$

where,  $(x_{1f},y_{1f},x_{2f},y_{2f},l_{2d},l_{3d})$  are known to the computational system of ordinary follower.

Hence,  $\|\vec{d\vec{s}}_3\|$  is defined as distance between the final and initial position of ordinary follower, where,  $\vec{s}_3$  a vector field along the trajectory curve of ordinary follower. It should be noted that  $(x_{3ln},y_{3ln})$  and  $(x_{3f},y_{3f})$  are always on  $\vec{s}_3$ . Then,  $\|\vec{d\vec{s}}_3\|$  can be determined as follows

$$\|\vec{d\vec{s}}_3\|^2 = (x_{3f}-x_{3ln})^2 + (y_{3f}-y_{3ln})^2 \quad (5.11)$$

Two equations in (5.10) represent two circles. They meet at two different points. The ordinary follower will follow the leader and first follower maintaining safe motion and moves to any one meeting point such that  $\|\vec{d\vec{s}}_3\|$  is minimum. By maintaining  $\|\vec{d\vec{s}}_3\|$  minimum, ordinary follower moves along shortest path to its final position. Thus, control law must be proposed for motion of first follower satisfying aforesaid conditions. In fact the whole problem can be treated as an optimization problem where minimization of objective function eq(5.11) under equality

constraints of eq (5.10) should be performed. Control law based on this optimization can be generated as

$$\mathbf{v}_3(t+3dt) = \mathbf{v}_{3f} = \frac{d\bar{s}_3}{dt} = \frac{dx_3}{dt} \hat{i} + \frac{dy_3}{dt} \hat{j} = v_{3xf} \hat{i} + v_{3yf} \hat{j} \quad (5.12)$$

where,  $v_{3xf} = \frac{dx_3}{dt}$  and  $v_{3yf} = \frac{dy_3}{dt}$ . and  $\hat{i}$  and  $\hat{j}$  are unit vectors along  $x$  and  $y$  direction of the global coordinate system.

The translational velocity control input  $\|\mathbf{v}_{3f}\| = \sqrt{v_{3xf}^2 + v_{3yf}^2}$  m/s.

Angular velocity (rad/s) control input is given by

$$\left. \begin{aligned} \omega_3(t+dt) = \omega_{3f} &= \tan^{-1} \left| \frac{dy_3}{dx_3} \right|, \text{ when both } dx_3 \text{ and } dy_3 \text{ are +ve} \\ &= \left( \pi - \tan^{-1} \left| \frac{dy_3}{dx_3} \right| \right), \text{ when } dx_3 \text{ is -ve and } dy_3 \text{ +ve} \\ &= - \left( \pi - \tan^{-1} \left| \frac{dy_3}{dx_3} \right| \right), \text{ when both } dx_3 \text{ and } dy_3 \text{ are -ve} \\ &= \left( \pi - \tan^{-1} \left| \frac{dy_3}{dx_3} \right| \right), \text{ when } dx_3 \text{ is +ve and } dy_3 \text{ is -ve} \\ &= -\frac{\pi}{2} \text{ or } \frac{\pi}{2}, \text{ when } dx_3 = 0 \text{ and } dy_3 \text{ is +ve or -ve} \end{aligned} \right\} \quad (5.13)$$

#### 5.5.4 Control Law for Ordinary Follower-2

Ordinary follower-2 attempts to satisfy two distance constraints i.e. it has two outgoing edges, first one  $l_{4d}$  is directed towards ordinary follower-1 and second one  $l_{5d}$  is directed towards first follower. Let the leader, first follower and ordinary follower-1 have been placed at their corresponding final positions. The ordinary follower senses the variation in position of first follower and ordinary follower-1 i.e. it senses error in actual and desired distances by sensing the

final position of the first follower and ordinary follower-1 staying at its initial position

$$\mathbf{p}_4(t) = \mathbf{p}_4(t+dt) = \mathbf{p}_4(t+2dt) = \mathbf{p}_4(t+3dt) = \mathbf{p}_{3ln} = (x_{3ln}, y_{3ln}).$$

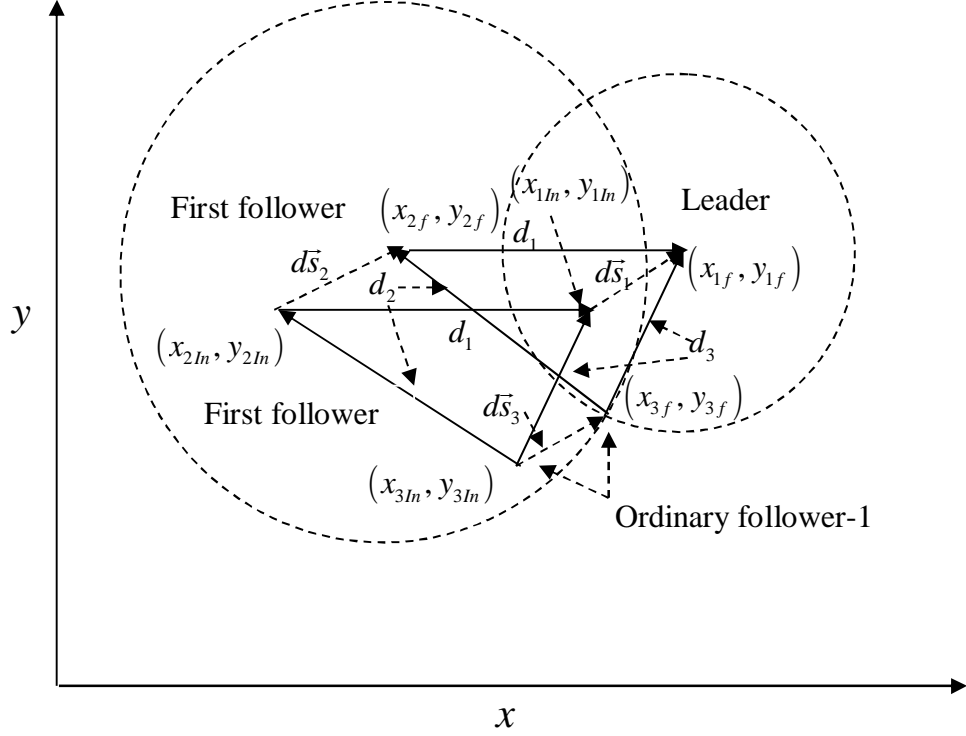


Fig.5.4 Motion of leader, first follower and ordinary follower-1 for a very small duration of time

It tries to satisfy these distance constraints to first follower and ordinary follower-1. Suppose, the ordinary follower-2 moves to its final position at the next instant of the time ( $dt$ ) after the instant during which ordinary follower-1 moves to its final position. During this movement leader, first follower and ordinary follower-1 are assumed to be stationary at the position  $\mathbf{p}_{1f}(t)$ ,  $\mathbf{p}_{2f}(t)$  and  $\mathbf{p}_{3f}(t)$  respectively. At the final position of ordinary follower-2 satisfies its distance constraints.

A condition is given to the ordinary follower-2 such that only when changes in positions of first follower as well as first follower-1 occur; ordinary follower-2 changes its position to final one.

This final position is assumed  $\mathbf{p}_3(t+4dt) = \mathbf{p}_{4f} = (x_{4f}, y_{4f}) \in \lambda_f$ . Now according to the desire

distance constraints  $l_{4d}$  and  $l_{5d}$ , two conditions are to be satisfied. They can be formulated as follows

$$\left. \begin{aligned} (x_{2f} - x_{4f})^2 + (y_{2f} - y_{4f})^2 - l_{5d}^2 &= 0 \\ (x_{3f} - x_{4f})^2 + (y_{3f} - y_{4f})^2 - l_{4d}^2 &= 0 \end{aligned} \right\} \quad (5.14)$$

where,  $(x_{2f}, y_{2f}, x_{3f}, y_{3f}, l_{4d}, l_{5d})$  are known to the computational system of ordinary follower-2.

Hence,  $\|\vec{d\bar{s}}_4\|$  is defined as distance between the final and initial position of ordinary follower-2.

Here,  $\vec{s}_4$  is a vector field along the trajectory curve of ordinary follower. It should be noted that

$(x_{4In}, y_{4In})$  and  $(x_{4f}, y_{4f})$  are always on  $\vec{s}_4$ . Then,  $\|\vec{d\bar{s}}_4\|$  can be determined as follows

$$\|\vec{d\bar{s}}_4\|^2 = (x_{4f} - x_{4In})^2 + (y_{4f} - y_{4In})^2 \quad (5.15)$$

Actually two equations in (5.9) are two circles. They meet at two different points. The ordinary follower will follow the leader and first follower maintaining safe motion and moves to any one meeting point such that  $\|\vec{d\bar{s}}_4\|$  is minimum. By maintaining  $\|\vec{d\bar{s}}_4\|$  minimum, ordinary follower moves along shortest path to its final position. Now it is the need to propose a control law for motion of first follower satisfying aforesaid conditions. Actually the whole problem may be treated as an optimization problem where minimization of objective function (5.15) under equality constraints of eq (5.14) should be performed. Control law based on this optimization is proposed as follows

$$\mathbf{v}_4(t+4dt) = \mathbf{v}_{4f} = \frac{d\bar{s}_4}{dt} = \frac{dx_4}{dt} \hat{i} + \frac{dy_4}{dt} \hat{j} = v_{4xf} \hat{i} + v_{4yf} \hat{j} \quad (5.16)$$



where,  $v_{4,xf} = \frac{dx_4}{dt}$  and  $v_{4,yf} = \frac{dy_4}{dt}$ . and  $\hat{i}$  and  $\hat{j}$  are unit vectors along  $x$  and  $y$  direction of the global coordinate system.

The translational velocity control input  $\|\mathbf{v}_{4f}\| = \sqrt{v_{4,xf}^2 + v_{4,yf}^2}$  m/s. Angular velocity (rad/s) control input is given by

$$\left. \begin{aligned} \omega_4(t+dt) &= \omega_{4f} = \tan^{-1} \left| \frac{dy_4}{dx_4} \right|, \text{ when both } dx_4 \text{ and } dy_4 \text{ are + ve} \\ &= \left( \pi - \tan^{-1} \left| \frac{dy_4}{dx_4} \right| \right), \text{ when } dx_4 \text{ is - ve and } dy_4 \text{ + ve} \\ &= - \left( \pi - \tan^{-1} \left| \frac{dy_4}{dx_4} \right| \right), \text{ when both } dx_4 \text{ and } dy_4 \text{ are - ve} \\ &= \left( \pi - \tan^{-1} \left| \frac{dy_4}{dx_4} \right| \right), \text{ when } dx_4 \text{ is + ve and } dy_4 \text{ is - ve} \\ &= -\frac{\pi}{2} \text{ or } \frac{\pi}{2}, \text{ when } dx_4 = 0 \text{ and } dy_4 \text{ is + ve or - ve} \end{aligned} \right\} \quad (5.17)$$

**Remarks 5.1:** Hence, according to Definition 5.9, during a *complete displacement* of the quadrilateral formation considered in section 5.4, the details of motion of all participating agents are described as follows. At the end of first instant of time  $dt$  the leader moves to its desired final position. Then at the end of second instant i.e.  $2dt$  the first follower moves to its final desired position to maintain distance constraints to the leader, during which leader remains stationary. At end of third instant i.e.  $3dt$  the ordinary follower-1 reaches to its final position to maintain distance constraints to both leader and first follower. At end of fourth instant i.e.  $4dt$  the ordinary follower-2 reaches to its final position to maintain distance constraints to both first follower and ordinary follower-1. Therefore the agents are not reaching their corresponding final position exactly at the same time. Consequently during the period starting from  $t$  to  $4dt$  desired distances

are not preserved among the agents, rather all agents are in the process of forming the desired formation. So it may be concluded that after every  $4dt$  time, the desired formation is obtained. Therefore, each agent starts to move to its new position (to be in a new position set) after every  $3dt$  time. That is there is a discontinuous motion occurs for every agent. Therefore, for formation of  $n$  number of agents, after every  $ndt$  time the desired formation is maintained. Each agent starts to move to its new position (to be in a new position set) after every  $(n-1)dt$  time.

## 5.6 Simulation Results and Discussions

In this section, effectiveness of proposed control laws eqs (5.4), (5.5), (5.8), (5.9), (5.12), (5.13), (5.16) and (5.17) have been tested successfully via three cases of simulations for below mentioned formation specifications, size of simulations steps in MATLAB R2012a simulation environment as mentioned in Table 5.2.

Table 5.2: Formation specifications, size of simulations steps

$l_{1d}(m)$	$l_{2d}(m)$	$l_{3d}(m)$	$l_{4d}(m)$	$l_{5d}(m)$	Time step size(s) for simulation
2	2	2	2	2	0.01

Lengths of different distances have been chosen same for easiness of showing the convergence of all distances to desired set satisfying corresponding to desired persistent formation.

Initial linear positions of agents and information about different trajectories tracked by leader are depicted in Table 5.3.

Table 5.3: Initial position of agents and information about leader trajectories

<i>Trajectories tracked by leader</i>	<i>Initial linear position</i>	$v_I$ (m/s)	$\omega_I$ (rad/s)	<i>Distance (m) traveled by leader</i>	<i>Angular frequency (Hz)</i>	<i>Time(s) travelled</i>
Case I: Straightline	(2, 4), (2, 2), (3.732, 3), (3.732, 1)	1	0	1.5	—	Corresponding to distance
Case II: Circular	-do-	1	0.00157	1.5	—	-do-
Case III: Sinusoidal  $x(t) = 0.03t$ $y(t) = \sin(0.03t)$	-do-	varying	varying	—	0.03	100

*Remarks 5.2:* Control laws given in equations (5.4), (5.8), (5.12) and (5.16) require the final position of the corresponding agent at each instant of time during their motion. For the leader, the final position at each instant of time is available as the path is specified for it, but for other agents, these positions must be calculated. To find out the final position at each instant of time  $t$ , the controller in each case requires optimization of a quadratic objective function under one or

two quadratic equality constraints as described in section 5.5. Several optimization methods are available for this purpose. The choice here is to exploit Sequential Quadratic Programming (SQP) as it is one of the most popular and robust algorithms for nonlinear continuous optimization. The method is based on solving a series of subproblems designed to minimize a quadratic model of the objective subject to a linearization of the constraints. In the proposed controller, the objective functions are chosen as quadratic whilst the constraints are taken as non-linear quadratic which can be linearized during course of optimization procedure. At the beginning of each instant of time  $t$  (i.e. at the beginning of a complete displacement of the whole formation), the position of each agent is used as the initial position in control law of that particular agent. This position coordinate is also assumed as starting point of that agent's complete iterative procedure (in optimization process using SQP) for finding out its final position. That iterative procedure follows the steps elaborated below.

(i) making a Quadratic Programming (QP) sub problem (based on a quadratic approximation of the Lagrangian function) using nonlinear objective function and equality constraints

(ii) solving that Quadratic Programming (QP) sub problem at each iteration

(iii) during (ii) (i) updating an estimate of the Hessian of the Lagrangian at each iteration using the BFGS (Broyden–Fletcher–Goldfarb–Shanno) formula [215],[216]

(iv) Quadratic Programming solution at each iteration performing appropriate Line Search using Merit Function [215],[216],[217].

### **5.6.1 Observations**

According to mentioned information of Table 5.3; straight line, circular and sinusoidal trajectory tracking of leader and corresponding estimated paths tracking of followers are shown in Fig. 5.5,

Fig.5.6 and Fig. 5.7 respectively. From these plots it is observed that while leader accurately tracks the desired path for a particular mission, followers also track their estimated paths accurately. As a result, the persistence property of desired CFMP formation is maintained during the mission such that distances among agents are maintained at their desired values after every specific interval of time. Thus, rigidity of the formation graph formed by agents are satisfied after every specific interval of time during the motion of formation which starts with desired set of distances among agents. The variations of distances among agents are observed for different trajectories for duration  $t=0s$  to  $t=0.08s$  is in Table 5.4.

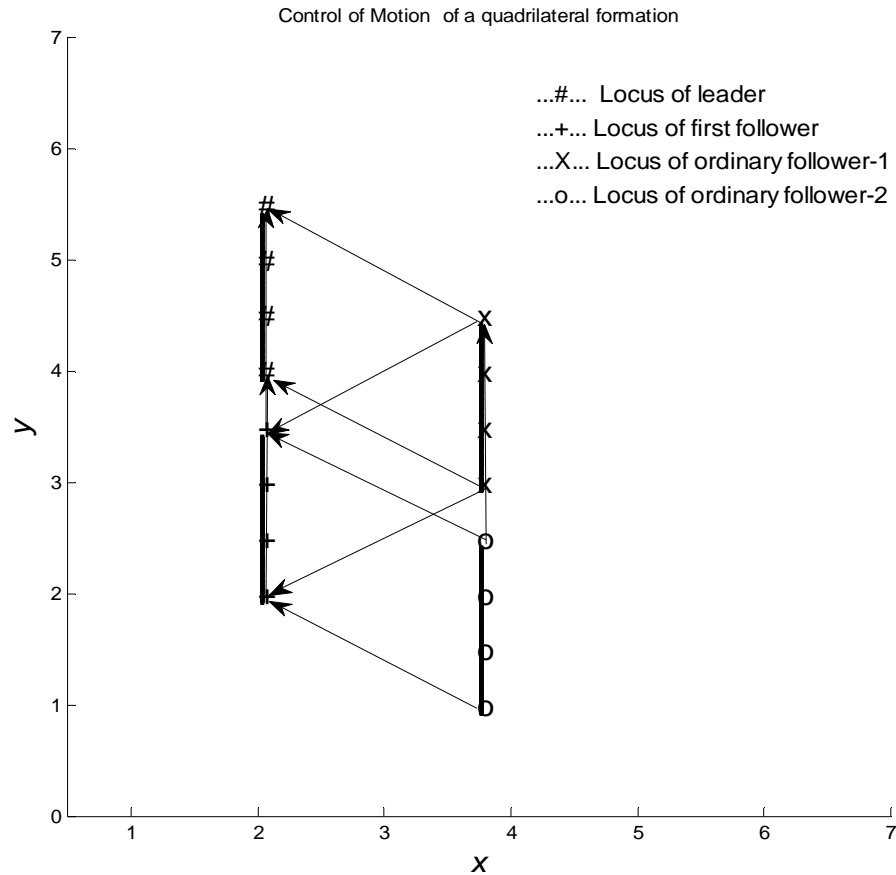


Fig 5.5. Straight line motion of formation of four agents with leader-follower structure

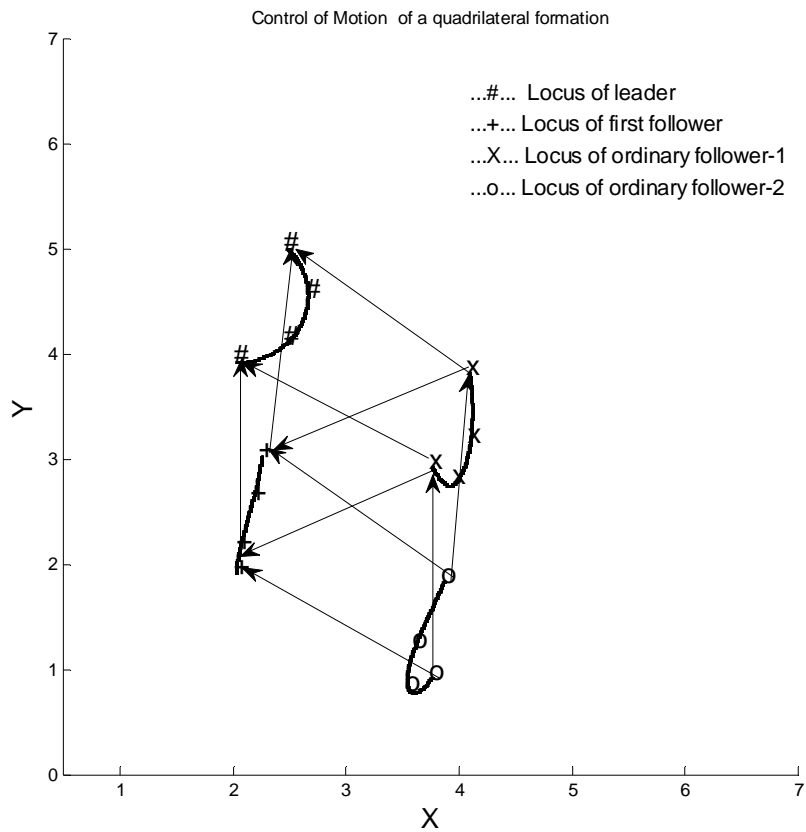


Fig. 5.6. Motion of formation of four agents with leader-follower structure corresponding to circular path tracked by leader

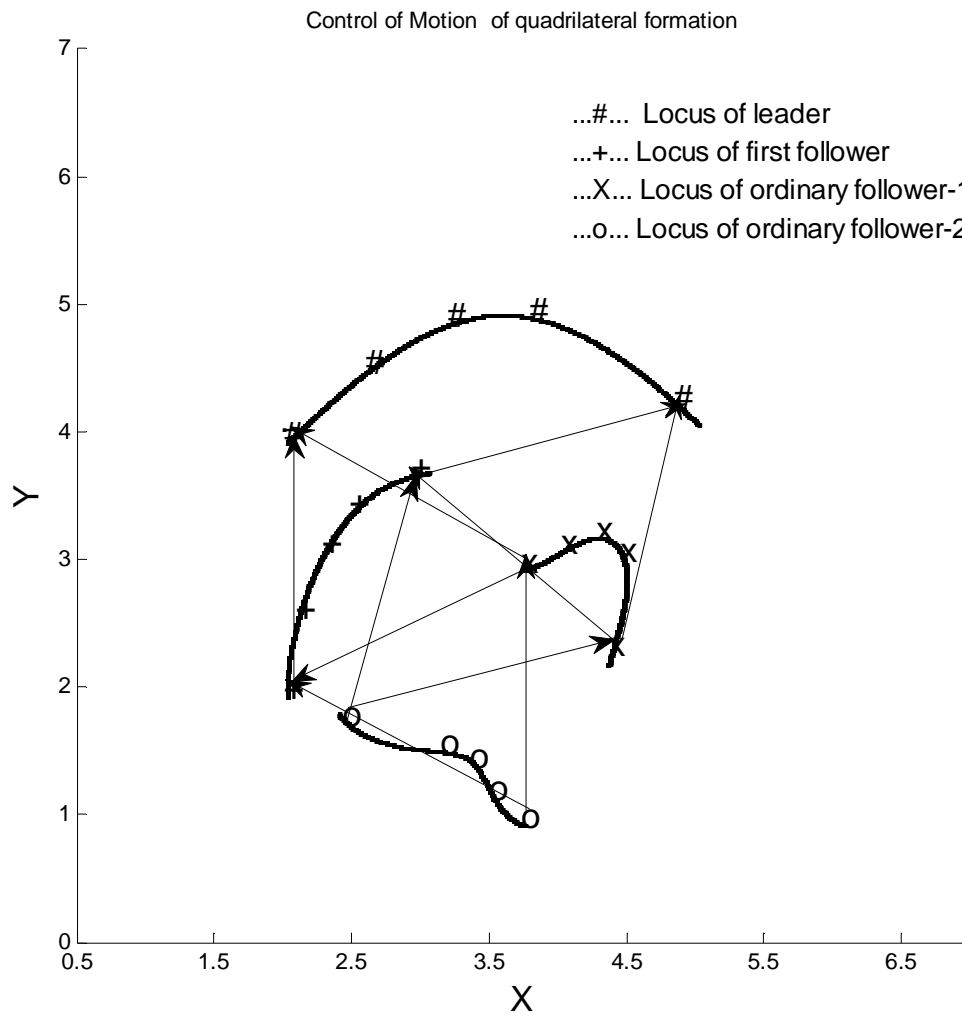


Fig. 5.7. Motion of formation of four agents with leader-follower structure corresponding to sinusoidal path tracking of leader

Table 5.4: Observation of distances from simulation for motion control of quadrilateral formation during the period  $t=0s$  to  $0.08s$

Time Instants(s)	$t=0$					$t=0.01$					$t=0.02$				
Distances(m)	$d_1$	$d_2$	$d_3$	$d_4$	$d_5$	$d_1$	$d_2$	$d_3$	$d_4$	$d_5$	$d_1$	$d_2$	$d_3$	$d_4$	$d_5$
Case:I	2	2	2	2	2	2.001	2.0005	2.0005	2	2	2	1.9995	2.0005	2.0005	2
Case:II	2	2	2	2	2	2	2	1.9991		2	2	2	1.9991	2	2
Case:III	2	2	2	2	2	2.0003	2	1.9998	2	2	2	1.9998	1.9998	2.0001	2

Time Instants(s)	$t=0.03$					$t=0.04$					$t=0.05$				
Distances(m)	$d_1$	$d_2$	$d_3$	$d_4$	$d_5$	$d_1$	$d_2$	$d_3$	$d_4$	$d_5$	$d_1$	$d_2$	$d_3$	$d_4$	$d_5$
Case:I	2	2	2	2.0005	2.001	2	2	2	2	2	2.001	2	2.0005	2	2
Case:II	2	2	2	2	1.9991	2	2	2	2	2	2	2	1.9991	2	2
Case:III	2	2	2	2.0001	2	2	2	2	2	2	2.0012	2	1.9996	2	2

Time Instants(s)	$t=0.06$					$t=0.07$					$t=0.08$				
Distances(m)	$d_1$	$d_2$	$d_3$	$d_4$	$d_5$	$d_1$	$d_2$	$d_3$	$d_4$	$d_5$	$d_1$	$d_2$	$d_3$	$d_4$	$d_5$
Case:I	2	1.9995	2.0005	2.0005	2	2	2	2	2.0005	2.001	2	2	2	2	2
Case:II	2	2	1.9991	2	2	2	2	2	2	1.9991	2	2	2	2	2
Case:III	2	1.9994	1.9996	2.0006	2	2	2	2	2.0006	2.0002	2	2	2	2	2



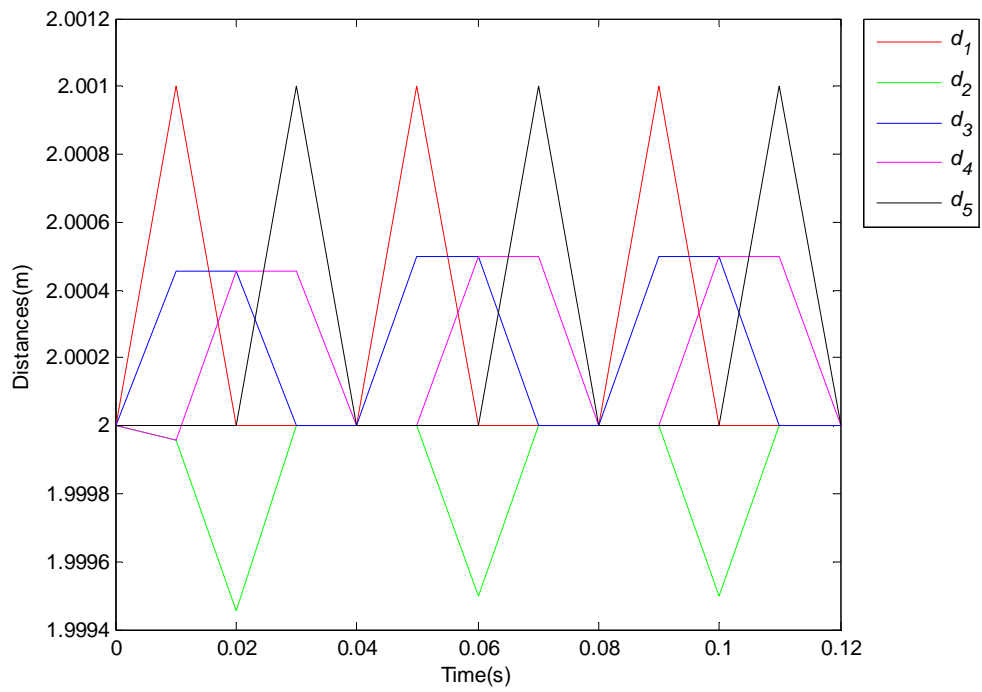


Fig. 5.8 Plot of  $d_1, d_2, d_3, d_4$  and  $d_5$  vs. time corresponding to straightline trajectory of leader

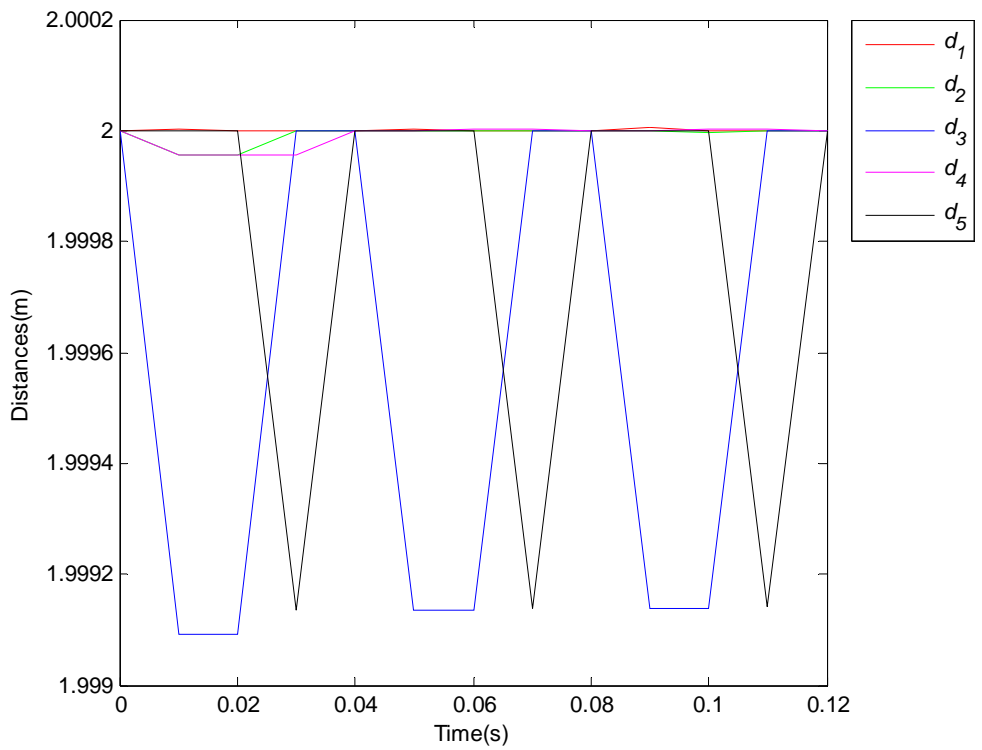


Fig. 5.9 Plot of  $d_1, d_2, d_3, d_4$  and  $d_5$  vs. time corresponding to circular trajectory of leader

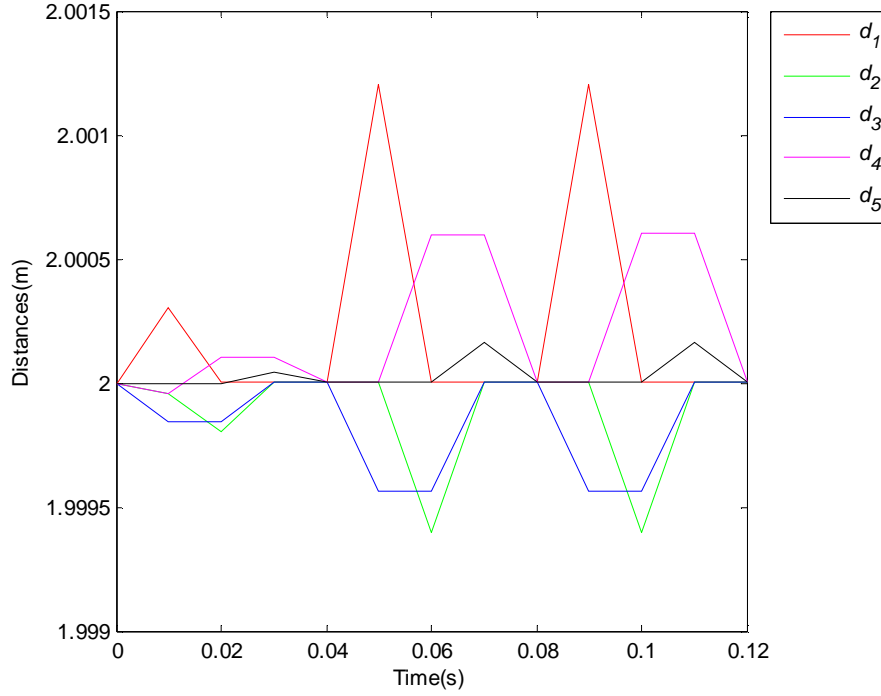


Fig. 5.10 Plot of  $d_1, d_2, d_3, d_4$  and  $d_5$  vs. time corresponding to sinusoidal trajectory of leader

For each of three cases of simulation mentioned above, the plots  $d_1, d_2, d_3, d_4$  and  $d_5$  vs.  $t$  are shown in Fig.5.7, Fig.5.8 and Fig.5.9 respectively. In these plots it is clearly observed that for every 0.04s interval instantaneous distances among four agents are maintained at desired values

## 5.7 CFMP Formation with AUV Dynamics

Previous sections discussed the strategy for implementation of a CFMP formation graph created by multiple nonholonomic point agents and proposed control algorithm for maintaining that formation structure during its motion. This section extends the concept of control of CFMP formation formed with simple kinematic model of point agent to complex dynamics of AUV[182]. However, the adopted implementation strategy of said CFMP formation in this case is different from that of point agents. A simple geometric technique is used for finding out the

states of unknown trajectories generated for followers AUVs during the course of tracking by global leader AUV along an unknown (e.g. navigation) or desired trajectory is different.

## 5.8 Problem Formulation

For simplicity, group of only three AUVs in two dimensional planes are considered for developing the proposed control algorithm. All AUVs are assumed to have similar kind of kinematics and dynamics of 3.2 and 3.3. These are placed in a CFMP triangular formation as shown in Fig.5.11. AUV-1, AUV-2, AUV-3 are assigned responsibilities of leader (also called global leader), first follower & the ordinary follower AUV respectively. Instantaneous distances among them are  $d_1, d_2$  and  $d_3$ . Desired distances are  $l_{1d}, l_{2d}, l_{3d}$ . A distance between two AUVs is the distance between the CoM (Centre of Mass) of one AUV to CoM of another AUV. It may be noted that for maintaining the said graph model of formation AUV-1 will have no outgoing edge i.e. it is free to move along a specified trajectory. AUV-2 will have to maintain one distance constraint  $l_{1d}$  i.e. to AUV-1 and AUV-3 will have to maintain two distance constraints  $l_{2d}$  and  $l_{3d}$  with respect to AUV-2 and AUV-1 respectively. Leader AUV needs to track a desired trajectory or it may move along an arbitrary trajectory according to requirement of any mission.

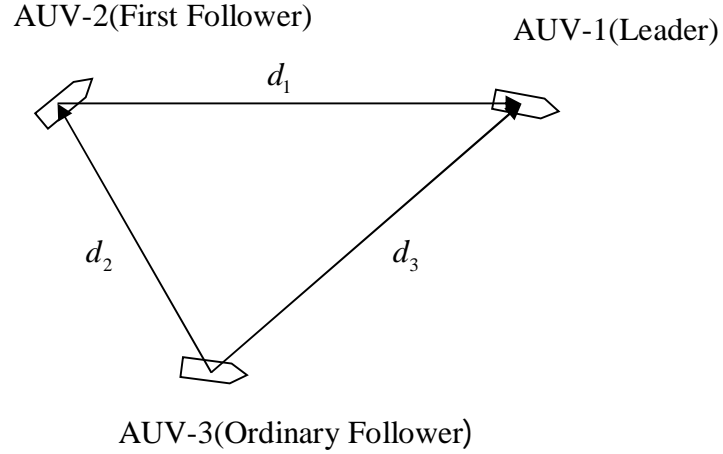


Fig. 5.11 Triangular formation of three AUVs with leader-follower structure

Before stating the main problem of the control of motion of CFMP formation some assumptions are made as mentioned below.

***Assumptions 5.3:***

- i. It has been assumed that each AUV communicates to other AUVs by electromagnetic wave as wireless communication medium. Due to its high absorption rate it cannot communicate with longer range. Therefore, each AUV is assumed to have limited communication range.
- ii. There is no delay among AUVs in communicating information
- iii. Each AUV can measure its linear position using the Inertial Navigation System (INS) navigation sensor and orientation by a magnetic compass respectively.
- iv. Leader AUV can communicate its position and orientation information to the first follower AUV and position information to ordinary follower AUV. Similarly first follower AUV can communicate its position and orientation to the ordinary follower AUV.

### 5.8.1 Problem Statement

Consider a triangular CFMP formation of three AUVs under the Assumptions 5.3. Each AUV follows the kinematics of and dynamics of (3.2) and (3.3). Assume initial structure of formation satisfies condition of (5.3). It is also assumed that initial formation preserves the desired inter-agent distances. It is intended to provide a set of decentralized control laws for the AUVs in this formation such that desired inter-agent distances are preserved after every fixed interval of time corresponding to desired tracking of leader for any mission. Control law is developed on the assumption that each agent accurately tracks its desired position state i.e stable trajectory tracking occurs.

A similar definition of a complete movement, as was discussed in section 5.5, between  $\lambda_n$  and  $\lambda_r$  (similar to  $\lambda_f$  in case of point agents) is also applied in proposing the control algorithm of CFMP formation with AUV dynamics. In this discussion,  $\lambda_n$  and  $\lambda_r$  are given by

$$\lambda_n = (x_{1n}, y_{1n}, \theta_{1n}, \dot{x}_{1n}, \dot{y}_{1n}, \dot{\theta}_{1n} = \omega_{1n}, u_{1n}, v_{1n}, \dots, x_{3n}, y_{3n}, \theta_{3n}, \dot{x}_{3n}, \dot{y}_{3n}, \dot{\theta}_{3n} = \omega_{3n}, u_{3n}, v_{3n}) \in \mathbb{R}^{8 \times 3} \quad (5.18a)$$

where,  $\theta_{1n} = \theta_{2n} = \theta_{3n} \in \lambda_n$ .

$$\lambda_r = (x_{1r}, y_{1r}, \theta_{1r}, \dot{x}_{1r}, \dot{y}_{1r}, \dot{\theta}_{1r} = \omega_{1r}, u_{1r}, v_{1r}, \dots, x_{3r}, y_{3r}, \theta_{3r}, \dot{x}_{3r}, \dot{y}_{3r}, \dot{\theta}_{3r} = \omega_{3r}, u_{3r}, v_{3r}) \in \mathbb{R}^{8 \times 3} \quad (5.18b)$$

where,  $\theta_{1r} = \theta_{2r} = \theta_{3r} \in \lambda_r$ . Before proceed to develop the control algorithm it is assumed that at any time  $t$  system of AUVs has reached a distance preserving state  $\lambda_f$  i.e. one complete movement has been achieved. Then how the AUVs move to their new positions and what amount of control inputs are required for another complete displacement is discussed below.

## 5.9 Development of Control Strategy of CFMP formation with AUV Dynamics

### 5.9.1 Trajectory Tracking and Development of Control Law of Global Leader

The global leader is not assigned any responsibility to maintain any distance constraint from any other agent in formation. Leader has information about the desired path (planned/given) to be tracked by it. Therefore, controller of leader may calculate the desired linear and angular velocity at every instant to reach the desired position. Suppose, at time  $t$  position state for leader is  $\boldsymbol{\eta}_l(t) = \boldsymbol{\eta}_{l_{ln}} = (x_{l_{ln}}, y_{l_{ln}}, \theta_{l_{ln}}) \in \lambda_{l_{ln}}$ . Let, the leader moves to a new linear position  $\boldsymbol{\eta}_{l_1}(t+dt) = \boldsymbol{\eta}_{l_{lr}} = (x_{l_r}, y_{l_r}) \in \lambda_r$  i.e. the final position, in very small period of time  $dt$  such that continuity preserves between  $\boldsymbol{\eta}_{l_{ln}}$  and  $\boldsymbol{\eta}_{l_{lr}}$  i.e. the distance between these two positions is sufficiently small. This motion of the leader and corresponding movement of the first follower is shown in Fig.5.15. According to Fig.5.16,  $d\boldsymbol{\eta}_{l_1} = dx_1 \hat{i} + dy_1 \hat{j}$ .  $\hat{i}$  and  $\hat{j}$  are unit vectors along  $x$  and  $y$  direction of the global coordinate system.  $dx_1 = x_{l_r} - x_{l_{ln}}$  and  $dy_1 = y_{l_r} - y_{l_{ln}}$ . The required  $x$  and  $y$  direction translational velocities in IRF to reach the desired position from its current position is

$$\dot{x}_1(t+dt) = \dot{x}_{l_r} = \frac{dx_1}{dt} \quad (5.19a)$$

$$\dot{y}_1(t+dt) = \dot{y}_{l_r} = \frac{dy_1}{dt} \quad (5.19b)$$

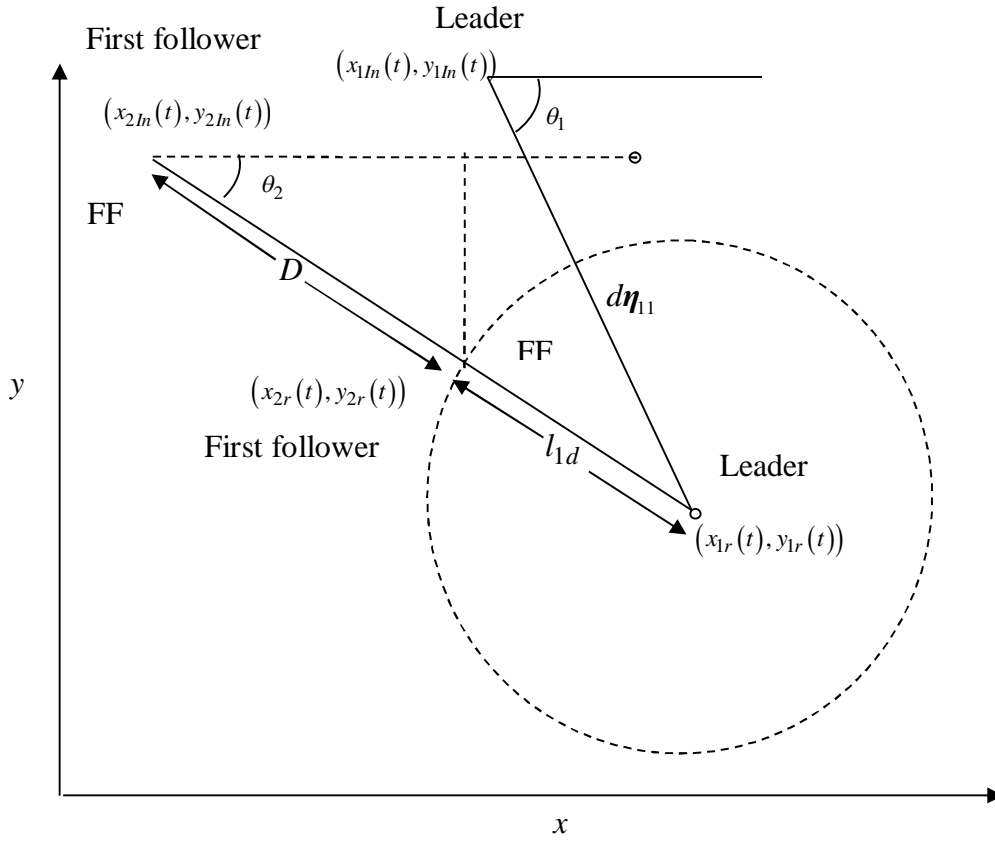


Fig. 5.12 Motion of Leader and First Follower for a very small duration of time ( $dt$ )

The angle made by straight line joining current and final position of leader, with respect to positive  $x$  axis of inertial reference frame, which is desired orientation of leader and is given by

$$\theta_1(t + dt) = \theta_{1r} = \tan^{-1} \left( \frac{dy_1}{dx_1} \right) \quad (5.20)$$

The convention of range of orientation is assumed to vary between 0 to 6.28 rad. The angular velocity required to track the desired orientation is given by

$$\omega_1(t + dt) = \omega_{1r} = \frac{d\theta_1}{dt} \quad (5.21)$$

where,  $d\theta_1 = \theta_{1r} - \theta_{1m}$ .

Substituting (5.19) and (5.21) in (3.2) the velocities in BRF can be obtained. Thus, required force and torque ( $F_{1r}$ ) can be obtained from (3.3) as follows

$$M\dot{v}_{1r} + C(v_{1r})v_{1r} + D(v_{1r})v_{1r} = F_{1r} = F_1(t+dt) \quad (5.22)$$

Thus, control law exclusively depends upon the dynamic model of AUV. It must be stated at this stage that  $v_{1r}$  follows (4.5) corresponding to curvature of the given/planned path to be tracked.

Proposed control structure for global leader AUV is shown in Fig. 5.13.

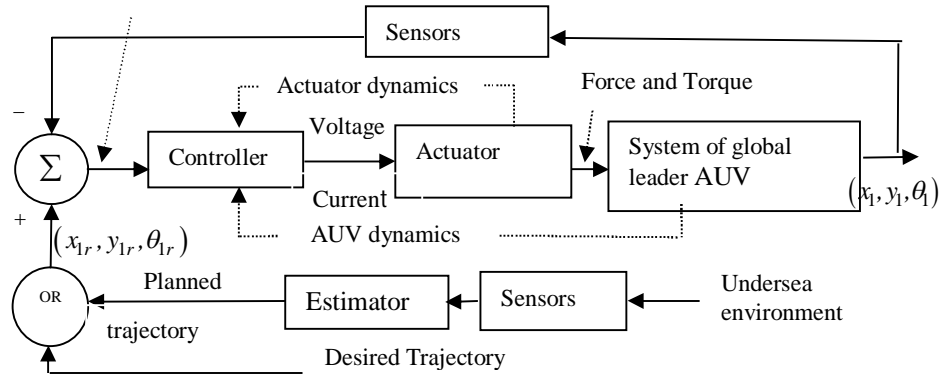


Fig 5.13 Controller Structure for Global Leader AUV

### 5.9.2 Trajectory Generation and Development of Control Law for Followers

Each  $k$ th follower AUV with identification number  $k=2,3$ , estimates its desired state using an estimator. Thus, how this kind of estimator functions for trajectory generation of first follower and ordinary follower in a triangular formation is elaborated below.

#### 5.9.2.1 Trajectory Generation and Development of Control Law for First Follower

First follower has been given responsibility to maintain a distance constraint i.e. desired distance  $l_{1d}$  to global leader. As shown in Fig 5.15, at any time instant  $t$ , current position state of ordinary



follower is assumed as  $\boldsymbol{\eta}_2(t)$  and thus  $\boldsymbol{\eta}_{2ln} = (x_{2ln}, y_{2ln}, \theta_{2ln}) = \boldsymbol{\eta}_2(t) = \boldsymbol{\eta}_2(t+dt)$ . Due to motion of leader the instantaneous distance  $d_1$  deviates from  $l_{1d}$ . First follower senses error between its actual and desired position state using communicated information of  $\boldsymbol{\eta}_{1f}$  staying at its initial position  $\boldsymbol{\eta}_2(t) = \boldsymbol{\eta}_2(t+dt) = \boldsymbol{\eta}_{2ln} = (x_{2ln}, y_{2ln})$ . In this process, it utilizes the error between actual and desired distances from leader. It attempts to satisfy this distance constraint and to track the orientation of leader. Suppose, it moves to its desired position state at the next instant of time  $dt$  after the instant during which the leader moves to its final position. It should be noted continuity preserves in the movement from  $\boldsymbol{\eta}_2(t)$  to  $\boldsymbol{\eta}_2(t+2dt) = \boldsymbol{\eta}_{2r} = (x_{2r}, y_{2r}) \in \lambda_r$ . During this movement of first follower, leader is assumed to be stationary at the position  $\boldsymbol{\eta}_1(t+2dt) = \boldsymbol{\eta}_{1f}$ . Let, to minimize error in distance, it tries to move to its desired position travelling along shortest path. This shortest path can be found out by drawing a circle centering at  $\boldsymbol{\eta}_{1r}$ , with radius  $l_{1d}$ . It can be found from the Fig.5.15, that shortest path exists along the straightline joining  $\boldsymbol{\eta}_{2ln}$  and  $\boldsymbol{\eta}_{1r}$ , and it has a length  $D$ .  $D$  is defined as

$$D = \sqrt{(x_{1r} - x_{2ln})^2 + (y_{1r} - y_{2ln})^2} - l_{1d} \quad (5.23)$$

The angle made by straight line joining initial and final position of first follower, with respect to positive  $x$  axis of inertial reference frame is

$$\theta_2 = \tan^{-1} \left( \frac{y_{1r} - y_{2ln}}{x_{1r} - x_{2ln}} \right) \quad (5.24)$$

Therefore,  $\boldsymbol{\eta}_{2r}$  can be estimated as

$$\left. \begin{aligned} x_{2r} &= D \cos(\theta_2) \\ y_{2r} &= D \sin(\theta_2) \end{aligned} \right\} \quad (5.25)$$

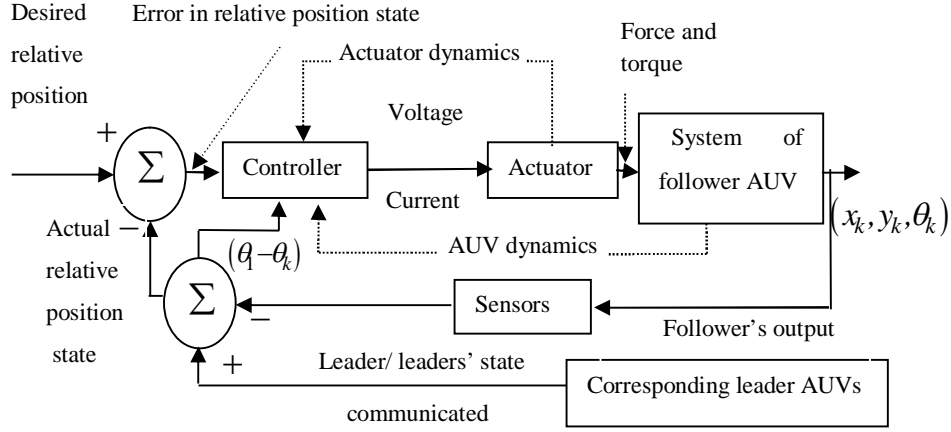


Fig. 5.14 Controller Structure of  $k$ th AUV

For reaching to desired final position from its initial position, the required  $x$  and  $y$  direction translational velocity in inertial frame is

$$\dot{x}_2(t + 2dt) = \dot{x}_{2r} = \frac{dx_2}{dt} \quad (5.26a)$$

$$\dot{y}_2(t + 2dt) = \dot{y}_{2r} = \frac{dy_2}{dt} \quad (5.26b)$$

where,  $dx_2 = x_{2r} - x_{2In}$  and  $dy_2 = y_{2r} - y_{2In}$  are error in position of first follower along its trajectory respectively in  $x$  and  $y$  direction.

Suppose, at the said instant  $(2dt)$  orientation of leader is  $\theta_1(t + dt) = \theta_1(t + 2dt)$ . Therefore,

$\theta_{2r}(t) = \theta_1(t + 2dt)$ . Error in orientation is

$$\theta_2(t + 2dt) = \theta_{2r} \quad (5.27a)$$

Required angular velocity is given by

$$\omega_2(t + 2dt) = \omega_{2r} = \frac{d\theta_2}{dt} \quad (5.27b)$$

where,  $d\theta_2 = \theta_{2r} - \theta_{2In}$ .

Substituting (5.26) and (5.27) in (3.2) the velocities in BRF can be obtained. Thus, required force and torque ( $F_{2r}$ ) may be obtained from eq.(3.3) as follows

$$M\dot{\mathbf{v}}_{2r} + C(\mathbf{v}_{2r})\mathbf{v}_{2r} + D(\mathbf{v}_{2r})\mathbf{v}_{2r} = \mathbf{F}_{2r} = \mathbf{F}_2(t+2dt) \quad (5.28)$$

It must be stated at this stage that  $\mathbf{v}_{2r}$  follows (4.5) as the global leader follows the same. The proof of this statement is given in the next chapter.

### 5.9.2.2 Trajectory Generation and Development of Control Law for Ordinary Follower

Ordinary follower has been given responsibility to maintain two distance constraints i.e. desired distance  $l_{2d}$  to global leader and  $l_{3d}$  to first follower. Assume, at any time instant  $t$ , current position state of ordinary follower is assumed as  $\boldsymbol{\eta}_3(t)$  and thus  $\boldsymbol{\eta}_{3In} = (x_{3In}, y_{3In}, \theta_{3In}) = \boldsymbol{\eta}_3(t) = \boldsymbol{\eta}_3(t+dt) = \boldsymbol{\eta}_3(t+3dt)$ . Due to motion of leader and the first follower instantaneous distances  $d_2$  and  $d_3$  deviates from  $l_{3d}$  and  $l_{2d}$ . First follower senses error between its actual and desired position state using communicated information of  $\boldsymbol{\eta}_{1r}$  staying at its initial position  $\boldsymbol{\eta}_2(t) = \boldsymbol{\eta}_2(t+dt) = \boldsymbol{\eta}_{2In}$ . In this process, it utilizes error between actual and desired distances from leader. It attempts to satisfy these distance constraints and to track the orientation of average of orientations of first follower and leader. Suppose, it moves to its desired position state at the next instant of time  $dt$  after the instant during which the leader moves to its

final position. It should be noted continuity preserves in the movement from  $\eta_2(t)$  to  $\eta_2(t+2dt)=\eta_{2r}=(x_{2r},y_{2r})\in\lambda_r$ . During this movement, first follower and leader are assumed to be stationary at their desired position  $\eta_{1r}$  and  $\eta_{2r}$ . A condition is given to the ordinary follower AUV such that only when changes in positions of both leader as well as first follower (not merely leader) occur; ordinary follower changes its position to final one.

Thus, according to the above discussions two desire distance constraints  $l_{3d}$  and  $l_{2d}$  are to be satisfied for final state. They can be formulated as follows

$$\left. \begin{aligned} (x_{1r} - x_{3r})^2 + (y_{1r} - y_{3r})^2 - l_{3d}^2 &= 0 \\ (x_{2r} - x_{3r})^2 + (y_{2r} - y_{3r})^2 - l_{2d}^2 &= 0 \end{aligned} \right\} \quad (5.29)$$

Two equations in (5.29) represent two circles. There are two meeting points of these circles. The ordinary follower has to move any of these meeting points avoiding collision with leader and first follower such that distance between initial and final positions must be minimum. That means ordinary follower follows the shortest path to reach the any of the meeting point on the circles where it will maintain distance constraints and respectively from first follower and leader. Two possible solutions of these equations are given by

$$\left. \begin{aligned} y_{r31} &= \frac{A+B}{C} \\ y_{r32} &= \frac{A-B}{C} \\ x_{r31} &= \frac{-b^* y_{r31} - c}{a} \\ x_{r32} &= \frac{-b^* y_{r32} - c}{a} \end{aligned} \right\} \quad (5.30)$$

Different parameters in (5.30) represent their expressions as follows

$$A = -(b(x_{r1}a + c) - a^2 y_{r1}), B = \sqrt{(b(x_{r1}a + c) - a^2 y_{r1})^2 - (b^2 + a^2)(a^2(y_{r1} - l_{3d})^2 + (x_{r1}a + c)^2)},$$

$$C = a^2 + b^2, a = 2^*(x_{r2} - x_{r1}), b = 2^*(y_{r2} - y_{r1}), c = x_{r1}^2 - x_{r2}^2 + y_{r1}^2 - y_{r2}^2 + l_{2d}^2 + l_{3d}^2$$

For reaching to desired final position from its initial position, the required  $x$  and  $y$  direction translational velocity in inertial frame is

$$\dot{x}_3(t + 3dt) = \dot{x}_{3r} = \frac{dx_3}{dt} \quad (5.31a)$$

$$\dot{y}_3(t + 3dt) = \dot{y}_{3r} = \frac{dy_3}{dt} \quad (5.31b)$$

where,  $dx_3 = x_{3r} - x_{3ln}$  and  $dy_3 = y_{3r} - y_{3ln}$  are error in position of ordinary follower along its trajectory respectively in  $x$  and  $y$  direction.

Suppose, at the said instant ( $3dt$ ) orientation of leader and first follower are  $\theta_{1r} = \theta_1(t + 3dt)$  and  $\theta_{2r} = \theta_2(t + 3dt)$ . Therefore,  $\theta_{3r} = \frac{\theta_{1r} + \theta_{2r}}{2}$ . Error in orientation is  $d\theta_3 = \theta_{3r} - \theta_{3ln}$ . Required angular velocity is given as

$$\omega_2(t + 3dt) = \omega_{3r} = \frac{d\theta_3}{dt} \quad (5.32)$$

Substituting (5.27) and (5.28) in (3.2) the velocities in BRF can be obtained. Thus, required force and torque ( $F_{3r}$ ) can be obtained from (3.3) as follows

$$M\dot{\mathbf{v}}_{3r} + C(\mathbf{v}_{3r})\mathbf{v}_{3r} + D(\mathbf{v}_{3r})\mathbf{v}_{3r} = \mathbf{F}_{3r} = \mathbf{F}_3(t + 3dt) \quad (5.33)$$

It must be stated at this stage that  $\mathbf{v}_{3r}$  follows (4.5) as the global leader follows the same. The proof of this statement is proved in the next chapter.

The proposed control structure for  $k$ th follower AUV, where,  $k=2,3$  is shown in Fig. 5.17.

From the above discussion it is concluded that trajectories of follower are continuous if the global leader follows a continuous trajectory.

### 5.10 Simulation Results and Observations

In this section, efficacy of simple geometric approach for implementation of CFMP formation of AUVs with simple control laws (5.22),(5.28),(5.32) have been verified using MATLAB 2012a. Formation specifications, size of simulations steps, initial position state of system of AUVs, trajectory information of leader are given in Table 5.5.

Table 5.5: Formation specifications, size of simulations steps, Initial position state, trajectory information of leader

$h_d(m)$	$l_{2d}(m)$	$l_{3d}(m)$	Time step size(s) for simulati -on	Trajectory tracked by leader: straightline		Initial position state of AUVs	Distancce (m) travelled by leader
				$v_l$ (m/s)	$\omega_l$ (rad/s)		
2	2	2	0.03	1	0	$\eta_1 = (2, 3.732, 1.57)$ $\eta_2 = (1, 2, 1.57)$ $\eta_3 = (3, 2, 1.57)$	3

Locus of leader, first follower and ordinary follower are shown in Fig. 5.15. Motion of different AUVs for first six instants has been shown in Fig. 5.16. Plots of distances among three AUVs during formation tracking is shown in Fig. 5.17.

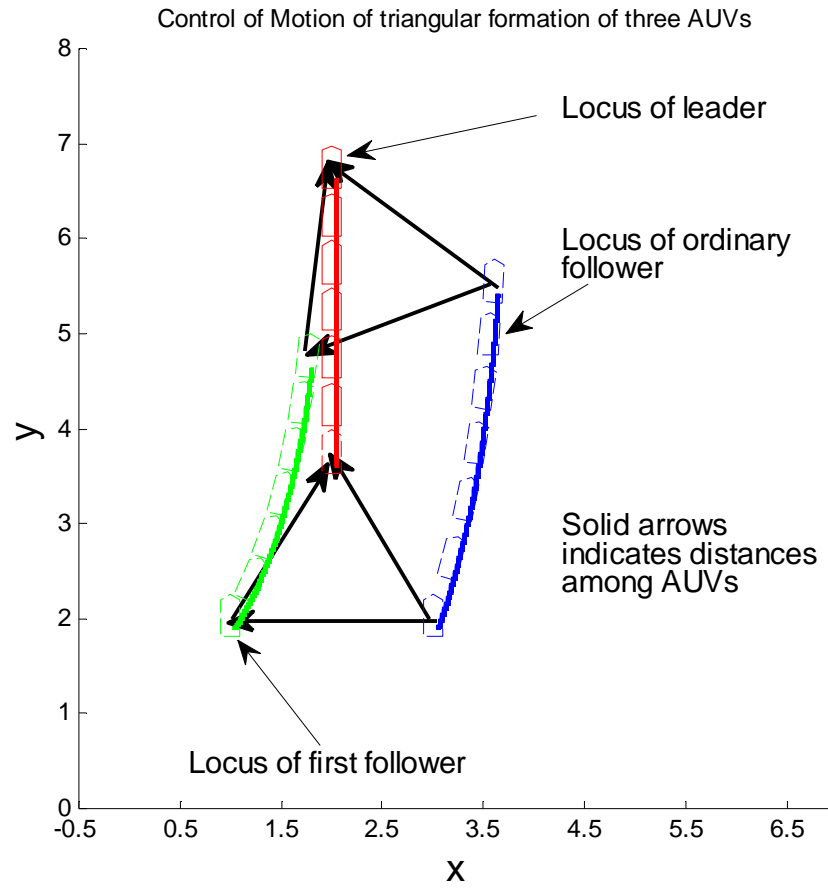


Fig. 5.15 Locus of first follower, ordinary follower with straightline trajectory tracking of leader

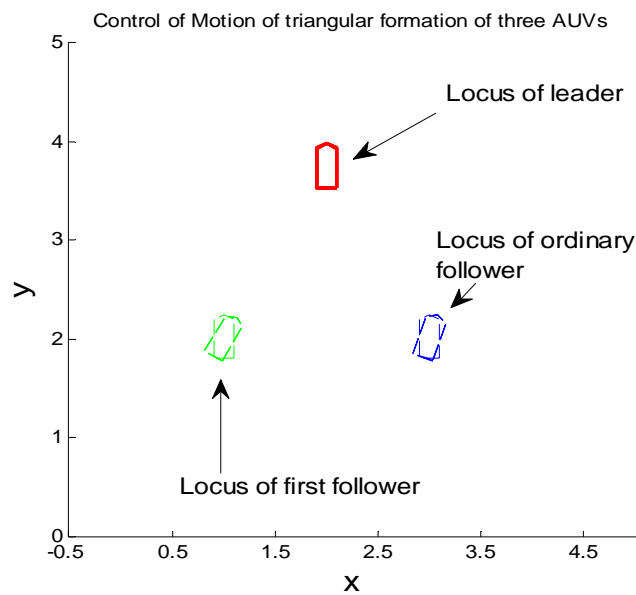


Fig. 5.16 Motion of different AUVs for first six instants of time corresponding to Fig. 5.15

## 5.11 Chapter Summary

In this chapter a new algorithm using a set of decentralized control laws based on optimization (using Sequential Quadratic Programming) of distance constraints has been proposed for the trajectory tracking control of leader in a CMFP formation of multiple nonholonomic autonomous point agents. The effectiveness of the proposed control schemes have been demonstrated through

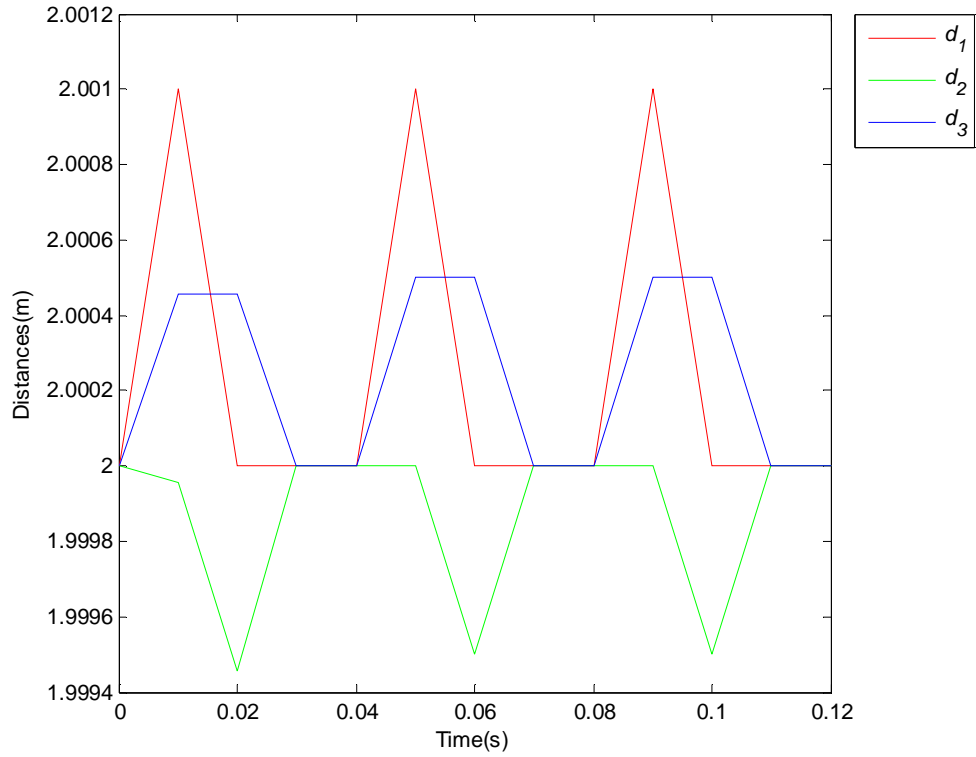


Fig. 5.17 Plots of distances among three AUVs during formation tracking

a number simulations corresponding to different trajectories tracking of leader. It is found that the inter-agent distances are maintained at desired values during the motion of formation. Proposed control algorithm is only suitable for non-time critical mission where it is not necessary that all point agents to reach to the goal at the same time. Next, proposed formation tracking control algorithm has been extended to CFMP formation of group of AUVs. But in this case, a



simple geometric technique has been used for estimating the desired linear position of a follower AUV. Control law exclusively depends upon the dynamic model of AUV i.e. controller is model based.

It is concluded from the design of control algorithms that finding out of desired state is easy in SQP method than the geometric method as no complete geometric description is required in earlier one. SQP merely needs to choose objective function and constraints in straightforward manner. But drawbacks of SQP method is that it takes more time than simple geometric method to estimate the desired state.



# Chapter-6

## Directed Distance-Based Decentralized Robust Formation Control of Multiple AUVs

### 6.1 Introduction

This chapter extends the work described in chapter 5 i.e. tracking control strategy of a leader-follower CFMP formation of multiple AUVs with uncertainties in their dynamic parameters and with limited torque generating capability from their actuators. Work considered of this chapter is to *i)* formulate the entire formation tracking problem described in chapter 5 for time-critical mission, where each AUV reaches around the goal point at the same time. This is different to the formulated problem in chapter 5 where control action of each AUV is generated in a specific order taking the available state of neighbours based on the scheme of a non-time critical mission which allows AUVs to converge to desired formation after every fixed interval of time. *ii)* further it is intended to launch N-PID like controller for directed graph based formation of AUVs. *iii)* In chapter 6, we also explore to design a suitable robust control strategy for achieving globally stable formation tracking as initial configuration of formation is always deviated from desired one a large due to several disturbances like ocean current in real underwater scenario.

The chapter is organised as follows. Section 6.2 presents the problem formulation. Section 6.3 provides the definitions on input to state stability (ISS) and cascaded system stability. Section 6.4 proposes a new control law for  $k^{\text{th}}$  AUV which is called Sliding Mode Nonlinear-PID controller with BI and BD. In section 6.5, the closed-loop dynamics of  $k$ -th AUV under the application of

said control law, is derived in terms of trajectory tracking error. Section 6.6 analyzes the stability formation control of CFMP formation of multiple AUVs under the application of control law SM-NPID with BI on each one; in the framework of input-to-state stability assuming the entire formation of AUVs as a system of several cascaded sub-systems. In section 6.7, efficacy of proposed control scheme is illustrated through a simulation for a group of AUVs in a CMFP formation. This chapter is concluded in section 6.8.

## 6.2 Preliminaries

### 6.2.1 Problem Description

A group of  $n$  number of AUVs are considered for said formation motion control in two dimensional (2D) oceanic space  $(\mathbb{R}^2)$ . The group is modeled as a CFMP formation [155] graph  $\vec{G}(N, \vec{E})$ , where,  $N$  and  $\vec{E} \subseteq N \times N$  represent the set of nodes which are Centre of Masses (CoMs) of AUVs and set of directed information flow (edges) among AUVs respectively. This directed graph is assumed constructed from initial leader-follower seed by Henneberg sequence with standard vertex additions [221], [155]. Minimal rigidity and constraint consistency are features of this kind of directed graph. Persistent graph, by feature of its construction, facilitates collision avoidance among AUVs. This said formation graph is shown in Fig.6.1, where cardinality  $|N| = n$  and dimension of  $E = |\vec{E}| = m$ . Following topological ordering [222] of Henneberg sequence construction method, the nodes are numbered as 1 for global leader (GB), 2 for first follower (FF) and  $k$  for  $k$ th follower. FF has only one neighbour i.e. GB.  $k$ th follower other than FF has two neighbours whose indices are less than  $k, \forall k \in \{3, 4, \dots, n\}$ . Edge set is oriented as  $\vec{E} = \{(\overline{2, 1}), \dots, (\overline{k, k\_less}), \dots\}, \forall k = (3, 4, \dots, n)$  and  $k\_less$  indicates the indices which are less than  $k$ . Entire CFMP may be considered as a collection of several triangular subgroups

each of which is formed taking a group of three AUVs at a time. In an example of this kind of triangular structure as depicted in Fig. 6.1, if indices  $k_L, k_R \in N_k$  where,  $N_k$  is set of neighbours of  $k$ th follower AUV,  $\forall k \in \{3, \dots, n\}$  then  $k_R < k_L < k$ . As an example,  $k_L=2$  and  $k_R=1$  for second follower ( $k=3$ ) in the basic triangular subgroup formed considering GB, FF, second follower AUV. The corresponding distance variables are denoted as  $l_{kk_L}, l_{kk_R}, l_{k_L k_R} \in E$ .

Each node in this formation represents an AUV. Kinematics and dynamics of AUV are eq (3.2) and eq (3.3) respectively. The state of  $k^{\text{th}}$  AUV is represented as  $\xi_k = (\eta_k, \dot{x}_k, \dot{y}_k, \dot{\theta}_k = \omega_k, u_k, v_k) \in \mathbb{R}^8$ , where,  $\eta_k = (\eta_{1k}, \eta_{2k}) \in \mathbb{R}^3$  is the position state.  $\eta_{1k} = (x_k, y_k) \in \mathbb{R}^2$  and  $\eta_{2k} = \theta_k \in \mathbb{R}$  denote for the linear position vector of CoM and orientation respectively.  $\dot{\eta}_{1k} = (\dot{x}_k, \dot{y}_k) \in \mathbb{R}^2$  represents linear velocity vector in IRF.  $\dot{\eta}_{2k} = \dot{\theta}_k = \omega_k \in \mathbb{R}$  denotes angular velocity.  $\mathbf{v}_k = [u_k \ v_k \ \omega_k]^T \in \mathbb{R}^3$  represents velocity vector of surge, sway and angular velocities in BRF.  $\mathbf{F}_k \in \mathbb{R}^3$  designates control inputs (force/torque). Let, the state vector of system of AUVs is denoted as

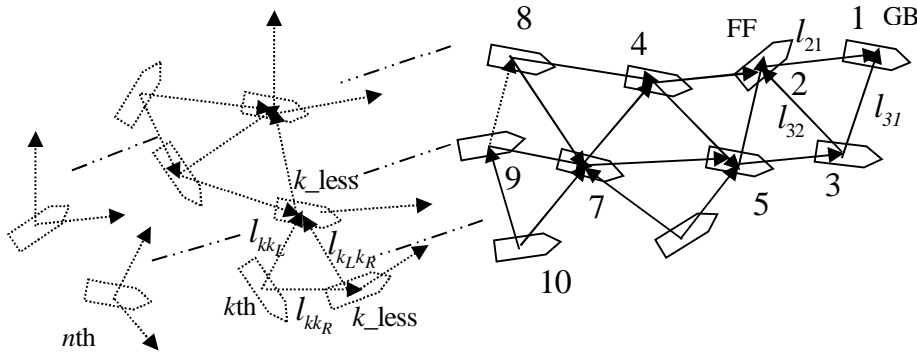


Fig. 6.1 Cycle free minimally persistent formation of a group of AUVs

$$\xi = [\xi_1 \quad \xi_2 \quad \dots \quad \xi_n]^T \in \mathbb{R}^{8n} \quad (6.1)$$

Position state vector of system of AUVs is denoted as

$$\varsigma = (\eta_{11}, \eta_{12}, \dots, \eta_{1n}, \eta_{21}, \eta_{22}, \dots, \eta_{2n}) \in \mathbb{R}^{3n} \quad (6.2)$$

Realization of the CFMP  $\bar{G}(N, \bar{E})$  of (Fig.6.1) is a function  $\mathbf{p}: N \rightarrow \mathbb{R}^2$ , where,

$\mathbf{p} = (\eta_{11}, \eta_{12}, \dots, \eta_{1n}) \in \mathbb{R}^{2n}$ . A pair  $(\bar{G}, \mathbf{p})$  is called framework and denoted as  $F$ . The instantaneous

distance variable between any pair of nodes  $(\overline{k, j}) \in E$  is defined as

$$l_{kj} = \|\eta_{1j} - \eta_{1k}\|, \forall (\overline{k, j}) \in E \quad (6.3)$$

According to persistence property of CFMP, it is necessary to put follower AUVs in fitting [155], [223] positions for a desired distance set for every desired realization. This distance set is defined as

$$l^d = \{l_{kj}^d, \forall (\overline{k, j}) \in E\} \in \mathbb{R}^m \quad (6.4)$$

In formation tracking, GB is assumed to track trajectory of a slowly moving reference AUV (RA)[208] along a sufficiently smooth predefined/planned trajectory. Then following definitions hold about the state of RA-GB.

*Definition 6.1:* Following eq (3.2c), the kinematic description of system of reference AUV to be tracked by global leader GB, is defined as follows

$$\dot{\eta}_{1r}(t) = J(\eta_{1r}) \mathbf{v}_{1r}(t) \quad (6.5)$$

$$\text{where, } \theta_{1r}(t) = \tan^{-1} \left( \frac{dy_1(t)}{dx_1(t)} \right) = \eta_{21r}(t) \quad (6.6)$$

The tracking control law proposed in this chapter does not need information about the acceleration state of the RA-GB. Boundary value of acceleration is only necessary. Feasible values of state of RA-GB along the curvature of its reference trajectory are restricted by

constraints on dynamics of GB. These constraints are specified bounds on velocities and accelerations. These bounds for all AUVs in general are mentioned as following

$$0 \leq \|\mathbf{v}_{1k}\| \leq v_{1kmax}, 0 \leq \|\dot{\mathbf{v}}_{1k}\| \leq a_{1kmax}, |\mathbf{v}_{21}| \leq v_{21max}, |\dot{\mathbf{v}}_{21}| \leq a_{2kmax}, \forall k = 1, \dots, n. \quad (6.7)$$

where,  $v_{1kmax}, a_{1kmax}, v_{21max}, a_{2kmax}$  are maximum values of quantities inside the norm.

Each follower AUV needs to track a dynamically generated trajectory (DGT) with respect to its linear position based on continuous time realization of desired CFMP. But, on the whole it tracks the trajectory of reference AUV (RA) which takes the reference linear state from DGT and reference angular state estimated from the angular state information of its own as well as neighbours. A desired state observer (DSO), as discussed in 6.2.2.1, is designed for each follower for estimating the state of corresponding RA. In this perspective, the state of  $k$ th reference AUV (RA- $k$ ) is defined as

$$\xi_{kr} = (x_{kr}, y_{kr}, \theta_{kr}, \dot{x}_{kr}, \dot{y}_{kr}, \dot{\theta}_{kr} = \omega_{kr}, u_{kr}, v_{kr}) \in \mathfrak{R}^8, k = 2, \dots, n \quad (6.8)$$

Before presenting the design procedure of observer and stating the problem of this research work a set of following assumptions are made.

**Assumptions 6.1:**

i) Distance variables for any triangular subgroup in the initial and desired realization of a CFMP formation graph of AUVs must satisfy the triangle inequalities to avoid collinearity [190], [188]. This type of formation refers to generically persistent [155] graph. Therefore, for any triangular subgroup in Fig.6.1, inequalities (6.9) and (6.10) must be fulfilled.

$$\left. \begin{aligned} l_{kk_L}(0) &< l_{kk_R}(0) + l_{k_L k_R}(0) \\ l_{kk_R}(0) &< l_{k_L k_R}(0) + l_{kk_L}(0) \\ l_{k_L k_R}(0) &< l_{kk_R}(0) + l_{kk_L}(0) \end{aligned} \right\}, \forall k \in \{3, \dots, n\} \quad k_L, k_R \in \{1, 2, 3, \dots, n\} \quad (6.9)$$

Thus, according to (6.11),  $F(\bar{G}, \mathbf{p}(0))$  is generically persistent [212].

$$\left. \begin{aligned} l_{kk_L}^d &< l_{kk_R}^d + l_{k_L k_R}^d \\ l_{kk_R}^d &< l_{k_L k_R}^d + l_{kk_L}^d \\ l_{k_L k_R}^d &< l_{kk_R}^d + l_{kk_L}^d \end{aligned} \right\}, \forall k \in \{3, \dots, n\} \text{ and } k_L, k_R \in \{1, 2, 3, \dots, n\} \quad (6.10)$$

- ii) Inter-agent distances are sufficiently larger than length of an AUV such that initial collision among AUVs can be avoided
- iii) Each AUV can measure its absolute linear position and orientation using navigational sensor [196] and magnetic compass. It is assumed that these measurements are free of noise.
- iv) Each AUV can estimate its translational velocities, angular velocities in IRF. These measured values are assumed noise free.
- v) Each AUV can receive transmitted information about the linear positions and orientations of its two (single neighbour for FF) neighbours in a triangular subgroup.
- vi) During motion of formation, failure of sensors do not occur
- vii) There is no time delay in receiving data from neighbours
- viii) Each AUV can estimate its desired state with the help of its desired state observer using the position and orientation state information of its neighbours.

## 6.2.2 Trajectory Generation and its boundedness and formulation of desired state

This subsection develops the method of trajectory generation and proves its boundedness corresponding to global leader's movement. Moreover, the desired state of formation is also established.

### 6.2.2.1 Trajectory generation and design of DSO

Trajectory generation problem refers to finding out a set of trajectories for followers corresponding to fulfilment of desired structure of CFMP, linked with the desired trajectory tracking of GB. Trajectory generation of a follower consists of finding out two state, namely linear state and angular state. Generation of linear state depends upon the theory of persistent



graph and property of underlying rigid graph. Generation of angular state is based on the assumption that FF and second follower ( $k=3$ ) track the orientation of GB and FF respectively and other followers track average of orientations of their neighbours. Combining both the generated trajectories, complete reference trajectory of a follower is obtained.

Desired trajectory wrt linear position for a particular follower AUV is a function which takes desired values of linear positions of that AUV at infinite number of instants during desired continuous time realization of CFMP formation corresponding to smooth motion of GB. Both actual and desired frameworks correspond to actual linear position of GB i.e  $\boldsymbol{\eta}_{11}(t)$ . Let,  $\boldsymbol{\eta}_{1k}(t), \forall k \in (2, \dots, n)$  and  $\boldsymbol{\eta}_{1kr}(t): \mathbb{R} \rightarrow \mathbb{R}^2$  actual and desired (reference) trajectory of  $k$ th follower AUV respectively wrt linear state. Then, actual and desired frameworks wrt actual trajectory of GB, are  $F(\vec{G}, \boldsymbol{p}(t))$  and  $F(\vec{G}, \boldsymbol{p}_r(t))$ , where,  $\boldsymbol{p}_r(t) = \{\boldsymbol{\eta}_{11}(t), (\boldsymbol{\eta}_{1kr}(t), \forall k = 1, 2, \dots, n)\}$   $\boldsymbol{p}(t) = \{\boldsymbol{\eta}_{1k}, \forall k = 1, 2, \dots, n\}$ . Desired framework should satisfy 6.4 and 6.10. Moreover, desired framework is time varying as the GB is tracking a path. Therefore, a desired framework is an element of a set of all possible frameworks congruent to a reference framework. This set is defined as follows  $F(\vec{G}, \hat{\boldsymbol{p}}), \forall \hat{\boldsymbol{p}} \in \mathbb{R}^{2n}$

*Definition 6.2:* Assume a generically persistent reference framework of graph  $\vec{G}$ , satisfying 6.4 and 6.10. Desired framework is a framework which is congruent to the reference framework. Thus, a set of desired frameworks is defined as follows

$$\boldsymbol{F}_r \triangleq \{F(\vec{G}, \boldsymbol{p}_r(t))\} \triangleq \{F(\vec{G}, \boldsymbol{p}(t)): \|\boldsymbol{\eta}_{1j} - \boldsymbol{\eta}_{1k}\| = \|\hat{\boldsymbol{\eta}}_{1j} - \hat{\boldsymbol{\eta}}_{1k}\|, \forall j, k \in N\} \quad (6.11)$$

Any framework  $\boldsymbol{p}(t)$  and its desired framework  $\boldsymbol{p}_r(t)$  are related through a set of optimization problems under a set of distance constraints 6.4.

FF has only one distance constraint and other followers has two distance constraints. Therefore, optimization problem for FF is stated combining its objective function (a distance minimization function) and distance constraints as follows

$$Op\_prob\_1 = \min(\|\boldsymbol{\eta}_{12r} - \boldsymbol{\eta}_{12}\|) \text{ subject to } \|\boldsymbol{\eta}_{11} - \boldsymbol{\eta}_{12r}\| = l_{21}^d \in l^d \quad (6.12)$$

For other followers with node indices  $k \in (3, \dots, n)$  have two constraints for two neighbours. Thus, optimization problem for  $k$ th follower other than FF is stated as

$$Op\_prob\_k = \min(\|\boldsymbol{\eta}_{1k} - \boldsymbol{\eta}_{1kr}\|) \text{ subject to} \quad (6.13)$$

$$(\|\boldsymbol{\eta}_{1k_L} - \boldsymbol{\eta}_{1kr}\| = l_{kk_L}^d, \|\boldsymbol{\eta}_{1k_R} - \boldsymbol{\eta}_{1kr}\| = l_{kk_R}^d) \in l^d, \forall k \in (3, \dots, n)$$

Set of optimization problems is defined as

$$Set\_Op\_prob = (Op\_prob\_1, Op\_prob\_2, Op\_prob\_3, \dots, Op\_prob\_n) \quad (6.14)$$

Therefore,  $\mathbf{p}(t)$  and  $\mathbf{p}_r(t)$  are interrelated by the following

$$\mathbf{p}_r(t) = (\boldsymbol{\eta}_{11}(t), \{\boldsymbol{\eta}_{1kr} : Op\_prob\_k \in Set\_Op\_prob, \forall \boldsymbol{\eta}_{1k} \in \mathbf{p}(t), \forall k \in (2, 3, \dots, n)\}) \in \mathbb{R}^{2n} \quad (6.15)$$

To implement 6.16 i.e. to estimate the values of  $\boldsymbol{\eta}_{1kr}(t)$ , each follower AUV exploits its desired state observer.

Tracking control objective of the said CFMP formation is divided into several sub tasks where each subtask is performed by an AUV. Subtask of GB is to generate control using reference state available from its reference AUV and its own state measured such that it can track the reference trajectory. Subtask of  $k$ th follower AUV is divided into two parts. In its first task, follower estimates the state of its RA- $k$  by introducing its *DSO*. Next task is to generate control input using desired and its own current measured state such that it can track its reference trajectory. Observer utilizes only local information about the linear and angular positions from its neighbours. Entire formation tracking is achieved by simultaneous execution of these individual subtasks at each time step. Hence the complete goal of formation control is decoupled (i.e. decentralized) although the AUVs are coupled at formation level. Based on assumptions made in Assumptions 6.1, the design procedure of observer for follower AUVs is presented below.

*Remarks 6.1:* CFMP formation using Henneberg's sequence suffers from unwanted flip realizations. But in this research work the desired linear position of a follower remains unique as it is found out based on shortest path based minimization and leader is assumed to move slowly. Thus, realizations are free from flip ambiguity problem during desired tracking of leader.

*Remarks 6.2:* Small change in time is inevitable for continuous realizations. On the other hand, the generation of control effort for an AUV is restricted by actuators' capability, the rate of change of linear position i.e. velocity and consequently acceleration should remain bounded. Hence, small change in linear positions of follower AUVs corresponding to small change in linear position of GB is essential during the motion of formation. Thus, if the AUVs start with non-collinear configuration they maintain same for all  $t \geq 0$ . Moreover, once formation reaches its desired configuration, rigidity of underlying undirected graph is clearly maintained for future time.

### ***DSO for FF***

Assume, for infinitesimal motion of GB, infinitesimal rigidity of entire formation is maintained by infinitesimal motion of followers. At each time instant, during a smooth motion of GB, FF determines state of RA-2,  $\xi_{2r}$  corresponding to actual state of GB ( $\eta_l$ ), which is available to FF by Assumptions 6.1. For this purpose FF introduces a DSO. Observer carries out this task by passing one parameter in DSO namely desired distance constraint ( $l_{21}^d$ ) to be maintained to GB and the state of GB. Set of values of  $\xi_{2r}(t)$  at infinite number of time steps for certain duration of time form the trajectory of RA-2.

In designing an observer, study of all possible movement of GB for bounded linear and angular displacement satisfying (6.7), at each time steps is essential. Suppose, the current state of GB at

$t=\tau$  is  $\xi_1(\tau)$  and state at next step  $t = \tau + \Delta\tau, \Delta\tau \rightarrow 0$ , is  $\xi_1(\tau+\Delta\tau)$ . Corresponding actual state and desired states of the FF at these instants are  $\{\xi_2(\tau), \xi_{2r}(\tau)\}$  and  $\{\xi_2(\tau+\Delta\tau), \xi_{2r}(\tau+\Delta\tau)\}$  respectively. Further, actual distance between GB and FF is assumed as  $l_{21}(t) = \|\eta_{11}(t) - \eta_{12}(t)\|$ . Till the  $l_{21} = l_{21}^d$  is not satisfied between FF and GB, two situations may arise for their motion at every instant of time. These take place when  $l_{21} > l_{21}^d$  and  $l_{21} < l_{21}^d$  respectively. Couple of examples of first situation have been explained in Fig. 6.2(a) and Fig. 6.2(b) when  $\theta_F > 0$  and  $\theta_F < 0$  respectively, where

$$\theta_F(t) = \tan^{-1} \left( \frac{y_1(t) - y_2(t)}{x_1(t) - x_2(t)} \right).$$

Fig. 6.3 (a) and Fig. 6.3(b) explains the second situation when  $\theta_F > 0$  and  $\theta_F < 0$  respectively.

*Remarks 6.3:* Practically, first situation may happen when GB is in an attempt to retreat from any obstacle whereas second situation indicates free forward motion of AUV. In the both figures Fig 6.2 and Fig 6.3, following two relations hold.

$$\left. \begin{aligned} l_{21} &= l_{21}^d - D \\ l_{21} &= l_{21}^d + D \end{aligned} \right\} \quad (6.16)$$

respectively, where,  $D(t) = \|\eta_{12r}(t) - \eta_{12}(t)\|$ . In both the cases, range of  $\theta_F$  is  $0 \leq \theta_F \leq \pi$  and  $0 \geq \theta_F \geq -\pi$  rad. Assume the convention of range for angle representation is 0 to  $2\pi$  rad. Using the value of  $\theta_F$ , the DSO of FF estimates its desired linear position for the first kind of situation as

$$\eta_{12r}(\tau + \Delta\tau) = \eta_{12}(\tau + \Delta\tau) + D\Omega(\theta_F) \quad (6.17)$$

For the second kind of situation is given by

$$\boldsymbol{\eta}_{12r}(\tau + \Delta\tau) = \boldsymbol{\eta}_{12}(\tau + \Delta\tau) + D\boldsymbol{\Omega}(\pi + \theta_F) \quad (6.18)$$

where,  $\boldsymbol{\Omega}(\theta) = [\cos(\theta) \quad \sin(\theta)]^T$ . Except at  $t=0$  (initially a desired velocity is assumed), the desired linear velocity in IRM at any instant  $t = \tau + \Delta\tau$  is estimated as follows

$$\dot{\boldsymbol{\eta}}_{12r}(\tau + \Delta\tau) = \lim_{\Delta\tau \rightarrow 0} \frac{L t}{\Delta\tau} \frac{\boldsymbol{\eta}_{12r}(\tau + \Delta\tau) - \boldsymbol{\eta}_{12r}(\tau)}{\Delta\tau} = \lim_{\Delta\tau \rightarrow 0} \frac{L t}{\Delta\tau} \frac{\Delta\boldsymbol{\eta}_{12r}(\tau + \Delta\tau)}{\Delta\tau} = \left. \frac{d\boldsymbol{\eta}_{12r}}{dt} \right|_{t=\tau+\Delta\tau} \quad (6.19)$$

It is assumed that FF tracks the orientation of its only one neighbour GB. Hence, desired orientation of FF at any instant  $t = \tau + \Delta\tau$  is given by

$$\theta_{2r}(t) \Big|_{t=\tau+\Delta\tau} = \theta_1(t) \Big|_{t=\tau+\Delta\tau} \quad (6.20)$$

Except at  $t=0$ , (initially a desired angular velocity is assumed), the desired angular velocity at any instant  $t = \tau + \Delta\tau$  is estimated by DSO as follows.

$$\omega_{2r}(\tau + \Delta\tau) = \lim_{\Delta\tau \rightarrow 0} \frac{L t}{\Delta\tau} \frac{\theta_{2r}(\tau + \Delta\tau) - \theta_{2r}(\tau)}{\Delta\tau} = \lim_{\Delta\tau \rightarrow 0} \frac{L t}{\Delta\tau} \frac{\Delta\theta_{2r}(\tau + \Delta\tau)}{\Delta\tau} = \left. \frac{d\theta_{2r}}{dt} \right|_{t=\tau+\Delta\tau} \quad (6.21)$$

*Remarks 6.4:* The problem arises when change over  $\Delta\theta_2$  takes place around a small region around 0 or  $2\pi$  line, in quadrant system, where a large value of angular velocity is estimated from (6.21). To overcome this problem, an angle of magnitude  $2\pi$  is subtracted from either of  $\theta_2(\tau)$  and  $\theta_1(\tau + \Delta\tau)$  which takes value very near but less than  $2\pi$  when other one takes positive value near zero. Following this conversion (6.21) is executed to estimate angular velocity within the limit of dynamic constraints eq (6.7).

Desired linear velocity in BRF for FF is obtained from the value of  $\dot{\boldsymbol{\eta}}_{12r}(t)$  and  $\theta_{2r}(t)$  respectively from (6.19) and (6.20) using (3.2c).

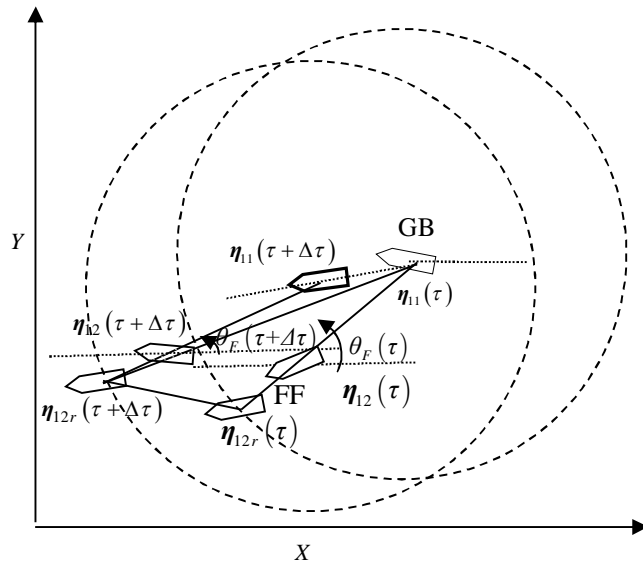


Fig. 6.2(a) Motion of FF and GB:  $\|\eta_{11} - \eta_{12}\| \leq l_{21}^d$

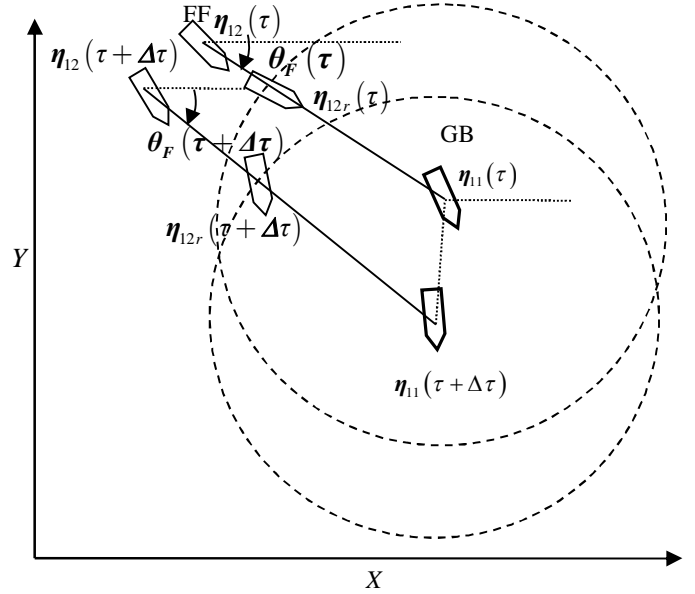


Fig. 6.2(b) Motion of FF and GB:  $\|\eta_{11} - \eta_{12}\| \geq l_{21}^d$

### DSO of $k^{\text{th}}$ follower

Assume, for infinitesimal motion of all AUVs in the group, state of  $k^{\text{th}}$  follower and its two neighbours are  $\xi_k(\tau + \Delta\tau), \xi_{k_L}(\tau + \Delta\tau), \xi_{k_R}(\tau + \Delta\tau)$  at  $t = \tau + \Delta\tau$  as shown in Fig. 6.3. It is also assumed that infinitesimal rigidity is maintained during their motion. According to Assumptions 6.1, at  $t = \tau + \Delta\tau$ ,  $k^{\text{th}}$  follower gets the information about the states of  $k_L$  and  $k_R$  follower, i.e.

$$\xi_{k_L}(\tau + \Delta\tau), \xi_{k_R}(\tau + \Delta\tau).$$

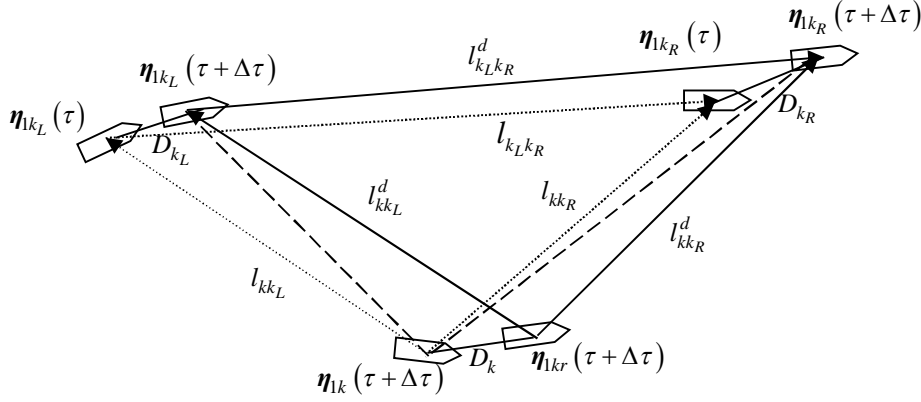


Fig. 6.3 Motion of three followers in a triangular subgroup of CFMP formation

$k$ th follower needs to satisfy two distance constraints to  $k_L$  and  $k_R$ . These are  $l_{kk_L}^d$  and  $l_{kk_R}^d$ . The desired state of  $k$ th follower is assumed as  $\xi_{kr}(\tau + \Delta\tau)$ . Hence,

$$\begin{cases} \|\eta_{1kr}(\tau + \Delta\tau) - \eta_{1k_L}(\tau + \Delta\tau)\| = l_{kk_L}^d \\ \|\eta_{1kr}(\tau + \Delta\tau) - \eta_{1k_R}(\tau + \Delta\tau)\| = l_{kk_R}^d \end{cases} \quad (6.22)$$

From chapter 5, it is known that there exist two possible solutions of  $\eta_{1kr}$  for two equations of centering at  $\eta_{1k_L}(\tau + \Delta\tau)$  and  $\eta_{1k_R}(\tau + \Delta\tau)$ . These are denoted as

$$\eta_{1kr} \in (\eta'_{1kr}, \eta''_{1kr})$$

where,

$$\begin{cases} \dot{\eta}'_{1kr} = \begin{bmatrix} \frac{-by'_{kr} - c}{a} & \frac{A+B}{C} \end{bmatrix}^T \\ \dot{\eta}''_{1kr} = \begin{bmatrix} \frac{-by''_{kr} - c}{a} & \frac{A-B}{C} \end{bmatrix}^T \end{cases} \quad (6.23)$$

where,  $A = (-b(x_{k_R}(\tau + \Delta\tau)a + c) - a^2y_{k_R}(\tau + \Delta\tau))$ ,

$$B = \sqrt{\left(b((x_{k_R}(\tau + \Delta\tau)a + c) - a^2y_{k_R}(\tau + \Delta\tau))^2 - (b^2 + a^2)\left(a^2(y_{k_L}(\tau + \Delta\tau) - l_{kk_R}^d)^2 + (x_{k_L}(\tau + \Delta\tau)a + c)^2\right)\right)},$$

$$C = a^2 + b^2, a = 2(x_{k_L}(\tau + \Delta\tau) - x_{k_R}(\tau + \Delta\tau)), b = 2(y_{k_L}(\tau + \Delta\tau) - y_{k_R}(\tau + \Delta\tau)),$$

$$c = x_{k_R}^2(\tau + \Delta\tau) - x_{k_L}^2(\tau + \Delta\tau) + y_{k_R}^2(\tau + \Delta\tau) - y_{k_L}^2(\tau + \Delta\tau) + (l_{kk_R}^d)^2 + (l_{kk_L}^d)^2.$$

Firstly, DSO estimates the  $\boldsymbol{\eta}'_{1kr}(\tau + \Delta\tau)$  and  $\boldsymbol{\eta}''_{1kr}(\tau + \Delta\tau)$ . Then it estimates the following

$$\begin{aligned} D'_k &= \|\boldsymbol{\eta}'_{1kr}(\tau + \Delta\tau) - \boldsymbol{\eta}_{1k}(\tau + \Delta\tau)\| \\ D''_k &= \|\boldsymbol{\eta}''_{1kr}(\tau + \Delta\tau) - \boldsymbol{\eta}_{1k}(\tau + \Delta\tau)\| \end{aligned} \quad (6.24)$$

Next, desired linear position of  $k^{\text{th}}$ -follower is found as

$$\boldsymbol{\eta}_{1kr}(\tau + \Delta\tau) = \left\{ \boldsymbol{\eta}_{1kr}(t) \Big|_{t=\tau+\Delta\tau} \in (\boldsymbol{\eta}'_{1kr}(\tau + \Delta\tau), \boldsymbol{\eta}''_{1kr}(\tau + \Delta\tau)) : \min(D'_k, D''_k) \right\} \quad (6.25)$$

Desired linear velocity in IRF

$$\dot{\boldsymbol{\eta}}_{1kr}(t) \Big|_{t=\tau+\Delta\tau} = \lim_{\Delta\tau \rightarrow 0} L\tau \frac{\boldsymbol{\eta}_{1kr}(\tau + \Delta\tau) - \boldsymbol{\eta}_{1k}(\tau + \Delta\tau)}{\Delta\tau} = \left( \frac{dx_{kr}(t)}{dt} \hat{i} + \frac{dy_{kr}(t)}{dt} \hat{j} \right) \Big|_{t=\tau+\Delta\tau} \quad (6.26)$$

It is assumed that the follower AUV other than FF and second follower ( $k=3$ ) tracks the average of the orientations of its neighbours. Hence, the DSO estimates the desired orientation of  $k^{\text{th}}$  follower using following expression

$$\theta_{kr}(t) \Big|_{t=\tau+\Delta\tau} = \frac{\theta_{k_L}(t) + \theta_{k_R}(t)}{2} \Big|_{t=\tau+\Delta\tau} \quad (6.27)$$

Consequently, the angular velocity is estimated as follows

$$\omega_{kr}(t) \Big|_{t=\tau+\Delta\tau} = \lim_{\Delta\tau \rightarrow 0} L\tau \frac{\theta_{kr}(\tau + \Delta\tau) - \theta_k(\tau + \Delta\tau)}{\Delta\tau} = \lim_{\Delta\tau \rightarrow 0} L\tau \frac{\Delta\theta_{kr}(\tau + \Delta\tau)}{\Delta\tau} = \frac{d\theta_{kr}(t)}{dt} \Big|_{t=\tau+\Delta\tau} \quad (6.28)$$

Eq. (6.28) also obeys the *Remarks 6.2* like FF. Desired linear velocity in BRF for  $k^{\text{th}}$  follower is obtained from the values of  $\dot{\boldsymbol{\eta}}_{1kr}(t)$  and  $\theta_{kr}(t)$  respectively from (6.26) and (6.27) using (3.2c).

*Remarks 6.5:* DSO of Second follower estimates the desired orientation using following expression



$$\theta_{3r}(t)\Big|_{t=\tau+\Delta\tau} = \frac{\theta_1(t) + \theta_2(t)}{2} \Big|_{t=\tau+\Delta\tau} \quad (6.29)$$

Consequently, the angular velocity is estimated as follows

$$\omega_{3r}(t)\Big|_{t=\tau+\Delta\tau} = \frac{d\theta_3(t)}{dt} \Big|_{t=\tau+\Delta\tau} \quad (6.30)$$

### 6.2.2.2 Boundedness of trajectories of followers corresponding to bounded trajectory of GB

It is required to prove that desired trajectories of followers remain under respective dynamic constraints mentioned in (6.17) as the trajectory tracked by global leader remains under given dynamic constraints mentioned in (6.12).

From the Fig.6.2, it is observed that for a sufficiently smooth motion of  $\vec{G}(N, \vec{E})$ , if  $\|\mathbf{v}_1(t)\|$  remains limited under dynamic constraints (6.7) for  $t \geq 0$ , then  $\Delta\boldsymbol{\eta}_{12r}(\tau + \Delta\tau)$  and consequently  $\|\mathbf{v}_{2r}(t)\|$  remains bounded for  $t \geq 0$ .

Similarly, from the Fig.6.3, it is observed that if  $\|\mathbf{v}_1(t)\|$  remains limited under dynamic constraints (6.7) for  $t \geq 0$ , then  $\Delta\boldsymbol{\eta}_{1k_L r}(\tau + \Delta\tau)$  and  $\Delta\boldsymbol{\eta}_{1k_R r}(\tau + \Delta\tau)$  and consequently  $\|\mathbf{v}_{kr}(t)\|$  remains bounded for  $t \geq 0$ .

### 6.2.2.3 Desired Steady State of system of AUVs

Before, presenting problem statement it is necessary to define the desired steady position state of system of AUVs. Desired steady state of system of AUVs corresponds to desired tracking of GB. As the motion control of system of AUVs is based on decentralized strategy, each AUV has the information only about the state of its neighbors. Thus, FF is assumed to get the information about the angular position of GB. Second follower is assumed to get the information about the

angular position of FF.  $k$ th follower is assumed to get information about  $k_L$ th and  $k_R$ th follower and so on.

The objective of this research work is to propose the motion control law based on maintaining the desired distance constraints among AUVs. Therefore, control for linear position of an AUV is straightforward and provided using the information of desired (from *DSO*) and current position. Linear position control only provides the structure of the formation but overall formation shape is achieved when the orientations of AUVs are also controlled in desired manner. Thus, to provide desired shape to the formation a specific desired orientation must be maintained by all AUVs. Hence, a criteria must be built up such that all AUVs finally follows same orientation. Although it has been set explicitly in (6.20) that FF has to track the orientation of GB, at this stage, it is explicitly set that orientation of FF needs to settle in the neighbourhood of  $\theta_1(t)$  instead of  $\theta_1(t)$ . Hence, desired steady orientation of FF is denoted as  $\theta_{2d}(t)$  and is specified as follows

$$\theta_1(t) - \theta_\epsilon \leq \theta_{2d}(t) \leq \theta_1(t) + \theta_\epsilon$$

where,  $\theta_\epsilon (< 1)$  is a very small positive number. In the same way, desired steady orientation of  $k$ th follower is set at  $\theta_1(t) - \theta_\epsilon \leq \theta_{kd}(t) \leq \theta_1(t) + \theta_\epsilon, \forall k = 3, 4, \dots, n$ . Thus, using (6.1) and (6.11), desired steady position state is defined below.

**Definition 6.3:** The desired steady position state of the CFMP formation  $\vec{G}(N, \vec{E})$  as shown in Fig. 6.1 for system of AUVs is defined as

$$\varsigma_d(t) = \left\{ \varsigma(t) : \boldsymbol{\eta}_1(t) = \boldsymbol{\eta}_{1r}(t); F(\vec{G}, \mathbf{p}(t)) \in \mathbf{F}_r; \eta_{2kr}(t) = \theta_{kd}(t), \forall k = 2, \dots, n \right\}. \quad (6.31)$$

### 6.2.3 Problem Statement

Consider a CFMP formation  $\vec{G}(N, \vec{E})$  of  $n$  number of AUVs as shown in Fig.6.1. Each AUV in the formation follows the kinematics and dynamics of (3.2c) and (3.3). It is assumed that initial framework is a perturbed version of desired realization. This perturbation is obvious in real underwater scenario due to the effect of ocean current disturbances. Hence, deviation in linear position and orientation for each AUV w.r.t its reference AUV at any time  $t$ , during tracking is defined as

$$\boldsymbol{\eta}_{ke}(t) = \boldsymbol{\eta}_k(t) - \boldsymbol{\eta}_{kr}(t) \quad (6.32)$$

where,  $\boldsymbol{\eta}_k = (x_k, y_k, \theta_k) \in \mathbb{R}^3$  and  $\boldsymbol{\eta}_{kr} = (x_{kr}, y_{kr}, \theta_{kr}) \in \mathbb{R}^3$  actual and desired position vector of  $k^{\text{th}}$  AUV in IRF.  $\boldsymbol{\eta}_{ke}(t) = (\boldsymbol{\eta}_k(t) - \boldsymbol{\eta}_{kr}(t)) = (x_{ke}(t), y_{ke}(t), \theta_{ke}(t)) \in \mathbb{R}^3$  is the error in position vector for  $k^{\text{th}}$  AUV.

Assume, initial position state of system of AUVs is

$$\boldsymbol{\varsigma}(0) = \left\{ (\boldsymbol{p}(0), \eta_{21}(0), \eta_{22}(0), \dots, \eta_{2n}(0)) : \boldsymbol{p}(0) \in F(\vec{G}, \boldsymbol{p}(0)) \right\} \in \mathbb{R}^{3n} \quad (6.33)$$

Initial error in position state for the system of AUVs is defined as

$$\boldsymbol{\varsigma}_e(0) = (\boldsymbol{\eta}_{11e}(0), \boldsymbol{\eta}_{12e}(0), \dots, \boldsymbol{\eta}_{1ne}(0), \boldsymbol{\eta}_{21e}(0), \boldsymbol{\eta}_{22e}(0), \dots, \boldsymbol{\eta}_{2ne}(0)) \in \mathbb{R}^{3n} \quad (6.34)$$

Statement: Initial position error  $\boldsymbol{\varsigma}_e(0)$  of a group of AUVs is such that (6.9) is satisfied. The objective is to design a set of decentralized control laws,  $\boldsymbol{F} \in \mathbb{R}^n$  under the Assumption 6.1 and constraints (6.7); on the application of which initial state  $\boldsymbol{\varsigma}_e(0)$  of system of AUVs reaches and remains in the neighbourhood of  $[\mathbf{0}] \in \mathbb{R}^{3n}, \forall t \geq 0$  in presence of bounded model parameter uncertainties as mentioned in Table 3.6, while global tracks a desired trajectory.

### 6.3 Notations and Definitions on Input to State Stability (ISS) and Cascaded System Stability

Before going to discuss input-to-state stability for a dynamic system following definitions must be stated.

*Definition 6.4* [225]:  $L_\infty^m$  space is space of all piecewise continuous functions  $\mathbf{u}: [0, \infty) \rightarrow \mathbb{R}^m$  satisfying

$$\|\mathbf{u}\|_{L_\infty^m} = \sup_{t \geq 0} \|\mathbf{u}(t)\|_\infty < \infty, \text{ where, } \|\mathbf{u}(t)\|_\infty = \max_i |u_i(t)|.$$

Now consider a nonlinear system

$$\dot{\mathbf{x}} = \mathbf{f}(\mathbf{x}, \mathbf{u}) \quad (6.35)$$

where,  $\mathbf{f}: \mathbb{R}^n \times \mathbb{R}^m \rightarrow \mathbb{R}^n$  with state  $\mathbf{x} \in \mathbb{R}^n$  and input  $\mathbf{u} \in \mathbb{R}^m$ .  $\mathbf{f}(\mathbf{x}, \mathbf{u})$  is locally Lipschitz in  $\mathbf{x}$  and  $\mathbf{u}$  with  $\mathbf{f}(\mathbf{0}, \mathbf{0}) = \mathbf{0}$ .

For the system of (6.35), the global input-to-state stability is defined as follows

*Definition 6.5* [218],[224],[225]: The system (6.35) is said to be globally ISS stable if there exist a class- $KL$  function  $\beta(\cdot)$  and class  $K_\infty$  function  $\gamma(\cdot)$ , called gain function and constants  $k_x, k_u \in \mathbb{R}^+$  such that the response  $\mathbf{x}(t)$  exists and satisfies the following

$$\|\mathbf{x}(t)\| \leq \beta(\|\mathbf{x}(0)\|, t) + \gamma(\|\mathbf{u}\|_{L_\infty^m}) \quad (6.36)$$

$$\forall t \geq 0, \text{ input: } \forall \mathbf{u} \in \mathbb{R}^m \|\mathbf{u}\|_{L_\infty^m} < k_u \text{ and initial state: } \mathbf{x}(0) \in \mathbb{R}^n, \|\mathbf{x}(0)\| < k_x.$$

ISS can be characterized as a dissipation notion which is stated in terms of Lyapunov function called ISS Lyapunov function. With respect to this function two theorems are referred.

*Theorem 6.1* [218],[224],[225]:The system (6.35) is input-to-state stable if and only if there exists an ISS Lyapunov function.

*Theorem 6.2* [218], [224],[225]: A continuously differentiable function  $V : \mathbb{R}^n \rightarrow \mathbb{R}$  is said to be an ISS global Lyapunov function for the system (6.35), if and only if there exist class  $K_\infty$  functions  $\alpha_i, i=1,2,3$  and a class- $K$  function  $\chi$  such that following two conditions are satisfied.

$$\alpha_1(\|\mathbf{x}\|) \leq V(\mathbf{x}) \leq \alpha_2(\|\mathbf{x}\|), \forall \mathbf{x} \in \mathbb{R}^n \quad (6.37a)$$

$$\|\mathbf{x}\| \geq \chi(\|\mathbf{u}\|) \Rightarrow \dot{V}(\mathbf{x}, \mathbf{u}) \leq -\alpha_3(\|\mathbf{x}\|), \forall \mathbf{u} \in \mathbb{R}^m \quad (6.37b)$$

Based on input-to-state stability, sufficient condition for stability of a cascaded system is mentioned as follows

*Theorem 6.3*[218],[225]: For a cascaded system

$$\Pi_1 : \dot{\mathbf{x}}_1 = \mathbf{f}_1(\mathbf{x}_1, \mathbf{x}_2, \mathbf{u}) \quad (6.38a)$$

$$\Pi_2 : \dot{\mathbf{x}}_2 = \mathbf{f}_2(\mathbf{x}_2, \mathbf{u}) \quad (6.38b)$$

with  $\mathbf{f}_1 : \mathbb{R}^{n_1} \times \mathbb{R}^{n_2} \times \mathbb{R}^m \rightarrow \mathbb{R}^{n_1}$  and  $\mathbf{f}_2 : \mathbb{R}^{n_2} \times \mathbb{R}^m \rightarrow \mathbb{R}^{n_2}$  are locally Lipschitz in  $\mathbf{x}_1, \mathbf{x}_2, \mathbf{u}$  and  $\mathbf{x}_2, \mathbf{u}$  respectively. Both functions satisfy, if the system (6.38a) is globally ISS with  $\mathbf{x}_2, \mathbf{u}$  as input and the system (6.38b) is globally ISS with input  $\mathbf{u}$ , then composite cascaded system  $\Pi$  of (6.39), is globally ISS i.e.

$$\Pi : \mathbf{u} \rightarrow \begin{bmatrix} \mathbf{x}_1 \\ \mathbf{x}_2 \end{bmatrix} \quad (6.39)$$

It should be noted here that, (6.38a) and (6.38b) are called driven system and driving system respectively.

## 6.4 Controller Design

In this section, on the basis of formulaion of problem in section 6.2.3, an individual trajectory tracking controller is proposed for each AUV using the combination N-PID with BI and SMC. This control strategy has already been used in chapter 4 for designing a tracking controller for an AUV to track a specified reference path. Work in this chapter proposes set of such kind of controllers for  $n$  number of AUVs in a group. In this group, only GB tracks the specified path. Each follower AUV considers a generated trajectory (as discussed in section 6.2) as the equilibrium trajectory for tracking.

Considering the trajectory tracking error of  $k^{\text{th}}$  AUV as defined in eq.(6.32), the error dynamics is defined as

$$\mathbf{s}_k(t) = [s_{1k} \quad s_{2k} \quad s_{3k}]^T = \rho \mathbf{J}^T(\boldsymbol{\eta}_k) \mathbf{f}_{pk}(\boldsymbol{\eta}_{ke}) + \mathbf{v}_{ke} \quad (6.40)$$

where,  $\mathbf{f}_{pk} \in L(\boldsymbol{\alpha}_{pk}, \boldsymbol{\beta}_{pk}, \boldsymbol{\delta}_{pk}, \cdot)$  and  $\rho > 0$  is used to vary the control bandwidth of the system of AUV.  $\boldsymbol{\eta}_{ke} = (x_{ke}, y_{ke}, \theta_{ke}) \in \mathbb{R}^3$  and  $\mathbf{v}_{ke} = (u_{ke}, v_{ke}, \omega_{ke}) \in \mathbb{R}^3$  are errors in position vector in IRF and velocity vector in BRF of AUV respectively. Nonlinear function [202], [203] of position error instead of linear position error has been used in robot manipulators to get faster convergence of actual state to desired state.  $s_k(t) = 0$  represents a surface (nonlinear switching surface) in the state space of order one (as AUV dynamics is a second order system). A thin boundary layer  $B_{ik}(t)$  is assumed neighboring each surface  $s_{ik}(t) = 0$  and all boundary layers are represented by the following set

$$\mathbf{B}_k(t) = \{(\boldsymbol{\eta}_{ke}, \mathbf{v}_{ke}) : |x_{ke}| \leq \mu_{1k}, |y_{ke}| \leq \mu_{2k}, |\theta_{ke}| \leq \mu_{3k}; |s_{ki}| \leq \varphi_{ki}, \forall i = 1, 2, 3\} \in \mathfrak{R}^3 \quad (6.41)$$

where,  $\mu_{3k}$  and  $\varphi_{ki}, \forall i=1,2,3$  are strictly positive constants. Outside each boundary layer, a control law has to be chosen such that it satisfies  $\eta$ -reaching condition [210]. This condition ensures that boundary layer  $\mathbf{B}_k(t)$  always remain attractive. Consequently, this attractiveness guarantees that any trajectory starts inside  $\mathbf{B}_k(t=0)$ , always remain in it for  $t \geq 0$ . With this objective and based on the discussion in the introduction section, a tracking control law which is a combination of N-PID and continuous SMC is proposed as follows

$$\mathbf{F}_k = -K_{dk}\mathbf{f}_d(\mathbf{v}_{ke}) - \mathbf{J}^T(\boldsymbol{\eta}_k)K_{pk}\mathbf{f}_p(\boldsymbol{\eta}_{ke}) - K_{sk}\mathbf{f}_s(\mathbf{s}_k) - K_{wk}\mathbf{f}_w(\boldsymbol{\chi}_{ke}), \forall k=1,2,n \quad (6.42)$$

where,  $\boldsymbol{\chi}_{ke} = \int_0^t [\mathbf{v}_{ke}(\xi) + \rho \mathbf{J}^T(\boldsymbol{\eta}_k)\mathbf{f}_p(\boldsymbol{\eta}_{ke})]d\xi$  and parameters of different nonlinear CPDI function vectors  $\mathbf{f}_k(\mathbf{v}_{ke}), \mathbf{f}_k(\boldsymbol{\eta}_{ke}), \mathbf{f}_w(\boldsymbol{\chi}_{ke})$  are set following similar procedure as described in (3.7).

Switching functions are defined as  $\mathbf{f}_s(\cdot) = \left[ \tanh\left(\frac{s_{1k}}{\phi_{1k}}\right) \quad \tanh\left(\frac{s_{2k}}{\phi_{2k}}\right) \quad \tanh\left(\frac{s_{3k}}{\phi_{3k}}\right) \right]^T$

$K_{sk}, K_{wk}, K_{dk}, K_{pk}$  are  $3 \times 3$  order diagonal positive definite gain matrices.  $\mathbf{J}^T(\boldsymbol{\eta}_k)$  is used to convert the error quantity of control law to BRF of AUV. Every moment  $\mathbf{v}_{ke}$  can be estimated from the estimated states  $(\dot{\boldsymbol{\eta}}_{ke})$  in IRF with help of  $\mathbf{J}(\boldsymbol{\eta}_k)$ . First part of this controller is the velocity damping term, which is bounded through a nonlinear function  $\mathbf{f}_d(\mathbf{v}_{ke})$  and facilitates to provide asymptotic stability of the closed loop system of AUV. Second part uses a filtered position error feedback using  $\mathbf{f}_p(\boldsymbol{\eta}_{ke})$  to enhance the global stability. Third part involving  $\mathbf{f}_s(\mathbf{s}_k)$  is the switching control part of SMC which uses  $\tanh(\cdot)$  function defined in (4.1) to reduce chattering. Last part contributes a bounded output from an integral action similar to 3.6. A differentiable potential function and its gradient like defined in (3.9) may also defined for tracking control.

## 6.5 Closed Loop Dynamics of $k^{th}$ AUV in terms of Trajectory Tracking Error

The closed-loop system dynamics can be obtained by substituting (6.42) into (3.3) for  $k^{th}$  AUV as follows,

$$M\dot{\mathbf{v}}_{ke} + C(\mathbf{v}_k)\mathbf{v}_{ke} + D(\mathbf{v}_k)\mathbf{v}_{ke} + K_{dk}\mathbf{f}_d(\mathbf{v}_{ke}) + J^T(\boldsymbol{\eta}_k)K_{pk}\mathbf{f}_p(\boldsymbol{\eta}_{ke}) + K_{sk}\mathbf{f}_s(s_k) - \mathbf{f}_{hk}(\cdot) = -K_{wk}\mathbf{f}_w(\boldsymbol{\chi}_{ke}) \quad (6.43a)$$

$$\text{where, } \mathbf{f}_{hk}(\mathbf{v}_{kr}, \boldsymbol{\eta}_{ke}) = -M \frac{d}{dt} (J^T(\boldsymbol{\eta}_k)J_r(\boldsymbol{\eta}_{kr})\mathbf{v}_{kr}) - C(\mathbf{v}_k)J^T(\boldsymbol{\eta}_k)J_{kr}(\boldsymbol{\eta}_{kr})\mathbf{v}_{kr}$$

$$-D(\mathbf{v}_k)J^T(\boldsymbol{\eta}_k)J_r(\boldsymbol{\eta}_{kr})\mathbf{v}_{kr} = -M \frac{d}{dt} (J^T(\boldsymbol{\eta}_{ke})\mathbf{v}_{kr}) - C(\mathbf{v}_k)J^T(\boldsymbol{\eta}_{ke})\mathbf{v}_{kr} - D(\mathbf{v}_k)J^T(\boldsymbol{\eta}_{ke})\mathbf{v}_{kr}$$

$$\text{Replacing, } \mathbf{v}_k = \mathbf{v}_{ke} + J^T(\boldsymbol{\eta}_k)J_{kr}(\boldsymbol{\eta}_{kr})\mathbf{v}_{kr} = \mathbf{v}_{ke} + J^T(\boldsymbol{\eta}_{ke})\mathbf{v}_{kr} - D(\mathbf{v}_k)J^T(\boldsymbol{\eta}_{ke})\mathbf{v}_{kr}, \quad (6.43a)$$

can further be expressed as

$$M\dot{\mathbf{v}}_{ke} = - \left[ C(\mathbf{v}_{ke} + J^T(\boldsymbol{\eta}_{ke})\mathbf{v}_{kr})\mathbf{v}_{ke} + D(\mathbf{v}_k)\mathbf{v}_{ke} + K_{dk}\mathbf{f}_d(\mathbf{v}_{ke}) + J^T(\boldsymbol{\eta}_k)K_{pk}\mathbf{f}_p(\boldsymbol{\eta}_{ke}) + K_{sk}\mathbf{f}_s(s_k) \right] + \mathbf{f}_{hk}(\mathbf{v}_{kr}, \boldsymbol{\eta}_{ke}, \mathbf{v}_{ke}) \quad (6.43b)$$

$$\text{where, } \mathbf{f}_{hk}(\mathbf{v}_{kr}, \boldsymbol{\eta}_{ke}, \mathbf{v}_{ke}) = -M \frac{d}{dt} (J^T(\boldsymbol{\eta}_{ke})\mathbf{v}_{kr}) - C(J^T(\boldsymbol{\eta}_{ke})\mathbf{v}_{kr})(\mathbf{v}_{ke} + J^T(\boldsymbol{\eta}_{ke})\mathbf{v}_{kr}) - D(\mathbf{v}_k)J^T(\boldsymbol{\eta}_{ke})\mathbf{v}_{kr}$$

$$= - \left\{ M J^T(\boldsymbol{\eta}_{ke}) \frac{d}{dt} (\mathbf{v}_{kr}) + M (J^T(\boldsymbol{\eta}_{ke}))\mathbf{v}_{kr} + C(J^T(\boldsymbol{\eta}_{ke})\mathbf{v}_{kr})J^T(\boldsymbol{\eta}_{ke})\mathbf{v}_{kr} + C(J^T(\boldsymbol{\eta}_{ke})\mathbf{v}_{kr})\mathbf{v}_{ke} + D(\mathbf{v}_k)J^T(\boldsymbol{\eta}_{ke}, \mathbf{v}_{kr}) \right\}$$

(6.43b) can also be expressed as

$$\dot{\mathbf{v}}_{ke} = -M^{-1} \left[ C(\mathbf{v}_{ke} + J^T(\boldsymbol{\eta}_{ke})\mathbf{v}_{kr})\mathbf{v}_{ke} + D(\mathbf{v}_k)\mathbf{v}_{ke} + K_{dk}\mathbf{f}_d(\mathbf{v}_{ke}) + J^T(\boldsymbol{\eta}_k)K_{pk}\mathbf{f}_p(\boldsymbol{\eta}_{ke}) + K_{sk}\mathbf{f}_s(s_k) \right] + M^{-1}\mathbf{f}_{hk}(\boldsymbol{\eta}_{ke}, \mathbf{v}_{ke}, \mathbf{v}_{kr}, \dot{\mathbf{v}}_{kr}) \quad (6.44)$$

Finally, assuming input  $\mathbf{u}_k = -\mathbf{v}_{kr} \in \mathbb{R}^3$  system (6.44) can be expressed for the state

$$\mathbf{x}_k = (\mathbf{x}'_k \quad \mathbf{x}''_k) \in (\mathbf{v}_{ke}, \boldsymbol{\eta}_{ke}) \in \mathbb{R}^6 \text{ as}$$



$$\Rightarrow \dot{\mathbf{v}}_{ke} = \mathbf{f}_{1k}(\mathbf{x}_k, \mathbf{u}_k, \dot{\mathbf{u}}_k) \in \mathbb{R}^3 \Rightarrow \dot{\mathbf{x}}'_k = \mathbf{f}_{1k}(\mathbf{x}_k, \mathbf{u}_k, \dot{\mathbf{u}}_k) \in \mathbb{R}^3 \quad (6.45)$$

where,  $\mathbf{f}_{hk}(\mathbf{u}_k, \dot{\mathbf{u}}_k, \boldsymbol{\eta}_{ke}, \mathbf{v}_{ke}) =$

$$= \mathbf{M}\mathbf{J}^T(\boldsymbol{\eta}_{ke})\dot{\mathbf{u}}_k + \left\{ \mathbf{M}\left(\dot{\mathbf{J}}^T(\boldsymbol{\eta}_{ke})\right) + \mathbf{C}\left(\mathbf{J}^T(\boldsymbol{\eta}_{ke})\mathbf{v}_{ke}\right) + \mathbf{D}(\mathbf{v}_k)\mathbf{J}^T(\boldsymbol{\eta}_{ke}) - \mathbf{C}\left(\mathbf{J}^T(\boldsymbol{\eta}_{ke})\mathbf{u}_k\right)\mathbf{J}^T(\boldsymbol{\eta}_{ke}) \right\} \mathbf{u}_k$$

Relative body fixed linear velocities between  $k^{\text{th}}$  AUV and its reference AUV is expressed as

$$\mathbf{v}_{1ke} = \mathbf{v}_{1k} - \mathbf{J}^T(\boldsymbol{\eta}_k)\mathbf{J}(\boldsymbol{\eta}_{kr})\mathbf{v}_{1kr} = \mathbf{Q}^T(\boldsymbol{\eta}_k)(\dot{\boldsymbol{\eta}}_{1k} - \dot{\boldsymbol{\eta}}_{1r}) = \mathbf{Q}^T(\boldsymbol{\eta}_k)\dot{\boldsymbol{\eta}}_{1e} \Rightarrow \dot{\boldsymbol{\eta}}_{1ke} = \mathbf{Q}^T(\boldsymbol{\eta}_{ke} + \boldsymbol{\eta}_{kr})\mathbf{v}_{1ke} \quad (6.46a)$$

where, expression of  $\mathbf{Q}$  is mentioned in section 3.2.

Relative angular velocities between  $k^{\text{th}}$  AUV and its reference AUV is expressed as

$$\dot{\boldsymbol{\eta}}_{2ke} = \mathbf{v}_{2ke} \quad (6.46b)$$

Combining both (6.46a) and (6.46b) one gets final expression

$$\dot{\mathbf{x}}''_k = \mathbf{f}_{2k}(\mathbf{x}_k, \boldsymbol{\ell}_k) \in \mathbb{R}^3, \text{ where, } \boldsymbol{\ell}_k = -\boldsymbol{\eta}_{kr} \quad (6.47)$$

Combining (6.45) and (6.47), the closed-loop system of  $k^{\text{th}}$  AUV may be described finally as

$$\dot{\mathbf{x}}_k = \mathbf{f}_k(\mathbf{x}_k, \mathbf{U}_k, \dot{\mathbf{U}}_k) \in \mathbb{R}^6, \text{ where, } \mathbf{U}_k = (-\mathbf{v}_{kr}, -\boldsymbol{\eta}_{kr}) = (\mathbf{u}_k, \boldsymbol{\ell}_k) \in \mathbb{R}^6 \quad (6.48)$$

## 6.6 Stability Analysis

Consider a group on  $n$  number of AUVs under the Assumptions 6.1, and control law for group is proposed as eq (6.37). In the motion control problem of this group, state of neighbours of each AUV facilitates the AUV to determine its desired position. Moreover, each AUV in this group acts as a subsystem in a cascaded system where driven and driving systems are  $k^{\text{th}}$  AUV and its neighbour  $(k-1)^{\text{th}}$  AUV (in case of first follower) or  $(k-1)^{\text{th}}$  and  $(k-2)^{\text{th}}$  AUV (for other follower) respectively. Hence, the objective of stability analysis is to ensure stable formation tracking corresponding to stable trajectory tracking of GB. The stability of this formation tracking problem is analysed based on input to state stability and cascaded system stability. Before going

to develop the main results of stability, it is intended to express the input to the driven system in terms of state and input variables of the driving system for a particular pair of cascaded system. For particular case of triangular formation of three AUVs namely global leader, first follower and ordinary follower-1 two individual cascaded systems exists. One is in between GB (driving) and FF (driven), whereas second one is in between Ordinary Follower ( $k=1$ ) called OF-1(driven) and GB and FF (both are driving OF-1).

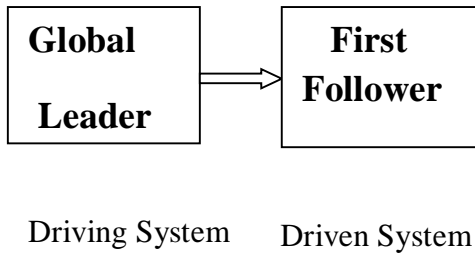


Fig. 6.4 Cascaded System of GB and FF

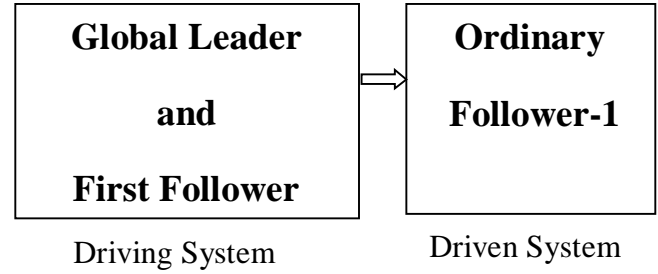


Fig. 6.5 Cascaded System of GB and FF with OF

Our goal is to prove stability of three systems individually; global input-to-state stability of GB w.r.t its input, global input-state stability of FF with respect to its input from GB, global input-to-state stability of OF with respect to its input from GB and FF both. Subsequently, we prove the global stability of combined system of GB, FF and OF-1 w.r.t input of GB.

Next, for the cascaded pair combining GB (driving system) and FF (driven system), the expression of input to FF in terms of input to GB state of GB and FF both; is developed.

*Lemma 6.1:* From 6.17 and 6.18, it can be concluded that

$$\eta_{12r} = \eta_{12} \pm \left\{ \|\eta_{11} - \eta_{12}\| - l_{21}^d \right\} \frac{(\eta_{11} - \eta_{12})}{\|\eta_{11} - \eta_{12}\|} \quad (6.49)$$

Taking derivative of both sides of (6.49) and rearranging the equations one can prove that

$$\mathbf{v}_{2r} = J(\eta_{2r}) \mathbb{C}_1 J^T(\eta_2) \mathbf{v}_{2e} + J(\eta_{2r}) \mathbb{C}_2 J^T(\eta_1) \mathbf{v}_{1e} + J(\eta_{2r}) \mathbb{C}_3 J^T(\eta_{1r}) \mathbf{v}_{1r} \quad (6.50)$$

where,  $\mathbb{C}_1 = \text{diag}[(\pm 1 - 1) \quad (\pm 1 - 1) \quad 0]$ ,  $\mathbb{C}_2 = \text{diag}[1 \quad 1 \quad 1]$ ,  $\mathbb{C}_3 = \text{diag}[1 \quad 1 \quad 1]$

Proof: From (6.49) one may write

$$-\boldsymbol{\eta}_{12e} = \pm \left\{ \frac{\|\boldsymbol{\eta}_{11} - \boldsymbol{\eta}_{12}\| - l_{21}^d}{\|\boldsymbol{\eta}_{11} - \boldsymbol{\eta}_{12}\|} \right\} (\boldsymbol{\eta}_{11} - \boldsymbol{\eta}_{12}) \quad (6.51a)$$

Taking derivative of both sides of (6.51a) with respect to time, one may obtain using (6.32)

$$-\dot{\boldsymbol{\eta}}_{12e} = \pm \left\{ \frac{\|\boldsymbol{\eta}_{11} - \boldsymbol{\eta}_{12e} - \boldsymbol{\eta}_{12r}\| - l_{21}^d}{\|\boldsymbol{\eta}_{11} - \boldsymbol{\eta}_{12e} - \boldsymbol{\eta}_{12r}\|} + \frac{l_{21}^d}{\|\boldsymbol{\eta}_{11} - \boldsymbol{\eta}_{12e} - \boldsymbol{\eta}_{12r}\|} \right\} (\dot{\boldsymbol{\eta}}_{11} - \dot{\boldsymbol{\eta}}_{12e} - \dot{\boldsymbol{\eta}}_{12r}) \quad (6.51b)$$

$$\dot{\boldsymbol{\eta}}_{12r} = (\pm 1 - 1) \dot{\boldsymbol{\eta}}_{12e} + \dot{\boldsymbol{\eta}}_{11e} + \dot{\boldsymbol{\eta}}_{11r} \quad (6.52a)$$

Regarding angular position of leader, (6.20) can be written with the help of (6.32) as,

$$\boldsymbol{\eta}_{22r} = \boldsymbol{\eta}_{21} = \boldsymbol{\eta}_{21e} + \boldsymbol{\eta}_{21r} \Rightarrow \dot{\boldsymbol{\eta}}_{22r} = \dot{\boldsymbol{\eta}}_{21e} + \dot{\boldsymbol{\eta}}_{21r} \quad (6.52b)$$

Combining (6.52a) and (6.52b),

$$\dot{\boldsymbol{\eta}}_{2r} = \mathbb{C}_1 \dot{\boldsymbol{\eta}}_{2e} + \mathbb{C}_2 \dot{\boldsymbol{\eta}}_{1e} + \mathbb{C}_3 \dot{\boldsymbol{\eta}}_{1r} \quad (6.53a)$$

Converting quantities in IRM to BRM for both sides of (6.53a), expression of (6.50) is proved as,

$$\begin{aligned} \mathbf{v}_{2r} &= J(\boldsymbol{\eta}_{2r}) \mathbb{C}_1 J^T(\boldsymbol{\eta}_{2e}) \mathbf{v}_{2e} + J(\boldsymbol{\eta}_{2r}) \mathbb{C}_2 J^T(\boldsymbol{\eta}_{1e}) \mathbf{v}_{1e} + J(\boldsymbol{\eta}_{2r}) \mathbb{C}_3 J^T(\boldsymbol{\eta}_{1r}) \mathbf{v}_{1r} \\ &= J(\boldsymbol{\eta}_{2r}) \mathbb{C}_1 J^T(\boldsymbol{\eta}_{2e} + \boldsymbol{\eta}_{2r}) \mathbf{v}_{2e} + J(\boldsymbol{\eta}_{2r}) \mathbb{C}_2 J^T(\boldsymbol{\eta}_{1e} + \boldsymbol{\eta}_{1r}) \mathbf{v}_{1e} + J(\boldsymbol{\eta}_{2r}) \mathbb{C}_3 J^T(\boldsymbol{\eta}_{1r}) \mathbf{v}_{1r} \end{aligned}$$

Assuming desired velocities as input as discussed previously one may reach to

$$\mathbf{v}_{2r} = \mathbf{f}_{32}(\mathbf{x}_1, \mathbf{x}_2, \mathbf{u}_1, \mathbf{u}_2) \quad (6.53b)$$

where,  $\mathbf{x}_2 = (\boldsymbol{\eta}_{2e}, \mathbf{v}_{2e}) \in \mathbb{R}^6$ .

Combining (6.45) and (6.48) for  $k=2$  and (6.53b), the system of FF is expressed as a combination

of three functions  $\dot{\mathbf{x}}_2' = \mathbf{f}_{12}(\mathbf{x}_2, \mathbf{u}_2, \dot{\mathbf{u}}_2) \in \mathbb{R}^3$ ,  $\dot{\mathbf{x}}_2'' = \mathbf{f}_{22}(\mathbf{x}_2, \ell_2) \in \mathbb{R}^3$  and  $\mathbf{v}_{2r} = \mathbf{f}_{32}(\mathbf{x}_1, \mathbf{x}_2, \mathbf{u}_1, \mathbf{u}_2)$ ,

as

$$\dot{\mathbf{x}}_2 = \mathbf{f}_2(\mathbf{x}_1, \mathbf{x}_2, \mathbf{U}_1, \mathbf{U}_2, \dot{\mathbf{U}}_2) \quad (6.54)$$

The following Lemma develops the expression of input to OF-1 in terms of input to GB, state of FF, GB and OF-1.

*Lemma 6.2:* Based on the equations (6.23)-(6.28) one can convert the the dynamics of Ordinary Follower-1 AUV in terms of states of first follower and global leader AUV and their inputs as

$$\dot{\mathbf{x}}_3 = \mathbf{f}_3(\mathbf{x}_1, \mathbf{x}_2, \mathbf{x}_3, \mathbf{U}_1, \mathbf{U}_2, \mathbf{U}_3, \dot{\mathbf{U}}_3) \quad (6.55a)$$

$\mathbf{x}_3 \in \mathbb{R}^6$  and  $\mathbf{U}_3 \in \mathbb{R}^3$  are states and inputs of ordinary follower-1. As the input of first follower may be expressed in terms inputs and states of global leader (6.55a) can be converted to

$$\dot{\mathbf{x}}_3 = \mathbf{f}_3(\mathbf{x}_1, \mathbf{x}_2, \mathbf{x}_3, \mathbf{U}_1, \mathbf{U}_3, \dot{\mathbf{U}}_3) \quad (6.55b)$$

Next theorem proves the global input-to-state stability of GB with respect to its desired input.

*Theorem 6.4:* Consider the closed-loop system (6.48) for  $k=1$  i.e.dynamics of global leader is

$$\dot{\mathbf{x}}_k = \mathbf{f}_1(\mathbf{x}_1, \mathbf{U}_1, \dot{\mathbf{U}}_1) \in \mathbb{R}^6, \text{ where } \mathbf{U}_1 = (-\mathbf{v}_{1r}, -\boldsymbol{\eta}_{1r}) = (\mathbf{u}_1, \boldsymbol{\ell}_1) \in \mathbb{R}^6 \quad (6.56)$$

with state  $\mathbf{x}_1 \in \mathbb{R}^6$  and locally essentially bounded input  $\mathbf{U}_1 \in \mathbb{R}^6$  and its derivatives in which

$\mathbf{f}(0,0,0)=0$  and  $\mathbf{f}_1(\mathbf{x}_1, \mathbf{U}_1, \dot{\mathbf{U}}_1)$  is locally Lipschitz on  $\mathbb{R}^6 \times \mathbb{R}^6 \times \mathbb{R}^6$ . Corresponding to

boundary layer

$$\mathbf{B}_1(t) = \{(\boldsymbol{\eta}_{1e}, \mathbf{v}_{1e}) : |x_{1e}| \leq \mu_{11}, |y_{1e}| \leq \mu_{21}, |\theta_{1e}| \leq \mu_{31}, |s_{1i}| \leq \varphi_{1i}, \forall i = 1, 2, 3\} \in \mathbb{R}^3$$

with respect to proposed Sliding Mode Nonlinear PID controller with BI and BD for global

leader, assume the following set  $H_1$  and  $H_2$  as  $H_1 = \{\|\mathbf{x}_1(0)\|_{max} : \|\mathbf{s}_1\|_{max}\}, H_2 = \{\|\mathbf{x}_{1b}\| : \|\mathbf{s}_1\|_{min}\},$

where,  $\|\mathbf{x}_{lb}\|$  is the value of  $\|\mathbf{x}_1(t)\|$  at the boundary of the sliding surface  $\mathbf{B}_1(t)$ . There exist gain matrices  $K_{d1}, K_{p1}, K_{w1}, K_{s1}$  such that Lemma 4.1 holds w.r.t. boundary layer  $\mathbf{B}_1(t)$  and following inequalities are satisfied,

$$i) \lambda_{\min} \{K_{p1}\} \rho_{\min}^p > \frac{\rho}{2} \lambda_{\max} \{M\} \quad (6.57a)$$

$$\begin{aligned} ii) \frac{P_2}{\sqrt{3}} + \lambda_{\min} \{D(\mathbf{v}_1)\} &\geq \rho \left( \sqrt{3} \delta_{pmax} \beta_{pmax} + \frac{1}{2} C_{max} V_{max} \right) + \frac{\rho}{2} \lambda_{\max} \{D(\mathbf{v}_1)\} \\ &+ \rho \frac{\lambda_{\max} \{K_{d1}\}}{2} \sigma_{2d} + \frac{1}{2} \lambda_{\max} \{M\} \omega_{max} + \rho \delta_{pmax} \lambda_{\max} \{M\} + \frac{1}{2} \lambda_{\max} \{D(\mathbf{v}_1)\} + N \|\mathbf{s}_1\|_{max} \end{aligned} \quad (6.57b)$$

where,  $P_2 = \lambda_{\min} \{K_{d1}\} \min_i \{\alpha_{di} \beta_{di}\}$ .

$$\begin{aligned} iii) P_1 + \lambda_{\min} \{D(\mathbf{v}_1)\} &\geq \rho \left( \sqrt{3} \delta_{pmax} \beta_{pmax} + \frac{1}{2} C_{max} V_{max} \right) + \frac{\rho}{2} \lambda_{\max} \{D(\mathbf{v}_1)\} \\ &+ \rho \frac{\lambda_{\max} \{K_{d1}\}}{2} \sigma_{2d} + \frac{1}{2} \lambda_{\max} \{M\} \omega_{max} + \rho \delta_{pmax} \lambda_{\max} \{M\} + \frac{1}{2} \lambda_{\max} \{D(\mathbf{v}_1)\} + N \|\mathbf{s}_1\|_{max} \end{aligned} \quad (6.57c)$$

where,  $P_1 = \lambda_{\min} \{K_{d1}\} \alpha_{dmin}$ .

$$iv) \lambda_{\min} \{K_{p1}\} \geq \frac{1}{2} C_{max} V_{max} + \frac{\lambda_{\max} \{K_{d1}\}}{2} + \frac{\lambda_{\max} \{D(\mathbf{v}_1)\}}{2} + \frac{\lambda_{\max} \{M\}}{2} \omega_{max} \quad (6.57d)$$

$$v) \min_i (K_{s1i}) \geq \lambda_{\max} (C_i) V_{1max}^2 + \max_i (h_{1imax}) + \frac{1}{2} \lambda_{\max} \{D(\mathbf{v}_1)\} + \max_i (K_{w1i}) \sqrt{3} \delta_{wmax} \beta_{wmax} \quad (6.57e)$$

then the system of global leader becomes globally input-to-state stable [225] with respect to its input  $\mathbf{U}_1 = (\mathbf{v}_{1r}, 0, 0, 0) \in \mathbb{R}^6$  and state  $\mathbf{x}_1(t) \in \mathbb{R}^6$  remains bounded below as  $\|\mathbf{x}_1(t)\| \leq \|\mathbf{x}_{lb}(t)\|$  for  $t \geq 0$ .

**Proof:** To verify input-to-state stability for the closed-loop system (6.48) with input  $\mathbf{U}_1$ , following ISS Lyapunov function is chosen

$$V_1(\mathbf{v}_{1e}, \boldsymbol{\eta}_{1e}) = \frac{1}{2} \mathbf{v}_{1e}^T M \mathbf{v}_{1e} + \rho \mathbf{f}_p^T(\boldsymbol{\eta}_{1e}) J(\boldsymbol{\eta}) M \mathbf{v}_{1e} + \sum_{i=1}^3 \int_0^{\eta_e(i)} f_{pi}^T(\boldsymbol{\eta}_{1e}(i)) K_{pli} d\boldsymbol{\eta}_{1e}(i) \quad (6.58)$$

which satisfies the following inequality for upper and lower limit of  $V_1$

$$\alpha_{11}(\|\mathbf{x}_1\|) \leq V(\|\mathbf{x}_1\|) \leq \alpha_{21}(\|\mathbf{x}_1\|), \mathbf{x}_1 = (\mathbf{x}_{11}, \mathbf{x}_{21}) \in (\mathbf{v}_{1e}, \boldsymbol{\eta}_{1e}) \in \mathbb{R}^6 \quad (6.59)$$

where,  $\alpha_{11}$  and  $\alpha_{21}$  are  $K_\infty$  functions given as

$$\begin{aligned} \alpha_{11}(\|\mathbf{x}_1\|) &= \frac{1}{2} \lambda_{\min}\{M\} \|\mathbf{v}_{1e}\|^2 - \frac{\rho}{2} \lambda_{\max}\{M\} \|\mathbf{f}_p(\boldsymbol{\eta}_{1e})\|^2 - \frac{\rho}{2} \lambda_{\max}\{M\} \|\mathbf{v}_{1e}\|^2 + \lambda_{\min}\{K_{p1}\} \wp_{\min}^p \|\mathbf{f}_p(\boldsymbol{\eta}_{1e})\|^2 \\ \Rightarrow \alpha_{11}(\|\mathbf{x}_1\|) &= \frac{1}{2} (\lambda_{\min}\{M\} - \rho \lambda_{\max}\{M\}) \|\mathbf{v}_{1e}\|^2 + \left( \lambda_{\min}\{K_{p1}\} \wp_{\min}^p - \frac{\rho}{2} \lambda_{\max}\{M\} \right) \sigma_{1p} \|\boldsymbol{\eta}_{1e}\|^2, \\ \Rightarrow \alpha_{11}(\|\mathbf{x}_1\|) &= \hat{\lambda}_1 \|\mathbf{x}_1\|^2 \end{aligned} \quad (6.60a)$$

where,  $\hat{\lambda}_1 = \lambda_{\min}[\text{diag}[Z_1 \quad Z_1 \quad Z_1 \quad Z_2 \quad Z_2 \quad Z_2]]$  and  $Z_1 = \frac{1}{2} (\lambda_{\min}\{M\} - \rho \lambda_{\max}\{M\})$ ,  
 $Z_2 = \left( \lambda_{\min}\{K_{p1}\} \wp_{\min}^p - \frac{\rho}{2} \lambda_{\max}\{M\} \right) \sigma_{1p}$ .

Thus, upper limit of  $V_1$  is expressed as follows

For,  $|\boldsymbol{\eta}_{1e}(i)| \leq 1, \forall i, \frac{1}{\sqrt{3}} \|\boldsymbol{\eta}_{1e}\|^2 \leq \|\boldsymbol{\eta}_{1e}\|$ , and  $\frac{1}{\sqrt{3}} \|\mathbf{v}_{1e}\|^2 \leq \|\mathbf{v}_{1e}\|$  as  $|\mathbf{v}_{1e}(i)| \leq 1, \forall i$

$$\begin{aligned} \alpha_{21}(\|\mathbf{x}_1\|) &= \frac{1}{2} \left( \lambda_{\max}\{M\} + \frac{\rho}{2} \lambda_{\max}\{M\} \right) \sqrt{3} \|\mathbf{v}_{1e}\| + \frac{\rho}{2} \lambda_{\max}\{M\} \sigma_{2p} \sqrt{3} \|\boldsymbol{\eta}_{1e}\| + \lambda_{\max}\{K_{p1}\} \max_i \left( |\delta_{pi} \beta_{pi}| \right) \|\boldsymbol{\eta}_{1e}\| \end{aligned} \quad (6.60b)$$

Thus,

$$\alpha_{21}(\|\mathbf{x}_1\|) = \mathbb{Q}_1 \|\mathbf{v}_{1e}\| + \mathbb{Q}_2 \|\boldsymbol{\eta}_{1e}\| = \Omega \|\mathbf{x}_1\|. \quad (6.60b.1)$$

where,  $\Omega = \sqrt{\lambda_{\max}[\text{diag}[\ell'_1 \quad \ell'_1 \quad \ell'_1 \quad \ell'_2 \quad \ell'_2 \quad \ell'_2]]}$ ,  $\ell'_1 = \mathbb{Q}_1^2 + \mathbb{Q}_1 \mathbb{Q}_2$ ,  $\ell'_2 = \mathbb{Q}_2^2 + \mathbb{Q}_1 \mathbb{Q}_2$  and

$$\mathbb{Q}_1 = \frac{\sqrt{3}}{2} \left( \lambda_{\max}\{M\} + \frac{\rho}{2} \lambda_{\max}\{M\} \right), \mathbb{Q}_2 = \frac{\sqrt{3}}{2} \rho \lambda_{\max}\{M\} \sigma_{2p} + \lambda_{\max}\{K_{p1}\} \max_i \left( |\delta_{pi} \beta_{pi}| \right)$$

For,  $|\boldsymbol{\eta}_{1e}(i)| > 1, \forall i$

$$\alpha_{21}(\|\mathbf{x}_1\|) = \frac{1}{2} \left( \lambda_{\max}\{M\} + \frac{\rho}{2} \lambda_{\max}\{M\} \right) \|\mathbf{v}_{1e}\|^2 + \frac{\rho}{2} \lambda_{\max}\{M\} \sigma_{2p} \|\boldsymbol{\eta}_{1e}\|^2 + \lambda_{\max}\{K_{p1}\} \max_i \left( |\delta_{pi} \beta_{pi}| \right) \|\boldsymbol{\eta}_{1e}\| \Rightarrow$$

$$\alpha_{21}(\|\mathbf{x}_1\|) = \frac{1}{2} \left( \lambda_{\max}\{M\} + \frac{\rho}{2} \lambda_{\max}\{M\} \right) \|\mathbf{v}_{1e}\|^2 + \left( \frac{\rho}{2} \lambda_{\max}\{M\} \sigma_{2p} + \lambda_{\max}\{K_{p1}\} \max_i \left( \|\delta_{pi} \beta_{pi}\| \right) \right) \|\boldsymbol{\eta}_{1e}\|^2 \quad (6.60b.2)$$

From (6.60b) it is concluded that

$$\Rightarrow \alpha_{21}(\|\mathbf{x}_1\|) = \bar{h}_1 \|\mathbf{x}_1\|^2 \quad (6.60c)$$

where,  $\bar{h}_1 = \lambda_{\max}[\text{diag}[Y_1 \quad Y_1 \quad Y_1 \quad Y_2 \quad Y_2 \quad Y_2]]$  and  $Y_1 = \frac{1}{2} \left( \lambda_{\max}\{M\} + \frac{\rho}{2} \lambda_{\max}\{M\} \right)$ ,

$$Y_2 = \frac{\rho}{2} \lambda_{\max}\{M\} \sigma_{2p} + \lambda_{\max}\{K_{p1}\} \max_i \left( \|\delta_{pi} \beta_{pi}\| \right).$$

Taking derivative of  $V_1$  with respect to time one gets,

$$\begin{aligned} \dot{V}_1 &= (\mathbf{v}_{1e} + \rho J(\boldsymbol{\eta}_1) \mathbf{f}_p(\boldsymbol{\eta}_{1e}))^T M \dot{\mathbf{v}}_{1e} + \rho \dot{\mathbf{f}}_p^T(\boldsymbol{\eta}_{1e}) J(\boldsymbol{\eta}_1) M \mathbf{v}_{1e} + \rho \mathbf{f}_p^T(\boldsymbol{\eta}_{1e}) \dot{J}(\boldsymbol{\eta}_1) M \mathbf{v}_{1e} + \mathbf{v}_{1e}^T J^T(\boldsymbol{\eta}_1) K_{p1} \mathbf{f}_p(\boldsymbol{\eta}_{1e}) \\ &\Rightarrow \dot{V} = (\mathbf{v}_{1e} + \rho J(\boldsymbol{\eta}_1) \mathbf{f}_p(\boldsymbol{\eta}_{1e}))^T (-C(\mathbf{v}_1) \mathbf{v}_{1e} - D(\mathbf{v}_1) \mathbf{v}_{1e} - K_{d1} \mathbf{f}_d(\mathbf{v}_{1e}) - J^T(\boldsymbol{\eta}_1) K_{p1} \mathbf{f}_p(\boldsymbol{\eta}_{1e}) - K_{s1} \mathbf{f}_s(s) - K_{w1} \mathbf{f}_w(\boldsymbol{\chi}_{1e})) \\ &\quad + \rho \dot{\mathbf{f}}_p^T(\boldsymbol{\eta}_{1e}) J(\boldsymbol{\eta}_1) M \mathbf{v}_{1e} + \rho \mathbf{f}_p^T(\boldsymbol{\eta}_{1e}) \dot{J}(\boldsymbol{\eta}_1) M \mathbf{v}_{1e} + (\mathbf{v}_{1e} + \rho J(\boldsymbol{\eta}_1) \mathbf{f}_p(\boldsymbol{\eta}_{1e}))^T \mathbf{f}_{h1}(\mathbf{u}_1, \dot{\mathbf{u}}_1, \boldsymbol{\eta}_{1e}, \mathbf{v}_{1e}) + \mathbf{v}_{1e}^T J^T(\boldsymbol{\eta}_1) K_{p1} \mathbf{f}_p(\boldsymbol{\eta}_{1e}) \end{aligned} \quad (6.61)$$

Using Property 3.4

$$\begin{aligned} \Rightarrow \dot{V}_1 &= - \left[ \mathbf{v}_{1e}^T D(\mathbf{v}_1) \mathbf{v}_{1e} + \mathbf{v}_{1e}^T K_{d1} \mathbf{f}_d(\mathbf{v}_{1e}) \right. \\ &\quad + \rho \left\{ \mathbf{f}_p^T(\boldsymbol{\eta}_{1e}) J(\boldsymbol{\eta}_1) C(\mathbf{v}_1) \mathbf{v}_{1e} + \mathbf{f}_p^T(\boldsymbol{\eta}_{1e}) J(\boldsymbol{\eta}_1) D(\mathbf{v}_1) \mathbf{v}_{1e} + \mathbf{f}_p^T(\boldsymbol{\eta}_{1e}) J(\boldsymbol{\eta}_1) K_{d1} \mathbf{f}_d(\mathbf{v}_{1e}) + \mathbf{f}_p^T(\boldsymbol{\eta}_{1e}) J(\boldsymbol{\eta}_1) J^T(\boldsymbol{\eta}_1) K_{p1} \mathbf{f}_p(\boldsymbol{\eta}_{1e}) \right\} \\ &\quad - \rho \dot{\mathbf{f}}_p^T(\boldsymbol{\eta}_{1e}) J(\boldsymbol{\eta}_1) M \mathbf{v}_{1e} - \rho \mathbf{f}_p^T(\boldsymbol{\eta}_{1e}) \dot{J}(\boldsymbol{\eta}_1) M \mathbf{v}_{1e} \left. \right] - \mathbf{s}^T K_w \mathbf{f}_w(\boldsymbol{\chi}_{1e}) \\ &\quad - \mathbf{s}^T K_s \mathbf{f}_s(s) + \mathbf{s}^T \left( M J^T(\boldsymbol{\eta}_{1e}) \dot{\mathbf{u}}_1 + \left\{ M \left( \dot{J}^T(\boldsymbol{\eta}_{1e}) \right) + C \left( J^T(\boldsymbol{\eta}_{1e}) \mathbf{v}_{1e} \right) + D(\mathbf{v}_1) J^T(\boldsymbol{\eta}_{1e}) - C \left( J^T(\boldsymbol{\eta}_{1e}) \mathbf{u}_1 \right) J^T(\boldsymbol{\eta}_{1e}) \right\} \mathbf{u}_1 \right) \end{aligned} \quad (6.62)$$

With the help of eq (4.37), in the domain  $\Delta_1 = \{\mathbf{v}_{1e} : V_{1\max} \geq \|\mathbf{v}_{1e}\| > \|\boldsymbol{\beta}_d\|\}$ , using (4.20-4.21), (4.23-4.28), (4.31-4.32a), (4.33), following Appendix A.6 and A.3 and replacing  $\mathbf{h}_1 = -M J^T(\boldsymbol{\eta}_{1e}) \dot{\mathbf{u}}_1$  and

$$\mathbf{s}_1^T C \left( J^T(\boldsymbol{\eta}_{1e}) \mathbf{u}_1 \right) J^T(\boldsymbol{\eta}_{1e}) \mathbf{u}_1 \geq - \sum_{i=1}^3 \lambda_{\max}(C_i) \|\mathbf{u}_1\|^2 |s_{1i}|$$

$$\begin{aligned} \dot{V}_1 &= - \left\{ \lambda_{\min}\{D(\mathbf{v}_1)\} \|\mathbf{v}_{1e}\|^2 + P_2 \|\mathbf{v}_{1e}\| \right. \\ &\quad \left. - \rho \left( \sqrt{3} \delta_{p\max} \beta_{p\max} C_{\max} \|\mathbf{v}_{1e}\|^2 + \frac{1}{2} C_{\max} V_{\max} \left( \|\mathbf{v}_{1e}\|^2 + \|\mathbf{f}_p(\boldsymbol{\eta}_{1e})\|^2 \right) \right) - \rho \lambda_{\max}\{D(\mathbf{v}_1)\} \frac{1}{2} \left( \|\mathbf{f}_p(\boldsymbol{\eta}_{1e})\|^2 + \|\mathbf{v}_{1e}\|^2 \right) \right. \end{aligned}$$

$$\begin{aligned}
& -\rho\lambda_{\max}\{K_{d1}\}\frac{1}{2}\left(\|\mathbf{f}_p(\boldsymbol{\eta}_{1e})\|^2 + \sigma_{2d}\|\mathbf{v}_{1e}\|^2\right) + \rho\lambda_{\min}\{K_{p1}\}\|\mathbf{f}_p(\boldsymbol{\eta}_{1e})\|^2 - \rho\delta_{p\max}\lambda_{\max}\{M\}\|\mathbf{v}_{1e}\|^2 \\
& -\rho\frac{1}{2}\lambda_{\max}\{M\}\omega_{\max}\left(\|\mathbf{f}_p(\boldsymbol{\eta}_{1e})\|^2 + \|\mathbf{v}_{1e}\|^2\right) - \left(\sum_{i=1}^3(K_{sli} - K_{wi}|f_{wi}(\chi_{1ei})| - \lambda_{\max}\{C_i\}\|\mathbf{u}_1\|^2 - h_{imax})|s_{li}|\right) \\
& + \left\{(C_{\max}\|\mathbf{v}_{1e}\| + \lambda_{\max}\{D(\mathbf{v}_1)\} + \lambda_{\max}\{M\}\|\mathbf{v}_{1e}\|)\|\mathbf{u}_1\|\right\}\|\mathbf{s}_1\|
\end{aligned} \tag{6.63a}$$

If linear and angular velocities are assumed to be set at less than unity, one gets  $\frac{1}{\sqrt{3}}\|\mathbf{v}_{1e}\|^2 \leq \|\mathbf{v}_{1e}\|$ .

Thus, eq (6.63a) can further be expressed as follows

$$\begin{aligned}
\Rightarrow \dot{V}_1 = & -\left\{A'_1 + \frac{P_2}{\sqrt{3}} - N\|\mathbf{s}_1\|_{\max} - \frac{1}{2}\lambda_{\max}\{D(\mathbf{v}_1)\}\right\}\|\mathbf{v}_{1e}\|^2 + \rho B\|\mathbf{f}_p(\boldsymbol{\eta}_{1e})\|^2 - \frac{1}{2}\lambda_{\max}\{D(\mathbf{v}_1)\}\|\mathbf{s}_1\|^2 \\
& + \left\{\sum_{i=1}^3(K_{sli} - K_{wi}|f_{wi}(\chi_{1ei})| - \lambda_{\max}\{C_i\}\|\mathbf{u}_1\|^2 - h_{imax})|s_{li}|\right\} - \left\{\frac{1}{2}\lambda_{\max}\{D(\mathbf{v}_1)\} + \frac{1}{2}N\|\mathbf{s}_1\|_{\max}\right\}\|\mathbf{u}_1\|^2
\end{aligned} \tag{6.63b}$$

$$\begin{aligned}
\text{where, } A'_1 = & \left\{(\lambda_{\min}\{D(\mathbf{v}_1)\} - \rho\left(\sqrt{3}\delta_{p\max}\beta_{p\max}C_{\max} + \frac{1}{2}C_{\max}V_{\max}\right) - \frac{\rho\lambda_{\max}\{D(\mathbf{v}_1)\}}{2}\right. \\
& \left. - \frac{\rho\lambda_{\max}\{K_{d1}\}\sigma_{2d}}{2} - \rho\frac{1}{2}\lambda_{\max}\{M\}\omega_{\max} - \rho\delta_{p\max}\lambda_{\max}\{M\}\right\} \\
B = & \lambda_{\min}\{K_{p1}\} - \frac{1}{2}C_{\max}V_{\max} - \frac{\lambda_{\max}\{D(\mathbf{v}_1)\}}{2} - \frac{\lambda_{\max}\{K_{d1}\}}{2} - \frac{\lambda_{\max}\{M\}}{2}\omega_{\max}, \quad N = C_{\max} + \lambda_{\max}\{M\}
\end{aligned}$$

Assume,  $|s_{li}| \leq 1, \forall i = 1, 2, 3$ . This implies,  $\sum_{i=1}^3|s_{li}| \geq \sum_{i=1}^3|s_{li}|^2$ . Thus, (6.63b) can further be expressed as

$$\Rightarrow \dot{V}_1 = -\left\{N'_1\|\mathbf{v}_{1e}\|^2 + \rho B\|\mathbf{f}_p(\boldsymbol{\eta}_{1e})\|^2 + L'_1\|\mathbf{s}_1\|^2 - N_2\|\mathbf{u}_1\|^2\right\} \tag{6.63c}$$

$$\begin{aligned}
\text{where, } L'_1 = & \left(\min_i(K_{sli}) - (\lambda_{\max}\{C_i\})V_{1\max}^2 - \max_i(h_{imax}) - \frac{1}{2}\lambda_{\max}\{D(\mathbf{v}_1)\} - \max_i(K_{wi})\sqrt{3}\delta_{w\max}\beta_{w\max}\right), \\
N'_1 = & A'_1 + \frac{P_2}{\sqrt{3}} - N\|\mathbf{s}_1\|_{\max} - \lambda_{\max}\{D(\mathbf{v}_1)\}, \quad N_2 = \frac{1}{2}N\|\mathbf{s}_1\|_{\max} + \frac{1}{2}\lambda_{\max}\{D(\mathbf{v}_1)\}
\end{aligned}$$

Considering the following fact

$$\|\mathbf{s}_1\|^2 \geq \left(\|\mathbf{v}_{1e}\| + \rho\|\mathbf{f}_p(\boldsymbol{\eta}_{1e})\| - 2\rho\|\mathbf{f}_p(\boldsymbol{\eta}_{1e})\|\right)^2 \geq \left(\|\mathbf{s}_1\| - 2\rho\|\mathbf{f}_p(\boldsymbol{\eta}_{1e})\|\right)^2 \Rightarrow \|\mathbf{s}_1\|^2 \geq \rho^2\|\mathbf{f}_p(\boldsymbol{\eta}_{1e})\|^2$$



eq (6.63c) implies

$$\dot{V}_1 = -\left\{ \aleph_1' \|\mathbf{v}_{1e}\|^2 + (\rho B + L_1') \min(\sigma_{1pi}) \|\boldsymbol{\eta}_{1e}\|^2 - \aleph_2 \|\mathbf{u}_1\|^2 \right\} \quad (6.63d)$$

Eq (6.63d) can further be written as

$$\Rightarrow \dot{V}_1 = -\left\{ Y_1 \|x_1\|^2 - \aleph_2 \|\mathbf{U}_1\|^2 \right\} \quad (6.63e)$$

where,  $Y_1 = \lambda_{\min} \left[ \text{diag} \begin{bmatrix} X_1' & X_1' & X_1' & Y_1' & Y_1' & Y_1' \end{bmatrix} \right]$ ,  $\mathbf{U}_1 = (\mathbf{u}_1, 0, 0, 0) \in \Re^6$ ,  $X_1' = \aleph_1'$ ,  $Y_1' = (\rho B + L_1' \rho^2) \min(\sigma_{1pi})$ . For any  $0 < \varepsilon_1 < 1$ , (6.63e) can be written as

$$\begin{aligned} \Rightarrow \dot{V}_1 &= -\left\{ Y_1 \|\mathbf{x}_1\|^2 - (1 - \varepsilon_1) \|\mathbf{x}_1\|^2 + (1 - \varepsilon_1) \|\mathbf{x}_1\|^2 - \aleph_2 \|\mathbf{U}_1\|^2 \right\} \\ \dot{V}_1 &= -\left\{ \varepsilon_1 Y_1 \|\mathbf{x}_1\|^2 + (1 - \varepsilon_1) \|\mathbf{x}_1\|^2 - \aleph_2 \|\mathbf{U}_1\|^2 \right\} \end{aligned} \quad (6.63f)$$

This is concluded from eq (6.63f) that the following must be guaranteed to ensure  $\dot{V}_1 \leq 0$ ,

$$(1 - \varepsilon_1) Y_1 \|\mathbf{x}_1\|^2 \geq \aleph_2 \|\mathbf{U}_1\|^2 \Rightarrow \|\mathbf{x}_1\| \geq \sqrt{\frac{\aleph_2}{(1 - \varepsilon_1) Y_1}} \|\mathbf{U}_1\| = \chi_1(r_1) \quad (6.63g)$$

As  $\|\mathbf{x}_1\|$  is positive. In (6.63g),  $\chi_1$  is a class -  $K$  function and  $r_1 = \|\mathbf{U}\|$ . Thus, when (6.63g) is true, next expression is also true

$$\|\mathbf{x}_1\| \geq \chi_1(\|\mathbf{U}_1\|) \Rightarrow \dot{V}_1 \leq -\varepsilon_1 Y_2 \|\mathbf{x}_1\|^2 = -\bar{\alpha}_1(\|\mathbf{x}_1\|) \quad (6.64)$$

where,  $\bar{\alpha}_1$  is a  $K_\infty$  function. Similar to (6.63g), in the region,  $\Delta_2 = \{\mathbf{v}_{1e} : \|\boldsymbol{\beta}_d\| \geq \|\mathbf{v}_{1e}\| \geq \|\mathbf{v}_{1e}\|_{\min}\}$

$$(1 - \varepsilon_1') Y_2 \|\mathbf{x}_1\|^2 \geq \aleph_2 \|\mathbf{U}_1\|^2 \Rightarrow \|\mathbf{x}_1\| \geq \sqrt{\frac{\aleph_2}{(1 - \varepsilon_1') Y_2}} \|\mathbf{U}_1\| = \chi_1'(r_1) \quad (6.65a)$$

where,

$Y_2 = \lambda_{\min} \left[ \text{diag} \begin{bmatrix} \hat{X}_1 & \hat{X}_1 & \hat{X}_1 & \hat{Y}_1 & \hat{Y}_1 & \hat{Y}_1 \end{bmatrix} \right]$ ,  $\mathbf{U}_1 = (\mathbf{u}_1, 0, 0, 0) \in \Re^6$ ,  $X_1' = \aleph_1'' = A_1' + P_1 - N \|s_1\|_{\max} - \lambda_{\max} \{D(\mathbf{v}_1)\}$ ,  $\hat{Y}_1 = (\rho B + L_1' \rho^2) \min(\sigma_{1pi})$  and  $0 < \varepsilon_1' < 0$ . In (6.65a),  $\chi_1'$  is a class -  $K$  function and  $r_1 = \|\mathbf{U}_1\|$ .

Thus, eq (6.65a) is true, if

$$\|\mathbf{x}_1\| \geq \chi'_1(\|\mathbf{U}_1\|) \Rightarrow \dot{V}_1 \leq -\varepsilon'_1 \gamma_2 \|\mathbf{x}_1\|^2 = -\bar{\alpha}'_1(\|\mathbf{x}_1\|) \quad (6.65b)$$

where,  $\bar{\alpha}'_1$  is a  $K_\infty$  function. As per the discussion in 10.21 and 10.22 of [225] the state remains bounded by the following inequality.

$$\|\mathbf{x}_1(t)\| \leq \beta(\|\mathbf{x}_1(0)\|, t) \in [0, t_{r(av)}], t_{r(av)} = \sum_{i=1}^3 t_{ri} / 3 \quad (6.65c)$$

where,  $\beta$  is a class- $KL$  function with initial state  $\mathbf{x}_1(0)$ . The expression of  $\beta$  is not unique for whole period of time  $t \in [0, t_{r(av)})$  before reaching boundary layer from initial state. Rather,  $t_{r(av)}$  is divided into two parts. First part corresponds to (6.63e). Second part corresponds to (6.65a). Suppose, first period continues upto  $t_1$  sec and cosequently second part persists  $(t_{r(av)} - t_1)$  sec. Utilizing eq(10.21) of [225] one may write with the initial state  $\mathbf{x}_1(0)$  and  $V(\mathbf{x}_1(0)) = V(0)$ .

$$\dot{V}_1(t) \leq \bar{\alpha}_1 \circ \alpha_{21}^{-1} \circ V_1(t) = -\frac{\varepsilon_1 \gamma_1}{\Omega^2} V_1^2(t) \quad (6.66a)$$

By solving (6.66a) with the help of Comparison Lemma [225], one gets

$$V_1(t) \leq \frac{1}{\frac{1}{V_1(0)} + \frac{\varepsilon_1 \gamma_1}{\Omega^2} t} = \pi_1(V_1(0), t) \quad (6.66b)$$

where,  $\pi$  is a class- $KL$  function.  $\beta_1$ , similar to eq (10.22) and Theorem 10.1.2 of [225], can be found as follows

$$\|\mathbf{x}_1(t)\| \leq \alpha_{11}^{-1}(\pi_1(\alpha_{21}(\|\mathbf{x}_1(0)\|), t)) = \beta_1(\|\mathbf{x}_1(0)\|, t) \quad (6.66c)$$

For the second period of time, one gets similar expression like (6.66c) as follows

$$\|\mathbf{x}_1(t)\| \leq \alpha_{11}^{-1}(\pi_2(\alpha_{21}(\|\mathbf{x}'_1(0)\|), t)) = \beta_2(\|\mathbf{x}'_1(0)\|, t) \quad (6.66d)$$

where,  $\pi_2$  is  $\beta_2$  is a class- $KL$  function and  $\|\mathbf{x}'_1(0)\| = \|\mathbf{x}_1(t_1)\|$  which is available from (6.66c) by putting  $t=t$  Final value of  $\|\mathbf{x}_1(t)\|$  is obtained from (6.66d) by putting  $t=(t_{r(av)} - t_1)$ .

$$\text{For, } \left| \frac{s_i}{\varphi_{li}} \right| \leq 1, \forall i = 1, 2, 3;$$

$$s^T K_s f_s(\cdot) = \sum_{i=1}^3 \left( \frac{K_{sli}}{\varphi_{li}} \right) |s_i|^2 \geq \frac{\min_i(K_{sli})}{\max_i(\varphi_{li})} \|s_i\|^2 \quad (6.67)$$

for  $\Delta_3 = \{v_e : \|v_e\| \leq \|v_e\|_{\min}, \|v_e\|_{\min} < \|\beta_d\|\}$ , with the help of (6.63) and (6.64)

$$\dot{V}_1 = - \left\{ \hat{\mathcal{N}}_1 \|v_{1e}\|^2 + \rho B \|\mathbf{f}_p(\boldsymbol{\eta}_{1e})\|^2 + L_1'' \|s_1\|^2 - \mathcal{N}'_2 \|u_1\|^2 \right\} \quad (6.68)$$

$$\text{where, } L_1'' = \left( \frac{\min_i(K_{sli})}{\max_i(\varphi_{li})} - \max_i(K_{wli}) \sqrt{3} \delta_{wmax} \beta_{wmax} - \max_i(\lambda_{max}\{C_i\}) V_{lmax}^2 - \max_i(h_{lmax}) - \frac{1}{2} \lambda_{max}\{D(v_1)\} \right)$$

$$\hat{N}_1 = A'_1 + P_1 - N \|s_1\|_{\min} - \frac{1}{2} \lambda_{max}\{D(v_1)\}, \mathcal{N}'_2 = \frac{1}{2} N \|s_1\|_{\min} + \frac{1}{2} \lambda_{max}\{D(v_1)\}.$$

Next, considering the following fact

$$\|s_1\|^2 \geq \left( \|v_{1e}\| + \rho \|\mathbf{f}_p(\boldsymbol{\eta}_{1e})\| - 2\rho \|\mathbf{f}_p(\boldsymbol{\eta}_{1e})\| \right)^2 \geq \left( \|s_1\| - 2\rho \|\mathbf{f}_p(\boldsymbol{\eta}_{1e})\| \right)^2 \Rightarrow \|s_1\|^2 \geq \rho^2 \|\mathbf{f}_p(\boldsymbol{\eta}_{1e})\|^2$$

eq (6.68) implies

$$\dot{V}_1 = - \left\{ \hat{\mathcal{N}}_1 \|v_{1e}\|^2 + (\rho B + L_1'' \rho^2) \min_i(\sigma_{1pi}) \|\boldsymbol{\eta}_{1e}\|^2 + \|s_1\|^2 - \mathcal{N}'_2 \|u_1\|^2 \right\} \quad (6.69a)$$

Thus, (6.69a) can further be written as

$$\Rightarrow \dot{V}_1 = - \left\{ E \|x_1\|^2 - \mathcal{N}'_2 \|u_1\|^2 \right\} \quad (6.69b)$$

$$E = \lambda_{\min} \left[ \text{diag} \left[ \hat{X}_1 \quad \hat{X}_1 \quad \hat{X}_1 \quad \hat{Y}_1 \quad \hat{Y}_1 \quad \hat{Y}_1 \right] \right], U_1 = (u_1 \quad 0 \quad 0 \quad 0) \in \mathbb{R}^n, \hat{X}_1 = \hat{\mathcal{N}}_1, \hat{Y}_1 = (\rho B + L_1'' \rho^2) \min_i(\sigma_{1pi}).$$

For any,  $0 < \hat{\varepsilon}_1 < 1$ , eq (6.69b) can be written as

$$\begin{aligned} \Rightarrow \dot{V}_1 &= - \left\{ E \|x_1\|^2 - (1 - \hat{\varepsilon}_1) E \|x_1\|^2 + (1 - \hat{\varepsilon}_1) E \|x_1\|^2 - \mathcal{N}'_2 \|u_1\|^2 \right\} \\ \dot{V} &= - \left\{ \hat{\varepsilon}_1 E \|x_1\|^2 + (1 - \hat{\varepsilon}_1) E \|x_1\|^2 - \mathcal{N}'_2 \|u_1\|^2 \right\} \end{aligned} \quad (6.69c)$$

Thus, following must be guaranteed to make  $\dot{V}_1 \leq 0$ ,

$$(1 - \hat{\varepsilon}_1) E \|\mathbf{x}_1\|^2 \geq \mathcal{N}'_2 \|\mathbf{U}_1\|^2 \Rightarrow \|\mathbf{x}_1\| \geq \sqrt{\frac{\mathcal{N}'_2}{(1 - \hat{\varepsilon}_1) E}} \|\mathbf{U}_1\| = \hat{\chi}_1(r_1) \quad (6.69d)$$

As  $\|\mathbf{x}_1\|$  is positive. In (6.69d),  $\chi_1$  is a class -  $K$  function and  $r_1 = \|\mathbf{U}_1\|$ .

Select,

$$\|\mathbf{x}_1\|_b = \hat{\chi}_1(\|\mathbf{U}_1\|_\infty) \geq \sqrt{\frac{\mathcal{N}'_2}{(1 - \hat{\varepsilon}_1) E}} \|\mathbf{U}_1\|_\infty, \text{ where, } \|\mathbf{U}_1\|_\infty \in L_\infty^m \quad (6.69e)$$

Assume,  $c_1 = \alpha_{21}(\hat{\chi}_1(\|\mathbf{U}_1\|_\infty))$ . Therefore, in the boundary layer set,  $\mathbf{B}_1(t)$  similar to (6.41) ; next expression may be defined true with respect to eq (6.69e)

$$\mathbf{B}_1(t) = \left\{ \left\{ \mathbf{x}_1 = (\mathbf{v}_{1e}, \boldsymbol{\eta}_{1e}) : |x_{1e}| \leq \mu_{11}, |y_{1e}| \leq \mu_{21}, |\theta_{1e}| \leq \mu_{31}, |s_{1i}| \leq \phi_{1i}, \forall i = 1, 2, 3 \right\} \in \mathfrak{R}^3, V_2(\mathbf{x}_2) \leq c_1 \right\} \quad (6.70)$$

whereas,  $\mathbf{B}_{1_{\hat{\chi}_1(\|\mathbf{U}_1\|_\infty)}} \subset \mathbf{B}_1$ . Thus, till  $\mathbf{x}_1(0) \in \mathbf{B}_1(t)$  is true, one may state with the help of eq (10.20) of [225], eq (6.60) and eq (6.69e) that,  $\mathbf{x}_1(t)$  satisfies

$$\|\mathbf{x}_1(t)\| \leq \gamma_1(\|\mathbf{U}_1\|_\infty) \leq \alpha_{11}^{-1}(\alpha_{21}(\chi'_1(\|\mathbf{U}_1\|_\infty))) \leq \sqrt{\frac{h_1}{\hat{\chi}_1}} \|\mathbf{x}_{1b}\| \Rightarrow \|\mathbf{x}_1(t)\| \leq \|\mathbf{x}_{1b}\| \quad (6.71)$$

where,  $\gamma_1$  is gain function which is a class -  $K_\infty$  function[225].

*Theorem 6.4:* Consider the closed-loop system (6.54) for FF with state  $\mathbf{x}_2 \in \mathfrak{R}^6$  and locally essentially bounded input  $\mathbf{U}_2 \in \mathfrak{R}^6$  and its derivatives  $\dot{\mathbf{U}}_2 \in \mathfrak{R}^6$ , bounded input  $\mathbf{U}_1 \in \mathfrak{R}^6$  and  $\mathbf{x}_1 \in \mathfrak{R}^6$  in which  $\mathbf{f}_2(0,0,0,0,0) = 0$  and  $\dot{\mathbf{x}}_2 = \mathbf{f}_2(\mathbf{x}_1, \mathbf{x}_2, \mathbf{U}_1, \mathbf{U}_2, \dot{\mathbf{U}}_2) \in \mathfrak{R}^6$  is locally Lipschitz on  $\mathfrak{R}^6 \times \mathfrak{R}^6 \times \mathfrak{R}^6 \times \mathfrak{R}^6 \times \mathfrak{R}^6$ . Corresponding to boundary layer

$$\mathbf{B}_2 = \left\{ (\mathbf{v}_{2e}, \boldsymbol{\eta}_{2e}) : x_{2e} \leq \mu_{12}, y_{1e} \leq \mu_{22}, \theta_{1e} \leq \mu_{32}, s_{2i} \leq \phi_{2i}, \forall i = 1, 2, 3 \right\} \in \mathfrak{R}^3$$

with respect to proposed Sliding Mode Nonlinear PID controller with BI and BD for global leader, assume the following set  $H_1$  and  $H_2$ , such that  $H_1 = \{\|\mathbf{x}_2(0)\|_{\max} : \|s_2\|_{\max}\}, H_2 = \{\|\mathbf{x}_{2b}\| : \|s_2\|_{\min}\},$

where,  $\|\mathbf{x}_{2b}\|$  is the value of  $\|\mathbf{x}_2(t)\|$  at the boundary of the sliding surface  $\mathbf{B}_2(t)$ . There exist gain matrices  $K_{d2}, K_{p2}, K_{s2}, K_{w2}$  such that Lemma 4.1 holds with respect boundary layer  $\mathbf{B}_2(t)$  and following inequalities are satisfied,

$$\left. \begin{aligned} & i) \lambda_{\min} \{K_{p2}\} \phi_{\min}^p > \frac{\rho}{2} \lambda_{\max} \{M\} \\ & ii) \frac{P_2}{\sqrt{3}} + \lambda_{\min} \{D(\mathbf{v}_2)\} \geq \rho \left( \sqrt{3} \delta_{pmax} \beta_{pmax} + \frac{1}{2} C_{max} V_{max} \right) + \frac{\rho}{2} \lambda_{\max} \{D(\mathbf{v}_2)\} \\ & \quad \frac{\rho}{2} \lambda_{\max} \{K_{d2}\} \sigma_{2d} + \frac{1}{2} \lambda_{\max} \{M\} \omega_{max} + \rho \delta_{pmax} \lambda_{\max} \{M\} + \lambda_{\max} \{D(\mathbf{v}_2)\} + N \|\mathbf{s}_2\|_{max} \\ & iii) P_1 + \lambda_{\min} \{D(\mathbf{v}_2)\} \geq \rho \left( \sqrt{3} \delta_{pmax} \beta_{pmax} + \frac{1}{2} C_{max} V_{max} \right) + \frac{\rho}{2} \lambda_{\max} \{D(\mathbf{v}_2)\} \\ & \quad + \frac{\rho}{2} \lambda_{\max} \{K_{d2}\} \sigma_{2d} + \frac{1}{2} \lambda_{\max} \{M\} \omega_{max} + \rho \delta_{pmax} \lambda_{\max} \{M\} + \lambda_{\max} \{D(\mathbf{v}_2)\} + N \|\mathbf{s}_2\|_{max} \\ & iv) \lambda_{\min} \{K_{p2}\} \geq + \frac{1}{2} C_{max} V_{max} + \frac{\lambda_{\max} \{K_{d2}\}}{2} + \frac{\lambda_{\max} \{D(\mathbf{v}_2)\}}{2} + \frac{1}{2} \lambda_{\max} \{M\} \omega_{max} \\ & v) \min_i (K_{s2i}) \geq \lambda_{\max} (C_i) V_{max}^2 + \max_i (h_{1imax}) + \frac{\lambda_{\max} \{D(\mathbf{v}_2)\}}{2} + \max_i (K_{w2i}) \sqrt{3} \delta_{wmax} \beta_{wmax} \end{aligned} \right\} \quad (6.72a)$$

then the system of eq (6.54) becomes globally input-to-state stable [225] with respect to two inputs  $\mathbf{U}_1 = (\mathbf{v}_{1r}, 0, 0, 0) \in \mathbb{R}^6$  and state  $\mathbf{x}_1(t) \in \mathbb{R}^6$  and  $\mathbf{x}_2(t)$  remains bounded as  $\|\mathbf{x}_2(t)\| \leq \|\mathbf{x}_{2b}(t)\|$  for  $t \geq 0$ .

**Proof:** To verify input-to-state stability for the closed-loop system (6.54) with input  $\mathbf{u}_1$  and  $\mathbf{x}_1$  following ISS Lyapunov function is chosen

$$V_2(\mathbf{v}_{2e}, \boldsymbol{\eta}_{2e}) = \frac{1}{2} \mathbf{v}_{2e}^T M \mathbf{v}_{2e} + \rho \mathbf{f}_p^T(\boldsymbol{\eta}_{2e}) J(\boldsymbol{\eta}_2) M \mathbf{v}_{2e} + \sum_{i=1}^3 \int_0^{\eta_{2e(i)}} f_{pi}^T(\boldsymbol{\eta}_{2e}(i)) K_{p2i} d\boldsymbol{\eta}_{2e}(i) \quad (6.72b)$$

Therefore,

$$\begin{aligned} \dot{V}_2 &= (\mathbf{v}_{2e} + \rho J(\boldsymbol{\eta}_2) \mathbf{f}_p(\boldsymbol{\eta}_{2e}))^T M \dot{\mathbf{v}}_{2e} + \rho \dot{\mathbf{f}}_p^T(\boldsymbol{\eta}_{2e}) J(\boldsymbol{\eta}_2) M \mathbf{v}_{2e} + \rho \mathbf{f}_p^T(\boldsymbol{\eta}_{2e}) \dot{J}(\boldsymbol{\eta}_2) M \mathbf{v}_{2e} + \mathbf{v}_{2e}^T J^T(\boldsymbol{\eta}_2) K_{p2} \mathbf{f}(\boldsymbol{\eta}_{2e}) \\ \Rightarrow \dot{V}_2 &= (\mathbf{v}_{2e} + \rho J(\boldsymbol{\eta}_2) \mathbf{f}_p(\boldsymbol{\eta}_{2e}))^T (-C(\mathbf{v}_2) \mathbf{v}_{2e} - D(\mathbf{v}_2) \mathbf{v}_{2e} - K_{d2} \mathbf{f}_d(\mathbf{v}_{2e}) - J^T(\boldsymbol{\eta}_2) K_{p2} \mathbf{f}_p(\boldsymbol{\eta}_{2e}) - K_{s2} \mathbf{f}_s(\mathbf{s}_2) - K_{w2} \mathbf{f}_w(\boldsymbol{\chi}_{2e})) \end{aligned}$$

$$\begin{aligned}
& + (\mathbf{v}_{2e} + \rho J(\boldsymbol{\eta}_2) \mathbf{f}_p(\boldsymbol{\eta}_{2e}))^T \mathbf{f}_{h2}(\mathbf{u}_2, \dot{\mathbf{u}}_2, \mathbf{v}_{2e}, \boldsymbol{\eta}_{2e}) + \rho \dot{\mathbf{f}}_p^T(\boldsymbol{\eta}_{2e}) J(\boldsymbol{\eta}_2) M \mathbf{v}_{2e} + \rho \mathbf{f}_p^T(\boldsymbol{\eta}_{2e}) \dot{J}(\boldsymbol{\eta}_2) M \mathbf{v}_{2e} + \\
& + \mathbf{v}_{2e}^T J^T(\boldsymbol{\eta}_2) K_{p2} \mathbf{f}_p(\boldsymbol{\eta}_{2e})
\end{aligned} \tag{6.73}$$

Using Property 3.4

$$\begin{aligned}
\Rightarrow \dot{V}_2 = & - \left[ \mathbf{v}_{2e}^T D(\mathbf{v}_2) \mathbf{v}_{2e} + \mathbf{v}_{2e}^T K_{d2} \mathbf{f}_d(\mathbf{v}_{2e}) \right. \\
& + \rho \left\{ \mathbf{f}_p^T(\boldsymbol{\eta}_{2e}) J(\boldsymbol{\eta}_2) C(\mathbf{v}_2) \mathbf{v}_{2e} + \mathbf{f}_p^T(\boldsymbol{\eta}_{2e}) J(\boldsymbol{\eta}_2) D(\mathbf{v}_2) \mathbf{v}_{2e} + \mathbf{f}_p^T(\boldsymbol{\eta}_{2e}) J(\boldsymbol{\eta}_2) K_{d2} \mathbf{f}_d(\mathbf{v}_{2e}) + \mathbf{f}_p^T(\boldsymbol{\eta}_{2e}) J(\boldsymbol{\eta}_2) J^T(\boldsymbol{\eta}_2) K_{p2} \mathbf{f}_p(\boldsymbol{\eta}_{2e}) \right\} \\
& - \rho \dot{\mathbf{f}}_p^T(\boldsymbol{\eta}_{2e}) J(\boldsymbol{\eta}_2) M \mathbf{v}_{2e} - \rho \mathbf{f}_p^T(\boldsymbol{\eta}_{2e}) \dot{J}(\boldsymbol{\eta}_2) M \mathbf{v}_{2e} \Big] - s_2^T K_{w2} \mathbf{f}_w(\boldsymbol{\chi}_{2e}) \\
& - s_2^T K_{s2} \mathbf{f}_s(s_2) + s_2^T \left( M J^T(\boldsymbol{\eta}_{2e}) \dot{\mathbf{u}}_2 + \left\{ M \left( \dot{J}^T(\boldsymbol{\eta}_{2e}) \right) + C \left( J^T(\boldsymbol{\eta}_{2e}) \mathbf{v}_{2e} \right) + D(\mathbf{v}_2) J^T(\boldsymbol{\eta}_{2e}) - C \left( J^T(\boldsymbol{\eta}_{2e}) \mathbf{u}_2 \right) J^T(\boldsymbol{\eta}_{2e}) \right\} \mathbf{u}_2 \right)
\end{aligned} \tag{6.74}$$

With the help of eq (4.37), in the domain  $\Delta_1 = \{ \mathbf{v}_{2e} : V_{1max} \geq \|\mathbf{v}_{2e}\| > \|\boldsymbol{\beta}_d\| \}$  using eq (4.20-4.21), (4.2

3-4. 28), (4.31-4.32a), (4.33), following Appendix A.6 and A.3 and replacing  $\mathbf{h}_2 = -M J^T(\boldsymbol{\eta}_{2e}) \dot{\mathbf{u}}_2$

$$\text{and } s_2^T C \left( J^T(\boldsymbol{\eta}_{2e}) \mathbf{u}_2 \right) J^T(\boldsymbol{\eta}_{2e}) \mathbf{u}_2 \geq - \sum_{i=1}^3 \lambda_{max}(C_i) \|\mathbf{u}_2\|^2 |s_{2i}|$$

$$\begin{aligned}
\dot{V}_2 = & \left[ \left( \lambda_{min}(D(\mathbf{v}_2)) + \frac{P_2}{\sqrt{3}} \right) \|\mathbf{v}_{2e}\|^2 \right. \\
& - \rho \left( \sqrt{3} \delta_{pmax} \beta_{pmax} C_{max} \|\mathbf{v}_{2e}\|^2 + \frac{1}{2} C_{max} V_{max} \left( \|\mathbf{v}_{2e}\|^2 + \|\mathbf{f}_p(\boldsymbol{\eta}_{2e})\|^2 \right) \right) - \rho \lambda_{max} \{ D(\mathbf{v}_2) \} \frac{1}{2} \left( \|\mathbf{f}_p(\boldsymbol{\eta}_{2e})\|^2 + \|\mathbf{v}_{2e}\|^2 \right) \\
& - \rho \lambda_{max} \{ K_d \} \frac{1}{2} \left( \|\mathbf{f}_p(\boldsymbol{\eta}_{2e})\|^2 + \sigma_{2d} \|\mathbf{v}_{2e}\|^2 \right) + \rho \lambda_{min} \{ K_p \} \|\mathbf{f}_p(\boldsymbol{\eta}_{2e})\|^2 \\
& - \rho \frac{1}{2} \lambda_{max} \{ M \} \omega_{max} \left( \|\mathbf{f}_p(\boldsymbol{\eta}_{2e})\|^2 + \|\mathbf{v}_{2e}\|^2 \right) - \rho \delta_{pmax} \lambda_{max} \{ M \} \|\mathbf{v}_{2e}\|^2 \Big] - \\
& \left( \sum_{i=1}^3 \left( K_{s2i} - K_{w2i} |\mathbf{f}_w(\boldsymbol{\chi}_{2ei})| - \lambda_{max}(C_i) \|\mathbf{u}_2\|^2 - h_{2imax} \right) |s_{2i}| \right) + \left\{ \left( C_{max} \|\mathbf{v}_{2e}\| + \lambda_{max}(D(\mathbf{v}_2)) + \lambda_{max} \{ M \} \|\mathbf{v}_{2e}\| \right) \|\mathbf{s}_2\| \right\} \|\mathbf{u}_2\|
\end{aligned} \tag{6.75a}$$

If linear and angular velocities are assumed to be set at less than unity one may get  $\frac{1}{\sqrt{3}} \|\mathbf{v}_{2e}\|^2 \leq \|\mathbf{v}_{2e}\|$ .

Thus, using this fact and replacing  $\|\mathbf{u}_2\| = \|\mathbb{C}_1\| \|\mathbf{v}_{2e}\| + \|\mathbb{C}_2\| \|\mathbf{v}_{1e}\| + \|\mathbb{C}_3\| \|\mathbf{u}_1\|$ , eq (6.75a) can further

be expressed as

$$\begin{aligned}
\dot{V}_2 = & \left[ \left( \lambda_{\min}(D(\mathbf{v}_2)) + \frac{P_2}{\sqrt{3}} \right) \|\mathbf{v}_{2e}\|^2 \right. \\
& - \rho \left( \sqrt{3} \delta_{pmax} \beta_{pmax} C_{max} \|\mathbf{v}_{2e}\|^2 + \frac{1}{2} C_{max} V_{max} \left( \|\mathbf{v}_{2e}\|^2 + \|\mathbf{f}_p(\boldsymbol{\eta}_{2e})\|^2 \right) \right) - \rho \lambda_{max} \{D(\mathbf{v}_2)\} \frac{1}{2} \left( \|\mathbf{f}_p(\boldsymbol{\eta}_{2e})\|^2 + \|\mathbf{v}_{2e}\|^2 \right) \\
& - \rho \lambda_{max} \{K_{d2}\} \frac{1}{2} \left( \|\mathbf{f}_p(\boldsymbol{\eta}_{2e})\|^2 + \sigma_{2d} \|\mathbf{v}_{2e}\|^2 \right) + \rho \lambda_{\min} \{K_{p2}\} \|\mathbf{f}_p(\boldsymbol{\eta}_{2e})\|^2 \\
& - \rho \frac{1}{2} \lambda_{max} \{M\} \omega_{max} \left( \|\mathbf{f}_p(\boldsymbol{\eta}_{2e})\|^2 + \|\mathbf{v}_{2e}\|^2 \right) - \rho \delta_{pmax} \lambda_{max} \{M\} \|\mathbf{v}_{2e}\|^2 \left. \right] - \left( \sum_{i=1}^3 (K_{si2} - \lambda_{max} \{C_i\} \|\mathbf{u}_2\|^2 - h_{imax}) |s_{i2}| \right) \\
& + \{N \|\mathbb{C}_1\| \|\mathbf{s}_2\| \|\mathbf{v}_{2e}\|^2 + \frac{1}{2} N \|\mathbb{C}_2\| \|\mathbf{s}_2\| \|\mathbf{v}_{2e}\|^2 + \frac{1}{2} N \|\mathbb{C}_2\| \|\mathbf{s}_2\| \|\mathbf{v}_{1e}\|^2 + \frac{1}{2} N \|\mathbb{C}_3\| \|\mathbf{s}_2\| \|\mathbf{v}_{2e}\|^2 + \frac{1}{2} N \|\mathbb{C}_3\| \|\mathbf{s}_2\| \|\mathbf{u}_1\|^2 \\
& + \frac{1}{2} \lambda_{max} \{D(\mathbf{v}_2)\} \|\mathbb{C}_1\| \|\mathbf{v}_{2e}\|^2 + \frac{1}{2} \lambda_{max} \{D(\mathbf{v}_2)\} \|\mathbb{C}_1\| \|\mathbf{s}_2\|^2 + \frac{1}{2} \lambda_{max} \{D(\mathbf{v}_2)\} \|\mathbb{C}_2\| \|\mathbf{v}_{1e}\|^2 + \frac{1}{2} \lambda_{max} \{D(\mathbf{v}_2)\} \|\mathbb{C}_2\| \|\mathbf{s}_2\|^2 \\
& + \frac{1}{2} \lambda_{max} \{D(\mathbf{v}_2)\} \|\mathbb{C}_3\| \|\mathbf{u}_1\|^2 + \frac{1}{2} \lambda_{max} \{D(\mathbf{v}_2)\} \|\mathbb{C}_3\| \|\mathbf{s}_2\|^2 \tag{6.75b}
\end{aligned}$$

Putting the values of  $\|\mathbb{C}_1\|$ ,  $\|\mathbb{C}_2\|$  and  $\|\mathbb{C}_3\|$  in eq (6.75b) one gets

$$\begin{aligned}
\dot{V}_2 = & \left[ \left( \lambda_{\min}(D(\mathbf{v}_2)) + \frac{P_2}{\sqrt{3}} \right) \|\mathbf{v}_{2e}\|^2 \right. \\
& - \rho \left( \sqrt{3} \delta_{pmax} \beta_{pmax} C_{max} \|\mathbf{v}_{2e}\|^2 + \frac{1}{2} C_{max} V_{max} \left( \|\mathbf{v}_{2e}\|^2 + \|\mathbf{f}_p(\boldsymbol{\eta}_{2e})\|^2 \right) \right) - \rho \lambda_{max} \{D(\mathbf{v}_2)\} \frac{1}{2} \left( \|\mathbf{f}_p(\boldsymbol{\eta}_{2e})\|^2 + \|\mathbf{v}_{2e}\|^2 \right) \\
& - \rho \frac{1}{2} \lambda_{max} \{M\} \omega_{max} \left( \|\mathbf{f}_p(\boldsymbol{\eta}_{2e})\|^2 + \|\mathbf{v}_{2e}\|^2 \right) - \rho \delta_{pmax} \lambda_{max} \{M\} \|\mathbf{v}_{2e}\|^2 \left. \right] - \left( \sum_{i=1}^3 (K_{si2} - \lambda_{max} \{C_i\} \|\mathbf{u}_2\|^2 - h_{imax}) |s_{i2}| \right) \\
& + \left( 2N \|\mathbf{s}_2\| \|\mathbf{v}_{2e}\|^2 + \frac{\lambda_{max} \{D(\mathbf{v}_2)\}}{2} \|\mathbf{v}_{2e}\|^2 + \left( N \|\mathbf{s}_2\| + \frac{\lambda_{max} \{D(\mathbf{v}_2)\}}{2} \right) \|\mathbf{v}_{1e}\|^2 + \right. \\
& \left. \left( \frac{N}{2} \|\mathbf{s}_2\| + \frac{\lambda_{max} \{D(\mathbf{v}_2)\}}{2} \right) \|\mathbf{u}_1\|^2 + \frac{3}{2} \lambda_{max} \{D(\mathbf{v}_2)\} \|\mathbf{s}_2\|^2 \right) \tag{6.75c}
\end{aligned}$$

$$\Rightarrow \dot{V}_2 = - \left[ \{\boldsymbol{\Sigma}'_1 \|\mathbf{v}_{2e}\|^2 + \rho B \|\mathbf{f}_p(\boldsymbol{\eta}_{2e})\|^2 + L'_1 \|\mathbf{s}_2\|^2 - (A_1 \|\mathbf{v}_{1e}\|^2 + A_2 \|\mathbf{u}_1\|^2) \right] \tag{6.75d}$$

$$\text{where, } \boldsymbol{\Sigma}'_1 = \left( A'_1 + \frac{P_2}{\sqrt{3}} - 2N \|\mathbf{s}_2\|_{max} - \frac{\lambda_{max} \{D(\mathbf{v}_2)\}}{2} \right),$$

$$\begin{aligned}
A'_1 &= \left\{ \lambda_{\min} \{D(\mathbf{v}_2)\} - \rho \left( \sqrt{3} \delta_{pmax} \beta_{pmax} C_{max} + \frac{1}{2} C_{max} V_{max} \right) - \frac{\rho \lambda_{max} \{D(\mathbf{v}_2)\}}{2} \right. \\
&\quad \left. - \frac{\rho \lambda_{max} \{K_{d2}\} \sigma_{2d}}{2} - \frac{\rho \lambda_{max} \{M\} \omega_{max}}{2} - \rho \delta_{pmax} \lambda_{max} \{M\} \right\}, N = C_{max} + \lambda_{max} \{M\}, \\
B &= \lambda_{\min} \{K_{p2}\} - \frac{1}{2} C_{max} V_{max} - \frac{\lambda_{max} \{D(\mathbf{v}_2)\}}{2} - \frac{\lambda_{max} \{K_{d2}\}}{2} - \frac{\lambda_{max} \{M\}}{2} \omega_{max}, \\
L'_1 &= \left( \min_i (K_{s2i}) - \lambda_{max} (C_i) V_{1max}^2 - \max_i (h_{1imax}) - \frac{3 \lambda_{max} \{D(\mathbf{v}_2)\}}{2} - \max (K_{w2i}) \sqrt{3} \delta_{wmax} \beta_{wmax} \right) \\
A_1 &= N \|s_2\|_{max} + \frac{\lambda_{max} \{D(\mathbf{v}_2)\}}{2}, A_2 = \frac{N}{2} \|s_2\|_{max} + \frac{\lambda_{max} \{D(\mathbf{v}_2)\}}{2}.
\end{aligned}$$

From (6.75d), one may get similar expression of (6.63d) as follows

$$\dot{V}_2 = - \left\{ \mathfrak{N}'_1 \|\mathbf{v}_{2e}\|^2 + (\rho B + L'_1) \min(\sigma_{1pi}) \|\boldsymbol{\eta}_{2e}\|^2 - (A_1 \|\mathbf{v}_{1e}\|^2 + A_2 \|\mathbf{u}_1\|^2) \right\} \quad (6.75e)$$

Eq (6.76) may further be written as

$$\Rightarrow \dot{V}_2 = - \left\{ \gamma_1 \|\mathbf{x}_2\|^2 - (A_1 \|\mathbf{v}_{1e}\|^2 + A_2 \|\mathbf{U}_1\|^2) \right\} \quad (6.75f)$$

where,  $\gamma_1 = \lambda_{\min} [\text{diag}[X'_1 \quad X'_1 \quad X'_1 \quad Y'_1 \quad Y'_1 \quad Y'_1]]$ ,  $\mathbf{U}_1 = (\mathbf{u}_1, 0, 0, 0) \in \Re^6$ ,  $X'_1 = \mathfrak{N}'_1$  and  $Y'_1 = (\rho B + L'_1 \rho^2)$

Let, choose any  $0 < \varepsilon < 1$ , and observe the following expression

$$\begin{aligned}
\Rightarrow \dot{V}_2 &= - \left\{ \gamma_1 \|\mathbf{x}_2\|^2 - (1-\varepsilon) \gamma_1 \|\mathbf{x}_2\|^2 + (1-\varepsilon) \gamma_1 \|\mathbf{x}_2\|^2 - (A_1 \|\mathbf{v}_{1e}\|^2 + A_2 \|\mathbf{U}_1\|^2) \right\} \\
\Rightarrow \dot{V}_2 &= - \left\{ \varepsilon \gamma_1 \|\mathbf{x}_2\|^2 + (1-\varepsilon) \gamma_1 \|\mathbf{x}_2\|^2 - (A_1 \|\mathbf{v}_{1e}\|^2 + A_2 \|\mathbf{U}_1\|^2) \right\}
\end{aligned} \quad (6.75g)$$

From the (6.75g), it is concluded that following must be guaranteed to ensure  $\dot{V}_2 \leq 0$ ,

$$(1-\varepsilon) \gamma_1 \|\mathbf{x}_2\|^2 \geq (A_1 \|\mathbf{v}_{1e}\|^2 + A_2 \|\mathbf{U}_1\|^2) \Rightarrow \|\mathbf{x}_2\| \geq \sqrt{\frac{1}{(1-\varepsilon)}} (A_1 \|\mathbf{v}_{1e}\|^2 + A_2 \|\mathbf{U}_1\|^2)$$

$$\|\mathbf{x}_2\| \geq \lambda_{max} [\text{diag}[X \quad Y]] \|\hat{\mathbf{U}}_2\| = \chi_2(r_2) \quad (6.77)$$

where,  $X = \frac{A_1}{(1-\varepsilon)} I_{6 \times 6}$ ,  $Y = \frac{A_2}{(1-\varepsilon)} I_{6 \times 6}$ ,  $\hat{\mathbf{U}}_2 = [\mathbf{x}_1 \quad \mathbf{U}_1] \in \Re^{12}$ , where,  $\mathbf{x}_1 = (\mathbf{x}'_1, 0, 0, 0)$ . In (6.77c),  $\chi_2$  is a class- $K$  function and  $r_2 = \|\hat{\mathbf{U}}_2\|$ .

Thus, eq (6.77) implies



$$\|\mathbf{x}_1\| \geq \chi_2(\|\hat{\mathbf{U}}_2\|) \Rightarrow \dot{V}_2 \leq -\varepsilon_1 \gamma_1 \|\mathbf{x}_2\|^2 = -\bar{\alpha}_2(\|\mathbf{x}_2\|) \quad (6.78)$$

where,  $\bar{\alpha}_2$  is a class  $K_\infty$  function.

Similar to (6.77c), in the domain,  $\Delta_2 = \{\mathbf{v}_{2e} : \|\boldsymbol{\beta}_d\| \geq \|\mathbf{v}_{2e}\| \geq \|\mathbf{v}_{2e}\|_{\min}\}$

$$(1 - \varepsilon'_1) \gamma_2 \|\mathbf{x}_2\|^2 \geq (A_1 \|\mathbf{v}_{1e}\|^2 + A_2 \|\mathbf{U}_1\|^2) \Rightarrow \|\mathbf{x}_2\| \geq \sqrt{\frac{1}{(1 - \varepsilon'_1)} (A_1 \|\mathbf{v}_{1e}\|^2 + A_2 \|\mathbf{U}_1\|^2)} \\ \Rightarrow \|\mathbf{x}_2\| \geq \lambda_{\max} [\text{diag}[X \quad Y]] \|\hat{\mathbf{U}}_2\| = \chi'_2(r_2) \quad (6.79a)$$

where,

$$\gamma_2 = \lambda_{\min} [\text{diag}[\hat{X}_1 \quad \hat{X}_1 \quad \hat{X}_1 \quad \hat{Y}_1 \quad \hat{Y}_1 \quad \hat{Y}_1]], \mathbf{U}_1 = (\mathbf{u}_1, 0, 0, 0) \in \mathfrak{R}^6, \hat{X}_1 = \mathfrak{N}_1'' = A'_1 + P_1 - 2N\|\mathbf{s}_2\|_{\max} \\ - \frac{\lambda_{\max}\{D(\mathbf{v}_2)\}}{2}, \hat{Y}_1 = (\rho B + L'_1 \rho^2) \min(\sigma_{1pi}) \text{ and } 0 < \varepsilon'_1 < 0. \text{ In (6.79a), } \chi_2 \text{ is a class - } K \text{ function}$$

and  $r_2 = \|\hat{\mathbf{U}}_2\|$ .

Similarly, all the expressions (6.79b), (6.79c), (6.80a)-(6.80d) are obtained corresponding to (6.65a), (6.65b), (6.66a)-(6.66d) assuming  $\mathbf{x}_2(0) \in H_1$  and  $\mathbf{x}_2(t_{r(av)}) \in H_2$ .  $\mathbf{x}_2(t)$  at  $t = t_{r(av)}$  is obtained from (6.80d) by putting  $t = t_{r(av)} - t_1$ .

Inside the boundary layer of SMC for the controller of FF, similar expressions of (6.80)-(6.84) are obtained, in the same these are created in (6.67)-(6.71). In (6.81), the following changes in expressions compared to (6.68) are made. Then after several expressions similar to Theorem 6.3,

$$\hat{\mathfrak{N}}_1 = A'_1 + P_1 - 2N\|\mathbf{s}_2\|_{\min} - \frac{1}{2} \lambda_{\max}\{D(\mathbf{v}_2)\} \text{ and} \\ A_1 = N\|\mathbf{s}_2\|_{\min} + \frac{\lambda_{\max}\{D(\mathbf{v}_2)\}}{2}, A_2 = \frac{N}{2} \|\mathbf{s}_2\|_{\min} + \frac{\lambda_{\max}\{D(\mathbf{v}_2)\}}{2}.$$

Select,

$$\|\mathbf{x}_{2b}\| = \hat{\chi}_2(\|\hat{\mathbf{U}}_2\|_\infty) = \lambda_{\max} [\text{diag}[X \quad Y]] \|\hat{\mathbf{U}}_2\|_\infty, \text{ where } \|\hat{\mathbf{U}}_2\|_\infty \in L_\infty^{12} \quad (6.82e)$$

Assume,  $c_1 = \alpha_{21}(\hat{\chi}_2(\|\hat{\mathbf{U}}_2\|_\infty))$ . Therefore, in the boundary layer set  $\mathbf{B}_2(t)$  similar to (6.41); next

expression may be defined true with respect to (6.69e).

$$\mathbf{B}_2(t) = \left\{ \left\{ \mathbf{x}_2 = (\mathbf{v}_{2e}, \boldsymbol{\eta}_{2e}) : |\mathbf{x}_{2e}| \leq \mu_{12}, |\mathbf{y}_{2e}| \leq \mu_{22}, |\theta_{1e}| \leq \mu_{32}, |s_{1i}| \leq \phi_{2i}, \forall i = 1, 2, 3 \right\} \in \mathfrak{R}^3, V_2(\mathbf{x}_2) \leq c_1 \right\} \quad (6.83)$$

whereas,  $\mathbf{B}_{\frac{\chi_2(\|\hat{\mathbf{U}}_2\|_\infty)}{\chi_2(\|\hat{\mathbf{U}}_2\|_\infty)}} \subset \mathbf{B}_2$ . Thus, till  $\mathbf{x}_2(0) \in \mathbf{B}_2(t)$  is true, one may states with the help of eq (10.20) of [225], (6.60) and (6.82e) that  $\mathbf{x}_2(t)$  satisfies

$$\|\mathbf{x}_2(t)\| \leq \gamma\left(\|\hat{\mathbf{U}}_2\|_\infty\right) \leq \alpha_{11}^{-1}\left(\alpha_{21}\left(\chi'_2\left(\|\hat{\mathbf{U}}_2\|_\infty\right)\right)\right) \leq \sqrt{\frac{\hbar}{\lambda}}\|\mathbf{x}_{2b}(t)\| \Rightarrow \|\mathbf{x}_2(t)\| \leq \|\mathbf{x}_{2b}(t)\| \quad (6.84)$$

where  $\gamma$  is gain function which is a class- $K_\infty$  function[225].

*Theorem 6.5:* Consider the closed-loop system (6.55b) for ordinary follower-1(k=2) with state

$\mathbf{x}_3 \in \mathfrak{R}^6$  and locally essentially bounded input  $\mathbf{U}_3 \in \mathfrak{R}^6$ , its derivatives  $\dot{\mathbf{U}}_3 \in \mathfrak{R}^6$ , bounded input

$\mathbf{U}_1 \in \mathfrak{R}^6$  and  $\mathbf{x}_1 \in \mathfrak{R}^6$  and  $\mathbf{x}_2 \in \mathfrak{R}^6$  which  $\mathbf{f}_3(0,0,0,0,0,0)=0$  and  $\mathbf{f}(\mathbf{x}_1, \mathbf{x}_2, \mathbf{x}_3, \mathbf{U}_1, \mathbf{U}_3, \dot{\mathbf{U}}_3)$  is

locally Lipschitz on  $\mathfrak{R}^6 \times \mathfrak{R}^6 \times \mathfrak{R}^6 \times \mathfrak{R}^6 \times \mathfrak{R}^6 \times \mathfrak{R}^6$ . Corresponding to boundary layer  $\mathbf{B}_3(t)$  like

$\mathbf{B}_2(t)$  and  $\mathbf{B}_1(t)$  with respect to proposed Sliding Mode Nonlinear PID controller with BI and BD

for ordinary folloer-1, assume the following set  $H_1$  and  $H_2$ ,

$H_1 = \left\{ \|\mathbf{x}_3(0)\|_{max} : \|\mathbf{s}_3\|_{max} \right\}, H_2 = \left\{ \|\mathbf{x}_{3b}\| : \|\mathbf{s}_3\|_{min} \right\}$ , where,  $\|\mathbf{x}_{3b}\|$  is the value of  $\|\mathbf{x}_3(t)\|$  at the

boundary of the sliding surface  $\mathbf{B}_3(t)$ . There exists gain matrices  $K_{d3}, K_{p3}, K_{s3}, K_{w3}$  such that

Lemma 4.1 holds with respect to boundary layer  $\mathbf{B}_3(t)$  like  $\mathbf{B}_2(t)$ ; and following inequalities

are satisfied.

$$\left. \begin{aligned}
& i) \lambda_{\min} \{K_{p3}\} \wp_{\min}^p > \frac{\rho}{2} \lambda_{\max} \{M\} \\
& ii) \frac{P_2}{\sqrt{3}} + \lambda_{\min} \{D(\mathbf{v}_3)\} \geq \rho \left( \sqrt{3} \delta_{pmax} \beta_{pmax} + \frac{1}{2} C_{max} V_{max} \right) + \frac{\rho}{2} \lambda_{\max} \{D(\mathbf{v}_3)\} \\
& \frac{\rho}{2} \lambda_{\max} \{K_{d3}\} \sigma_{2d} + \frac{1}{2} \lambda_{\max} \{M\} \omega_{max} + \rho \delta_{pmax} \lambda_{\max} \{M\} + \lambda_{\max} \{D(\mathbf{v}_3)\} + N \|\mathbf{s}_2\|_{max} \\
& iii) P_1 + \lambda_{\min} \{D(\mathbf{v}_3)\} \geq \rho \left( \sqrt{3} \delta_{pmax} \beta_{pmax} + \frac{1}{2} C_{max} V_{max} \right) + \frac{\rho}{2} \lambda_{\max} \{D(\mathbf{v}_3)\} \\
& + \frac{\rho}{2} \lambda_{\max} \{K_{d3}\} \sigma_{2d} + \frac{1}{2} \lambda_{\max} \{M\} \omega_{max} + \rho \delta_{pmax} \lambda_{\max} \{M\} + \lambda_{\max} \{D(\mathbf{v}_3)\} + N \|\mathbf{s}_3\|_{max} \\
& iv) \lambda_{\min} \{K_{p3}\} \geq \frac{1}{2} C_{max} V_{max} + \frac{\lambda_{\max} \{K_{d3}\}}{2} + \frac{\lambda_{\max} \{D(\mathbf{v}_3)\}}{2} + \frac{1}{2} \lambda_{\max} \{M\} \omega_{max} \\
& v) \min_i (K_{s3i}) \geq \lambda_{\max} (C_i) V_{max}^2 + \max_i (h_{1imax}) + \frac{\lambda_{\max} \{D(\mathbf{v}_3)\}}{2} + \max_i (K_{w3i}) \sqrt{3} \delta_{wmax} \beta_{wmax}
\end{aligned} \right\} \quad (6.85)$$

then (6.55b) is globally input-to-state stable with respect to input  $\mathbf{U}_1, \mathbf{x}_1$  and  $\mathbf{x}_2$  and state  $\mathbf{x}_3(t)$  remains bounded below a value which corresponds to its boundary layer  $\|\mathbf{x}_3(t)\| \leq \|\mathbf{x}_{3b}(t)\|, \forall t \geq 0$ .

*Proof:* Similar proof as described in Theorem 6.5

*Theorem 6.6:* As the global leader is globally input-to-state stable with respect to  $\mathbf{U}_1$ , first follower is globally input-to-state stable with respect to  $\mathbf{x}_1$  and  $\mathbf{U}_1$  and ordinary follower is globally input-to-state stable with respect to  $\mathbf{x}_1, \mathbf{x}_2$  and  $\mathbf{U}_1$ , then entire system of global leader, first follower and ordinary Follower in a CFMP formation is input-to-state stable with respect to  $\mathbf{U}_1$ .

*Proof:* Theorem is direct consequences of Theorem 6.4 and Theorem 6.5 with the help of Theorem 6.3.

## 6.7 Results and Discussion

For simplicity, the triangular formation of three AUVs namely GB, FF, OF-1 are taken consideration as shown in Fig 5.14, for simulation. The distance variables among GB, FF and OF-1 are  $d_1, d_2, d_3$ . It is assumed that the global leader AUV needs to track the sinusoidal trajectory of eq (4.22) in chapter-4 which is given as follows

$$\left. \begin{array}{l} x(t) = 0.03t \\ y(t) = \sin(0.03t) \end{array} \right\} \quad (6.86)$$

Table 6.1: Information about initial state and initial error in state of global leader

	x-position	y-position	orientation	Surge velocity	Sway velocity	Angular velocity
Initial state	2	1	1.4720	0.1044	-0.0399	-0.0172
Initial error in state	12.02	12.985	0.003	0.1454	0.0547	0.0341

Table 6.2: Information about desired distances and initial errors in distances

Distance variables	$d_1$	$d_2$	$d_3$
Desired distances	10	12	14
Initial error in distances	4	3.5	4

Table 6.3 Values of parameters of controllers for different controller

Gains →				
Controller ↓	$K_p$	$K_d$	$K_s$	$K_w$
Global leader	$diag[1000,1000,1000]$	$diag[1200,1200,1200]$	$diag[400,400,100]$	$diag[1.4,1.5,.3]$
First follower	$diag[1080,1080,900]$	$diag[1240,1220,1200]$	$diag[450,450,120]$	$diag[1.4,1.5,.3]$
Ordinary follower	$diag[1080,1080,900]$	$diag[1230,1230,1100]$	$diag[430,420,110]$	$diag[1.4,1.5,.3]$

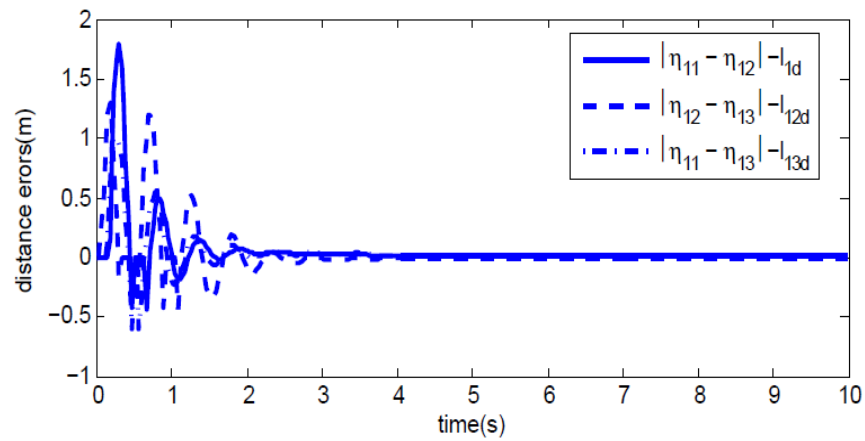


Fig.6.6:Distance errors among AUVs vs.time

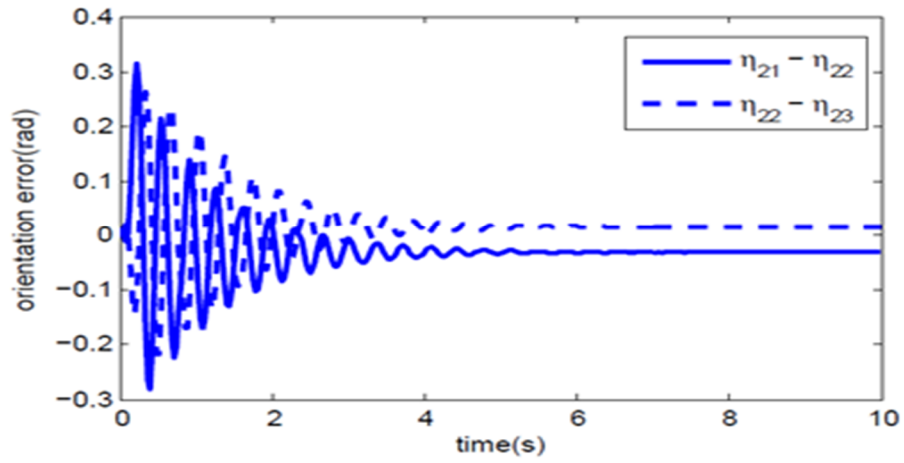


Fig.6.7:Error in orientations among AUVs vs.time

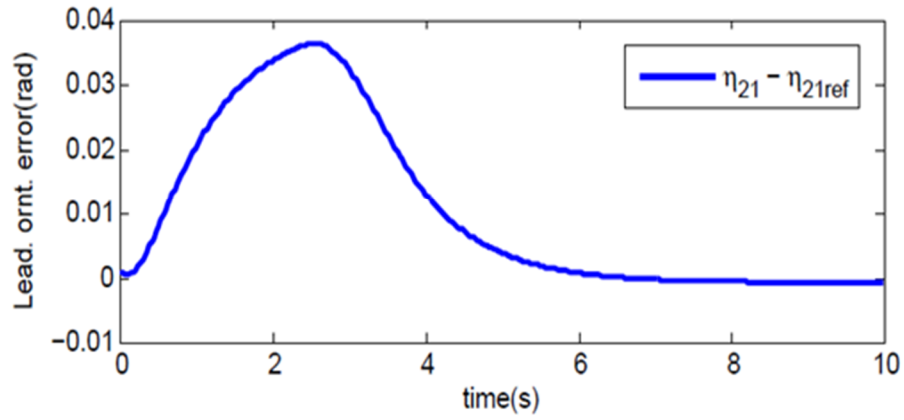


Fig.6.8: Orientation error of leader vs. time

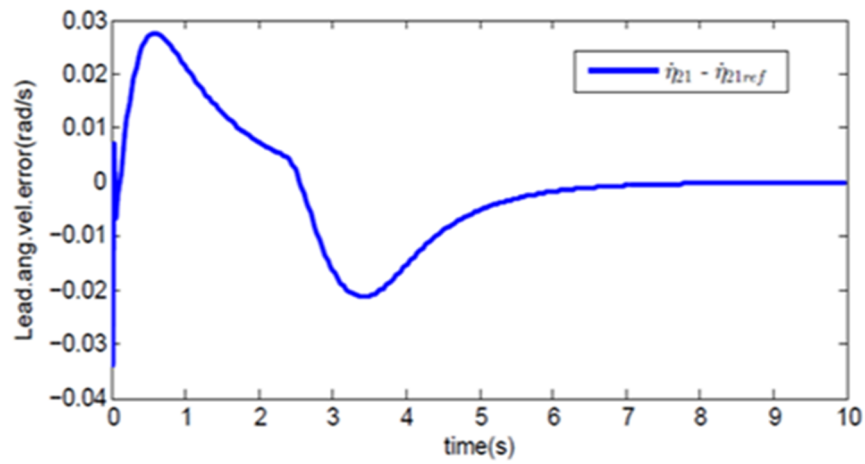
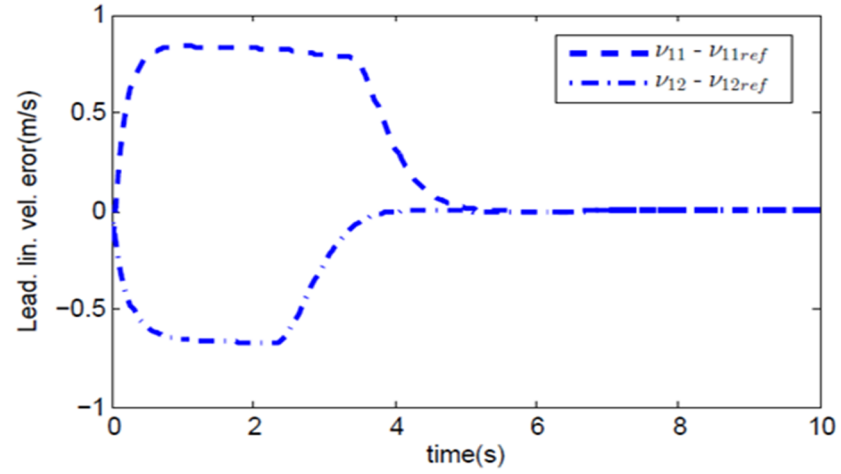


Fig 6.9:Error in angular velocity of leader vs. time



6.10: Error in linear velocities of leader vs. time

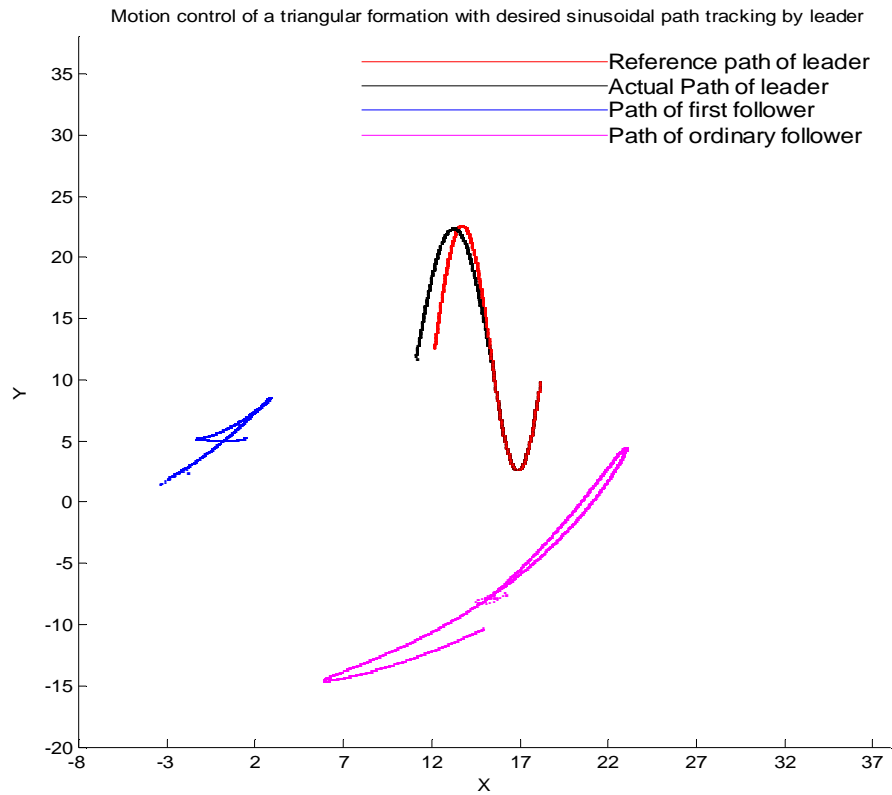


Fig.6.11 Tracking of sinusoidal path by global leader and corresponding generated trajectory tracking of first follower and ordinary follower-1 in a CFMP formation

From the simulation of three AUVs in a formation it is concluded that the desired distances are maintained during the course of motion of group of AUVs as the simulation envisages distance errors (Fig 6.6) converge to a very small value around zero. Orientation errors (Fig 6.7) among GB and FF and FF and PF-1 also converge to a narrow region around zero finally within a short interval of time. The leader also successfully follows its desired orientation (Fig 8) angular velocity (Fig 6.9) and linear velocities (Fig 6.10). Therefore, SM-NPID with BI and BD efficiently works to achieve desired formation and to maintain it during course of motion for  $\forall t \geq 0$ . In Fig 6.11, it is observed that for a successful desired sinusoidal path tracking by global leader, the other followers also track their corresponding generated paths successfully to maintain desired distance preserving Cycle Free Minimally Persistent formation of three AUVs.

## 6.8 Chapter Summary

In this chapter, a new Sliding Mode Nonlinear PID with BI and BD controller has been developed for tracking of the reference by the global leader AUV and corresponding to the generated trajectory tracking by the followers in a cycle free minimally persistent formation of multiple AUVs. This proposed algorithm has been verified for cooperative formation control of three AUVs. From the simulation results envisage that followers track their desired configurations at every instant of time corresponding to tracking of a desired sinusoidal path by the global leader without breaking of formation structure.



# Chapter 7

## Conclusion and Suggestions for Future Work

### 7.1 Overall Conclusions of the Thesis

The thesis has first developed, a robust set-point controller namely N-PID with BI and BD in chapter 3 which has been applied to AUV. The stability of this controller has been verified considering parametric uncertainties existing in the dynamic model of AUV and actuators with specific torque constraints. From the simulation studies it has been verified that this controller works well in the face of parametric uncertainties and actuators' torque limitation.

Secondly, the thesis has developed a robust tracking controller, namely Sliding Mode Nonlinear PID with Bounded Integral and Bounded Derivative in chapter 4. This controller has been applied on AUV for tracking a desired path. The stability of the proposed SM-N-PID controller with BI and BD has been proved with the assumption that parametric uncertainties in the dynamic model of AUV and actuators' torque constraints. From the obtained results it is envisaged that SM-N-PID controller with BI and BD provides efficient performances while tracking a desired sinusoidal path in face of uncertainties and actuators' torque constraints.

Control input demand of the proposed controllers namely N-PID controller with BI and BD and SM-N-PID controller with BI and BD; is reduced that arises due to the upper bounds of parameter matrices of AUV dynamics for tuning the gains. This is accomplished by considering the parameters of nonlinear functions in relation with gains of the controller such that the control demand does not go beyond the specified limit of actuator. Moreover Nonlinear PID controller

with BI and BD and SM-N-PID controller with BI and BD provide very good transient and steady state responses meeting the desired criteria of less settling time, less overshoot, which are essential requirements for achievement of useful performance of an AUV in underwater scenario.

In chapter 5, the formation of group of point agents has been modeled using the Cycle Free Minimally Persistent directed graph where only one-way communication among agents is required. The implementation of this graph has been accomplished based on shortest or minimized path. These facilitate the development of control algorithm for entire formation with lesser requirements of communication and energy compared to two-way communication in undirected graph model. Each agent generates its velocity control inputs estimated from the position errors between its final and current positions at each instant. Simulation envisages that for a desired trajectory tracking by leader, each participating agent in the CFMP formation accurately tracks its corresponding generated trajectory by applying the above velocity control inputs.. Next, the above implementation scheme of CFMP formation has been applied to a group of AUVs where a model based controller exhibits efficient performances during the course of the motion of the above CFMP formation of AUVs.

In chapter 6, SM-N-PID controller with BI and BD has been deployed to each AUV which is applied in a CFMP formation. A detailed analysis of the input-state stability based on the formulation of cascaded AUVs in a CFMP formation has been presented. From the obtained results it is observed that SM-N-PID controller with BI and BD exhibits superior performances for large initial deviation in desired distances among AUVs.

## **7.2 Contributions of the Thesis**

The thesis has following contributions. In chapter 3, a set-point controller namely a Nonlinear

PID with BI and BD has been proposed for an AUV. This controller copes up with the parametric uncertainties in the dynamic model of the AUV. It also overcomes the problems of saturation of actuator due to high demand of control effort to achieve stable motion in face of uncertainties in hydrodynamic parameters. Complete stability of the above controllers has been proved considering the motion of AUV in two dimensional plane. Simulation using MATLAB R2012a has been pursued to compare the performance of proposed N-PID controller with BI and BD over existing Nonlinear PID controller considering the time domain specifications such as overshoot, convergence time to desired state under specified limit of parameter variation and torque produced by the actuators.

In chapter 4, a Sliding Mode Nonlinear PID controller with BI and BD has been proposed for trajectory tracking of an AUV. Similar to the set point controller developed in chapter 3, this controller also successfully overcomes the parametric uncertainties in the dynamics of an AUV and suppresses the inherent problem of limitation in torque producing capability of actuators. The proposed controller is proved to be more efficient than the existing Sliding Mode nonlinear PID controller without Bounded Integral and Bounded Derivative in terms of less overshoot, convergence time to the desired state under the specified limit of parameter variation and actuator torque constraints. Performance of the proposed controller i.e. SM-N-PID controller with BI and BD has been verified through simulation for which AUV is intended to track a desired sinusoidal path.

Moreover, the proposed controllers namely N-PID with BI and BD and SM-N-PID with BI and BD in chapter 3 and chapter 4 use a nonlinear function for velocity errors in the derivative part of the controllers which further reduces for limiting the torque generation and subsequently possibility of reducing actuator saturation effects.

In the chapter 5, a trajectory tracking controller has been proposed for tracking a desired trajectory by the global leader in a Cycle Free Minimally Persistent Formation of multiple autonomous point agents. Simulation results envisage that proposed position-error based controller provides efficient tracking performance while the global leader tracks straight line, circular and sinusoidal path. The desired distances are maintained among the agents after every fixed interval of time during the motion in non-time-critical fashion.

In chapter 6, stability of a CFMP formation of AUVs in a triangular formation is analyzed by formulating the entire formation as a combination of several cascaded AUV pairs, where each AUV uses Sliding Mode Nonlinear PID with Bounded Integral and Bounded Derivative designed in chapter 4. The notion of input-to-state stability has been exploited for pursuing direct Lyapunov analysis of the above cascaded AUV pairs. The global input to state stability for motion control of AUVs in the said formation is proved in respect of input (desired velocity) of the global leader.

### **7.3 Suggestions for Future Work**

***Control design for three dimensional motion of AUVs:*** Controllers proposed in chapter 3 and chapter 4 i.e. N-PID controller with BI and BD and SM-N-PID controller with BI and BD may then be extended to a three dimensional motion (3D) of the AUV. Further, selection of controller gains in these controllers for ensuring complete stability of the AUV system is a challenging task as in the 3D motion several limitations arise in the angular motion of AUV.

***Generalization of input to state analysis:*** Generalization of the proposed input-to-state stability based analysis of Cycle Free Minimally Persistent formation can be extended to a large number of AUVs rather than considering only three AUVs in a triangular formation.

## APPENDIX

**A.1:** Based on the assumption of  $\pm p\%$  variation in values of a parameters of AUV the entries of  $M$  matrix may be given below

$$M|_{uncertain} = diag \left[ m \pm pm - (X_{\dot{u}} \pm pX_{\dot{u}}), m \pm pm - (Y_{\dot{v}} \pm pY_{\dot{v}}), I_z \pm pI_z - (N_{\dot{\omega}} \pm pN_{\dot{\omega}}) \right] \quad (A1.1)$$

Element-wise maximum values of  $M$ , are

$$M_{11max} = m + pm - (X_{\dot{u}} - pX_{\dot{u}}), M_{22max} = m + pm - (Y_{\dot{v}} - pY_{\dot{v}}), M_{33max} = I_z + pI_z - (N_{\dot{\omega}} - pN_{\dot{\omega}}) \quad (A1.2)$$

**A.2:** Based on the assumption of  $\pm p\%$  variation in values of a parameters of AUV the entries of  $D(v)$  matrix may be given below

$$D(v)|_{uncertain} = \begin{bmatrix} X_u \pm pX_u + (X_{u|u|} \pm pX_{u|u|})|u| & 0 & 0 \\ 0 & Y_v \pm pY_v + (Y_{v|v|} \pm pY_{v|v|})|v| & 0 \\ 0 & 0 & N_{\omega} \pm pN_{\omega} + (N_{\omega|\omega|} \pm pX_{\omega|\omega|})|\omega| \end{bmatrix}$$

$$D_{11max} = X_u + pX_u + (X_{u|u|} + pX_{u|u|})|\pm u_{max}|, D_{22max} = Y_v + pY_v + (Y_{v|v|} + pY_{v|v|})|\pm v_{max}|,$$

$$D_{33max} = N_{\omega} + pN_{\omega} + (N_{\omega|\omega|} + pX_{\omega|\omega|})|\pm \omega_{max}|$$

$$D_{11min} = X_u - pX_u + (X_{u|u|} - pX_{u|u|})|\pm u_{min}|, D_{22min} = Y_v - pY_v + (Y_{v|v|} - pY_{v|v|})|\pm v_{min}|,$$

$$D_{33min} = N_{\omega} - pN_{\omega} + (N_{\omega|\omega|} - pX_{\omega|\omega|})|\pm \omega_{min}|$$

**A.3:** The vector  $C(m, X_{\dot{u}}, Y_{\dot{v}}, x)y, \forall x, y \in \mathfrak{R}^3$ , can be expressed in the form below

$$C(m, X_{\dot{u}}, Y_{\dot{v}}, x)y = \begin{bmatrix} x^T C_1(m, Y_{\dot{v}})y \\ x^T C_2(m, X_{\dot{u}})y \\ x^T C_3(Y_{\dot{v}}, X_{\dot{u}})y \end{bmatrix}, \quad \dots\dots\dots(\text{A3.1})$$

where,  $C_1(m, Y_{\dot{v}}), C_2(m, X_{\dot{u}}), C_3(Y_{\dot{v}}, X_{\dot{u}})$  are symmetric matrices. Their expressions are mentioned below

$$C_1(m, Y_{\dot{v}}) = \begin{bmatrix} 0 & 0 & 0 \\ 0 & 0 & \frac{-m+Y_{\dot{v}}}{2} \\ 0 & \frac{-m+Y_{\dot{v}}}{2} & 0 \end{bmatrix}, C_2(m, X_{\dot{u}}) = \begin{bmatrix} 0 & 0 & \frac{-X_{\dot{u}}+m}{2} \\ 0 & 0 & 0 \\ \frac{-X_{\dot{u}}+m}{2} & 0 & 0 \end{bmatrix}$$

$$C_3(X_{\dot{u}}, Y_{\dot{v}}) = \begin{bmatrix} 0 & \frac{X_{\dot{u}}-Y_{\dot{v}}}{2} & 0 \\ \frac{X_{\dot{u}}-Y_{\dot{v}}}{2} & 0 & 0 \\ 0 & 0 & 0 \end{bmatrix}. \quad \dots\dots\dots(\text{A3.2})$$

From (A3.1), the norm  $\|C(m, X_{\dot{u}}, Y_{\dot{v}}, x)y\|^2$  of vector  $C(m, X_{\dot{u}}, Y_{\dot{v}}, x)y$  is

$$\|C(m, X_{\dot{u}}, Y_{\dot{v}}, x)y\|^2 = \sum_{l=1}^3 (x^T C_l(m, x_{\dot{u}}, Y_{\dot{v}})y)^2 = \sum_{l=1}^3 |x^T C_l(m, X_{\dot{u}}, Y_{\dot{v}})y|^2 \leq \left[ \sum_{l=1}^3 \|C_l(m, X_{\dot{u}}, Y_{\dot{v}})\|^2 \right] \|x\|^2 \|y\|^2. \quad \dots\dots\dots(\text{A3.3})$$

(A3.3) is true as for any two vectors  $x$  and  $y$  and dimensionally matched square matrix  $P$ ,

$$|x^T P y| \leq \|P\| \|x\| \|y\|. \quad \text{As } C_l(m, X_{\dot{u}}, Y_{\dot{v}}), l = 1, 2, 3, \text{ are symmetric matrices, therefore,}$$

$$(\lambda_{\min} \{C_l\})^2 \leq \|C_l(m, X_{\dot{u}}, Y_{\dot{v}})\|^2 \leq (\lambda_{\max} \{C_l\})^2 \quad \dots\dots\dots (\text{A3.4})$$

$$\text{Thus, } \left[ \sum_{l=1}^3 \|C_l(m, X_{\dot{u}}, Y_{\dot{v}})\|^2 \right] \leq \sum_{l=1}^3 [\lambda_{\max}(C_l)]^2 \leq \sqrt{3} \max[\lambda_{\max}\{C_1\}, \lambda_{\max}\{C_2\}, \lambda_{\max}\{C_3\}] = C_{\max} \quad \dots(\text{A3.5})$$

and

$$\left[ \sum_{l=1}^3 \|C_l(m, X_{\dot{u}}, Y_{\dot{v}})\|^2 \right] \geq \sum_{l=1}^3 [\lambda_{\min}(C_l)]^2 \geq \sqrt{3} \min[\lambda_{\min}\{C_1\}, \lambda_{\min}\{C_2\}, \lambda_{\min}\{C_3\}] = C_{\min} \quad \dots(\text{A3.6})$$

$\lambda_{\min}\{C_l\}$  and  $\lambda_{\max}\{C_l\}, \forall l$  can be found out in same way as discussed in case of  $M$  in A1.

From (A3.3)

$$C_{\min} \|x\| \|y\| \leq \|C(m, X_{\dot{u}}, Y_{\dot{v}}, x) y\| C_m \|x\| \|y\| \quad \dots(\text{A3.7})$$

#### A.4: Proof of Lemma 3.1(iii)

From Lemma 3.1 (i),

$$\text{If } \|x\| < \|\beta\|, \|f(x)\| \leq \delta_{\max} \|x\| \Rightarrow \|f(x)\|^2 \leq \delta_{\max}^2 \|x\|^2 \Rightarrow \sigma_1 \|x\|^2$$

$$\text{If } |x_i| \geq |\beta_i|, \forall i \Rightarrow \sqrt{n} \beta_{\min} \leq \|x\|,$$

$$\|f(x)\| \leq \sqrt{n} \delta_{\max} \beta_{\max} \Rightarrow \|f(x)\|^2 \leq n \delta_{\max}^2 \beta_{\max}^2 \leq \frac{\delta_{\max}^2 \beta_{\max}^2}{\beta_{\min}^2} n \beta_{\min}^2 \leq \frac{\delta_{\max}^2 \beta_{\max}^2}{\beta_{\min}^2} \|x\|^2 \leq \sigma_2 \|x\|^2$$

#### A.5: Proof of Lemma 3.2

Case I: When  $\forall x_i \in R: |x_i| < \beta_i$ , for upper and lower limits of  $\int f_i(x) dx$  and  $f_i^2(x_i)$  one has

$$\frac{\delta_i x_i^2}{2} \geq \int f_i(x_i) dx_i \geq \frac{\alpha_i x_i^2}{2} \text{ and } \delta_i^2 x_i^2 \geq f_i^2(x_i) \geq \alpha_i^2 x_i^2 \quad \dots(\text{A5.1})$$

Therefore, for lower limits of (A5.1), following relation holds for  $\kappa_i > 0$

$$\int f_i(x_i) dx_i - \kappa_i f_i^2(x_i) = \frac{\alpha_i x_i^2}{2} - \kappa_i \alpha_i^2 x_i^2 \quad \dots\dots(A5.2)$$

$$\text{Selecting } 0 < \kappa_i \leq \frac{1}{2\alpha_i} \text{ one has } \left( \int f_i(x_i) dx_i - \kappa_i f_i^2(x_i) \right) \geq 0; \text{ for } x \neq 0 \quad \dots\dots(A5.3)$$

For upper limits in (A5.1), following relation holds for  $\zeta_i > 0$

$$\frac{\delta_i x_i^2}{2} - \zeta_i \delta_i^2 x_i^2 = \left( \int f_i(x_i) dx_i - \zeta_i f_i^2(x_i) \right) \quad \dots\dots(A5.4)$$

$$\text{Selecting, } 0 < \zeta_i \leq \frac{1}{2\delta_i} \text{ one has } \left( \int f_i(x_i) dx_i - \zeta_i f_i^2(x_i) \right) \geq 0; \text{ for } x \neq 0 \quad \dots\dots(A5.5)$$

Hence, for any  $\wp_i > 0$  and  $\frac{1}{2\delta_i} \leq \wp_i \leq \frac{1}{2\alpha_i}$ ; one has

$$\left( \int f_i(x_i) dx_i - \wp_i f_i^2(x_i) \right) \geq 0; \text{ for } \forall x_i \in R : |x_i| < \beta_i, \text{ and } x \neq 0 \quad \dots\dots(A5.6)$$

*Case II:* When,  $\forall x_i \in R : |x_i| \geq \beta_i$  for upper and lower limits of  $\int f_i(x_i) dx_i$  and  $f_i^2(x_i)$  one has

$$|\delta_i \beta_i| |x_i| \geq \int f_i(x_i) dx_i \geq |\alpha_i \beta_i| |x_i| \text{ and } \delta_i^2 \beta_i^2 \geq f_i^2(x_i) \geq \alpha_i^2 \beta_i^2 \quad \dots\dots(A5.7)$$

Therefore, for upper limits of (A5.7), following relation holds for  $\kappa_i > 0$

$$\int f_i(x_i) dx_i - \kappa_i f_i^2(x_i) = |\delta_i \beta_i| |x_i| - \kappa_i \delta_i^2 \beta_i^2 \quad \dots\dots(A5.8)$$

$$\text{Selecting, } 0 < \kappa_i \leq \frac{|x_i|}{|\delta_i \beta_i|} \text{ one gets } \left( \int f_i(x_i) dx_i - \kappa_i f_i^2(x_i) \right) \geq 0. \quad \dots\dots(A5.9)$$

For lower limits in (A5.7), following relation holds true for  $\zeta_i > 0$

$$\int f_i(x_i) dx_i - \zeta_i f_i^2(x_i) = |\alpha_i \beta_i| |x_i| - \zeta_i \alpha_i^2 \beta_i^2 \quad \dots\dots(A5.10)$$

$$\text{Selecting, } 0 < \zeta_i \leq \frac{|x_i|}{|\alpha_i \beta_i|}, \text{ one gets } \left( \int f_i(x_i) dx_i - \zeta_i f_i^2(x_i) \right) \geq 0 \quad \dots\dots(A5.11)$$



Hence, for  $\frac{|x_i|}{|\delta_i \beta_i|} \leq \wp_i \leq \frac{|x_i|}{|a_i \beta_i|}$ ; one has

$$\left( \int f_i(x_i) dx_i - \wp_i f_i^2(x_i) \right) \geq 0; \text{for } \forall x_i \in R: |x_i| \geq \beta_i \quad \dots\dots(A5.12)$$

A.6

$$\mathbf{h}_1 = - \left\{ M J^T(\boldsymbol{\eta}) J(\boldsymbol{\eta}_r) \dot{\mathbf{v}}_r + C \left( J^T(\boldsymbol{\eta}) J_r(\boldsymbol{\eta}_r) \mathbf{v}_r \right) J^T(\boldsymbol{\eta}) J_r(\boldsymbol{\eta}_r) \mathbf{v}_r + D(\mathbf{v}) J^T(\boldsymbol{\eta}) J_r(\boldsymbol{\eta}) \mathbf{v}_r \right\}$$

For the first term of  $\mathbf{h}_1$  i.e.

$$\mathbf{h}_{11} = M J^T(\boldsymbol{\eta}) J(\boldsymbol{\eta}_r) \dot{\mathbf{v}}_r = \begin{bmatrix} M_{11}(\dot{v}_{11r} \cos \theta_e + \dot{v}_{12r} \sin \theta_e) \\ M_{22}(\dot{v}_{12r} \cos \theta_e - \dot{v}_{11r} \sin \theta_e) \\ M_{33} \dot{v}_{21r} \end{bmatrix} = \begin{bmatrix} X_1 \\ X_2 \\ X_3 \end{bmatrix} = \mathbf{X}, \text{ where, } \theta_e = (\theta - \theta_r) \quad \dots(A.6.1)$$

Differentiating  $F_1$  with respect to  $\theta_e$  assuming  $\dot{v}_{11r}$  and  $\dot{v}_{12r}$  constants,

$$\frac{dX_1}{d\theta_e} = 0 \Rightarrow M_{11}(-\dot{v}_{11r} \sin(\theta_e) + \dot{v}_{12r} \cos(\theta_e)) = 0 \quad \dots\dots(A.6.2)$$

$$\text{From (A.6.1), } \cos(\theta_e) = \pm \frac{\dot{v}_{11r}}{\sqrt{\dot{v}_{11r}^2 + \dot{v}_{12r}^2}} = \pm a, \sin(\theta_e) = \pm \frac{\dot{v}_{12r}}{\sqrt{\dot{v}_{11r}^2 + \dot{v}_{12r}^2}} = \pm b \quad \dots(A.6.3)$$

$$\text{From A.6.2, } \frac{d^2 X_1}{d\theta_e^2} = -M_{11}(\dot{v}_{11r} \cos(\theta_e) + \dot{v}_{12r} \sin(\theta_e)) \quad \dots(A.6.4)$$

With the help of (A.6.3), from (A.6.4), following table is obtained.

Table A.6.1: The value of second derivative of  $F_1$  correspond to  $\cos(\theta_e)$  and  $\sin(\theta_e)$

Sl.No.	$\cos(\theta_e)$	$\sin(\theta_e)$	$\frac{d^2 X_1}{d\theta_e^2}$
1.	$+a$	$+b$	$-M_{11}(\dot{v}_{11r}^2 + \dot{v}_{12r}^2) / \sqrt{\dot{v}_{11r}^2 + \dot{v}_{12r}^2}$
2.	$-a$	$-b$	$M_{11}(\dot{v}_{11r}^2 + \dot{v}_{12r}^2) / \sqrt{\dot{v}_{11r}^2 + \dot{v}_{12r}^2}$
3.	$+a$	$-b$	$M_{11}(\dot{v}_{12r}^2 - \dot{v}_{11r}^2) / \sqrt{\dot{v}_{11r}^2 + \dot{v}_{12r}^2}$
4.	$-a$	$-b$	$M_{11}(\dot{v}_{12r}^2 + \dot{v}_{11r}^2) / \sqrt{\dot{v}_{11r}^2 + \dot{v}_{12r}^2}$

As,  $\left| \pm (\dot{v}_{12r}^2 - \dot{v}_{11r}^2) \right| < \left| (\dot{v}_{11r}^2 + \dot{v}_{12r}^2) \right|$  the values of  $F_1$  takes maximum and minimum when second derivative of it correspond to the value of it in the 2<sup>nd</sup>. and 3<sup>rd</sup>. row of Table 4.1.

$$\text{Therefore, } X_{1max} = \max \left\{ M_{11} \sqrt{\dot{v}_{11r}^2 + \dot{v}_{12r}^2} \right\} = M_{11max} A_{1max} \quad \dots (A.6.5a)$$

$$\text{Similarly, } X_{2max} = \max \left\{ M_{22} \sqrt{\dot{v}_{11r}^2 + \dot{v}_{12r}^2} \right\} = M_{22max} A_{1max} \quad \dots (A.6.5b)$$

$$\text{From (A.6.1), it is clear that } X_{3max} = \max \left\{ M_{33} \dot{v}_{21r} \right\} = M_{33max} A_{2max} \quad \dots (A.6.5c)$$

For the second term of  $\mathbf{h}_1$ , with the help of A.3

$$\mathbf{h}_{12} = C \left( J^T(\boldsymbol{\eta}) J_r(\boldsymbol{\eta}_r) \mathbf{v}_r \right) J^T(\boldsymbol{\eta}) J_r(\boldsymbol{\eta}_r) \mathbf{v}_r = \begin{bmatrix} J^T(\boldsymbol{\eta}) J_r(\boldsymbol{\eta}_r) \mathbf{v}_r C_1(m, Y_{\dot{v}}) J^T(\boldsymbol{\eta}) J_r(\boldsymbol{\eta}_r) \mathbf{v}_r \\ J^T(\boldsymbol{\eta}) J_r(\boldsymbol{\eta}_r) \mathbf{v}_r C_2(m, X_{\dot{u}}) J^T(\boldsymbol{\eta}) J_r(\boldsymbol{\eta}_r) \mathbf{v}_r \\ J^T(\boldsymbol{\eta}) J_r(\boldsymbol{\eta}_r) \mathbf{v}_r C_3(X_{\dot{u}}, Y_{\dot{v}}) J^T(\boldsymbol{\eta}) J_r(\boldsymbol{\eta}_r) \mathbf{v}_r \end{bmatrix} = \begin{bmatrix} Y_1 \\ Y_2 \\ Y_3 \end{bmatrix} \dots (A.6.6)$$

$$\text{Thus, } \begin{bmatrix} Y_1 \\ Y_2 \\ Y_3 \end{bmatrix} \leq \begin{bmatrix} \lambda_{max} \{C_1\} \|\mathbf{v}_r\|^2 \\ \lambda_{max} \{C_2\} \|\mathbf{v}_r\|^2 \\ \lambda_{max} \{C_3\} \|\mathbf{v}_r\|^2 \end{bmatrix} \leq \begin{bmatrix} \lambda_{max} \{C_1\} V_{max}^2 \\ \lambda_{max} \{C_2\} V_{max}^2 \\ \lambda_{max} \{C_3\} V_{max}^2 \end{bmatrix} = \begin{bmatrix} Y_{1max} \\ Y_{2max} \\ Y_{3max} \end{bmatrix} \quad \dots (A.6.7)$$

For the third term of  $\mathbf{h}_1$ , similar to A.6.1

$$\mathbf{h}_{13} = D(\mathbf{v}) J^T(\boldsymbol{\eta}) J_r(\boldsymbol{\eta}) \mathbf{v}_r = \begin{bmatrix} D_{11}(v_{11r} \cos \theta_e + v_{12r} \sin \theta_e) \\ D_{22}(v_{12r} \cos \theta_e - v_{11r} \sin \theta_e) \\ D_{33} v_{21r} \end{bmatrix} = \begin{bmatrix} Z_1 \\ Z_2 \\ Z_3 \end{bmatrix} \quad \dots (A.6.7)$$

$$\text{Hence, } \begin{bmatrix} Z_1 \\ Z_2 \\ Z_3 \end{bmatrix} \leq \begin{bmatrix} D_{11max} V_{1max} \\ D_{22max} V_{1max} \\ D_{33max} V_{2max} \end{bmatrix} = \begin{bmatrix} Z_{1max} \\ Z_{2max} \\ Z_{3max} \end{bmatrix} \quad \dots (A.6.8)$$

$$\text{Consequently, } \mathbf{h}_1 = \mathbf{X} + \mathbf{Y} + \mathbf{Z} \leq \begin{bmatrix} X_{1max} + Y_{1max} + Z_{1max} \\ X_{2max} + Y_{2max} + Z_{2max} \\ X_{3max} + Y_{3max} + Z_{3max} \end{bmatrix} = \begin{bmatrix} h_{11max} \\ h_{12max} \\ h_{13max} \end{bmatrix}$$

## References

- [1] Leibniz Institute of Marine Sciences (IFM-GEOMAR), Kiel, Germany.  
[Online]. Available: <http://www.ifm-geomar.de>.
- [2] National Oceanic Atmospheric Administration(NOAA), United State Department of Commerce, USA. Operated by Wood Whole Oceanographic Institution, USA.[Online]. Available: <http://www.whoi.edu>.
- [3] Hawaii Undersea Research Laboratory(HURL). [Online]. Available: <http://www.soest.hawaii.edu/HURL/subops/piscesV.html>.
- [4] Wood Whole Oceanographic Institution, USA. [Online]. Available: <http://www.whoi.edu>.
- [5] National Oceanic Atmospheric Administration (NOAA), United State Department of Commerce, USA. [Online]. Available: <http://www.oceanexplorer.noaa.gov>.
- [6] Centre for Marine Environmental Sciences, Germany.[Online]. Available: <http://www.marum.de>.
- [7] Japan Agency for Marine-Earth Science and Technology (JAMSTEC), Japan.[Online]. Available: <http://www.jamstec.go.jp>.
- [8] M. S. Triantafyllou and G. S. Triantafyllou, "An efficient swimming machine," *Scientific American*, 272(3), 64-70 (1995).
- [9] C. Alt, B. Allen, T. Austin, N. Forrester, R. Goldsborough, M. Purcell, and R. Stokey, "Hunting for mines with REMUS: A High performance, affordable, free swimming underwater robot," in *Proc. OCEANS, MTS/IEEE 2001 Conference and Exhibition*, vol.1, pp.117-122, 2001.
- [10] Bellingham, J. G., Goudey, C. A., et al. "A Second Generation Survey AUV", *Proc. IEEE*

*Symp. on Autonomous Underwater Vehicle Technology*, July 1994, pp. 148-155.

- [11] Promode R. Bandyopadhyay, "Trends in Bio-Robotic Autonomous Undersea Vehicles", IEEE Journal of Oceanic Engineering, vol. 30, no.1, January 2005.
- [12] Autonomous Systems Laboratory, College of Engineering, University of Hawaii, Manoa, USA. [Online]. Available: <http://eng.hawaii.edu/~index.html>.
- [13] Seamor ROVs, Seamor Marine, Canada. [Online]. Available: [www.seamor.com](http://www.seamor.com)
- [14] R. Gisiner, J. Tague, and P. Moore, ONR Biosonar Program Review, SPAWAR Systems Center, San Diego, CA, Aug. 13–14, 2002.
- [15] Alexander V. Inzartsev, *Underwater Vehicles*, 1<sup>st</sup>. Ed., ISBN 978-953-7619-49-7, 582 pages, Croatia, Austria, I-Tech, January 2009. [Online]. Available: [www.intechweb.org](http://www.intechweb.org).
- [16] Yonghui Hu, Wei Zhao, Long Wang, "Vision-Based Target Tracking and Collision Avoidance for two Autonomous Robotic Fish," IEEE Transactions on Industrial Electronics, vol.56, no.5, May 2009.
- [17] P. R. Bandyopadhyay, "Maneuvering hydrodynamics offish and small underwater vehicles," J. Integrative and Comparative Biology, vol. 42, no. 1, pp. 102–117, 2002.
- [18] Webb, D. C., Simonetti, P. J., Jones, C.P. (2001). "SLOCUM: an underwater glider propelled by environmental energy," IEEE J. Oceanic Engineering, vol. 26, issue 4, pp.447 – 452, Oct. 2001.
- [19] Edward A. Fiorelli, "Cooperative Vehicle Control, Feature Tracking and Ocean Sampling," PhD Dissertation at Department of Mechanical & Aerospace Engineering, Princeton University, USA, November 2005.
- [20] Samuel M. Smith and Stanley E. Dunn, "The Ocean Voyager-II: An AUV Designed for Coastal Oceanography," in *Proc. IEEE AUV'94, Symposium on Autonomous Underwater Vehicle Technology*, pp.139-147, 1994.

- [21] Luke Stutters, Honghai Liu, Carl Tiltman and David J Brown ,”Navigation Technologies for Autonomous Underwater Vehicles”, IEEE Transactions on Systems, Man and Cybernetics-Part C: Applications and Reviews,vol.38, no..4,pp.581 – 589, 2008.
- [22] O.-E. Fjellstad and T. Fossen, “Position and attitude tracking of AUV’s: quaternion feedback approach,” *IEEE J. Ocean. Eng.*, vol. 19, no. 4, pp. 512–518, Oct. 1994.
- [23] F. Alonge, F. D’Ippolito, and F. Raimondi, “Trajectory tracking of underactuated underwater vehicles,” in *Proc. 40th IEEE Conf. Decis. Control 2001*, Orlando, FL, vol. 5, pp. 4421–4426, Jul. 2001.
- [24] Filoktimon Repoulas, Evangelos Papadopoulos,” Planar trajectory planning and tracking control design for underactuated AUVs,” *Ocean Engineering*, Elsevier, vol. 34, Issues 11-12,pp.1650–1667, Elsevier, 2007.
- [25] K.D. Do, J. Pan, Z.P. Jiang,”Robust and adaptive path following for underactuated autonomous underwater vehicles”, *Ocean Engineering*, Elsevier,vol.31,issue 16, pp.1967-1997, 2004.
- [26] M. Breivik and T. Fossen, “Guidance-based path following for autonomous underwater vehicles,” in *Proc. MTS/IEEE OCEANS 2005*, Washington, DC, Sep., vol. 3, no. 4, pp. 2807–2814,2005.
- [27] L. Lapierre, D. Soetanto, and A. Pascoal, “Nonlinear path following with applications to the control of autonomous underwater vehicles,” in *Proc.42nd IEEE Conf. Decis. Control*, Maui, HI, vol. 2, pp. 1256–1261, Dec. 2003.
- [28] Daniel J. Stilwell and Bradley E. Bishop, “Platoon of Underwater Vehicles”, *IEEE Control System Magazine*,vol.20,issue 6,pp.45-52, December 2000.

- [29] A. Pedro Aguiar, Jo˜ao P. Hespanha, Antˆonio M. Pascoal “Switched seesaw control for the stabilization of underactuated vehicles” *Automatica*, Elsevier, vol.43, issue 12, pp.1997–2008, 2007.
- [30] A. Aguiar and A. Pascoal, “Dynamic positioning and way-point tracking of underactuated AUVs in the presence of ocean currents,” in *Proc. 41<sup>st</sup> IEEE Conference on Decision and Control*, Las Vegas, NV, Dec. 2002, vol. 2, pp. 2105–2110.
- [31] C.A. Woolsey, L. Techy “Cross-track control of a slender, underactuated AUV using potential shaping”, *Ocean Engineering*, Elsevier, Issue 36, pp.82-91, 2009.
- [32] S. Li, X.P. Hou, C.C. Cheah, “Adaptive Region Tracking Control for Autonomous Underwater Vehicle,” in *Proc. 2010 11<sup>th</sup> Intl. Conf. on Control, Automation, Robotics and Vision*, pp. 2129-2134, Singapore, 7<sup>th</sup>-10<sup>th</sup> December 2010
- [33] M. Feezor, F. Sorrell, P. Blankinship, and J. Bellingham, “Autonomous Underwater Vehicle homing/docking via electromagnetic guidance,” *IEEE J. Ocean. Eng.*, vol. 26, no. 4, pp. 515–521, Oct. 2001.
- [34] P. Jantapremjit and P. Wilson, “Control and guidance for homing and docking tasks using an autonomous underwater vehicle,” in *Proc. IEEE/RSJ Intl. Conf. Intell. Robots Syst.*, San Diego, CA, Oct. 2007, pp. 3672–3677.
- [35] Y. Park, H.H. Jun, P.M. Lee, F.Y. Lee and J.-H. Oh, “Experiment on underwater docking of an autonomous underwater vehicle ‘ISiMI’ using optical terminal guidance,” in *Proc. OCEANS 2007*, Vancouver, BC, Canada, Jun., vol. 2, pp. 1–6.
- [36] Pedro Batista, Carlos Silvestre, Paulo Oliveira, “A Sensor-Based Controller for Homing of Underactuated AUVs,” *IEEE Transactions on Robotics*, Vol. 25, No. 3, June 2009.

- [37] E. Coste-Maniere, H. H. Wang, and A. Peuch, "Control architectures: What's going on?" in *Proc. US-Portugal Workshop on Undersea Robotics and Intelligent Control*, Lisbon, Portugal, Published by the University of S.W. Lousiana, 1995, pp. 54–60.
- [38] P. Ridao, J. Battle, J. Amat, and G. N. Roberts, "Recent trends in control architectures for autonomous underwater vehicles," *Int. J. Syst. Sci.*, vol.30, no. 9, pp. 1033–1056, 1999.
- [39] K. P. Valavanis, D. Gracanin, M. Matijasevic, R. Kolluru, and G. A. Demetriou, "Control architectures for autonomous underwater vehicles," *IEEE Contr. Syst. Mag.*, vol. 17, no. 6, pp. 48–64, 1997.
- [40] P. Ridao, J. Yuh, K. Sugihara, and J. Battle, "On AUV control architecture," in *Proc. Int. Conf. Robots and Systems*, vol.2, pp.855-860, Japan, 2000.
- [41] M. Carreras, J. Battle, P. Ridao, "An overview on behavior-based methods for AUV-control," in *Proc. MCMC 2000, 5th. IFAC Conf. on Maneuvering and Control of Marine Crafts*, Alborg, Denmark, 2000.
- [42] A. M. Meystel and J. S. Albus, *Intelligent Systems, Architecture, Design and Control*. New York: Wiley, 2002.
- [43] R. Arkin, *Behavior-Based Robotics*. Cambridge, MA: MIT Press, 1998.
- [44] R. C. Arkin, "Path planning for a vision-based autonomous robot," in *Proc. SPIE Conf. Mobile Robots*, vol.727, pp.240-249, Cambridge, MA, 1986.
- [45] E. Gat, "Reliable goal-directed reactive control for real-world autonomous mobile robots," Ph.D. Thesis, Virginia Polytech. State University, Blacksburg, 1991
- [46] T. I. Fossen, *Guidance and Control of Ocean Vehicles*. 1<sup>st</sup>. Ed., 489 pages, Chichester, Newyork, John Wiley & Sons, 1994
- [47] B. Jalving, "The NDRE-AUV Flight Control System," *IEEE Journal of Oceanic Engineering*, Vol.19, No.4, pp. 497-501, October 1994.

- [48] A. Chellabi, M.Nahon,"Feedback Linearization control of Undersea Vehicles,"in *Proc.OCEANS'93.'Engineering in Harmony with Ocean'*, Vol.1, pp.1410-1451,18-21 Oct.1993.
- [49] Ola-Erik Fjellstad and Thor I. Fossen,"Position and attitude Tracking of AUV's: A Quaternion Feedback Approach,"*Journal of Oceanic Engineering*, Vol.19, No.4, October 1994.
- [50] A.Trebi-Ollennu, B.White, "Nonlinear Robust Control Designs for a Remotely Operated Underwater Vehicle Depth Control System," in *Proc.of International Mechanical Engineers*, pp.201-214, Vol.210, 1996.
- [51] B.White,"Robust Control of Unmanned Underwater Vehicle," in *Proc. of the 37<sup>th</sup>. IEEE Conf. on Decision & Control*, pp.2533-2534, Tampa, Florida USA, December, 1998.
- [52] T.Koh, M.Lau,E.Low,G.Seet,S.Swei, P.Cheng,"A study of the Control of an Underactuated Underwater Robotic Vehicle," in *Proc. of the 2002 IEEE/RSJ Intl. Conf. on Intelligent Robots and Systems*, Vol.2,pp.2049-2054,Lausanne, Switzerland,Sept.30-Oct.5,2002.
- [53] J. Park, W. Chung, J. Yuh,"Nonlinear  $H_\alpha$  Optimal PID Control of Autonomous Underwater Vehicles," in *Proc. of IEEE International Symposium on Underwater Technology*, pages 193-198, 23rd. -26th. May 2000, Tokyo, Japan.
- [54] T.Chatchanayuenyong, M. Parnichkun,"Time Optimal Hybrid Sliding Mode-PI Control for an Autonomous Underwater Robot," *International Journal of Advanced Robotic Systems*, Vol.5, No.1, 2008, ISSN1729-8806, pp.91-98.
- [55] S. Arimoto, F. Miyazaki, Stability and robustness of PID feedback control for robot manipulators of sensory capability, in: M. Brady, R.P. Paul (Eds.), *Robotics Research First International Symposium*, MIT Press, Cambridge, MA, 1984, pp. 228–235.



- [56] Premysla Herman, "Modified set-point controller for underwater vehicles," *Mathematics and Computers in Simulation*, Elsevier, vol.80, pp. 2317-2328, May, 2010
- [57] V.Parra-Vega, S.Arimoto, Y.H.Liu,"Dynamic Sliding PID Control for Tracking of Robot Manipulators: Theory and Experiments,"*IEEE Transactions on Robotics and Automation*, vol.19, No.6, December 2003.
- [58] David A. Smallwood and Louis L.Whitcomb, "Model-based dynamic positioning of underwater robotic vehicles: theory and experiment," *IEEE Journal of Ocean Engineering*, vol.29 (1), pp.169-186, January, 2004.
- [59] D.R.Yoerger and J.E.Slotline," Robust Trajectory Control of Underwater Vehicles," *IEEE Journal of Ocean Engineering* vol.10 (4), pp.462-470, 1985.
- [60] A. J. Healey and D. Lienard, "Multivariable sliding mode control for autonomous diving and steering of unmanned underwater vehicles," *IEEE J. Oceanic Engineering.*, vol. 18, pp. 327–339, 1993
- [61] D. Macro, A. Healy, R. Mcghee, D. Brutzman, R. Cristi,"Control System, Architecture, Navigtion and Communication Research Using NPS Phoenix Underwater Vehicle," 6<sup>th</sup> Intl. Advanced Robotics Program Workshop on Underwater Robotics, Toulon, France, March 27-29, 1996.
- [62] J. Riedel, A. Healy,"Shallow water Station Keeping of AUVs Using Multi-sensor Fusion for Wave Disturbance Prediction and Compensation," in *Proc. OCEANS'98*,vol.2, pp.1064-1068, 1998.
- [63] M.Innoceti, G.Campa," Robust Control of Underwater Vehicles: Sliding Mode vs. LMI Synthesis," in *Proc.American Control Conference*, vol.5,pp.3422-3426,San Diego, CA, 1999.

- [64] Pan-Mook Lee, Seok-Won Hong, Yong-Kon Lim, Chong-Moo Lee, Bong-Hwan Jeon, Jong Won Park, "Discrete-Time Quasi-Sliding Mode Control of an Autonomous Underwater Vehicle," IEEE Journal of Ocean Engineering, vol.24,vol. 24, no.3, July 1999.
- [65] Fernando Castaños and Leonid Fridman, "Analysis and Design of Integral Sliding manifolds for Systems With Unmatched Perturbations," IEEE Transactions on Automatic Control, vol. 51, no. 5, pp. 853-858,May 2006.
- [66] R. Prasanth Kumar, A. Dasgupta, C.S. Kumar,"Robust trajectory control of underwater vehiclesusing time delay control law," Ocean Engineering, Elsevier, vol.34,pp.842 849,2007.
- [67] M. Triantafyllu and M. Grosenbaugh," Robust Control of underwater Vehicle system with Time Delays,"IEEE Journal of Ocean Engineering, Vol.16, No.1, pp.146-151, January 1991.
- [68] G. Conte, A.Serrani," Global Robust Tracking and Disturbance Attenuation for Unmanned Underwater Vehicle, " in *Proc. of the 1998 IEEE Conf. on Control Applications*, vol.2, pp.1094-1098, Trieste, Italy, 1-4<sup>th</sup> September, 1998.
- [69] D. Boskovic, M Krstic," Global Attitude/Position Regulation for Underwater Vehicles," International Journal of System Science, 1999, vol.30, no.9, pp.939-946.
- [70] A. Menozzi, T. Galiardi," Dynamics and Control of MTV: A Multipurpose Unmanned Underwater Vehicle," in*Proc. of American Control Conference*, vol.1,no.6,pp.70-74, Chicago, Illinois, June 2000.
- [71] C. Wit, E. Diaz, M.Perrier," Nonlinear Control of an Underwater Vehicle/Manipulator with Composite Dynamics," IEEE Transactions on Control System Technologyvol.8,pp.948-960, No.6,November 2006.
- [72] J.Kim, L.Lee, Y.Cho, H.Lee and H. Park, " Mixed $H_\infty/H_2$  control with Regional Pole Placements for Underwater Vehicle Systems," in *Proc. of American Control Conference*, vol.1, no.6, pp.80-84,Chicago,Illinois, June 2000.

- [73] Z.Feng, R.Allen,"  $H_\infty$ Autopilot Design for an Autonomous Underwater Vehicle," in*Proc. of IEEE Intl. Conf. on Control Applications*,vol.1,pp.350-354, Glasgow, Scotland, U.K., September 18-20, 2002.
- [74] Lucia Moreira, C. Guedes Soares " $H_\infty$  and  $H_2$  Designs for Diving and Course Control of an Autonomous Underwater Vehicle in Presence of Waves," *IEEE Journal of Ocean Engineering*, vol.33, no.2, pp.69-88, April, 2008.
- [75] J.Petrich, D.J.Stilwell,"Robust Control for an Autonomous Underwater Vehicle that suppresses pitch and yaw coupling," *Ocean Engineering*,Elsevier, vol.38, no.1,pp.197-204, 2011.
- [76] C.Silvestre, C.Pascoal,"Control of an AUV in the vertical and horizontal planes: system design and test at sea", *Transactions of Institute of Measurement and Control* 19(3), 126-138, 1997.
- [77] Loc, Mai Ba; Choi, Hyeung-Sik; You, Sam-Sang; Kim, Joonyoung; Kim, Yun-Hae, "Mu-Synthesis Depth Controller Design for a Small Autonomous Underwater Vehicle, "Advanced Science Letters," American Scientific Publishers, vol. 15, no.1, pp. 202-209(8), August 2012.
- [78] Cedric L. Logan"A Comparison Between H-Infinity/Mu-Synthesis Control and Sliding-Mode Control for Robust Control of a Small Autonomous Underwater Vehicle," in *Proc. of 1994 IEEE Symp. on Autonomous Underwater Vehicle Technology, AUV'94*, pp-399-416, Cambridge, MA, 19-20 Jul 1994.
- [79] M.Innoceti, G.Campa," Robust Control of Underwater Vehicles: Sliding Mode vs. LMI Synthesis", *American Control Conference*, vol. 5, pp.3422-3426, San Diego, CA, 1999.
- [80] Robert Playter, "Control System Design Using  $H_\infty$  Optimization" Master of Science thesis, Massachusetts Institute of Technology, USA, July 7, 1988.

- [81] J. Biggs, W. Holderbaum, "Optimal Kinematic Control of an Autonomous Underwater Vehicle," *IEEE Transactions on Automatic Control*, vol.54, no.7, pp.1623-1626, July 2009.
- [82] T. W. McLain and R. W. Beard, "Successive galerkin approximations to the nonlinear optimal control of an underwater robotic vehicle," in *Proc. 1998 IEEE Int. Conf. on Robotics and Automation*, vol.1, pp.762 – 767, 16-20th May 1998, Leuven, Belgium.
- [83] R. Prasanth Kumar, A. Dasgupta, C.S. Kumar, "Real-time optimal motion planning for autonomous underwater vehicles," *Ocean Engineering*, Elsevier, vol.32, no.11-12, pp.1431–1447, 2005.
- [84] H. Yuan Z. Qu, "Optimal real-time collision-free motion planning for autonomous underwater vehicles in a 3D underwater space," *IET Control Theory Appl.*, 2009, vol. 3, no. 6, pp. 712–721.
- [85] A. J. Healey, "Model-based maneuvering controls for autonomous underwater vehicles," *ASME Journal of Dynamic Systems, Measurement, and Control*, 114(4):614–622, December 1992.
- [86] T.I. Fossen, S.I. Sagatun, "Adaptive Control of Nonlinear Underwater Robotic Systems," in *Proc. of IEEE Intl. Conf. on Robotics and Automation*, vol.2, Sacramento, California, Vol.2, pp.1687-1695, April, 1991.
- [87] Sadegh, N. and Horowitz, R., "Stability Analysis of a Class of Adaptive Controllers for Robotic Manipulators," *Intl. Journal of Robotics Research*, vol.9, no.3, pp.74-94, 1990.
- [88] G. Antonelli, S. Chiaverini, N. Sarkar, M. West, "Adaptive Control of an Autonomous Underwater Vehicle: Experimental results on ODIN," *IEEE Transactions on Control System Technology*, vol. 9, no.5, pp.756-765, 2001.

- [89] X.Li, S.P.Hou, C.C.Cheah," Adaptive Region Tracking Control for autonomous Underwater Vehicle," in *Proc.IEEE 2010 11th. Intl. Conf. on Control, Automation, Robotics and Vision*, pp.2129-2134,Singapore,7-10th. December 2010.
- [90] S.K. Choi, J.Yuh," Experimental Study on a Learning Control System with Bound Estimation for Underwater Robots," in *Proc of the Intl. Conf. on Robotics and Automation*, vol.3, pp.2160-2165, April, 1996.
- [91] Side Zhao, "Advanced Control of Autonomous Underwater Vehicles," a PhD dissertation, University of Hawaii,Honolulu, USA August 2004.
- [92] Jean-Jacques E. Slotine and Weiping Li,"On the Adaptive Control of Robot Manipulators," *International Journal of Robotics Research*, vol.3,no.6,pp49-59,1st.September, 1987.
- [93] Junku Yuh,"A Neural Net Controller for Underwater Robotic Vehicle,"*IEEE Ocean Engineering Journal*, vol.15, no.3, pp.161-166,July 1990.
- [94] J.Yuh,"Learning Control for Underwater Robotic Vehicles," *IEEE Control Systems*, vol.14,no.2,pp.39-46, April 1994.
- [95] N.Seube," Neural Learning Rules for Control: Application to AUV Tracking Control," 1991 in *Proc. IEEE Conf. on Neural Networks for Ocean Engineering*, pp.185-196,August 15-17, 1991.
- [96] K.Benugopal, R.Sudhakar,"Online Learning Control of Autonomous Underwater Vehicles Using Feedforward Neural Network," *IEEE Journal of Ocean Engineering*, vol.17, no.4, pp.308-319,October1992
- [97] R.Sutton, C.Johnson, G.Roberts,"Depth Control of an Unmanned Underwater Vehicle Using Neural Networks," in*Proc. of the OCEANS'94*, vol.3,pp. III/121-III/125,13-16<sup>th</sup>. September,1994.

- [98] K. Asakawa N.Kato,Y.Ito,J.Kojima,S.Takagi,Y.Shirasaki,N. Kato, "Control Performance of Autonomous Underwater Vehicle' AQUA EXPLORER 1000' for Inspection of Underwater Cables," in *Proc. of OCEAN '94, Ocean Engineering for Today's Technology and Tomorrow's Preservation*, pp.135-140. Vol.1, 1994.
- [99] P. DeBietto,"Fuzzy Logic for Depth Control of Unmanned Undersea Vehicles," *IEEE Journal of Ocean Engineering*, vol.20, no.3, July 1995.
- [100] J.Guo, S.Huang,"Control of an Autonomous Underwater Vehicle Testbed Using Fuzzy Logic and Genetic Algorithms," in*Proc. of 1996 Symposium on Autonomous Underwater Vehicle Technology*, pp.485-489, June 2-6, 1996.
- [101] W.Lee, G.Kang,"A Fuzzy Model-based Controller of an Underwater Vehicle under the Influence of Thruster Dynamics," in*Proc. of the 1998 IEEE Intl. Conf. on Robotics and Automation*,vol.1, pp.750-755, Leuven, Belgium, May 1998.
- [102] M. Carreras, J. Batlle, P. Ridaoand G.N. Roberts, "An Overview of Behavior-based Methods of AUV Control," in *Proc.MCMC2000, 5th IFAC Conf. on Maneuvering and Control of Marine Crafts*, pp.141-146,Aalborg, Denmark, 23-25 August, 2000.
- [103] Mark Carreras Perez, "A Proposal of a Behavior-Based Control Architecture with Reinforcement Learning for an Autonomous Underwater Robot," PhD Thesis, Dept. of Electronics, Informatics and Automation, University of Gerona, Catalonia, Spain,2003.
- [104] J K Rosenblatt, S B Williams, H Durrant-Whyte,"Behavior-Based Control of Autonomous Underwater Exploration," *International Journal of Information Sciences*, vol 145, no.1-2, pp 69-87, 2002.
- [105] Junaed Sattar, Philippe Giguère, Gregory Dudek,"Sensor-based Behavior Control for an Autonomous Underwater Vehicle," *International Journal of Robotics Research*, June vol. 28 no. 6701-713,2009.

- [106] Naomi Ehrich Leonard, "Geometric Methods for Robust Stabilization of Autonomous Underwater Vehicles," in *Proc. IEEE AUV'96 on Autonomous Underwater Vehicle Technology*, pp.470-476, 1996,
- [107] Francesco Bullo and Andrew D. Lewis. *Geometric Control of Mechanical Systems*. Springer, 2005.
- [108] M. Chyba and R.N. Smith, "A First Extension of Geometric Control Theory to Underwater Vehicles," in *Proc. of the 2008 IFAC Workshop on Navigation, Guidance and Control of Underwater Vehicles*, vol.2, Part 1, Killaloe, Ireland, 2008.
- [109] M. Andonian, D. Cazzaro, L. Invernizzi, M. Chyba, S. Grammatico, "Geometric Control for Autonomous Underwater Vehicles: Overcoming a Thruster failure," in *Proc. 49<sup>th</sup>. IEEE Conf. on Decision and Control*, pp.7051-7056, December 2010, Hilton Atlanta, GA, USA.
- [110] S. Singh, a Sanyal, R. Smith, N. Nordkvist, M. Chyba, "Robust Tracking of Autonomous Underwater Vehicles in the Presence of Disturbance Inputs," in *Proc. of the ASME 28<sup>th</sup>. Intl. Conf. on Ocean, Offshore and Arctic Engineering, OMAE2009*, May 31-June 1 2009, Honolulu, Hawaii.
- [111] T.I. Fossen, Mogens Blanke, "Nonlinear Output feedback Control of Underwater Vehicle Propellers Using Feedback Form Estimated Axial Flow Velocity," *IEEE Journal of Ocean Engineering*, vol.25, No.2, pp.241-255, April 2000.
- [112] Y. Nakamura, S. Savant, "Nonlinear Tracking Control of Autonomous Underwater Vehicles," in *Proc. of 1992 IEEE Intl. Conf. on Robotics and Automation*, vol.3, pp.A4-A9, Nice, France, May 1992.
- [113] J. Guo, F. C. Chiu, S. W. Cheng, Y. J. Joeng, "Motion control and way-point tracking of a biomimetic underwater vehicle," in *Proc. 2002 International Symposium on Underwater Technology*, pp.73-78, Taipei, Taiwan, 2002.

- [114] A. Pedro Aguiar, Jo˜ao P. Hespanha, Antˆonio M. Pascoal, "Switched seesaw control for the stabilization of underactuated vehicles," *Automatica*, Elsevier, vol.43, no.12, pp.1997-2008, Dec.2007.
- [115] A.J. van der Schaft, " $L_2$ -Gain Analysis of Non-linear Systems and Nonlinear state feedback  $H_\infty$ ," *IEEE Transactions on Automatic Control*, vol.37, no.6, pp.770-784, 1992.
- [116] T.W. McLain and R.W.Beard, "Successive galerkin approximations to the nonlinear optimal control of an underwater robotic vehicle," in *Proc. 1998 Intl. Conf. on Robotics and Automation*, 1998, pp.762-767.
- [117] A.Isidori and A. Astolfi, "Disturbance Attenuation and  $H_\infty$ -Control Via Measurement Feedback in Nonlinear Systems," *IEEE Trans. on Automat. Contrl.* vol.37, no.6, pp.1283-1293, 1992.
- [118] R. Cristi, F. Papoulias, A Healy, "Adaptive Sliding Mode Control of Autonomous Underwater Vehicles in Diving Plane," *IEEE Journal of Ocean Engineering*, pp.152-160, vol.15, no.3, July 1990.
- [119] D. Yoerger, J.Slotine, "Adaptive Sliding Mode Control for an Experimental Underwater Vehicle," *Proc. of 1991 IEEE Intl. Conf. on Robotics and Automation*, pp.2746-2751, Sacramento, California, April 1991.
- [120] Mukund Narasimhan, Sahjendra N.Singh, "Adaptive optimal control of an AUV in the dive plane using dorsal fins," *Ocean Engineering*, Elsevier, vol.33, issue 3-4, pp. 404-416, March 2006.
- [121] Antonio Pedro Aguiar and Jo˜ao Pedro Hespanha, "Logic-Based Switching Control for Trajectory-Tracking and Path-Following of Underactuated Autonomous Vehicles with Parametric Modeling Uncertainty," in *Proc. of ACC'04-American Control Conf.*, vol.4, pp.3004-3010, Boston, MA, 30th. June-2<sup>nd</sup>.July 2004.



- [122] F. Chiu, G Guo, C.Huang,"Application of Sliding Mode Fuzzy Controller to the Guidance and Control of an Autonomous Underwater Vehicle," in *Proc. ofUT00*, 2000 Intl. Symposium on Underwater Technology, pp.181-186, Tokyo,Japan,2000.
- [123] J.Guo, F.C.Cjiu, C.Huang,"Design of a Sliding mode Fuzzy Controller for Guidance and Control of an autonomous Underwater Vehicles," *Ocean Engineering*, Elsevier, vol.30,no.16, pp. 2137-2155, Nov.2003.
- [124] F.Song, S.Smith," Design of Sliding Mode Fuzzy Controllers for an Autonomous Underwater Vehicles without System Model," in *Proc. OCEANS 2000 MTS/IEEE Conf. and Exhibition*,vol.2 pp.835-840, Boca Raton, Florida, USA,2000.
- [125] F.Song, S.Smith,"A Comparison of Sliding Mode Fuzzy Controller and Fuzzy Sliding Mode Controller," in *Proc. NAFIPS 2000*, The 19<sup>th</sup> Intl. Conf. of North American Fuzzy Information Processing Society, pp.480-484,Atlanta,USA, 2000.
- [126] Arjuna Balasuriya and Li Cong,"Adaptive Fuzzy Sliding Mode Controller for Underwater Vehicles," in *Proc. 4<sup>th</sup>. Intl. Conf. on Control and Automation (ICCA'03)*, pp.917-921,10th.-12th. June 2003, Montreal, Canada.
- [127] M.Lee, H.Choi,"A Robust Neural Controller for Underwater Robot Manipulators," *IEEE Transactions on Neural Networks*, pp.1465-1470, vol.11, no.6, November 2000.
- [128] T. Chatchanayuenyong, M.Parnichkun,"Neural network based-time optimal sliding mode control for an autonomous underwater robot," *Mechatronics*, Elsevier,vol.16.,issue.8, pp.471-478, 2006.
- [129] T.Kim, J.Yuh.,"A Novel Neuro-Fuzzy Controller for Autonomous Underwater Vehicle," in *Proc. of 2001, IEEE Intl. Conf. on Robotics and Automation*, vol. 3, pp.2350-2355, Seoul,Korea, May,2001.

- [130] C.S. Lee, G.S.Wang, J Yuh, "Self-adaptive neuro-fuzzy systems for autonomous underwater vehiclecontrol," Journal of advanced Robotics, Taylor & Francis, vol.15, issue 5,pp.589-608,2001
- [131] Jeen-Shing Wang and C.S.George Lee," Self-Adaptive Recurrent Neuro-Fuzzy Control of an Autonomous Underwater Vehicle," IEEE Transactions on Robotics and Automation, vol.19, no.2,pp.283-295,April, 2003.
- [132] Ji-Hong Li, Pan-Mook Lee, and Bong-Huan Jun,"A Neural Network Adaptive Controller for Autonomous Diving Control of an Autonomous Underwater Vehicle," Intl. Journal of Control, Automation, Systems, Springer,vol.2, no.3, pp.374-383, September 2003.
- [133] Mark Carreras Perez, "A Proposal of a Behavior-Based Control Architecture with Reinforcement Learning for an Autonomous Underwater Robot," PhD Thesis, Dept. of Electronics, Informatics and Automation, University of Girona, 2003.
- [134] Marc Carreras, Junku Yuh, Joan Batlle, and Pere Ridao, "A Behavior-Based Scheme Using ReinforcementLearning for Autonomous Underwater Vehicles," IEEE Journal of Oceanic Engineering, vol. 30, no. 2, pp.416-427,April, 2005
- [135] Yu Tian, Wei Li, Aiqun Zhang, and Jiancheng Yu, "Behavior-Based Control of an Autonomous Underwater Vehicle forAdaptive Plume Mapping," in *Proc. 2nd Intl. Conf. on Intelligent Control and Information Processing*, IEEE, pp.719-724,2011.
- [136] Przemyslaw Herman "Decoupled PD set-point controller for underwater vehicles," Elsevier, Ocean Engineering, vol.36, issue 6-7, pp.529-534, 2009.
- [137] Y.C. Sun and C.C. Cheah,"Adaptive Setpoint Control for Autonomous Underwater Vehicles," in *Proc. of the 42<sup>nd</sup>. IEEE Conf. on Decision and Control*, vol.2,pp.1262-1267,Maui, Hawaii, USA,9<sup>th</sup>-12<sup>th</sup>. December, 2003.

- [138] Y. Wang, W. Yan J. Li, "Passivity-based formation control of autonomous underwater vehicles," *IET Control Theory and Applications*, vol.6, issue 4, pp.518-525, 1<sup>st</sup> March, 2012.
- [139] S.P.Hou, C.C.Cheah, "Can a simple Control Scheme Work for a Formation Control of Multiple Autonomous Underwater Vehicles," *IEEE Trans. on Automat. Control*, vol.19, no.5, pp.1090-1101, September 2011.
- [140] D. B. Edwards, T.A. Bean, D.L. Odell, M.J. Anderson "A Leader-Follower Algorithm for Multiple AUV Formations," in *Proc. IEEE/OESon Autonomous Underwater Vehicles*, vol. 1, pp. 40-46, 2004.
- [141] Nikolay Burlutskiy, Yaniss Touahami, Beom H. Lee, "Power efficient formation configuration for centralized leader-follower AUVs control," *Journal of Marine Science and Technology*, 7 March 2012, pp. 1-15, doi:10.1007/s00773-012-0167-0.
- [142] Rongxin Cui, Shuzhi Sam Ge, Bernard Voon Ee How, and Yoo Sang Choo "Leader-Follower Formation Control of Underactuated AUVs with Leader Position Measurement," 2009 IEEE Internatl. Conf. on Robot. and Automat. Kobe Internl. Conf. Center, Kobe, Japan, May 12-17, 2009.
- [143] D.Atta, B.Subudhi, M.M.Gupta "Cohesive Motion Control Algorithm for Formation of Multiple Autonomous Agents," *Journal of Robotics*, Hindawi Publishing Corporation, Volume 2010, Article ID 360925, 12 pages, doi:10.1155/2010/360925.
- [144] Daniel J. Stilwell and Bradley E. Bishop, "Platoon of Underwater Vehicles", *IEEE Control System Magazine*, December 2000.
- [145] B.K Sahu, B.Subudhi, B.K.Dash, "Flocking Control of Multiple Autonomous Underwater Vehicles," in *Proc. IEEE INDICON 2012*, pp.257-262, Kochi, India, 7<sup>th</sup>-9<sup>th</sup> December 2012,.

- [146] Rongxin Cui a, ShuzhiSamGe, BernardVoonEeHow, YooSangChoo,” Leader–follower formation control of underactuated autonomous underwater vehicles,” *Ocean Engineering*,Elsevier, vol.37,issue 17-18, pp.1491–1502, Dec.2010.
- [147] A.Nag,S.S.Patel,S.A.Akbar,“Fuzzy Logic Based Depth Control of an Autonomous Underwater Vehicle,” in *ProcIntl. Multi Conf. on Automation, Computing, Control and Compressed Sensing(iMAC4s)*,pp.117-123,Kottayam,2013.
- [148] A. Pedro Aguiar, Reza Ghabcheloo, Antonio M. Pascoal, and Carlos Silvestre,“Coordinated Path-Following Control of Multiple Autonomous Underwater Vehicles,” in *Proc. of the Sixteenth (2007) International Offshore and Polar Engineering Conf. Lisbon, Portugal, July 1-6, 2007.*
- [149] Reza Olfati-Saber, J. Alex Fax, Richard M. Murray, “Consensus and Cooperation inNetworkedMulti-Agent Systems,” in *Proc. of the IEEE*, vol. 95, no. 1, pp.215-233,January 2007.
- [150] Matthew A. Joordens, Mo Jamshidi,”Consensus Control for a System of Underwater Swarm Robots,” *IEEE Systems Journal*, vol. 4, no. 1, pp.65-73, March 2010.
- [151] Edward A. Fiorelli,”Cooperative Vehicle Control, Feature Tracking and Ocean Sampling,”PhD Thesis,Princeton University, USA, November, 2005.
- [152] Edward Fiorelli, Naomi Ehrich Leonard, Pradeep Bhatta, Derek A. Paley, Ralf Bachmayer, David M. Fratantoni, “Multi-AUV Control and Adaptive Sampling in Monterey Bay”, *IEEE Journal of Oceanic Engineering*, Vol. 31, No. 4, pp.935-948,.October, 2006.
- [153] J. Baillieul and A. Suri, “Information patterns and hedgingBrockett’s theorem in controlling vehicle formations,” in*Proc. of the 42nd IEEE Conf. on Decision andControl*, vol. 1, pp. 556–563, December 2003.

- [154] C. Yu, J. M. Hendrickx, B. Fidan, B. D. O. Anderson, and V. D. Blondel, "Three and higher dimensional autonomous formations: rigidity, persistence and structural persistence," *Automatica*, vol. 43, no. 3, pp. 387–402, 2007.
- [155] J. M. Hendrickx, B. D. O. Anderson, J.-C. Delvenne, and V. D. Blondel, "Directed graphs for the analysis of rigidity and persistence in autonomous agent systems," *International Journal of Robust and Nonlinear Control*, vol. 17, no. 10-11, pp. 960–981, 2007.
- [156] Y. Deng, P. P. J. Beaujean, E. An, and Edward Carlson, "Task allocation and Path Planning for Collaborative Autonomous Underwater Vehicles Operating through an Underwater Acoustic Communication," *Journal of Robotics*, vol. 2013, Article ID 483095, 15 pages, 2013.
- [157] A. Pedro Aguiar, Reza Ghabcheloo, Antonio M. Pascoal, and Carlos Silvestre, "Coordinated Path-Following Control of Multiple Autonomous Underwater Vehicles," in *Proc. of the Seventeenth (2007) Intl. Offshore and Polar Engineering Conference Lisbon*, pages 7 nos., Portugal, July 1-6, 2007.
- [158] M. Bayat, F. Vanni and A. Pedro Aguiar, "Online Mission Planning for Cooperative Target Tracking of Marine Vehicles," in *Proc. of MCMC'09 - 8th Conf. on Maneuvering and Control of Marine Craft*, IFSC Proc., Elsevier, vol. 42, issue 8, pp. 185-189, Guarujá (SP), Brazil, Sep. 2009.
- [159] A. Okamoto, J. J. Feeley, D. B. Edwards, and R. W. Wall, "Robust control of a platoon of underwater autonomous vehicles," in *Proc. IEEE Conf. on Ocean 2004 and Techno-Ocean'04*, vol. 1, pp. 505–510, December 2005.
- [160] Saing Paul Hou and Chien Chern Cheah, "Can a Simple Control Scheme Work for a Formation Control of Multiple Autonomous Underwater Vehicles?," *IEEE Transactions on Control Systems Technology*, vol. 19, no. 5, pp. 1090-1191, September 2011.

- [161] A.Nag, S.S.Patel, K.Kishore, S.A.Akbar,"A Robust H-Infinity Based Depth Control of an Autonomous Underwater Vehicle," in *Proc. 2013 IEEE Intl. Conf. on Advanced Electronic Systems*, 21-23<sup>rd</sup>. September, pp.68-73, Pilani, India.
- [162] Sebastien Varrier, "Robust control of Autonomous Underwater Vehicles,"INRIA Rhone-Alps, Gipsa-Lab, June 14, 2010.
- [163] Jian-sen Shen, Xu-chang Zhou, Hong-gang Zhang, "Research on Sliding Mode Control forNear-Surface AUV Depth Regulation in Waves Circumstance," IEEE International Conference on Electrical and Control Engineering, Wuhan, China, 25-27th. June 2010, pp.1760-1764.
- [164] R.Kelley, "A Tuning Procedure for Stable PID Control of Robot Manipulators," *Robotica*, pt.2, Vol.13, Mar/April,1995,pp.141-148.
- [165] M.Perrier, C.Canudas-De-Wit,"Experimental Comparison of PID vs.PID Plus Nonlinear Controller for Subsea Robots,"*Autonomous Robots* 3,195-212(1996)@1996 Kluwer Academic Publishers.
- [166] Karl Johan Astram and Lars Rundqwist,"Integrator Windup and How to Avoid It,"*American Control Conference*, Pittsburgh, PA, USA, 21-23 June, 1989,pp.1693-1698.
- [167] Z. Lin"Global Control of Linear Systems with Saturating Actuators,"*Automatica*, 1998, 34(7):897-905.
- [168] T.Chatchanayuenyong, M. Parnichkun,"Time Optimal Hybrid Sliding Mode-PI Control for an Autonomous Underwater Robot," *International Journal of Advanced Robotic Systems*, Vol.5, No.1, 2008, ISSN1729-8806, pp.91-98.
- [169] John-Erik Loberg," Plannar Docking Algorithm for Underactuated Marine Vehicles," Master's Thesis, June 2010, Norwgein University of Science & Technology.

- [170] Lynn Andrew Gish, "Design of AUV Charging System," Master's Thesis, Massachusetts Institute of Technology, USA, June 2004.
- [171] S. Arimoto, "A class of quasi-natural potentials and Hyper-stable PID servo-loops for nonlinear robotic system," Transactions of the Society of Instrument and Control Engineers, vol. 30, No. 9, pp. 1005–1012, September 1994.
- [172] R. Kelley, "Global positioning of Robot Manipulators via PD Control Plus a Class of Nonlinear, Integral actions, "IEEE Transactions on Automatic Control vol.43, no.7, July 1998.
- [173] R. Ortega, A. Loria, and R. Kelly, "A semiglobally stable output feedback PI<sup>2</sup>D regulator for robot manipulators," IEEE Transactions on Automatic Control, vol. 40, no. 8, pp. 1432–1436, August 1995.
- [174] E.M.Jafarov, M.N.A.Parlaker, "A New Variable Structure PID-Controller Design for Robot Manipulators," IEEE Transactions on Control System Technology, vol.13, no.1, January 2005.
- [175] Cui, S. S. Ge, B. V. E. How, and Y. S. Choo, "Leader-Follower Formation Control of Underactuated AUVs with Leader Position Measurement," in *Proc. IEEE Intl. Conf. on Robotics and Automation*, Kobe, Japan, 2009, pp. 979-984.
- [176] R. Carelli, C. De La Cruz. F. Roberti, "Centralized Formation Control of Non-Holonomic Mobile Robots," Latin American Applied Research, vol.36, pp.63-69, June 2006.
- [177] Cui, S. S. Ge, B. V. E. How, and Y. S. Choo, "Leader-Follower Formation Control of Underactuated AUVs with Leader Position Measurement," in *Proc. IEEE Intl. Conf. on Robotics and Automation*, pp. 979-984, Kobe, Japan, 2009.
- [178] Jos'e Rodrigues, Dario Figueira, Carlos Neves, Isabel Ribeiro, "Leader-Following Graph-Based Distributed Formation Control," in *Proc. Robotica'2008*, pp.71-77, 2008.

- [179] Reza Olfati-Saber, Richard M. Murray, "Consensus Problems in Networks of Agents With Switching Topology and Time-Delays," *IEEE Transactions on Automatic Control*, Vol. 49, No. 9, September, 2004.
- [180] A. Jadbabaie, J. Lin, and S. A. Morse, "Coordination of groups of mobile agents using nearest neighbor rules," *IEEE Trans. Automat. Control*, vol. 48, issue 6, pp. 988–1001, June 2003.
- [181] Kwang-Kyo Oh and Hyo-Sung Ahn, "Distance-based Formation Control Using Euclidean Distance Dynamics Matrix: General Cases," in *Proc. 2011 American Control Conf.*, pp. 4816–4821, O'Farrell Street, San Francisco, CA, USA, June 29 - July 01, 2011.
- [182] D. Atta, B. Subudhi, "Decentralized Formation Control of Multiple Autonomous Underwater Vehicles," *International Journal of Robotics and Automation, ACTA Press*, vol. 28, no. 4, pp. 303–310, 2013.
- [183] Suiyang Khoo, Lihua Xie and Zhihong Man, "Robust Finite-Time Consensus Tracking Algorithm for Multi-robot Systems," *IEEE/ASME Transactions on Mechatronics*, vol. 14, no. 2, 219–227, April 2009.
- [184] Xiaoyu Cai, "Graph Rigidity-Based Formation Control of Planar Multi-Agent Systems," PhD Thesis, Dept. of Mechanical and Industrial Engineering, Louisiana State University and Agricultural and Mechanical College, August 2013.
- [185] Kwang-Kyo Oh and Hyo-Sung Ahn, "Formation Control of Mobile Agents Based on Distributed Position Estimation," *IEEE Transactions on Automatic Control*, Vol. 58, No. 3, pp. 737–742, March 2013.
- [186] L. Krick, M. Broucke and B. Francis, "Stabilization of infinitesimally rigid formations of multi-robot networks," *International Journal of Control*, vol. 82, issue 3, pp. 423–439, 2009.



- [187] Kwang-Kyo Oh, Hyo-Sung Ahn, "Distance-based formation Control Using Euclidean Distance Dynamics Matrix: General Cases," in *Proc. Of 2011 American Control Conference* pp.4816-4821, San Francisco, CA, USA, June 29-July 01, 2011.
- [188] M. Cao, A. S. Morse, C. Yu, B. D. O. Anderson and S. Dasgupta, "Controlling a triangular formation of mobile autonomous agents," in *Proc. of the 47th IEEE Conf. on Decision and Control*, pp. 3603-3608, 2007.
- [189] M. Cao, A. S. Morse, C. Yu, B. D. O. Anderson, and S. Dasgupta, "Maintaining a directed, triangular formation of mobile autonomous agents," *Communications in Information and Systems*, vol. 11, no. 1, pp. 1-16, 2011.
- [190] F. Dörfler and B. Francis, "Geometric analysis of the formation problem for autonomous robots," *IEEE Trans. Autom. Control*, vol 55, no. 10, pp. 2379-2384, 2010.
- [191] B. Fidan, C. Yu, and B.D.O. Anderson, "Acquiring and maintaining persistence of autonomous multi-vehicle formations," *IET Control Theory Applications*, vol. 1, no. 2, pp. 452-460, 2007.
- [192] B. D. O. Anderson, C. Yu, B. Fidan, and J. M. Hendrickx, "Rigid graph control architectures for autonomous formations," *IEEE Control Systems Magazine*, vol. 28, no. 6, pp. 48-63, 2008.
- [193] J. Baillieul and A. Suri, "Information patterns and hedging brockett's theorem in controlling vehicle formations," in *Proc. IEEE Conf. Decision and Control*, Maui, HI, 2003, vol. 1, pp. 556-563.
- [194] Laura Krick, "Application of Graph Rigidity in Formation Control of Multi-Robot Networks," Master Degree Thesis, University of Toronto, Canada, 2007.

- [195] Xianbo Xiang, Bruno Jouvencel, Olivier Parodi, "Coordinated Formation Control of Multiple Autonomous Underwater Vehicles for a pipeline inspection," *International Journal of Advanced Robotic System*, vol.7, no.1, pp.075-084, ISSN 1729-8806, 2010.
- [196] N. H. Kussat, C. D. Chadwell, and R. Zimmerman, "Absolute positioning of an autonomous underwater vehicle using GPS and acoustic measurements," *IEEE J. Ocean. Eng.*, vol. 30, no. 1, pp. 153–164, Jan. 2005.
- [197] C. Q. Huang, X. G. Wang, and Z. G. Wang, "A Class of Transpose Jacobian-based NPID Regulators for Robot Manipulators with an Uncertain Kinematics," *Journal of Robotic Systems* 19(11), 527–539 (2002) © 2002 Wiley Periodicals, Inc.
- [198] S. Arimoto, "Fundamental problems of robot control: Part I, Innovations in the realm of robot servo-loops", *Robotica*, vol. 13, Issue 1, pp.19 -27., 1995.
- [199] C.C. Cheah, S. Kawamura, S. Arimoto, and K. Lee, "PID control of robotic manipulator with uncertain Jacobian matrix," in *Proc. IEEE Intl. Conf. Robotics and Automation*, Michigan, 1999(b), pp. 494–499.
- [200] S. Arimoto, "Control Theory of Nonlinear Mechanical Systems-A passivity-Based and Circuit-Theoretic Approach," 1<sup>st</sup>. Ed. Clarendon Press, Oxford Engineering Science Series (Book 49), Oxford, Dec. 1996.
- [201] Yury Stepanenko and Chun-Yi Su, "Variable Structure Control of Robot Manipulators with Nonlinear Sliding Manifolds," *International Journal of Control*, Taylor and Francis, vol.58, no.2, pp.285-300, 1993.
- [202] C.Y. Su, Y. Stepanenko, "On Using Nonlinear Sliding Manifolds in Robotic Control," in *Proc. of the 32<sup>nd</sup>. Conf. on Decision and Control*, vol.3, pp.2121-2124, San Antonio, Texas, December 1993.

- [203] Vadim Utkin, Hoon Lee, "Chattering Problem in Sliding Mode Control System," in *Proc. VSS'06, Intl. Workshop on Variable Structure System*, pp.346-350, Alghero, Italy, 5-7<sup>th</sup>. June 2006.
- [204] E.M.Jafarov, M.N.A.Parlaker,"A New Variable Structure PID-Controller Design for Robot Manipulators,"*IEEE Transactions on Control System Technology*, vol.13, no.1, pp.122-130,January 2005.
- [205] Takegaki, M. & Arimoto, S. , "A new feedback method for dynamic control ofmanipulators," *ASME Journal of Dynamic Systems, Measurement, and Control*, vol. 103,pp. 119–125,1981.
- [206] Keng Peng Tee and Shuzhi Sam Ge,"Control of Fully Actuated Ocean Surface Vessels Using a Class of Feedforward Approximators,"*IEEE Transactions on Control Systems Technology*, vol. 14, no. 4,pp.750-756, July 2006.
- [207] M. Egerstedt, X. Hu, and A. Stotsky,"Control of Mobile Platforms Using a Virtual VehicleApproach,"*IEEE Transactions on Automatic Control*, vol. 46, no. 11, pp.1777-1782,November 2001.
- [208] Wilfrid Perruquetti and Jean Pierre Barbot, "Sliding Mode Control in Engineering," edited version, pages:432nos., Marcel Dekker Inc., Network, USA, 2002.
- [209] Jean Jacques E.Slotine, Weiping Li,"*Applied Nonlinear Control*," 1<sup>st</sup> Ed., pages459, Englewood Cliffs,NJ: Prentice-Hall,Englewood Cliffs, New Jersey, USA, 1991,
- [210] Eric Vaughn Wallar,"Design and Full-Scale Testing of a Sliding Mode Controller for a small Underwater Vehicle," Master of Science (in Aeronautics and Astronautics ) Thesis, Massachusetts Institute of Technology, USA, June, 1989.
- [211] J. M. Hendrickx, B. Fidan, C. Yu, B. D. O. Anderson, and V.D. Blondel, "Elementary operations for the reorganization of minimally persistent formations," in *Proc. of the 17<sup>th</sup> Intl.*

Symposium on Mathematical Theory of Networks and Systems (MTNS '06), pp. 859–873, Kyoto, Japan, 2006.

- [212] B. D. O. Anderson, C. Yu, B. Fidan, and J. M. Hendrickx, “Rigid graph control architectures for autonomous formations,” *IEEE Control Systems Magazine*, vol. 28, no. 6, pp. 48–63, 2008.
- [213] B. D. O. Anderson, S. Dasgupta, and C. Yu, “Control of directed formations with a leader-first follower structure,” in *Proc. of the 46th IEEE Conf. on Decision and Control (CDC '07)*, pp. 2882–2887, New Orleans, La, USA, December 2007.
- [214] S. Sandeep, B. Fidan, and C. Yu, “Decentralized cohesive motion control of multi-agent formations,” in *Proc. of the 14<sup>th</sup> Mediterranean Conf. on Control and Automation (MED'06)*, pp. 1-6, 28-29<sup>th</sup>. June 2006.
- [215] M. J. D. Powell, “A fast algorithm for nonlinearly constrained optimization calculations,” in *Numerical Analysis*, G.A. Wat-son, Ed., vol. 630 of *Lecture Notes in Mathematics*, Springer, London, UK, 1978.
- [216] M. J. D. Powell, “The Convergence of variable metric methods for nonlinearly constrained optimization calculations,” in *Nonlinear Programming*, J.B. Rosen, O.L. Mangasarian, K. Ritter, Robinson, eds., Academic Press, pp. 27-63, New York, USA, 1978.
- [217] S. P. Han, “A globally convergent method for nonlinear programming,” *Journal of Optimization Theory and Applications*, vol. 22, no. 3, pp. 297–309, 1977.
- [218] Hassan K. Khalil, “Nonlinear Systems,” 3<sup>rd</sup>. Edition, pp. 750, Prentice Hall Inc., Upper Saddle River, NJ 07458, USA, 2002.
- [219] David Gray Roberson, Jr. “Environmental Tracking and Formation Control for an Autonomous Underwater Vehicle Platoon with Limited Communication” PhD Thesis, Dept., Electrical Engineering, Virginia Polytechnic Institute and State University, USA, 2008.

- [220] Julien M. Hendrickx, Baris Fidan, Changbin (Brad) Yu, Brian D. O. Anderson and Vincent D. Blondel, "Formation Reorganization by Primitive Operations on Directed Graphs," *IEEE Transactions on Automatic Control*, vol. 53, No. 4, pp.968-979, May 2008.
- [221] Tolga Eden, Walter Whitely B. D. O. Anderson, A. Stephen Morse, Peter N. Belhumeur, "Information Structures to Secure Control of Rigid Formations with Leader-Follower Architecture," in *Proc. of the American Control Conf.*, pp. 2966–2971, Portland, Oregon, June 2005.
- [222] D. J. Lajer, "Topological ordering of a list of randomly numbered elements of network," *Communications of the ACM*, vol.4, no.4, pp.167-168, 1961.
- [223] M. Hendrickx, B. Fidan, B.D.O. Anderson, and V.D.Blondel, "Three and higher dimensional autonomous formations: rigidity, persistence and structural persistence rigidity, persistence and structural persistence," *Automatica*, vol.43, no.3, pp.387-402, 2007.
- [224] Eduardo D. Sontag, "Smooth Stabilization Implies Coprime Factorization," *IEEE Transactions on Automatic Control*, vol. 34, no. 4, April 1989.
- [225] Alberto Isidori, "Nonlinear Control system-II," 1<sup>st</sup>. Ed., Springer-Verlag London Limited, June, 1999, ISSN: 0178-5354.
- [226] David Angeli, Eduardo D. Sontag, Yuan Wang, "Input-to-state stability with respect to inputs and their derivatives," *Int. J. of Robust and Nonlinear Control*, vol.13, pp.1035–1056, 2003.
- [227] Vladimir Filaretov, Dmitry Yukhimetes, "Synthesis Method of Control System for Spatial Motion of Autonomous Underwater Vehicle," *International Journal of Industrial Engineering and Management*, vol., pp.3, pp.133-141, 2012.



## **Thesis Dissemination**

### **Journal**

- [1] D.Atta, B. Subudhi,"Decentralized Formation Control Algorithm for Multiple Autonomous Underwater Vehicles,"*International Journal of Robotics and Automation*, ACTA Press, vol. 28, no. 4,pp.303-310, 2013
- [2] D. Atta, B. Subudhi, Madan M. Gupta,"Cohesive Motion Control Algorithm for Formation of Multiple Autonomous Agents,"*Journal of Robotics (Hindawi Publishing Corporation)*, Article ID 360925, doi:10.1155/2010/360925,2010.
- [3] B. Subudhi, D.Atta,"Design of a path following controller for an underactuated AUV," *Jounl. of Archives of Contrl. Sciencess*, vol 19. (LV, no.4, pp. 355-368), 2009.
- [4] D. Atta and B.Subudhi ,"Robust Set-Point Control of Autonomous Underwater Vehicle using Nonlinear PID Controller with Bounded Integral and Bounded Derivative," Transactions of the Institute in Measurement and Control, Sage Publications. (Under Review)

### **Conferences**

- [1]. D. Atta, B. Subudhi,"A New Algorithm for Motion Control of Acyclic Minimally Persistent Formation of Mobile Autonomous Agents," IEEE-INDICON - 2009, Gandhinagar, India, 18th-20<sup>th</sup>. December 2009.





# Author's biography

Debabrata Atta was born to Late Sudhansu Sekhar Atta and Smt. Manju Rani Atta on 1<sup>st</sup>. January, 1973 at Kharagpur, West Bengal, India. He obtained a Bachelor's degree in Electrical Engineering from Jalpaiguri Govt. Engineering Collge, West Bengal, India in 1995 and a Master in Mechatronics Enginerring from Maulana Abul Kalam Azad University of Technology (erstwhile, West Bengal University of Technology), Kolkata, West Bengal, India in 2007. He joined as a Institute PhD Scholar in the Department of Electrical Engineering, National Institute of Technology Rourkela in September 2008. His areas of academic pursuit include Robotics, Autonomous Underwater Vehicle, Control System, Robust Control.

## **Communications:**

Address: Department of Electrical Engineering, National Institute of Technology Rourkela, Orissa, PIN: 769008.

*e-mail:* attadebabrata@gmail.com